

THE INFLUENCE OF FLOOR MEMBERS ON THE BEHAVIOR OF
REINFORCED CONCRETE BEAM-COLUMN JOINTS SUBJECTED
TO SEVERE CYCLIC LOADING

APPROVED BY SUPERVISORY COMMITTEE:

To my parents

THE INFLUENCE OF FLOOR MEMBERS ON THE BEHAVIOR OF
REINFORCED CONCRETE BEAM-COLUMN JOINTS SUBJECTED
TO SEVERE CYCLIC LOADING

by

ROBERTO T. LEON, M.S.

DISSERTATION

Presented to the Faculty of the Graduate School of

The University of Texas at Austin

in Partial Fulfillment

of the Requirements

for the Degree of

DOCTOR OF PHILOSOPHY

THE UNIVERSITY OF TEXAS AT AUSTIN

December, 1983

ACKNOWLEDGEMENTS

The experimental work reported herein was carried out at the Phil M. Ferguson Structural Engineering Laboratory, Balcones Research Center, The University of Texas at Austin.

This research was sponsored by the National Science Foundation under Grant Numbers ENV-77-20816 and PRF-7720816.

The research project was under the direction of Dr. James O. Jirsa, the writer's dissertation advisor. The writer is deeply indebted to Dr. Jirsa for the continuous support, advice, and humor that made this work possible. The encouragement of Dr. John E. Breen, Director of the Ferguson Structural Engineering Laboratory, is also gratefully acknowledged. The friendship and opportunities provided by them and the rest of the faculty at the Ferguson Laboratory are greatly appreciated.

The author is indebted to his fellow graduate students, Joe Longwell, Sam Burguières, and Jeff Reeder, who supervised various phases of the project and provided the manpower, ingenuity, and friendship necessary to carry it to completion. The help of

undergraduates Mike Ritch and Jeff Fox is also gratefully acknowledged.

The help of the technical staff at the Ferguson Lab, composed of Blake Stasney, George Moden, Dick Mershall, Dan Perez, and Gorham Hinckley, was invaluable in making this work possible. The help of the clerical staff of Maxine DeButts, Laurie Golding, Pat Henderson, Norm Halsted, and Al Garcia is gratefully acknowledged. The author is deeply indebted to Alex Tahmassebi and Conrad Paulson for their work on the data acquisition and reduction parts of this project. The help of fellow graduate students Julio Ramirez, Terry Kohutek, Randy Poston, Mark Moore, Milind Joglekar, and Paul Murray during different phases of the project is also acknowledged.

A special thanks is extended to all Pacos, the Friday Gang, and Sheryl Davis for their continuous support and friendship.

Roberto T. Leon

The University of Texas at Austin
December, 1983

ABSTRACT

Eight reinforced concrete beam-column joint subassemblages were tested to investigate the influence of floor members on their response under large cyclic load reversals. The tests were divided into three series. The first dealt with specimens with different framing beam sizes; the second with specimens with floor slabs; and the third with a comparison between interior and exterior joints. The intent was to clarify the effect of different floor member sizes and shapes on the behavior of these subassemblages.

Typically the subassemblages were 13 ft. high and consisted of four 13 in. by 18 in. beams framing into a 15 in. by 15 in. column. They were intended to represent a beam-column joint in the bottom stories of a moment resisting frame. The structural components between the midheight of adjacent floors and the points of inflection along the beams were modelled. The subassemblages were subjected to a severe load history consisting of 3 cycles at drifts of 2%, 4%, and 6%. The loads were applied biaxially simultaneously, and were intended to model the worst loading condition to be expected from a major earthquake.

The tests showed that the framing beam geometry and the presence of a slab can have a significant influence on the behavior of beam-column joints. Most of the specimens tested exhibited severe stiffness and strength degradation with cycling. This was more pronounced in specimens with very narrow beams and without slabs. The test proved that the shear strength of beam-column joints is very high, and that in general, flexural considerations should govern their design. The severe bond deterioration and yield penetration observed in most tests proves the need for strict anchorage requirements for beam-column joints.

A design approach was developed to integrate the parameters found by this and other experimental studies to be important in moment-resisting frame design. The design approach, still under development, leads to frames with wide beams with low reinforcement percentages and to flexurally strong columns.

TABLE OF CONTENTS

Acknowledgements	iv
Abstract	vi
Table of Contents	viii
Chapter 1. Introduction	1
1.1. Background	2
1.2. The Moment-Resisting Frame	3
1.3. The Joint Problem	5
1.4. Objectives	9
Chapter 2. Review of Past Research and Practice	11
2.1. Review of Past Research	11
2.1.1. Research in the U.S. and Canada	13
2.1.2. Research in New Zealand	16
2.1.3. Other Research	17
2.2. Shear Strength of Joints	19
2.2.1. Factors Affecting Joint Performance and Shear Stren	19
2.2.2. The Concrete Strut	20
2.2.3. The Panel Truss Mechanism	22
2.3. Current Design Procedures	26
2.3.1. The ACI-ASCE Committee 352 Method	26
2.3.2. The ATC3-06 Approach	30
2.3.3. The New Zealand Standard	32
2.3.4. The Japanese Design Procedure	34
2.3.5. Comparison of Design Methods	35
2.4. Limitations of Past Research	40
Chapter 3. Experimental Program	43
3.1. Test Series Description	43

3.2. Specimen Design	48
3.3. Specimen Details	49
3.3.1. Beam and Column Details	49
3.3.2. Specimen Fabrication	53
3.3.3. Material Properties	53
3.4. Testing Setup and Procedure	54
3.5. Instrumentation	59
3.6. Load History	63
3.7. Summary	67
Chapter 4. Experimental Results	69
4.1. General	69
4.2. Load History	71
4.3. Principal Load vs. Deformation Relationships	74
4.3.1. Beam Load-Beam Displacement	75
4.3.2. Joint Shear - Joint Shear Strain	81
4.4. General Specimen Behavior	89
4.4.1. Dead Load and Initial Cracking Cycle	90
4.4.2. First Deflection Level	90
4.4.3. Second and Third Deflection Levels	96
4.5. Other Measures of Response	98
4.5.1. Interstory Displacement vs. Joint Shear Strain	98
4.5.2. Joint Rotation vs. Interstory Displacement	100
4.5.3. Column Rotation vs. Interstory Displacement	100
4.5.4. Beam Rotations vs. Interstory Displacement	102
4.5.5. Beam Longitudinal Displacement vs. Interstory Displ	102
4.6. Reinforcing Bar Slip	104
4.7. Reinforcing Bar Stresses and Strains	107
4.7.1. Beam Bars	107
4.7.2. Column Bars	113
4.7.3. Joint Ties	115
4.8. Components of Displacement	117
4.8.1. Definitions of Components	117
4.8.2. Beam End Deflection Components	118
4.8.3. Interstory Displacement Components	120
4.9. Summary	125
Chapter 5. Description of Other Tests	126
5.1. Introduction	126
5.2. Effect of Beam Size	127
5.2.1. BCJ5 - Control Specimen [Area Ratio = 86%]	128
5.2.1.1. Behavior of Test Specimen	128

5.2.1.2. Deflection Measurements	133
5.2.2. Steel Strains	136
5.2.2.1. Evaluation of Performance	140
5.2.3. BCJ11 - Narrow Beams [Area Ratio =58%]	140
5.2.3.1. Behavior of Test Specimen	141
5.2.3.2. Deflection Measurements	144
5.2.3.3. Steel Strains	147
5.2.3.4. Evaluation of Performance	150
5.2.4. BCJ12 - Wide Beams [Area Ratio = 120%]	150
5.2.4.1. Behavior of Test Specimen	151
5.2.4.2. Deflection Measurements	155
5.2.4.3. Steel Strains	157
5.2.4.4. Evaluation of Performance	159
5.3. BCJ10 - Wide Beam [Area Ratio =120% , $f_c = 2800$ psi]	159
5.4. Behavior of Specimen	159
5.5. Effect of Slab	161
5.5.1. BCJ8 - Control Test	162
5.5.2. BCJ9 and BCJ9A - Specimens with Slab	162
5.5.2.1. Behavior of Test Specimen	162
5.5.2.2. Deflection Measurements	167
5.5.2.3. Steel Strains	169
5.5.2.4. Evaluation of Performance	172
5.6. Exterior vs. Interior Joints	172
5.6.1. BCJ13 - Exterior without Slab	173
5.6.1.1. Behavior of Test Specimen	173
5.6.1.2. Deflection Measurements	179
5.6.1.3. Steel Strains	180
5.6.1.4. Evaluation of Performance	181
5.6.2. BCJ14 - Exterior with Slab	181
5.6.2.1. Behavior of Test Specimen	181
5.6.2.2. Deflection Measurements	185
5.6.2.3. Steel Strains	185
5.6.2.4. Evaluation of Performance	188
5.7. Conclusions	188

Chapter 6. Evaluation of Experimental Data 190

6.1. Introduction	190
6.2. Shear Strength	191
6.3. Hysteretic Behavior	205
6.4. Bond Conditions and Bar Slip	214
6.5. Effect of Framing Member Size	232
6.5.1. Framing Beam Size	240
6.5.2. Effect of a Slab	250
6.5.3. Effect of Column Axial Load	252

6.6. Conclusions	253
6.6.1. Lateral Restraint	253
6.6.2. Nominal Shear Stress Levels	254
6.6.3. Bond Conditions	255
6.6.4. Transverse Joint Shear Reinforcement	255
Chapter 7. Preliminary Design Approach for Beam-Column Joints in Moment Resisting Frames in Seismic Regions	257
7.1. Introduction	257
7.2. Evaluation of Parameters Governing Design	258
7.3. Selection of Governing Parameter	260
7.3.1. The Moment Ratio	261
7.3.1.1. Effect on Construction Costs	262
7.3.1.2. Structural Effects	263
7.4. Determination of the Beta Factor	263
7.4.1. Experimental Data	263
7.4.2. Conclusion form BCJ Test Series	275
7.4.3. Structural Considerations	276
7.4.4. Current Design Values	277
7.4.5. Suggested Values for the Moment Ratio	277
7.5. Proposed design approach	279
7.5.1. Background	279
7.6. Basis for Design Approach	279
7.7. Derivation of Equations	281
7.7.1. Uniaxial Loading	284
7.7.1.1. Beam Flexural Strength	284
7.7.1.2. Column Flexural Strength	284
7.7.1.3. Flexural Reinforcement Limits	285
7.7.1.4. Joint Shear Capacity	285
7.7.1.5. Bond Stresses	286
7.7.1.6. Geometric Considerations	286
7.7.2. Biaxial Loading	287
7.7.2.1. Beam Moment Capacity	287
7.7.2.2. Column Moment Capacity	287
7.7.2.3. Joint Shear Strength	288
7.7.2.4. Geometric Parameters	288
7.7.2.5. Synthesis	288
7.7.3. Discussion	289
7.7.4. Minimum Transverse Steel Requirements	292
7.8. design approach	293
7.9. Evaluation and Comparison of Design Approach	295
Chapter 8. Conclusions	303

8.1. Summary of Test Program	303
8.2. Summary of Results	304
8.2.1. Experimental Results	304
8.2.2. Design Recommendations	305
8.3. Proposed Design Approach	306
8.4. Additional Research Needs	307
REFERENCES	309

LIST OF TABLES

Table 3-1:	Summary of test series	45
Table 4-1:	Equivalent stiffness	78
Table 6-1:	Summary of shear strengths	194
Table 6-2:	Maximum Shears - Positive Peaks	197
Table 6-3:	Allowable shear strengths	199
Table 6-4:	Contributions of steel and concrete	200
Table 6-5:	Comparison of design procedures	203
Table 6-6:	Equivalent P-P stiffnesses	208
Table 6-7:	Loops	211
Table 6-8:	Strut size calculations	246
Table 7-1:	Summary of Past Research	264
Table 7-2:	Summary of Past Research	265
Table 7-3:	Summary of Past Data	266
Table 7-4:	Suggested values for Beta	278
Table 7-5:	Design Examples	297

LIST OF FIGURES

Figure 1-1:	Elastic frame behavior	4
Figure 1-2:	Inelastic frame behavior	4
Figure 1-3:	Forces acting on a deformed joint.	7
Figure 2-1:	Test specimens used in past research	12
Figure 2-2:	Concrete strut mechanism	21
Figure 2-3:	The panel truss mechanism	23
Figure 2-4:	Concrete strut contribution	36
Figure 2-5:	Maximum allowable shear stresses	37
Figure 2-6:	Contribution of different mechanisms	38
Figure 3-1:	Dimensions of beam-column joint subassemblage	44
Figure 3-2:	Uniaxial interaction diagram	50
Figure 3-3:	Biaxial interaction diagram	50
Figure 3-4:	Beam and column details	52
Figure 3-5:	Real vs. idealized model	55
Figure 3-6:	Test set-up	56
Figure 3-7:	Loading system	58
Figure 3-8:	Inserts and deflection transducers in the joint area	60
Figure 3-9:	Joint shear strain measurement	61
Figure 3-10:	Components of beam end deflection	62
Figure 3-11:	Location of strain gages near the joint	64
Figure 3-12:	Slip-wire instrumentation	65
Figure 3-13:	Load history applied	68
Figure 4-1:	Reinforcement in the joint area	70
Figure 4-2:	Load history for BCJ8	72
Figure 4-3:	Equivalent interstory displacement	72
Figure 4-4:	Load-deformation for North beam [BCJ8]	76
Figure 4-5:	Load-deformation for South beam [BCJ8]	76
Figure 4-6:	Equivalent stiffness	78
Figure 4-7:	Total joint shear vs. interstory displacement	80
Figure 4-8:	calculation of shear in the joint	82
Figure 4-9:	Joint shear vs. joint shear strain - NS - BCJ8	84
Figure 4-10:	Joint shear vs. joint shear strain - EW - BCJ8	84
Figure 4-11:	Effect of strain incompatibility on joint shear strain	87
Figure 4-12:	Joint equilibrium with and without strain compatibility	88

Figure 4-13:	Cracking of the South and West Beams	91
Figure 4-14:	Joint SW corner at LS 7	93
Figure 4-15:	Joint SW corner at LS 12	93
Figure 4-16:	Joint SW corner at LS 68	95
Figure 4-17:	Joint SW corner at LS 124	95
Figure 4-18:	JSS vs. ID for North-South direction	99
Figure 4-19:	JSS vs. ID for East-West direction	99
Figure 4-20:	Joint rotation vs. interstory displacement	101
Figure 4-21:	Inelastic column rotation vs. interstory displacement	101
Figure 4-22:	Beam rotation vs. interstory displacement	103
Figure 4-23:	Longitudinal beam displacement vs. interstory displacement	103
Figure 4-24:	Slip vs interstory displacement - Top bar West face	106
Figure 4-25:	Slip vs interstory displacement - Top bar East face	106
Figure 4-26:	strain profile - Top EW bar	108
Figure 4-27:	strain profile - Bottom EW bar	108
Figure 4-28:	Stress profile - Top EW bar	110
Figure 4-29:	Stress profile - Bottom EW bar	110
Figure 4-30:	Stress vs. strain for BEBN	111
Figure 4-31:	Stress vs. interstory displacement -BWBN	111
Figure 4-32:	Strain vs. moment resultant- NW column bar top	114
Figure 4-33:	Strain vs. moment resultant- NW column bar bottom	114
Figure 4-34:	Stress vs. ID - TNT	116
Figure 4-35:	Stress vs. ID - TNB	116
Figure 4-36:	Contributions to beam end deflection - East - BCJ8	119
Figure 4-37:	Contribution due to elastic deformation	122
Figure 4-38:	Contribution due to beam inelastic rotation	122
Figure 4-39:	Contribution due to column inelastic rotation	123
Figure 4-40:	Contribution due to joint shear strain	123
Figure 4-41:	Components of interstory displacement	124
Figure 5-1:	Total Moment vs Interstory dis. - BCJ5	129
Figure 5-2:	P-delta Correction	129
Figure 5-3:	Beam load vs. deflection - West beam - bcj5	130
Figure 5-4:	Shear cracking at joint - LS 7	130
Figure 5-5:	BCJ5 at end of first three cycles	132
Figure 5-6:	BCJ5 at end of test	132
Figure 5-7:	Contributions to total deformation	134
Figure 5-8:	Joint rotation vs. interstory displacement - bcj5	134
Figure 5-9:	Stress vs. strain for top beam bar	137

Figure 5-10:	Stress vs strain for column bar	137
Figure 5-11:	Top joint hoop stress vs. displacement.	138
Figure 5-12:	Bottom joint hoop stress vs. displacement	138
Figure 5-13:	Moment vs. interstory displacement for BCJ11	142
Figure 5-14:	Comparison of first cycles for BCJ5 and BCJ11	142
Figure 5-15:	BCJ11 at LS 68	145
Figure 5-16:	BCJ11 at LS end of test	145
Figure 5-17:	Deflection components for BCJ11	146
Figure 5-18:	Joint rotations for BCJ11	146
Figure 5-19:	Strain profile for top column SE corner	148
Figure 5-20:	Stress vs strain joint hoop - BCJ11	149
Figure 5-21:	Total moment vs interstory dis. -BCJ12	152
Figure 5-22:	Cracking in the joint area - BCJ12	152
Figure 5-23:	BCJ24 at LS 24	153
Figure 5-24:	BCJ12 at LS 124	153
Figure 5-25:	Deflection components for BCJ12	156
Figure 5-26:	Joint rotation vs interstory displacement.	156
Figure 5-27:	Stress vs interstory displacement for CSEB	158
Figure 5-28:	Joint hoop stresses - BC12	158
Figure 5-29:	BCJ9 - Specimen with a slab	163
Figure 5-30:	Load-deflection for BCJ9	164
Figure 5-31:	BCJ9 at LS 12	166
Figure 5-32:	BCJ9 at LS 68	166
Figure 5-33:	Deflection components for BCJ9	168
Figure 5-34:	Joint rotations for BCJ9	168
Figure 5-35:	cracks in the joint area	170
Figure 5-36:	BCJ9 at end of test	170
Figure 5-37:	Stress vs ID for top east tie -BCJ9	171
Figure 5-38:	Stress vs ID for bottom east tie - BCJ9	171
Figure 5-39:	Steel in the joint area for exterior joints	174
Figure 5-40:	Load-deflection for BCJ13 NS	175
Figure 5-41:	Load-deflection for BCJ13 EW	175
Figure 5-42:	BCJ13 at LS 12	177
Figure 5-43:	BCJ13 at LS 68	177
Figure 5-44:	Deflection components for BCJ13	178
Figure 5-45:	Joint rotations for BCJ13	178
Figure 5-46:	Load-deflection for BCJ14 NS	182
Figure 5-47:	Load-deflection for BCJ14 EW	182
Figure 5-48:	BCJ14 at LS 7	184
Figure 5-49:	BCJ14 at LS 68	184
Figure 5-50:	deflection components for BCJ14	186
Figure 5-51:	joint rotations for BCJ14	186
Figure 5-52:	Stress-strain for BCJ14	187
Figure 5-53:	Stress-strain for BCJ14	187
Figure 6-1:	Shear demand on typical joint	192
Figure 6-2:	Joint shear calculations	195

Figure 6-3:	Hysteretic behavior of R.C.	207
Figure 6-4:	Types of hysteretic behavior	207
Figure 6-5:	Bond stresses in a bar through a joint	215
Figure 6-6:	Top East gage	217
Figure 6-7:	Top West gage	218
Figure 6-8:	Top west gage 8 in. from joint	221
Figure 6-9:	Top west gage 16 in. from joint	222
Figure 6-10:	Bond stress history	223
Figure 6-11:	Bar slip versus strain model	225
Figure 6-12:	Slip on East side	227
Figure 6-13:	Slip on West side	227
Figure 6-14:	Calculations of slip and elongation	228
Figure 6-15:	Bottom East gage	230
Figure 6-16:	Bottom west gage	230
Figure 6-17:	Bond stress history bottom	231
Figure 6-18:	Forces on biaxially loaded joint	233
Figure 6-19:	NZ tests - Contributions of steel and concrete	236
Figure 6-20:	Zhang and Jirsa's model	238
Figure 6-21:	Biaxially loaded joint - mechanisms	239
Figure 6-22:	Realistic distribution of stresses in joint	241
Figure 6-23:	Diagonal strut	242
Figure 6-24:	Strut for BCJ11	244
Figure 6-25:	Strut for BCJ12	244
Figure 6-26:	Crack pattern for interior joint	251
Figure 6-27:	Crack pattern for exterior joint	251
Figure 7-1:	Moment ratio vs joint reinforcement- Interior	268
Figure 7-2:	Moment ratio vs joint shear stress level	269
Figure 7-3:	Performance classification for Table 7-1	271
Figure 7-4:	Definition of variables used.	283
Figure 7-5:	Beam reinforcement vs. moment ratio limits - Uniaxial	290
Figure 7-6:	Beam reinforcement vs. moment ratio limits - Biaxial	290
Figure 7-7:	Outline of design approach	296
Figure 7-8:	Comparison	301

Chapter 1

Introduction

The damage to large population centers caused by earthquakes during the past two decades has sparked a growing concern with seismic design and seismic safety. Earthquakes such as those that destroyed Tangshan (1976), Guatemala City (1976), and Managua (1972) and damaged the San Fernando Valley (1971) have yielded very valuable information to researchers and engineers on the behavior of reinforced concrete structures under seismic loading. However, there are still many areas of earthquake engineering where there is no consensus among experts as to the best analytical and design procedures [12, 85].

One of these areas is the analysis and design of beam-column joints in reinforced concrete moment-resisting frames [78, 54]. While a large amount of research has been carried out in this area in the past 10 years, design recommendations based on the research vary substantially from one study to another. There is disagreement as to the basic mechanism controlling the transfer of forces across a joint as well as to the relative importance of the parameters to be used in design. As will be discussed later there are valid reasons for such discrepancies.

The experimental work reported herein will not resolve the contradictions mentioned. In this study the results of tests on seven full-scale reinforced concrete beam-column joints will be discussed. A summary of the state-of-the-art in beam-column joint design as well as the experimental data will then provide the background for the derivation of new design guidelines.

1.1 Background

The explosive growth of urban areas in developing countries and the soaring prices for prime real state in industrialized nations have created a strong demand for highrise buildings. While the design of such structures for gravity loads presents few problems, their design for lateral loads (wind, earthquakes, etc.) is a completely different and infinitely more complex task. With recent seismic rezoning, large parts of the U.S. which were previously considered to be seismically safe have been upgraded to low or moderate intensity zones. This has made seismic design and seismic retrofitting a very important consideration in areas where previously no earthquake design or analysis was necessary.

To withstand large lateral loads without appreciable damage, buildings need strength and energy-absorption capacity. In the design process, this need for stiffness and ductility has to be balanced against economic constraints. Different framing schemes, or

structural systems, are usually examined before a satisfactory solution is reached. For the case of earthquake loading a satisfactory solution will be determined only when the building is subjected to actual ground motions. It can seldom be decided analytically because the effect of non-structural components on overall structural response cannot be accurately modelled and the actual ground motion will not be known.

1.2 The Moment-Resisting Frame

After the San Fernando earthquake (1971), researchers and engineers in the U. S. became concerned with the inability of some common structural systems to dissipate seismic energy without suffering considerable structural and non-structural damage. Spurred by dramatic failures such as that of the Olive View Hospital, the engineering profession began to look for ways of improving existing systems and to experiment with new ones. Among the former, the "strong column-weak girder" design philosophy for the class of structures known as moment-resisting frames gained widespread acceptance. In moment-resisting frames all the lateral deformations caused by an earthquake are taken by the frame, without the help of shear walls or other lateral bracing. As shown in Fig 1-1, if a moment-resisting frame is subjected to a small earthquake, the deformations in the members will be primarily elastic and only limited yielding would be expected. If subjected to a very strong

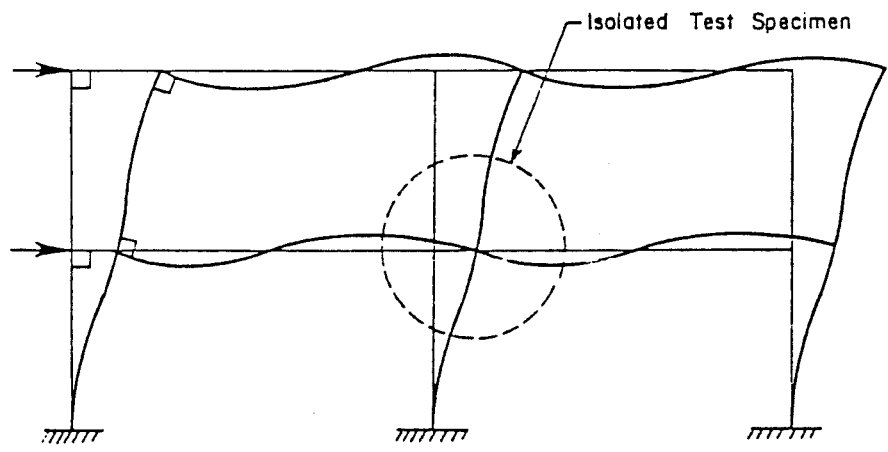


Figure 1-1 : Elastic frame behavior

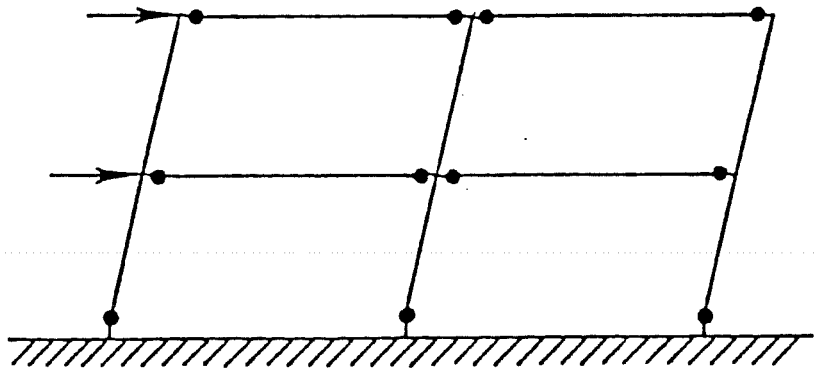


Figure 1-2 : Inelastic frame behavior

earthquake, on the other hand, the building will have to absorb and dissipate some energy to avoid a brittle failure. Energy absorption can be provided by detailing the structure such that plastic hinges occur in the beams in the vicinity of the joints and the lower story columns, as shown in Fig. 1-2. Rotations in the plastic hinges provide the necessary energy-dissipation mechanism without significant damage to the gravity load carrying capacity of the structure.

A key to this design philosophy is that, except for the hinges which must form at their bases, the columns should remain essentially elastic throughout the earthquake so that neither appreciable stiffness nor strength degradation can occur. If this cannot be prevented the building will collapse because of the instability due to P-delta effects. The beam-column connection, or joint, is an integral part of the column and thus must remain elastic even though very large forces are transmitted from the beam into the column. The joint thus becomes the key structural element for satisfactory performance in moment-resisting frames.

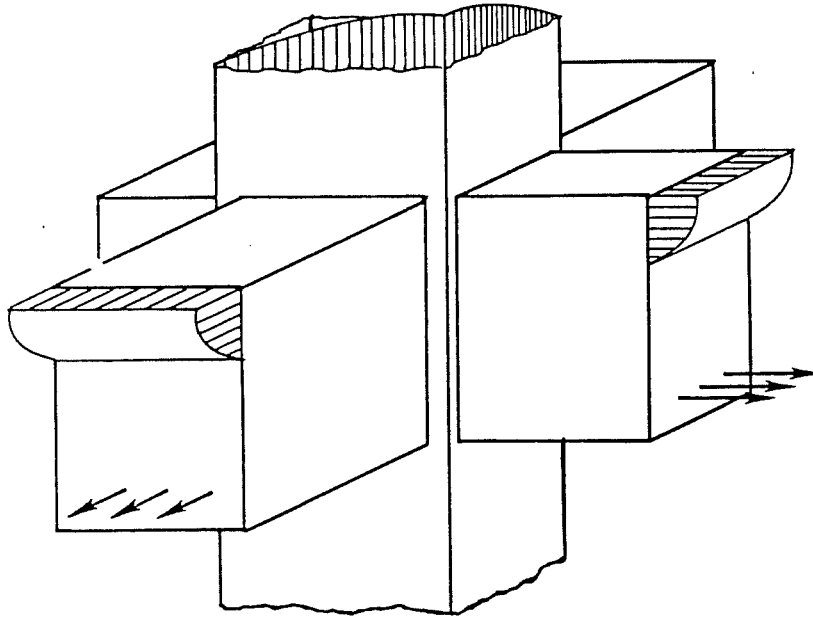
1.3 The Joint Problem

Prior to 1970 the design of connections in reinforced concrete structures subjected to seismic actions received little attention. Most designers considered the joint to be infinitely

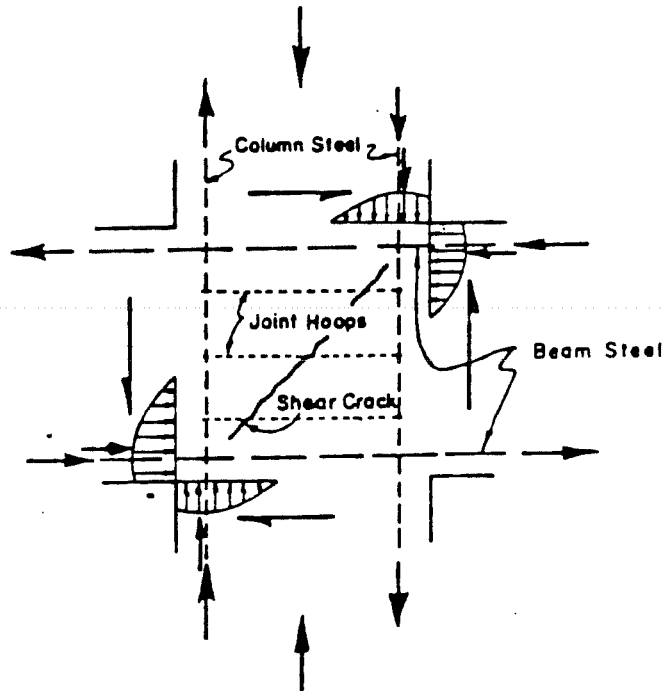
strong, and thus to have non-deteriorating strength and stiffness. With improved construction details for beams and columns based on experimental and analytical research, it became obvious that the joint was a weak link in the structure. While beam and column members can be detailed to perform well during earthquakes, there is a lack of information on connecting the members so that the assemblage behaves well also. A free-body diagram of the area near an interior beam-column joint (Fig. 1-3) shows that if plastic hinges are to be formed near the joint, large flexural forces in the beams result in very large shear and bond stresses through the joint. Anchorage conditions may be critical if it is assumed that the bars have to be in tension on one side of the joint and compression on the other for the energy dissipation mechanism to perform satisfactorily.

Tests have shown that for typical joint details used today the anchorage length available in the joint region is insufficient, and thus bond deterioration will occur [107, 12, 11]. If we further assume that under a severe earthquake a building can undergo several large cycles of reversed loading, it becomes clear that this bond deterioration can result in slippage of these bars through the joint. If the bars begin to slip through the joint, the stiffness of the system is reduced considerably, and thus instability can follow.

Moreover, the bond stresses are transferred as horizontal shear to the joint, resulting in very large shear stresses. If we



(a) Forces acting on a biaxially loaded joint



(b) Free body diagram of forces in the joint area

Figure 1-3 : Forces acting on a beam-column joint

consider that the nominal shear strength of concrete in beams is only between 2 and $4\sqrt{f'_c}$, and that the typical joint can receive anywhere from 5 to 10 times that amount under a severe earthquake, it is obvious that shear strength deterioration must also occur, unless completely different force transfer mechanisms are involved.

The primary effect of the loss of bond and shear strength is a significant loss of stiffness of the overall system. A reduction of stiffness produces a large increase of the natural period of the structure, substantially changing the magnitude of the forces and deflections to be expected. The building becomes damaged as the earthquake progresses and is required to absorb less energy. Inclusion of this phenomenon results in a rather complex analytical problem that is handled in design through the use of elastic and inelastic response spectra. Designing for a constant period structure in the region of greatest amplification in the spectrum will yield a conservative solution.

A large number of tests on beam-column joint subassemblages have been conducted in the past 10 years. Most of these tests were carried out on planar specimens without floor slabs and with beam sizes very similar to the column size. Tests on planar specimens clarified the importance of adequate transverse reinforcement and anchorage of bars through the joint. However, the restraint on the boundaries of the joint provided by floor members in the orthogonal

plane and by a floor slab have not been adequately explored. The effect of biaxial loading on joint behavior is another area where research is needed to clarify the parameters to be used in their design.

The lateral restraint provided by the floor system is the main subject of this dissertation. A review of past research will be presented and existing code provisions discussed. The experimental work conducted in this investigation will be described. The influence of shear, bond, and lateral restraint on the behavior of the specimens will then be examined. Finally, the results of this project, as well as those of other tests reported in the literature, will be used to develop a design approach in which the requirements for acceptable joint performance are considered at the same time that the main structural members are proportioned.

1.4 Objectives

The objectives of this dissertation are:

- To report on the behavioral aspects of a test series aimed at clarifying the effect of lateral restraint from the floor system on beam-column joints.
- To analyze the influence of shear and bond deterioration on the stiffness and strength of the subassemblages tested.
- To examine the applicability of models based on response of joints in planar frames to the response of joints in a three-dimensional floor system.

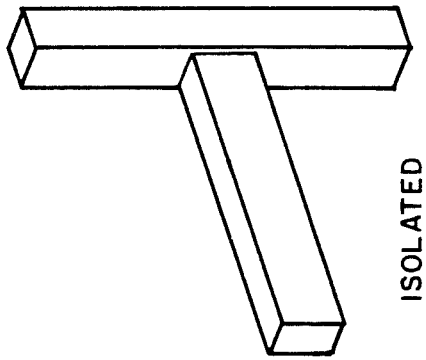
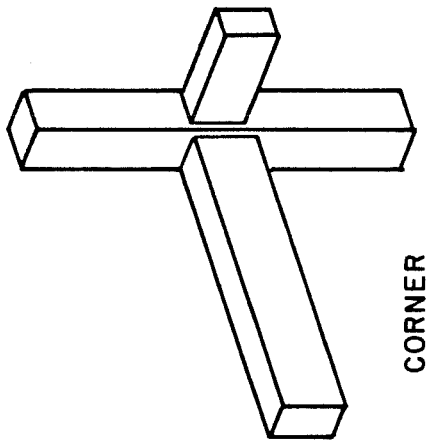
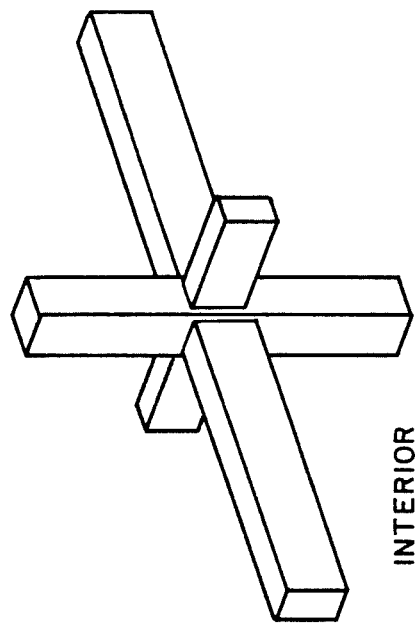
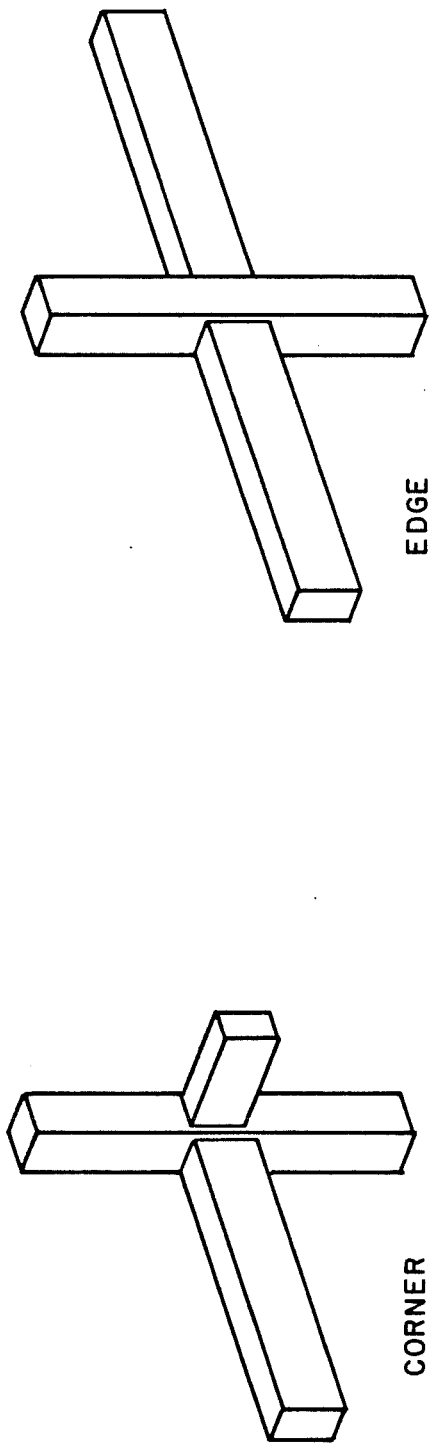
- To develop an approach to integrate the requirements for acceptable joint performance in moment resisting frames into the initial proportioning of the main structural members.

Chapter 2

Review of Past Research and Practice

2.1 Review of Past Research

A large amount of research has been carried out in the area of beam-column joints during the past 15 years mainly in the U.S. (UC-Berkeley, UM-Ann Arbor, and UT-Austin), in New Zealand (U. of Christchurch, U. of Auckland), in Canada (U. of Toronto), in the U.S.S.R. and in Japan. Some of the specimens used in these studies are shown schematically in Fig. 2-1. Unfortunately, the experimental data from Japan and the U.S.S.R. is not widely known because of it has not been translated into English. In Japan much of the research has been carried out by private construction companies and is not reported in the technical literature. A summary of most of the available data is found in Zhang and Jirsa [114], and is reproduced in Appendix F. All the tests to be discussed here refer to planar joint specimens loaded uniaxially unless otherwise specified.



INTERIOR TYPE

CORNER TYPE

Figure 2-1 : Specimens used in past research on beam-column joints

2.1.1 Research in the U.S. and Canada

The first studies in the U.S. on the behavior of beam-column joints were carried out at the U. of Illinois in the early 1950's by McCollister et al. [61], and in the early 1960's by Burns et al. [22]. Both of these studies were conducted on beam specimens with column stubs, and were aimed at determining the strength and ductility characteristics of beam-column joints.

The importance of proper detailing for these elements was not fully appreciated until the work of Hanson and Conner [41, 42, 43, 28] in the late 1960's. Those studies were aimed primarily at insuring the ductility of members using Grade 60 steel, and at finding suitable design methods for members under earthquake loads. Their studies consisted of 16 tests on exterior and interior joints, and the variables studied included column load, amount of joint reinforcement, and material properties. All the specimens failed flexurally in the beams, and showed that transverse joint reinforcement was necessary if the members were to perform satisfactorily. Detailing for shear, anchorage, and confinement were clearly the keys to satisfactory behavior. Hanson and Conner advocated extending the beam shear equations to beam-column joints since very little data was available on actual joints.

Additional data became available in the early 1970's through the work of Meinheit and Jirsa at the U. of Texas at Austin

[48, 49, 50, 51, 52, 53, 1]. A series of 14 full-scale joints were subjected to severe cyclic loads; the tests were aimed at defining the shear strength of the concrete in the joint area and developing realistic design recommendations. The main variables used were column load, joint reinforcement, lateral beam size, column size, load history, and concrete strength. Diagonal cracking in the joint occurred early in the load history and could be predicted by existing beam shear equations. However, the shear at diagonal cracking was found to be a poor indicator of ultimate joint shear strength. It was found that the ultimate shear strength of the joint was about twice that of its cracking strength, and that it was significantly different from that of a beam. The main factors affecting shear strength were found to be column load, joint reinforcement, and the restraining effect of lateral beams. An increase in any of these parameters resulted in higher shear strengths; the increase, however, was not linear. The main conclusion with regard to cyclic loading was that the contribution of the concrete to the shear strength decreased as cycling progressed. The joint reinforcement was unable to assume the additional load and the shear capacity decreased. On the basis of this test series new recommendations for joint design were developed by a Joint ACI-ASCE committee, and they will be discussed in Section 2.3.1 .

The work of Jirsa and Meinheit, which dealt with interior joints, was complemented by that of Uzumeri and Seckin

[105, 106, 89, 90, 91] at the U. of Toronto. They carried out a study of 17 exterior joint specimens, in which column load, joint reinforcement, and anchorage details were the main variables. It was clear from these tests that bond deterioration could lead to very unsatisfactory behavior. The anchorage of beam bars into exterior columns was clearly shown to be a problem since typical element dimensions did not allow for adequate anchorage. The tests pointed out that joints cannot be analyzed as rigid members, and that joint deformation is undesirable. It confirmed that the largest drop in shear strength and stiffness occurs between the first and second cycles at any deflection level, and that a conservative lower bound to stiffness and strength could be given by the envelope provided by the second cycle.

Most recently, work in this area has been conducted at UC-Berkeley by Bertero et al. [13, 96, 36, 107, 108, 10, 79, 80, 81], and at UM-Ann Arbor by Wight [29, 31, 88, 58, 59]. In the Berkeley tests, bond and anchorage in the joint region were shown to be the critical problems for beam-column joints, and it was clearly shown that slippage of the bars through the joint can cause very large concentrated inelastic beam rotations at the column faces. A joint model was derived from the test results, and a computer program (ZAP) [95] was calibrated to predict the behavior of beam-column joints subjected to earthquake loads.

With the exception of the some tests conducted by Bertero, most of the tests carried out in the U.S. have indicated some stiffness and strength losses with cycling. The prevalent view is that while stiffness and strength deterioration are undesirable, some must be allowed in order to keep the size of the joint and the volumetric shear reinforcement at practical levels.

2.1.2 Research in New Zealand

A large amount of research has been carried out in New Zealand, primarily by the group led by Park and Paulay [72, 77]. The focus of the research in New Zealand has been to develop and test design details to improve joint behavior, with the intent of obtaining joints with non-deteriorating stiffness and strength.

In one series at the U. of Canterbury , thirteen full-scale exterior and interior joints were tested. The main variables were the column load and the joint reinforcement details. The tests dealt with general behavior characteristics of exterior [87] and interior joints [82, 74, 75] and included consideration of joints in the elastic range [15] ; prestressed joints [16, 56]; the use of anchor blocks in exterior joints [62]; the relocation of plastic hinges away from the joint [21]; biaxially loaded interior joints [9]; and joints with low levels of axial load in the column [94].

All the studies showed that it is possible to detail joints

to perform well under extreme seismic loads. The keys to satisfactory behavior are maintaining the joint in an uncracked state as long as possible by partial prestressing, by low shear and bond stresses, and by providing sufficient joint reinforcement. Through the use of Grade 40 steel, small diameter bars, large anchorage lengths, mechanical anchors, etc., favorable bond conditions can be developed, and deterioration due to bond problems kept to a minimum.

The tests by Park and Paulay, and those conducted by Fenwick [33, 34] and Blakeley [16, 17, 18, 19, 20], have been the basis for the development of the requirements for joints now present in the N.Z. concrete code [97]. The tests were interpreted to indicate that the contribution of the concrete to the shear strength of the joint was uncertain when hinging occurred at the column face, and should therefore be disregarded in design. It was also shown that the use of details such as welding additional bars through the joint and welding anchor plates to the bars limit slippage of the bars and thus markedly decrease the loss of stiffness and shear strength .

2.1.3 Other Research

As mentioned before, a large amount of data concerning beam-column joints has become available due to work conducted in Japan. A good summary of this data can be found in Zhang and Jirsa [115]. The tests of Ohwada [70, 71] dealt mostly with the effect of

lateral beams, those of Hamada and Kamimura [39, 40] dealt with the applicability of the strut mechanism to joints, and those of Ishibashi [45, 46, 47] dealt with the effect of large reinforcement bars. The Japanese results confirmed the importance of adequate bond provisions as well as the importance of accounting for the lateral restraint effect provided by side beams. Other important research on beam-column joints has been carried out in Japan by Bessho [14], Higashi [44], Kokusho [57], Nakada [66], Ogura [69], Sekine [93], Tada [100], Minami [63, 64], Wakabayashi [109], and Yamaguchi [110, 111].

Additional research has been carried out by Bychenkov in the U.S.S.R. [23]; by Taylor [103], Swan [99] and Balint [8] in the U.K; by Calcerano [24] in Italy; by Nilsson [67] in Denmark; by Gavrilovic in Yugoslavia [38]; by Carvalho in Portugal [25]; by Tassios et al. in Greece [102]; and by researchers in the People's Republic of China [83].

Some analytical work has also been conducted in an effort to model beam-column joints and their deteriorating behavior. Among them the works of Riddel [84], Saiidi [86], Takizawa [101], Gates [37], Moss [65], Edgar [30], Soleimani [95], and particularly Fillippou [35] and Noguchi [68] represent the most successful attempts.

2.2 Shear Strength of Joints

2.2.1 Factors Affecting Joint Performance and Shear Strength

The research described in the previous paragraphs has led to the identification of the most important variables affecting shear strength of beam-column joints. Among them are :

1. The amount of joint reinforcement : It has been shown that transverse column hoops surrounding the joint core are necessary to maintain the shear strength capacity, or at least to decrease its rate of deterioration. The relationship is not linear, and there is evidence that there is an upper limit to the effectiveness of joint reinforcement.
2. The effect of lateral beams : Tests have shown that joints with lateral beams framing from the unloaded direction behave better than planar joints. It has been speculated that the larger the area of the joint covered by passive members, the larger the shear capacity of a joint.
3. The effect of column axial load : Originally this parameter had been thought to be very important in joint behavior. It has been shown, though, that the effect of axial load is not significant unless very large compressive stresses are present. Since most columns designed for earthquake resistance are generally loaded below the balance point, and possibly might go into tension if the drifts are large, this parameter has become less and less significant for design purposes.
4. The effect of anchorage : This is of particular importance for exterior joints, where hooks are needed to anchor the beam bars into the column. Adequate anchorage must be provided, since pullout of the hooks can constitute a failure mechanism for this type of joint. The case for anchorage can be extended to interior joints, where it is necessary to go from tension in one side of the joint to compression on the other over a very short distance. It can be shown that most joints designed today do not meet current development lengths requirements.

5. The bond conditions : This refers to the size and cover of the longitudinal reinforcement in the beams and column; the larger the bars used the more severe the bond requirements, and thus the longer anchorage length needed in the joint core.
6. The material properties : It has been observed that the higher the compressive strength of the concrete the higher the shear capacity of a joint , all other variables being equal. Once again, this is not a linear relationship and more work is needed in this area. The strength of the reinforcement is also important, since the use of Grade 40 steel can reduce the bond requirements significantly from those of Grade 60 steel.
7. Others : Some investigators [12] have proposed that geometric ratios, such as the depth of the beam vs. depth of the column or the beam bar diameter vs. the column depth are important parameters and should be considered when formulating codes.

To understand the importance of the variables, the mechanisms of shear transfer across the joint must be examined.

2.2.2 The Concrete Strut

Two main mechanisms have been proposed to account for the shear transfer across the joint. The first is labelled the "concrete strut" because a band of concrete carrying compression is formed between diagonally opposite corners of the joint. The joint shear corresponds to the horizontal component of that strut, see Fig 2-2. The formation of a strut depends on the presence of favorable end conditions, that is the presence of equilibrating compressive forces in the adjoining columns and beams. As shown in Fig.2-2, the orientation and size of the strut are hypothesized to depend on

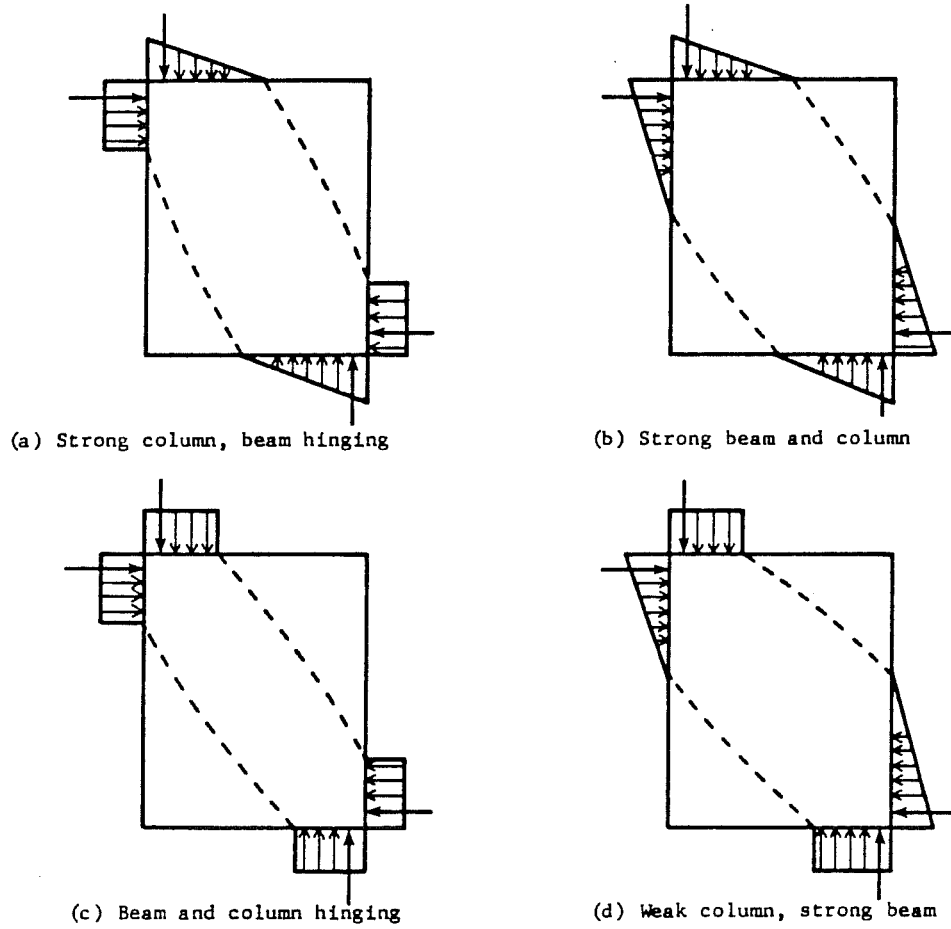


Figure 2-2 : The concrete strut mechanism

whether the beam or the column are hinging at any particular moment. It must be noted that when a beam yields or when the beam longitudinal bars slip, cracks form at the face of the joint; the width of those cracks will depend on the magnitude of drift of the structure. Conceivably, the cracks could be wide enough that they will not close instantaneously upon reversal of the load. Thus the compressive blocks shown on the beams would not be present at certain times during the load history and the efficiency of the strut mechanism could be impaired. The factors affecting the performance of a strut are the amount of joint reinforcement, the bond requirements, and whether the beams are hinging at that point in the load history.

2.2.3 The Panel Truss Mechanism

The other mechanism proposed for the transfer of shear across a joint is the panel truss mechanism, see Fig. 2-3. The panel truss mechanism was formulated to account for cracking of the concrete as the loading progressed; it was felt that when the concrete in the joint area cracked severely, a strut mechanism could not be sustained. In this case, shear must be transferred by a series of smaller inclined struts, which were held in place by the horizontal forces in the joint hoops and the vertical forces provided by additional vertical reinforcement. A major drawback of this theory is that it would seem to require the presence of vertical as well as

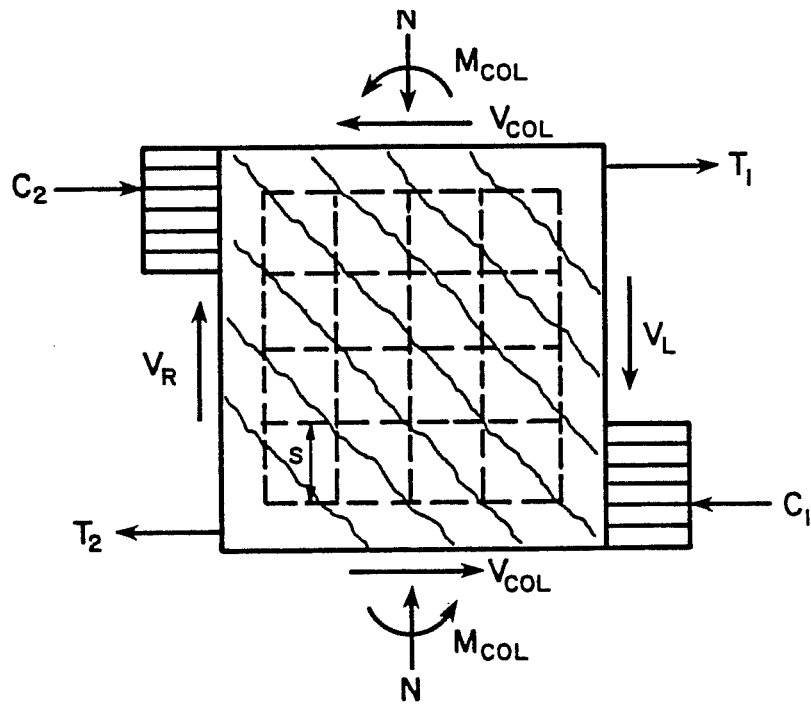


Figure 2-3 : The panel truss mechanism

horizontal hoops to confine the joint. It has been shown that the intermediate bars in the column can be used to provide this same function. The factors affecting this mechanism are the amounts of horizontal and vertical joint reinforcement , and the column axial load.

If the intermediate longitudinal bars in the column and the joint hoops in the joint can be counted to form a small truss mechanism, the main longitudinal reinforcement in the beams and column will also be able to act as a truss. It is very hard, if not impossible, to separate this contribution to joint shear strength. In the past investigators have disregarded this additional truss mechanisms, whose contribution can be very large if the joint reinforcement is small and the longitudinal beam and column reinforcement is large.

Both the concrete strut and the panel truss mechanism are feasible in a joint loaded by seismic forces, and probably the two mechanisms work together to transfer the horizontal shear load across the joint. Efforts to isolate the contribution of each have not proved successful for two main reasons. The first is the lack of a reliable technique for measuring concrete strains, particularly strains in the confined core or on the cracked surface of the concrete. The second has to do with limited ability to differentiate between the levels of strains in the joint reinforcement due to axial

extension created by horizontal shear and those due to local bending created by bulging of the joint core. Thus the contributions of the steel and the concrete to the shear strength of the joint are not clear.

It should be noted, however, that the large differences in the design procedures to be examined next stem from the different emphasis given to these mechanisms. The New Zealand tests, with their excellent bond conditions, show no significant slip or bond deterioration. If no bond deterioration is present, and if the amounts of top and bottom steel present in the beams is unequal, it is possible that the cracks at the joint-beam interface might not close completely when the loads are reversed. Thus the steel in the beams might go from yielding in tension on one side to yielding in compression on the other. In this case the beam compressive blocks are not present, and the efficiency of the concrete strut mechanism is impaired; thus, the New Zealand design procedures require large amounts of joint transverse steel so that a truss mechanism able to carry the full shear load can be developed. The U.S. and Canadian tests, on the other hand, show some bond deterioration and some bar slip. As these phenomena become more important, the concrete strut begins to dominate over the truss mechanism, particularly if the amounts of transverse joint reinforcement are small. Thus the emphasis in the U.S. is on design procedures based on a concrete strut model to carry large portions of the shear. These differences

must be kept in mind when making comparisons between the different design procedures to be described next.

2.3 Current Design Procedures

Only recently have provisions for the design of beam-column joints been incorporated into design recommendations or building codes. The best known of these are the ACI-ASCE Committee 352 recommendations [2, 7], the ATC3-06 proposal [6], and the New Zealand Standard [97]. Additionally, Meinheit and Jirsa [50] in the U.S. and Sugano and Koreishi [98] in Japan have proposed other design approaches. New guidelines for the design of joints will also be incorporated into the revised Appendix A to appear in the next edition of the ACI code [3, 4, 5]. The C.E.B. [27] provisions are very similar to those present in the new New Zealand code. Each of these procedures will be reviewed briefly.

2.3.1 The ACI-ASCE Committee 352 Method

To determine joint shear strength a beam shear analogy is used. The shear contributed by the shear reinforcement may be developed from the truss analogy. Assuming that a diagonal crack (at about 45 degrees) extends through the joint, the transverse column reinforcement crosses the crack as it would in a beam . The required contribution of the transverse reinforcement can then be easily calculated. The contribution of the concrete is assumed to be equal

to the shearing force causing diagonal cracking, and the total shear strength is the algebraic sum of these two contributions. The equations for the concrete shear strength have been modified to fit the data available from beam-column joint tests as follows.

$$v_j = V_j / bd = v_s + v_c$$

where,

- b = width of the compression face of the column acting in the plane of the joint
- d = distance from the extreme compression fiber to the centroid of the tension steel in the column

The shear strength assigned to the concrete is

$$v_c = 3.5 \beta \gamma \sqrt{f'_c} (1.0 + 0.002 N_u / A_g) \text{ (psi)}$$

where,

- β = factor reflecting the severity of the loading. Equal to 1.4 for normal joints and 1.0 for seismic joints
- γ = factor reflecting the effect of perpendicular confining beams. Equal to 1.4 if the beams cover over 75% of the width and depth of both joint faces; otherwise equal to 1.0
- f'_c = concrete compressive strength, psi
- N_u = magnitude of factored column axial load, lbs
- A_g = gross area of the column, in²

The shear resistance assigned to the steel is

$$v_s = A_{sv} f_y / bs < 15 \sqrt{f'_c}$$

where

- A_{sv} = area of steel crossing a shear crack within a distance s , in²
- f_y = yield strength of the steel, psi
- b = width of the column framing into the joint , in
- s = vertical spacing of the reinforcement, in

An upper limit on total joint shear stress is applied as

$$v_j = v_c + v_s < 20 \sqrt{f'_c}$$

A substantial review of these provisions has been proposed in a new draft of the ACI-ASCE Committee 352 recommendations currently under study. In these new provisions, the total shear strength would not be proportioned between the concrete and the steel. Rather, a minimum amount of joint shear reinforcement would be required, as given by :

$$A_s = [0.3 s_h f'_c h'' / f_y] [(A_g/A_c)-1.0]$$

or,

$$A_s = [0.09 s_h f'_c h'' / f_y]$$

where

- s_h = spacing of the hoops , in.
- h'' = depth of the column, in.
- A_g = gross area of the column, in.²
- A_c = confined area of the column, in.²
- A_s = required transverse steel in the joint, in.²

The transverse reinforcement would have to be closely spaced (4. in or less), and be continued above and below the joint for a distance at least equal to the greatest of 18 in., one-sixth the clear height of the column, or the maximum column dimension. In addition, the maximum longitudinal bar size would be controlled by :

$$h_{\text{column}} > 20 d_{\text{beam bar}}$$

or

$$h_{\text{beam}} > 20 d_{\text{column bar}}$$

The minimum anchorage lengths for hooked hooked bars within in the joint by :

$$l_{dh} > [\phi f_y d_{\text{beam bar}} / 65 \sqrt{f'_c}]$$

The total shear through the joint would be limited to within

$$V_j < \alpha b d \sqrt{f'_c}$$

where α = 12 for corner, 15 for exterior, and 20 for interior joints. Thus the emphasis in the revision to the ACI-ASCE 352 report is shifted from a more complex and realistic approach that assigns

some shear to the steel and to the concrete, to a simpler and design-oriented procedure requiring some minimum transverse reinforcement and nominal joint shear stress level criteria to be satisfied.

The revisions to the ACI-ASCE Joint Committee 352 report are similar to the provisions that will appear in Appendix A of the new ACI Code [5]. This Appendix A requires that:

$$\phi M_{n,col} > 1.2 M_{n,beam}$$

and requires the same minimum amount of transverse steel in the joint as those given by the ACI-ASCE 352 report. The nominal shear stress is limited to $15 f'_c$ for unconfined joints and $20 f'_c$ for confined ones. Confinement depends on whether all faces of the joint are covered with framing members for at least 75% of their area.

2.3.2 The ATC3-06 Approach

The recommendations of the "Tentative Provisions for the Development of Seismic Regulations for Buildings" (ATC3-06) are based on an equation for ultimate shear strength developed by Jirsa and Meinheit [50], as follows :

$$V_u = 5.1 \beta S (f'_c)^{2/3} \text{ (psi)}$$

where

$$- \beta = 1 + 0.25 [W_L / h_c]$$

$$- S = 1 + 6p_s$$

- W_L = width of lateral beam perpendicular to applied shear
- h_c = width of the column into which lateral beams frame
- ρ_s = volumetric percentage of joint hoop reinforcement

In this equation, the importance not only of the concrete and steel contributions but also the effect of framing beams is recognized.

The ATC3-06 document requires that the column transverse reinforcement be continued through the joint to provide adequate confinement and shear reinforcement. It provides an upper limit for joint shear stress such that :

$$v_u = V_u / \phi b d = V_u / 0.85 b d < 16\sqrt{f'_c}$$

is the limit for joints confined by members on all sides, while a 25% reduction in capacity is necessary if the joint is unconfined by beams. For this procedure, minimum volumetric shear reinforcement would range from 0.6% to 1.2% for spiral reinforcement and 0.8% to 1.2% for rectangular hoop reinforcement. The ATC3-06 approach typically will result in less shear reinforcement than specified by the old ACI-ASCE Committee 352 report.

2.3.3 The New Zealand Standard

The New Zealand Standard recognizes two types of joints, and approaches each separately. This differentiation is based upon the experimental work conducted by Park and Paulay, and separates joints designed to remain essentially elastic from those where hinging adjacent to the joint is acceptable.

When the joints remain "elastic", a large amount of the shear is allocated to the concrete, and the remainder to the steel reinforcement. The shear is allocated as follows

- if the column load is higher than $0.1f'_c/C_j$,

$$V_{ch} = 2/3 \left((C_j P_e / A_g) - (f'_c / 10) \right)^{0.5} b_j h_c$$

- if no plastic hinges can be formed next to the joint face,

$$V_{ch} = 0.5 (A'_s / A_s) V_{jh} (1 + \{C_j P_e\} / 0.4 a_g f'_c)$$

- if the joint is prestressed

$$V_{ch} = 0.7 P_{cs}$$

where

- $C_j = V_{jh} / [V_{jx} + V_{jz}]$
- V_{ch} = horizontal shear resisted by concrete, N
- V_{jx} = horizontal shear in x-direction, N
- V_{jz} = horizontal shear in z-direction, N

- P_e = maximum design axial load in compression, N
- A_g = gross area of section, mm^2 .
- f'_c = compressive strength of the concrete, MPa
- b_j = effective width of joint, mm.
- h_c = overall depth of column in the direction considered, mm.
- P_{sc} = force after all losses in the prestressing in the middle third of the beam, N

If the joint is designed such that beam hinges can form at the column faces, the concrete is not assigned any of the shear load. All of it is taken by the steel. To prevent early stiffness and strength deterioration, the following limit is imposed on total shear,

$$V_{jh} < 1.5\sqrt{f'_c} \quad (\text{MPa units})$$

If none of the conditions mentioned above with regard to elastic joints is met, the entire shear force is to be taken by the steel as follows

$$A_{jh} = V_{sh} / f_y$$

Vertical joint shear reinforcement is also required to take care of the vertical forces needed to maintain a panel truss mechanism.

2.3.4 The Japanese Design Procedure

While the Japanese code for reinforced concrete design is based on working stress rather than ultimate strength, and no provisions for joint design are present in the codes, the work of Sugano and Koreishi [97] must be noted. After a series of experiments at the U. of Tokyo, they proposed a design procedure for joints based on ultimate strength. They assigned contributions to both the steel and the concrete as follows,

$$v_c = 0.51f'_c - 0.001f'_c{}^2 \quad (\text{kg./cm}^2)$$

$$v_s = 2.7 (r_w f_y)^{1/2}$$

for f'_c less than 6000 psi, where

- $r_w = A_s / b s$
- b = width of the column, cm.
- s = spacing of the hoops, cm.
- A_s = total area of hoop reinforcement, cm^2 .

Sugano and Koreishi also make a distinction between cracking and ultimate strength. For cracking the following expression was proposed :

$$v_{cr} = (f_t^2 + f_t(P_u/A_g))$$

- f_t = tensile strength of concrete, kg/cm^2
- P_u = column load, kg.
- A_g = gross column area, cm^2

2.3.5 Comparison of Design Methods

In comparing the first three design procedures discussed above, the background to each is important. The ACI-ASCE Committee 352 design procedures are based on tests carried out on reinforced concrete members subjected to axial loads. Most of these tests, therefore, were not on joints but on members with quite different shear spans from the aspect ratios of joints. Since in a typical joint the column depth is approximately equal to the beam depth, the applicability of the results of tests with shear spans in excess of 2.0 is questionable. In the New Zealand Standard, the concrete is assumed to carry no shear unless strict requirements are met. However, Zhang and Jirsa [113] state that :

By checking 19 specimens available from the U.S., Japan, Canada, and New Zealand, which had volumetric percentages of joint transverse reinforcement less than 1%, a lateral or no lateral beam, and with hinges at the column face, it was observed that the average shear carried by the joint under cyclic loading is about 66% of that under monotonic loading. The ratios of the value of shear strength at the worst peak under cyclic loading to the test value of shear strength at maximum peak after yielding under monotonic loading were distributed from 0.40 to 0.90 (See Fig.2-4). This indicates that even under cyclic loading concrete in joints can make a contribution to the shear capacity... Accordingly, the shear resistance of the concrete as a diagonal strut in the joint core need not be ignored in design [113].

The provisions of the ATC3-06 document seem to assign more shear to the concrete than other methods, but it must be remembered that by limiting the total allowable shear, the size of the column may have to be increased. The resulting shear stress levels will not

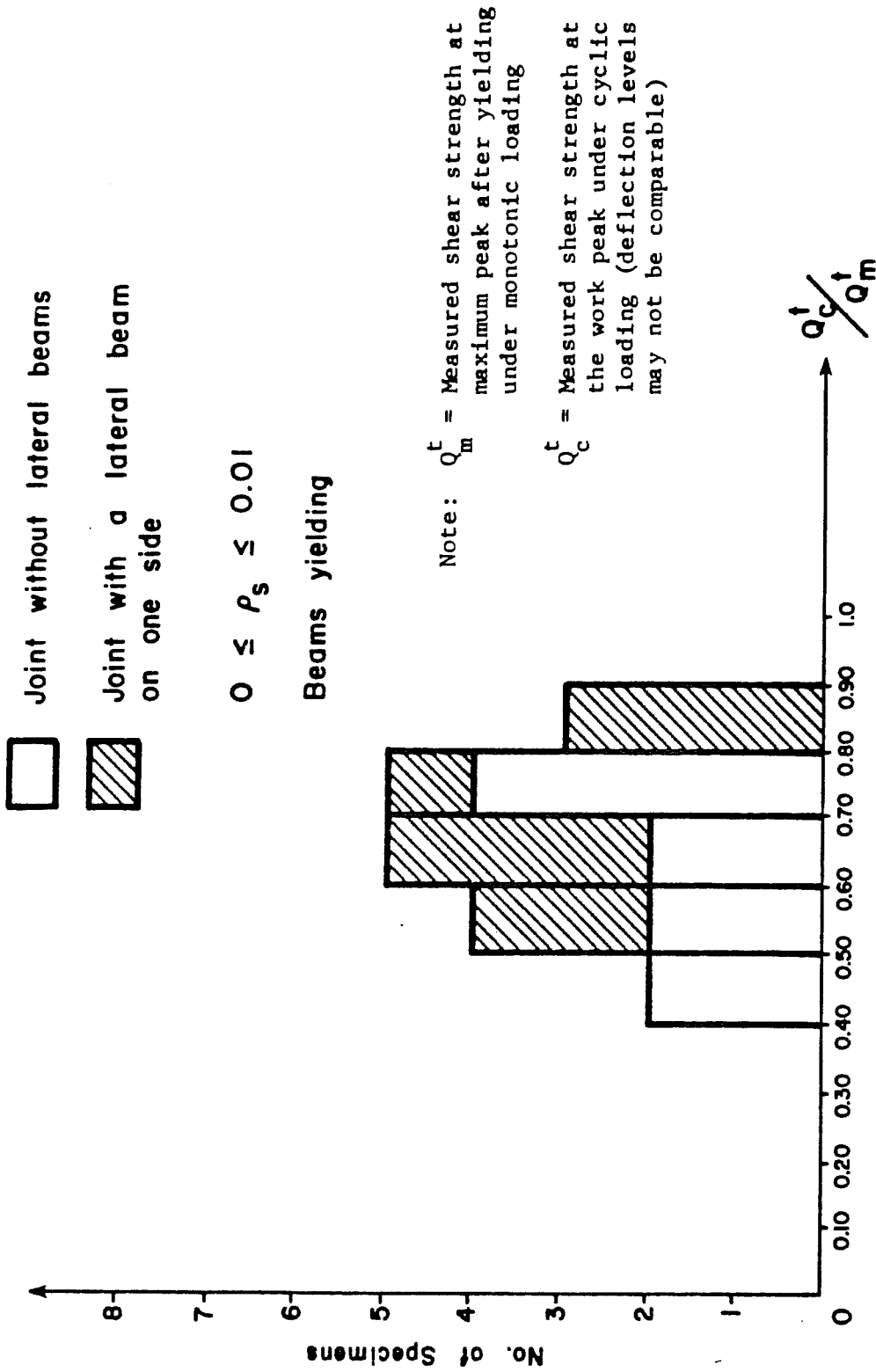


Figure 2-4 : Contribution of the concrete strut mechanism (110)

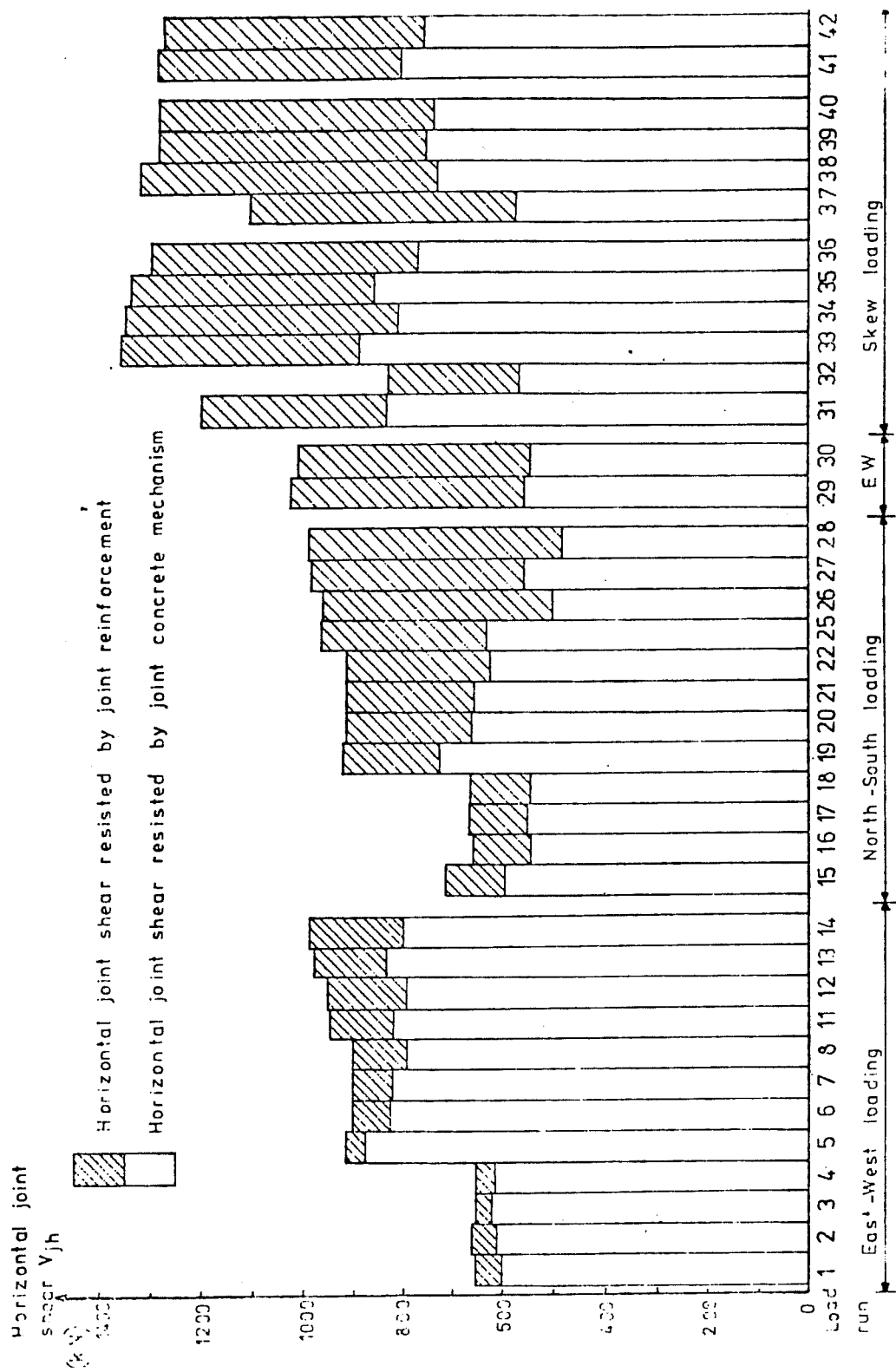


Figure 2-6 : Contribution of the different mechanisms to joint shear resistance (9)

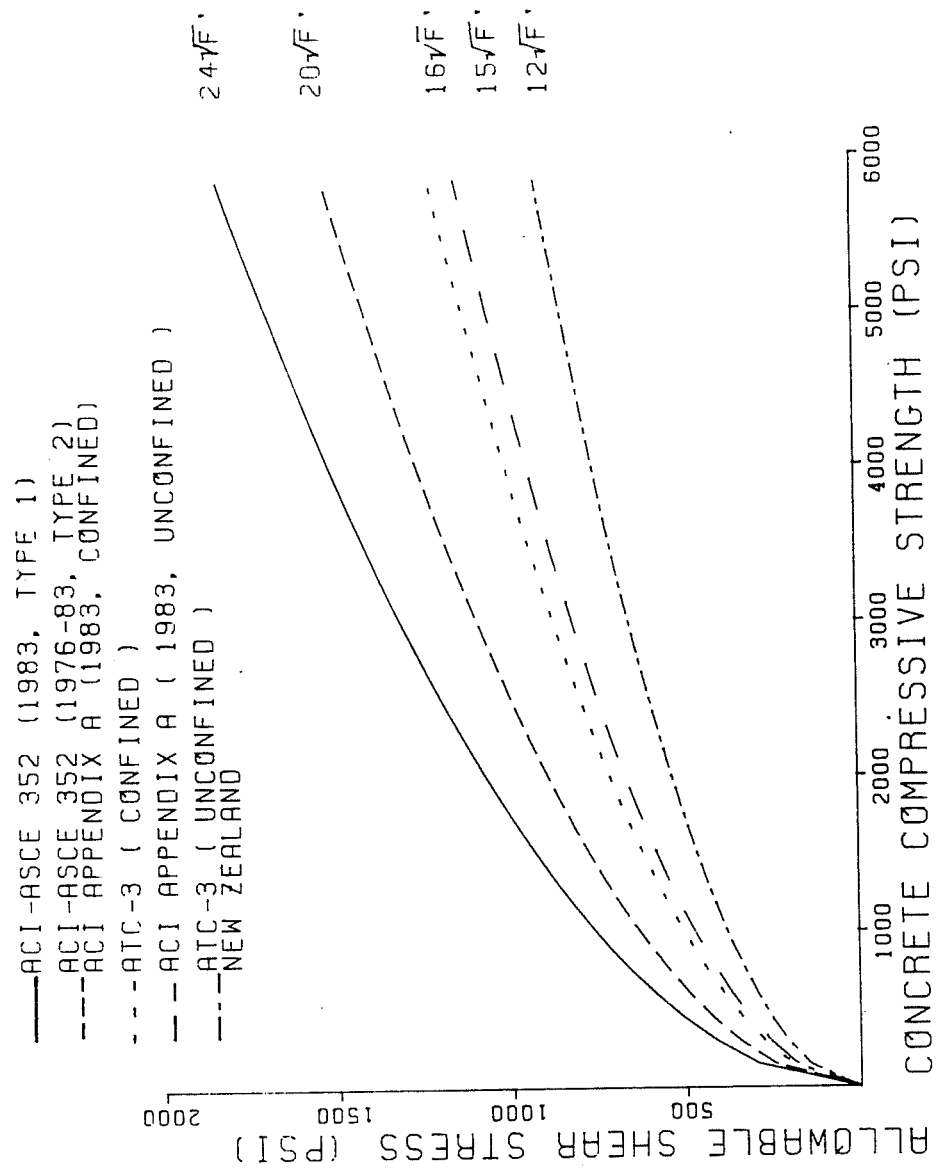


Figure 2-5 : Allowable shear stresses under current codes

x

be very different from those of of the Committee 352 recommendations. One can conclude that the New Zealand approach provides maximum reinforcement for the joint, while the ATC3-06 document suggests a minimum. The ACI-ASCE Committee 352 recommendations provide a compromise between these two extremes. A comparison of the maximum shear stress allowed under all methods is shown in Fig. 2-5.

It should be noted that the cracking joint shear strength for beam-column joints is on the order of 7 to $10\sqrt{f'_c}$, with the higher values associated with large transverse joint reinforcement ratios. Thus the limits imposed by the New Zealand Standard would imply much less joint shear cracking than the ACI-ASCE 352 procedures would allow. Thus one would expect the procedures that allow nominal joint shear stresses greater than about $15\sqrt{f'_c}$ to imply some degree of joint shear distress, and consequently some loss of stiffness and strength with cycling.

It is difficult to compare the amount of shear assigned by each procedure to the steel and the concrete. For example, for a typical interior joint with hinges next to the column face the New Zealand Standard will assign all the shear to the steel; the ATC3-06 procedure would require about an 0.8% volumetric reinforcement ($f'_c=4000$ psi and $f_y= 60$ ksi); and the ACI-ASCE Committee 352 would assign about 300 psi to the concrete and the rest to the steel.

Attempts to quantify the contributions of the steel and concrete to the overall shear strength have not been very successful. One such attempt is shown in Fig. 2-6. It comes from a New Zealand test [9], and shows that the concrete strut mechanism contributed as much as 60% to 80% of the total strength even at very large deformations and after a large number of cycles. The contribution of the concrete strut is higher at the peaks than at the intermediate load stages, and one would expect, based on the work of Zhang [114], that the concrete contribution should be about 50% to 70% at these stages.

2.4 Limitations of Past Research

Several limitations of past research must be noted. First, there is an absence of tests in which joints were loaded biaxially. Because of economic and physical constraints, all but one of the test series [9] were carried out on planar joints loaded uniaxially. In some cases stub beams were used to simulate members framing perpendicularly, but they were never loaded. In a real earthquake a structure would likely be loaded in some direction which does not correspond with the principal structural axis, and thus the joints would be loaded biaxially. There is little or no information on the strength of joints under this loading condition and few design recommendations have been proposed.

The second limitation is a lack of data regarding the influence of the size of the member producing the shear on the joint behavior. Except for the ACI-ASCE Committee 352 recommendations, the effect of wide or narrow beams framing into the joint has not been addressed. Most of the research has been carried out on specimens with beam widths close but smaller than the column width. Thus data regarding the influence of beam width is needed.

A third limitation is the lack of uniformity in the loading histories used by different investigators. Comparisons among test series are difficult and often impossible. In many cases test specimens have been subjected to many small cycles of deformation before the peak strength is reached. The effect of the smaller cycles on the ultimate strength is unknown.

A fourth limitation is that the large losses of stiffness reported from many tests have not been adequately studied. Thus, while the joint might be able to carry the shear input from the beams, the loss of stiffness due to yield penetration and bond deterioration can represent a separate failure mechanism that has not been adequately investigated.

In most past research the specimens tested did not have a slab. In typical cast-in-place construction, beams, columns and slabs are cast simultaneously and therefore act as a single structural

unit. There is very little data on the effect of the slab on overall joint behavior.

Several other aspects of the behavior of joints have not been clarified by past research. Among them are the upper and lower limits of transverse reinforcement necessary for good behavior; the anchorage requirements for beam bars in exterior joints; and the effect of axial load on the deterioration of joint strength and stiffness.

Chapter 3

Experimental Program

3.1 Test Series Description

To study the main parameters affecting the shear strength of beam-column joints a test series comprising 15 full-scale tests was devised, utilizing the subassemblages shown in Fig. 3-1. This report deals with the last eight tests only, but a summary of the test series, shown in Table 3-1, is important to understand the scope of the project. The first three tests were conducted on identical specimens and were aimed at clarifying the effect of load history. Specimen BCJ1 was loaded uniaxially, and was the control specimen for the following two biaxially loaded specimens. In test BCJ1 racking deformations were applied only to the North-South beams, while the East-West beams were held at a constant dead load deflection. Specimen BCJ2 was cycled simultaneously in both the North-South and East-West directions, simulating the condition where lateral forces are skewed at a 45 degree angle from the building's principal axis. Specimen BCJ3 was also loaded biaxially, but in this case the deformations were applied alternately to the North-South and East-West beams. For example, the North-South beams were cycled once while

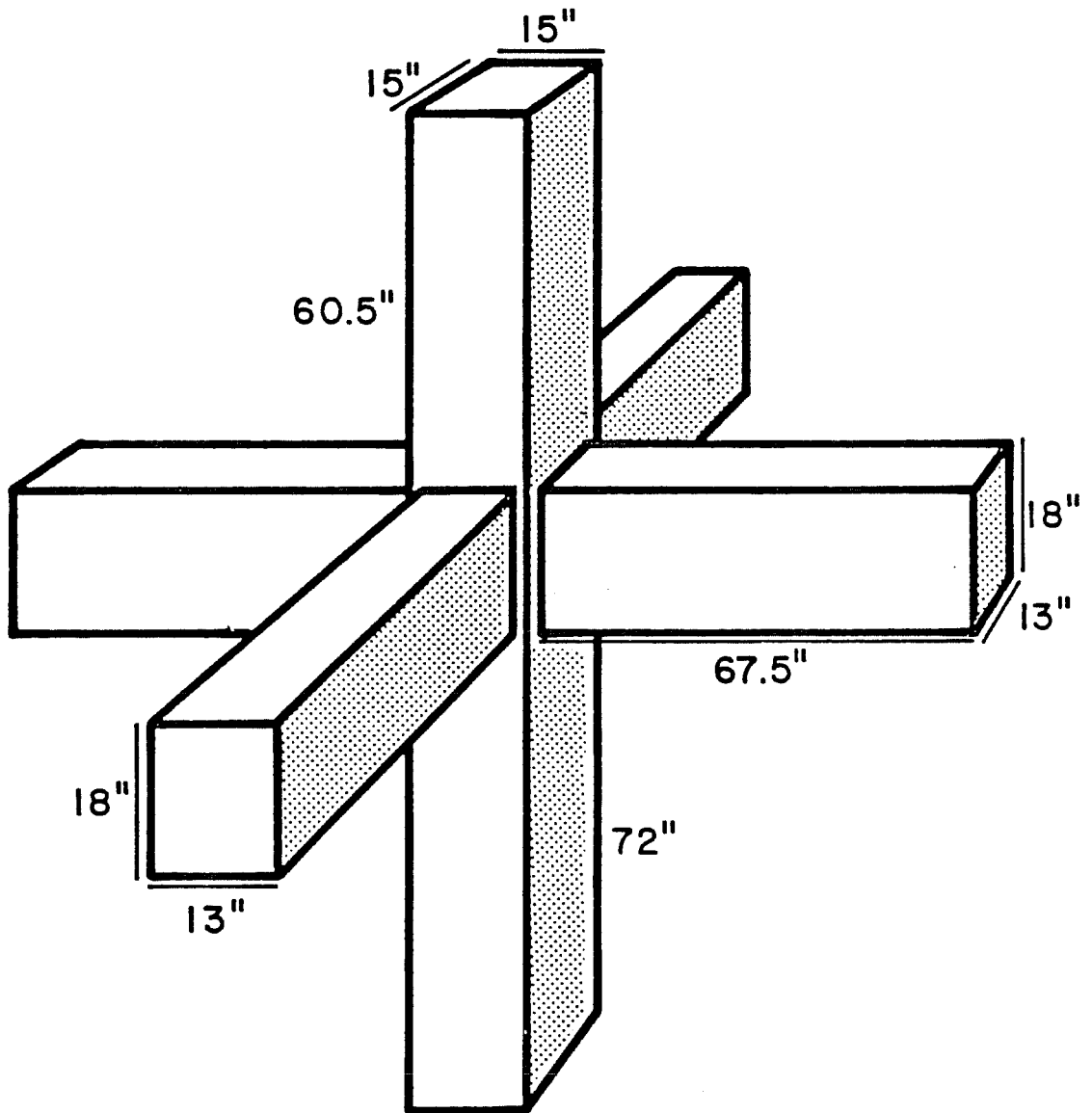


Figure 3-1 : Dimensions of beam-column subassemblages

Test	Column	Reinforcement		Load	Purpose
		Beam Neg.	Beam Pos.		
BCJ1	12 # 9	3 # 10	3 # 8	UC	Uniaxial
BCJ2	12 # 9	3 # 10	3 # 8	BS	Biax. Sim.
BCJ3	12 # 9	3 # 10	3 # 8	BA	Biax. Alt.
BCJ4	12 # 9	2 # 10	2 # 8	BS	Bar number
BCJ5	12 # 9	3 # 8	3 # 6	BS	Bar size
BCJ6	12 # 9	3 # 8	3 # 6	MS	Biax. Mon.
BCJ7	12 # 9	3 # 8	3 # 6	BS	Joint rein.
BCJ8	12 # 9	3 # 8	3 # 6	BS	P(col) = 0
BCJ9	12 # 9	3 # 8	3 # 6	BS	Slab
BCJ9A	12 # 9	3 # 8	3 # 6	BS	Slab
BCJ10	12 # 9	3 # 8	3 # 6	BS	Wide beams
BCJ11	8 # 11	2 # 10	2 # 8	Bs	Narrow beams
BCJ12	12 # 9	3 # 8	3 # 6	BS	Wide beams
BCJ13	12 # 9	3 # 8	3 # 6	BS	Exterior
BCJ14	12 # 9	3 # 8	3 # 6	BS	Ext. w/slab

Loading - UC = Cyclic uniaxial
 BS = Cyclic biaxial simultaneous
 MS = Monotonic biaxial simultaneous
 BA = Cyclic biaxial alternate

Dimensions - All columns 15 in. by 15 in.
 All beams 13 in. by 18 in.,
 except BCJ11 8.75 in. by 18.0 in.
 BCJ10 18.0 in. by 18.0 in.
 BCJ12 18.0 in. by 18.0 in.

Joint Reinforcement - all units had 2 # 4 ties at 5 in. in the joint,
 except BCJ7 which had 10 # 4 ties grouped as
 5 sets of double ties at 2.5 in.

Table 3-1: Summary of test series

the East-West beams were held at the dead load position, and then the East-West beams were cycled while the North-South were held in the dead load position. For both specimens BCJ1 and BCJ3, the failure occurred in the joint area, while for specimen BCJ2 a column failure was observed. Since a column failure was considered undesirable, a redesign of the specimen was necessary in order to conduct the remaining tests under a biaxially simultaneous loading.

In order to increase the capacity of the column with respect to the beam, the amount of beam reinforcement was decreased in the following two specimens. In specimen BCJ4 the beam reinforcement was decreased by 1/3 to two # 10 at the top and two # 8 at the bottom; in specimen BCJ5, the bar configuration was changed to three #8 at the top and three #6 at the bottom. The total areas of steel, however, were not significantly different for these two tests. A direct comparison of bond characteristics between specimens BCJ2, BCJ4, and BCJ5 was possible. Test BCJ6 was similar to specimen BCJ5 but the load was applied monotonically to establish an envelope for the shear deformation relationships and to compare with the cyclic response. In test BCJ7, the amount of shear reinforcement in the joint was increased substantially, from two #4 ties to ten #4 ties, in order to check the effectiveness of additional steel in the joint.

For the second part of the project it was decided to test specimens with slabs to model frame structures more accurately. In

order to facilitate testing, it was decided to remove the axial load from the column since maintaining column loads would have meant significant changes in the testing frame. Specimen BCJ8 was the control specimen for this series, and its behavior will be discussed in detail in Chapter 4. This specimen can be compared directly with BCJ5, to examine the effect of axial load. Specimens BCJ9 and BCJ9A were identical specimens with an octahedrally-shaped slab large enough to simulate the effect of a floor slab on the joint.

The test series continued with tests on specimens having different size beams; specimen BCJ11 had very narrow (8.75") beams, and specimen BCJ12 had very wide (18") beams compared to the 13 in. beams used in the other specimens. These tests were run using an axial load and are directly comparable to BCJ5. Specimen BCJ10 also had large beams but because of problems during the casting, it only achieved a compressive strength of 2800 psi, as opposed to an average of about 4500 psi for all the other specimens. Comparisons between BCJ10 and BCJ12 give an indication of the effect of concrete strength.

The last two tests were conducted on exterior joints, since no data is available on the performance of such joints under bidirectional loading. Both tests were conducted without axial load. Specimen BCJ13 had no slab while BCJ14 did. The behavior of the exterior joint with no slab could be compared directly to that of

specimen BCJ8, while that of the exterior joint with the slab can be compared to that of specimens BCJ9 and BCJ9A.

3.2 Specimen Design

The beam-column specimens in this series were specifically designed so that the joint core strength would be the controlling factor. The design of all the specimens was based on the equations proposed by Meinheit and Jirsa for shear strength. It was anticipated that the specimens would exhibit severe shear strength deterioration as well as bond degradation.

The specimen was also designed to have proportions similar to those typical of joint elements in reinforced concrete multistory buildings. The specimen extended to the midstory height above and below the joint, based on the assumption that a point of contraflexure occurs at that point. This is a common assumption in frame design, and is valid for upper story columns. The point of inflection in the bottom story columns will most likely be much nearer the joint than the midstory height.

The dimensions of the test specimen used are shown in Fig. 3-1, and the design calculations are included in Appendix B .

3.3 Specimen Details

As previously mentioned, the specimens were designed in order to maximize the shear input into the joint while maintaining a reasonable specimen size and proportions. The resulting specimen has a much larger column longitudinal reinforcement ratio than commonly used in frames in seismic areas. The beam lengths were kept to about 6.5 ft. on each side of the subassemblage for practical reasons; this would correspond to a column spacing of 13 ft., smaller than the 20 ft. to 24 ft. spacing that the beam size would indicate for a typical frame.

3.3.1 Beam and Column Details

All specimens had 15 in by 15 in. columns reinforced with 12 #9 bars, giving a reinforcement ratio of about 5.33%. This very large reinforcement ratio was needed to obtain the necessary column flexural capacity without affecting the proportions of the beam-column joint. The uniaxial interaction diagram for the column is shown in Fig 3-2, while the biaxial interaction diagram for the case of zero axial load is shown in Fig 3-3. It was observed that due to the severity of the loading, crushing of the concrete at the corner of the column was possible. Crushing and spalling of the cover results in a much smaller capacity and can lead to column yielding, as observed in several tests. The column shear reinforcement consisted of closed #4 ties spaced at 4 in. through the column and at

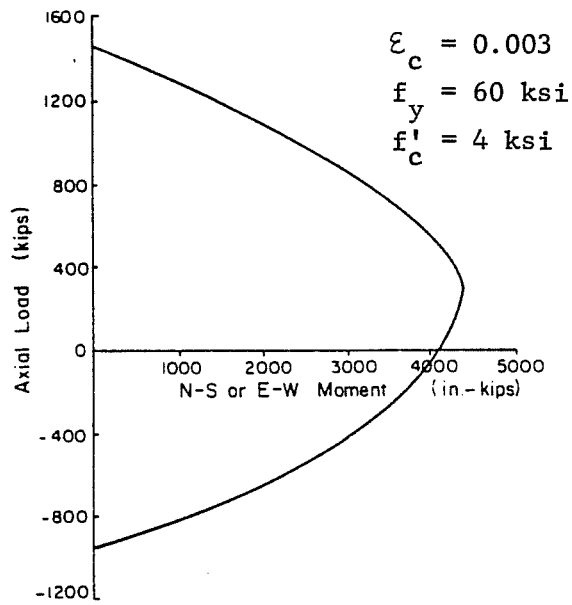


Figure 3-2 : Interaction diagram for BCJ column

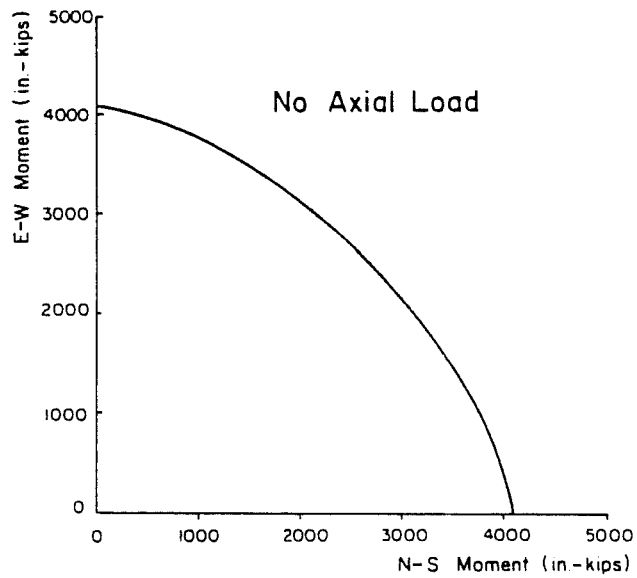


Figure 3-3 : Biaxial interaction for BCJ column

5. in. in the joint area. The ties were closed by 135 degree hooks having legs with development lengths of 10 bar diameters as recommended by the SEAOC Code [91]. No intermediate ties or crossties were used, and a 1.5 in. nominal cover was employed. The details of the beam and column are shown in Fig 3-4 .

The typical beam size for all the specimens was 13 in. by 18 in. The exceptions were tests BCJ10 and BCJ12 which had 18 in. by 18 in. beams, and test BCJ11 which had 8.75 in. by 18 in. beams. For the specimens described in this study, the typical beam had 3 #8 bars at the top and 3 #6 bars at the bottom; the only exception was test BCJ11 which had 2 #10 at the top and 2 #8 at the bottom. Crossing of the beam steel at the joint required the placement of the North-South reinforcement above the East-West , resulting in a slight increase of positive moment capacity and a decrease of negative moment capacity of the East-West direction with respect to the North-South one. Shear reinforcement for the beams consisted of #3 closed stirrups spaced at about 4 in. beginning about 2 in. from the column face. The cover was 1.5 in. and the spacing between beam bars was 2.2 in., see Fig. 3.4 .

The slab, as tested, had an average thickness of 3.75 in. and was reinforced at the top only with #3 bars; the slab bars did not have hooks at either end of the bar and were spaced at 12 in. beginning at 6.0 in. from the column face.

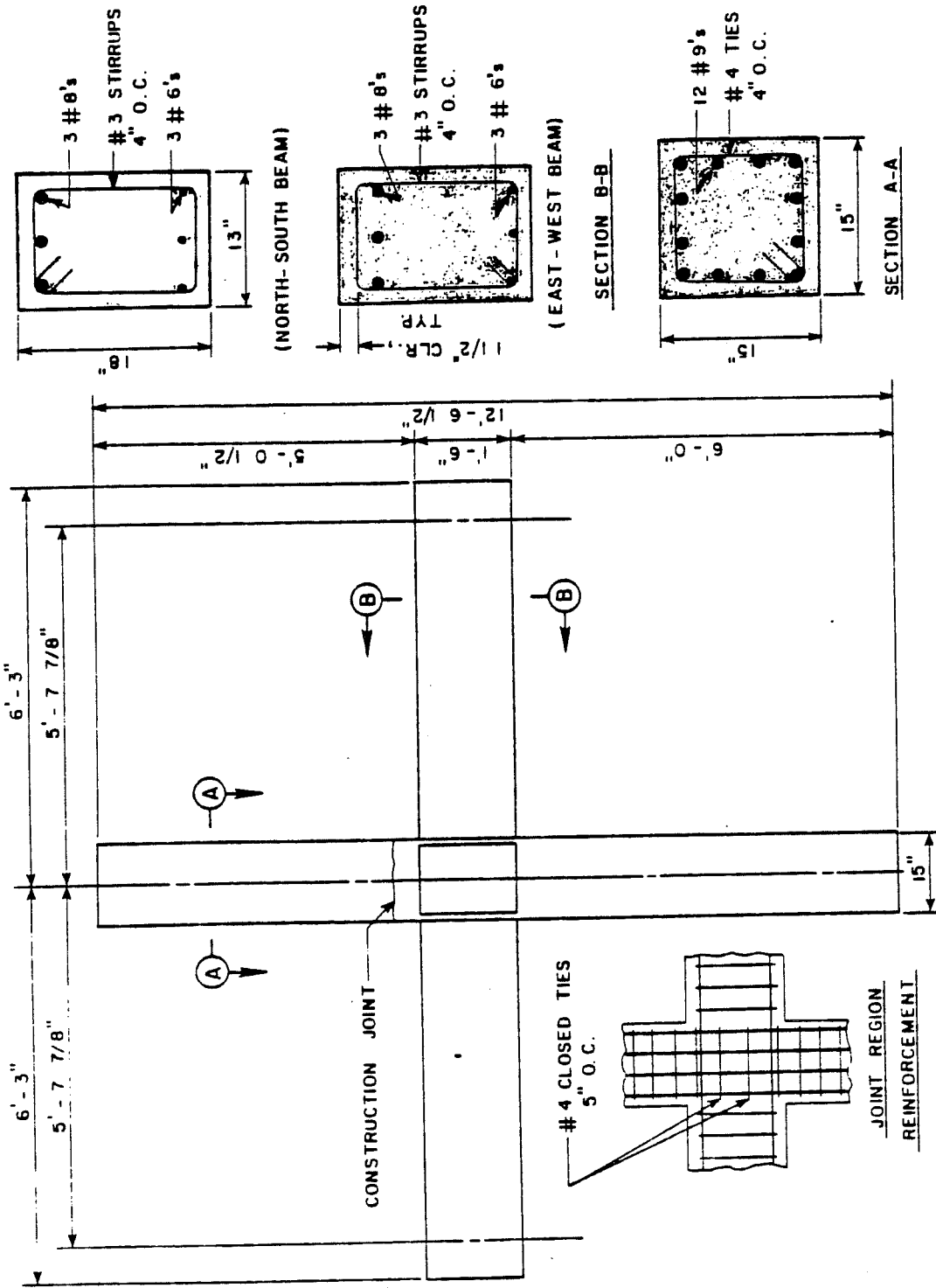


Figure 3-4 : Beam and column details for BCJ series

3.3.2 Specimen Fabrication

Fabrication of each specimen consisted of instrumenting the desired steel bars, tying the beam and column cages, placing them securely in the forms, attaching the instrumentation reference inserts, placing the concrete and curing the specimen.

The lower column cage was fabricated first and lowered into the forms; four bolts were inserted at the bottom of the column cage to provide the connection to the testing frame. Then the beam cages, along with the two joint ties, were lowered into position. At this stage the concrete in the bottom column, beams, slab, and 4 in. of the upper column was cast. Approximately a week later the specimen was removed from the forms, the ties in the upper column placed and the upper column cast [60].

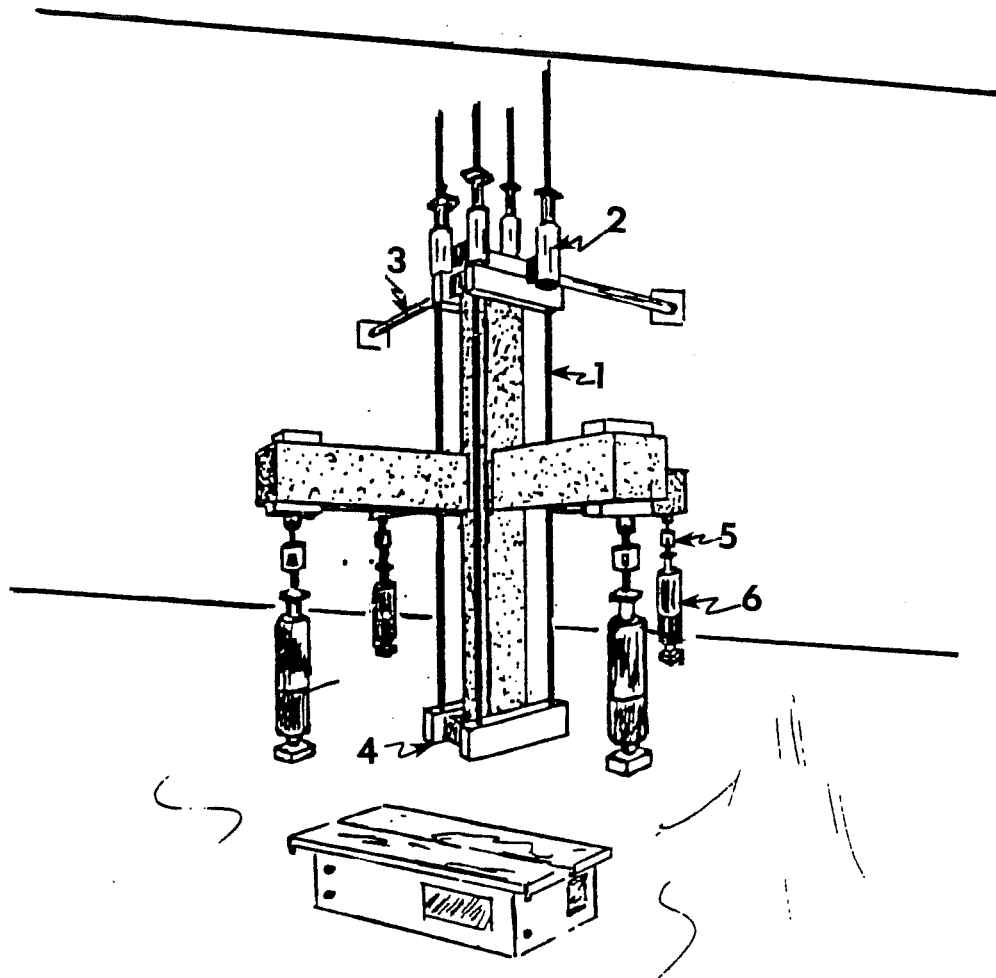
3.3.3 Material Properties

Although an effort was made throughout the test series to maintain uniform material properties, this was not always possible. The desired concrete compressive strength was 4500 psi, and it was successfully achieved for most of the lower specimen casts. Since the bottom cast included the joint, it was felt that the larger compressive strengths achieved in the top casts did not significantly affect the specimen behavior. The specified yield strength of the steel was 60 ksi, but in many instances this lower bound was exceeded significantly. The material properties are shown in Appendix A.

3.4 Testing Setup and Procedure

As shown in Fig. 3-5, the deflected shape assumed by a beam-column joint subassemblage in a high-rise frame structure under lateral load can be achieved by moving the column ends in opposite directions horizontally while pinning the beam ends. The same deflected shape can be obtained by pinning the column ends and displacing the beam ends vertically in opposite directions. In this test series the second approach was used for economical and practical reasons. This setup cannot account directly for P- Δ effects, but they can be added mathematically to the load-deformation curves.

The testing apparatus, shown in Fig 3-6, consisted of upper and lower loading heads, two column shear struts, and a reaction wall. Both the upper and lower loading heads were grouted and bolted to the column. The lower column was also bolted to the floor, providing a moment-resisting connection at the bottom. In order to model a true pin connection, the lower column was longer than the upper one, so that when the specimen was loaded a point of contraflexure formed about 12 in. from the bottom of the column. The main reason for fixing the bottom of the column to the reaction floor was the anticipated case of imposing tensile loads in the column. The upper loading head was connected through 2 pins to the column shear struts, providing a true moment-free connection at the top. The shear struts were also pinned-connected to the reaction wall.



- (1) Axial load rods
- (2) Axial load rams
- (3) Shear struts to reaction wall
- (4) Semi-fixed base
- (5) Load cell
- (6) Loading rams

Figure 3-5 : Test set-up

Although the column did not have a true pin at the bottom, an elastic analysis showed that the horizontal displacement of the lower point of inflection during loading would be small, and lead to less than 5% errors in the calculations for elastic flexural deformations. The semi-fixity at the bottom also provided for some moment transfer. An elastic analysis showed that the differences between assuming a pin at 12 in. from the bottom of the column, and a fixed base would lead to a maximum of 55%-to-45% split of column moments between the bottom and top of the joint. Thus the assumed even split of column moments to be made in latter calculations will not introduce significant errors. It was assumed that when the specimen went into the inelastic range these differences would not increase. Calculations for the actual position of the bottom point of inflection as the tests progressed indicated that it was very close to the bottom of the column for the load stages close to the peaks.

To apply the axial load, four rods attached to the rams placed on the top loading head were used. Each rod was loaded by a 100 ton hydraulic jack connected to a single manifold, thus keeping a constant load on all four rods. As the rams extended, the rods went into tension and the column was subjected to compression.

Beams were loaded using double-rod hydraulic rams. Two independent, manually controlled systems were used to apply the racking loads. The system illustrated in Fig. 3-7 permitted the application of both dead and racking loads.

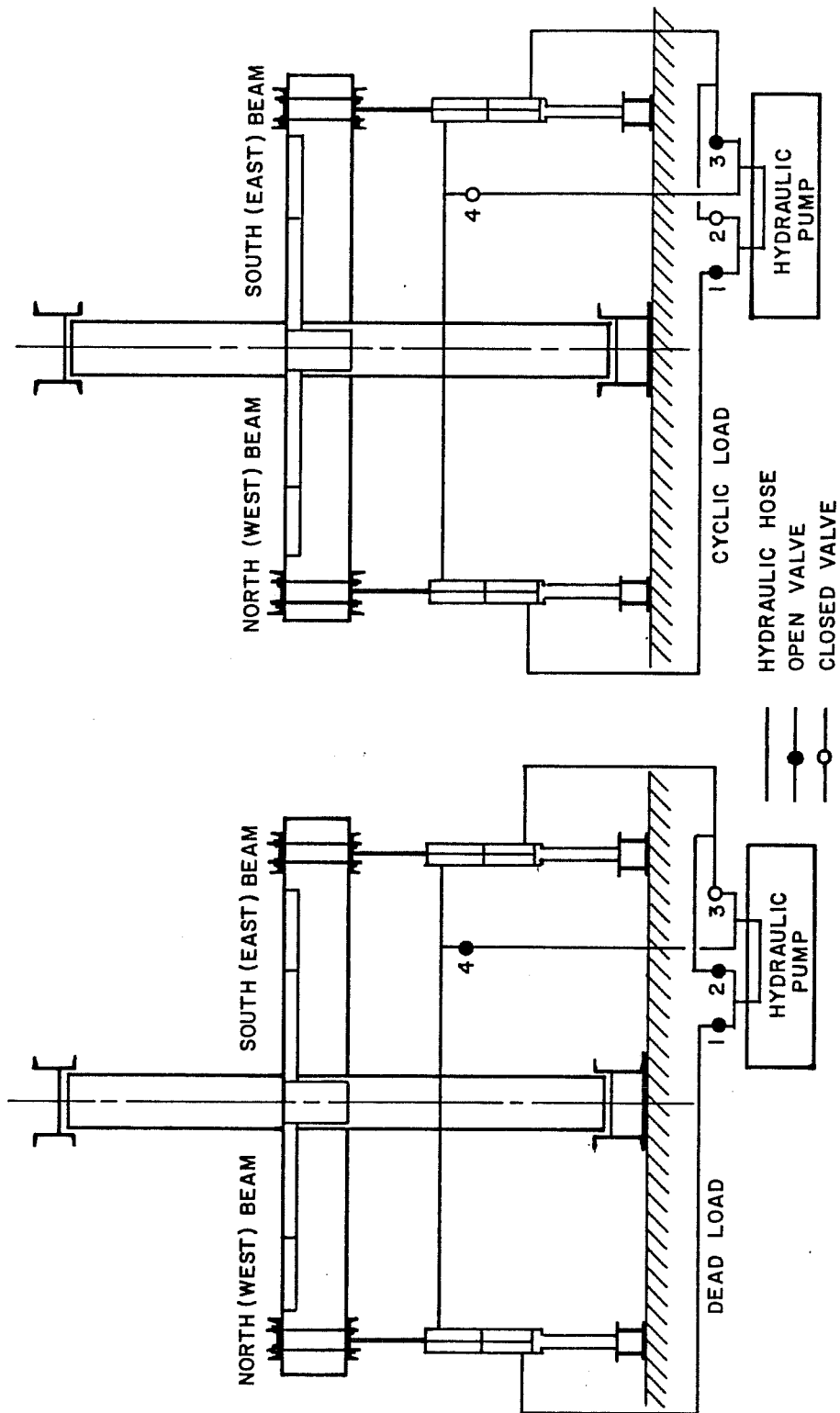


Figure 3-6: Loading system.

3.5 Instrumentation

The specimens were heavily instrumented in order to obtain as much information as possible from these tests. Three kinds of measuring devices were used: load cells, displacement transducers, and strain gages.

The loads applied to the beam ends were monitored by the use of load cells. The axial loads on the top shear struts were measured with full-bridge strain gages. The beam end deflections were measured using 12 in. stroke linear potentiometers, and deflections in the joint area were monitored using 2 in. stroke linear potentiometers.

One of the main purposes of the tests was to separate the components of interstory drift in order to improve the understanding of the stiffness deterioration phenomenon. Five main components, or mechanisms, were identified, and are shown in Fig. 3-10. The first two of these components are beam and column elastic deformations, and these can be found from static equilibrium, if we assume that the points of inflection are known. The third and fourth important components are beam and column inelastic rotations, and include the contribution of hinging and bar slip. The fifth is the deformation produced by joint shear distortion. The last three cannot be measured directly, but can be estimated by measuring the relative rotation between the beam and the column face, the movement of the column with respect to a fixed point, and the joint shear strain.

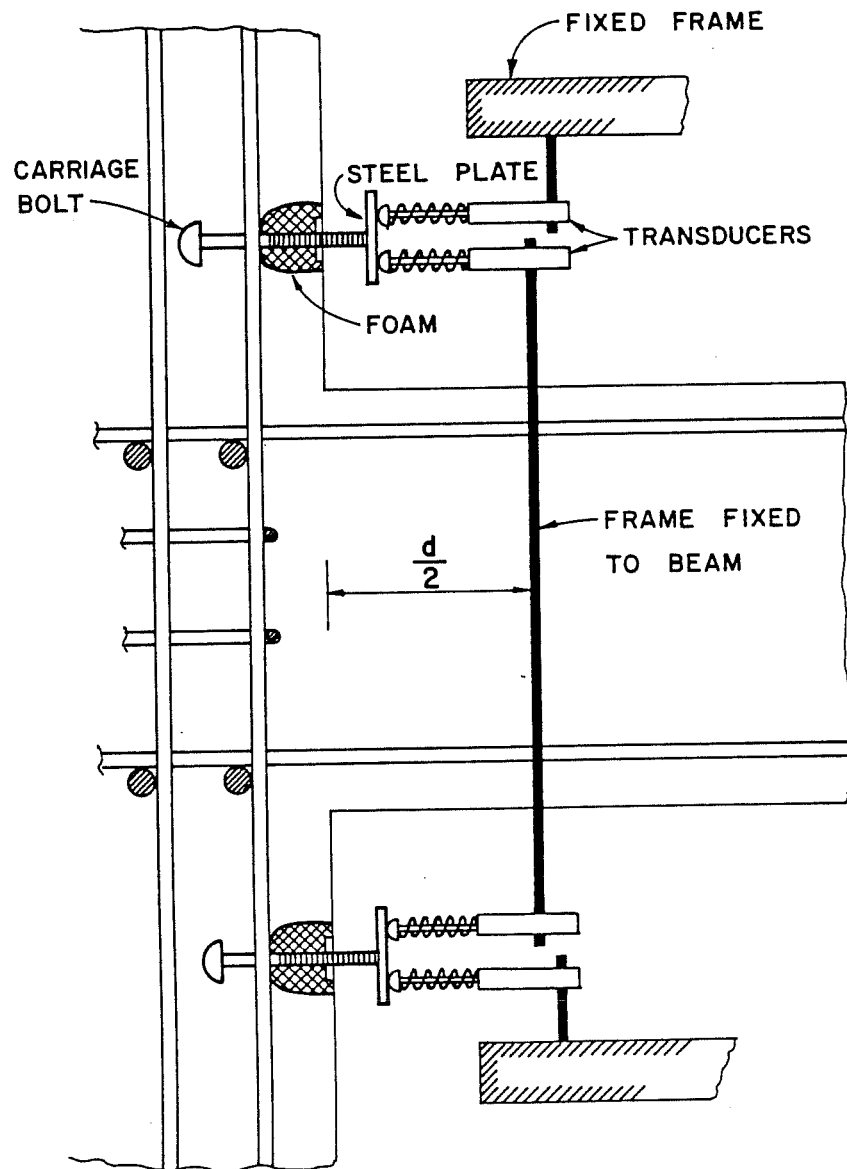


Figure 3-7 : Inserts and transducers in the joint area

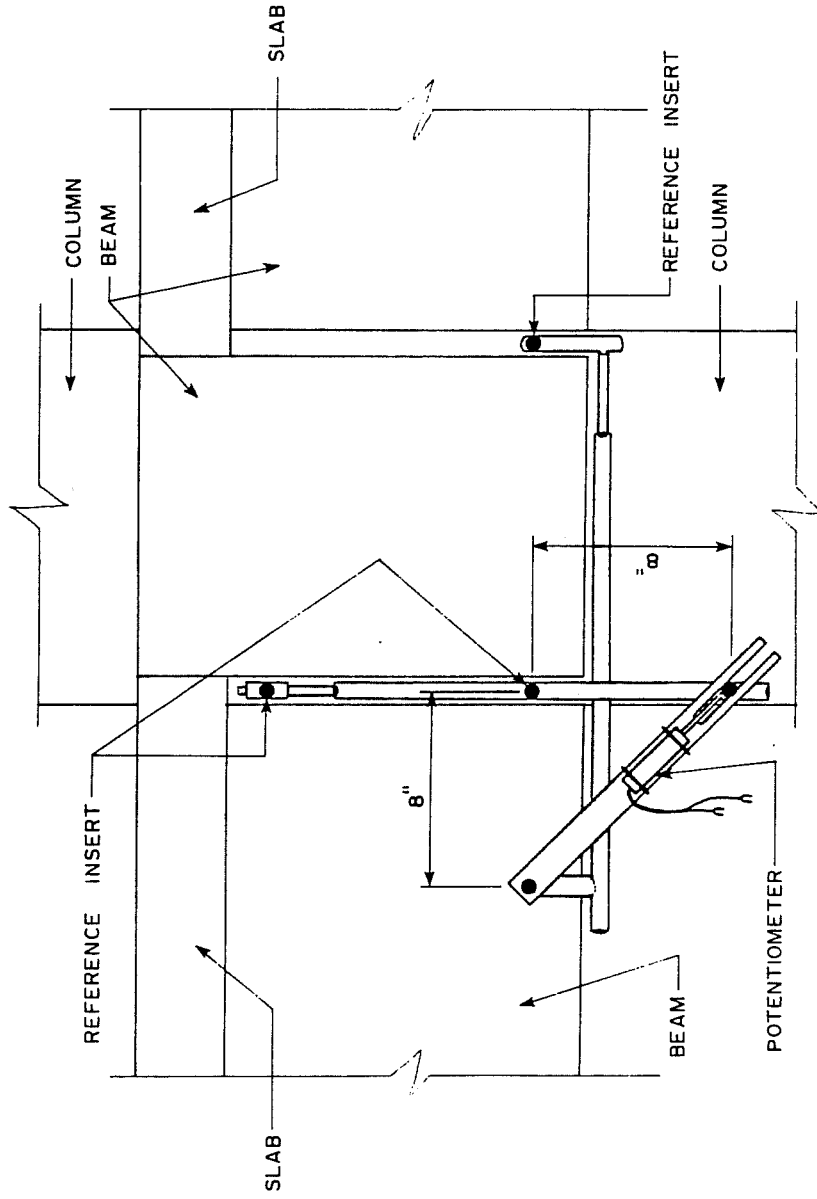
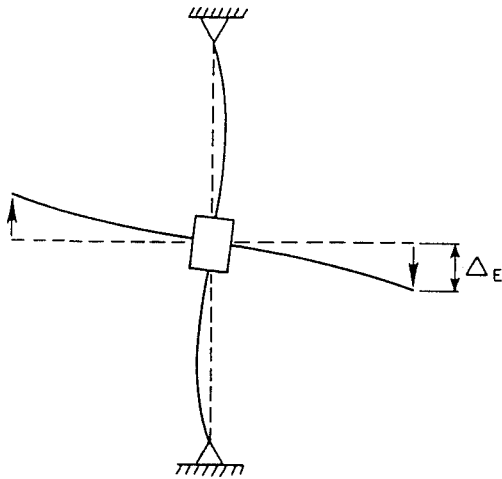
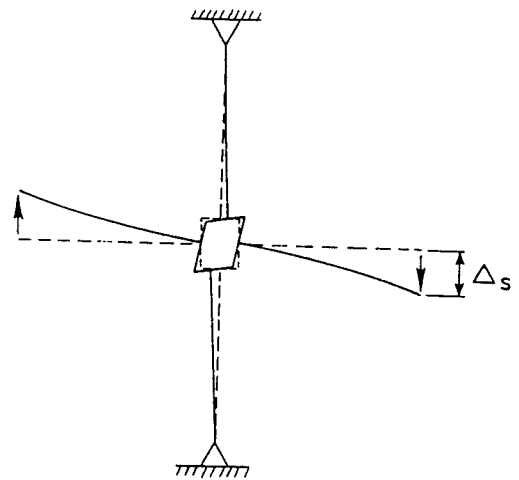


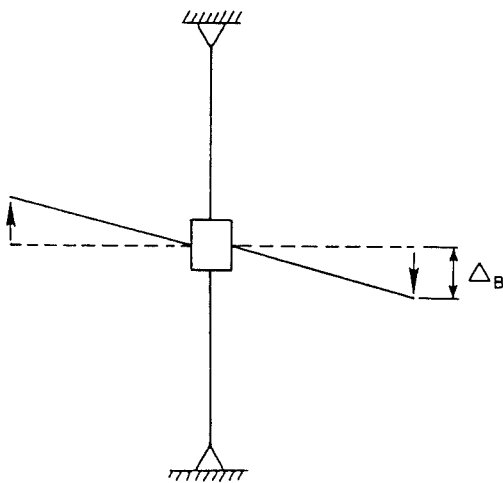
Figure 3-8: Joint shear strain instrumentation.



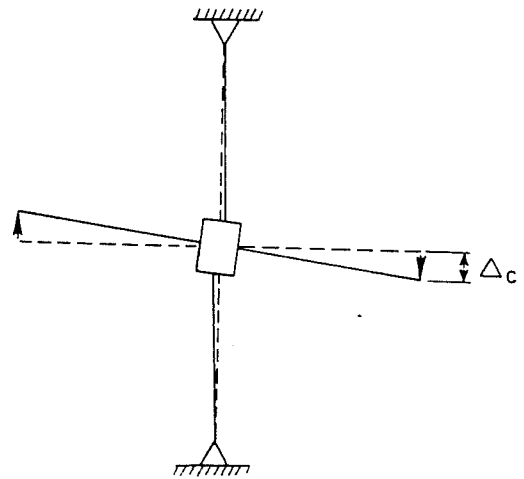
(1-2) Beam and column elastic flexural deformation.



(2) Joint shear strain.



(3) Inelastic beam rotation.



(4) Inelastic column rotation.

Figure 3-9 : Components of beam deflection

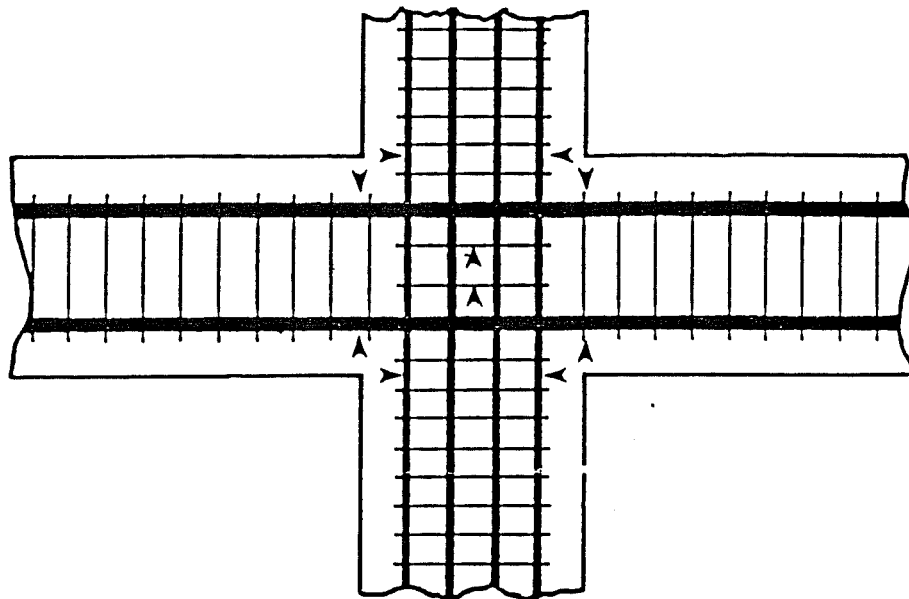
All these measurements were taken using bolts imbedded in the concrete core, as shown in Fig 3-8. The bolts were covered with foam through the cover concrete to prevent spalling of the cover concrete from influencing the readings. This arrangement seemed to perform well during all tests. The shear strain was measured from similar inserts using the apparatus shown in Fig 3-9. A complete description of these measurements is given in Appendix C.

Over 50 resistance strain gages were distributed through the specimen as shown in Fig. 3-11, to provide information on the strains in the reinforcing bars. To measure the bar slip, stiff wires were attached to the reinforcing bars and permitted measurement of the relative movement of the bars with respect to the surrounding concrete. The "slip-wire" instrumentation is shown in Fig. 3-12.

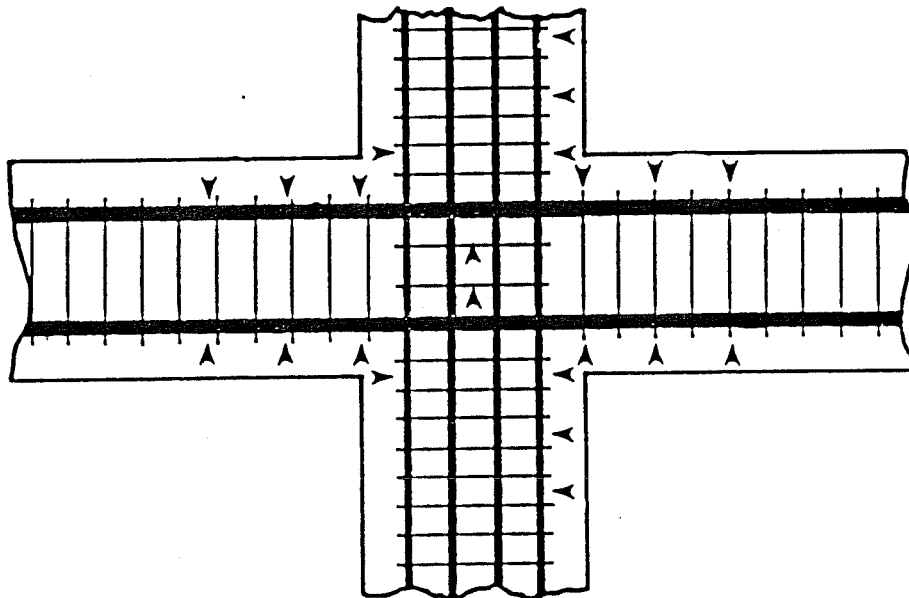
All the data was taken with a VIDAR Data Acquisition System, and processed used a DG Nova-3 minicomputer. Selected channels were then plotted to evaluate, both qualitatively and quantitatively, the behavior of each specimen.

3.6 Load History

As previously mentioned, the selection of a load history for a test series is a critical decision. It was felt that since the major interest was to establish the ultimate capacity of the subassemblage, few small or no elastic cycles would be applied. To



(a) Gages in the NS direction, West face and in the EW direction, North face.



(b) Gages in the NS direction, East face and in the EW direction, South face.

Arrows indicate position of strain gages. All stirrups and ties spaced at 4.0 in. on center.

Figure 3-10 : Location of strain gages near the joint

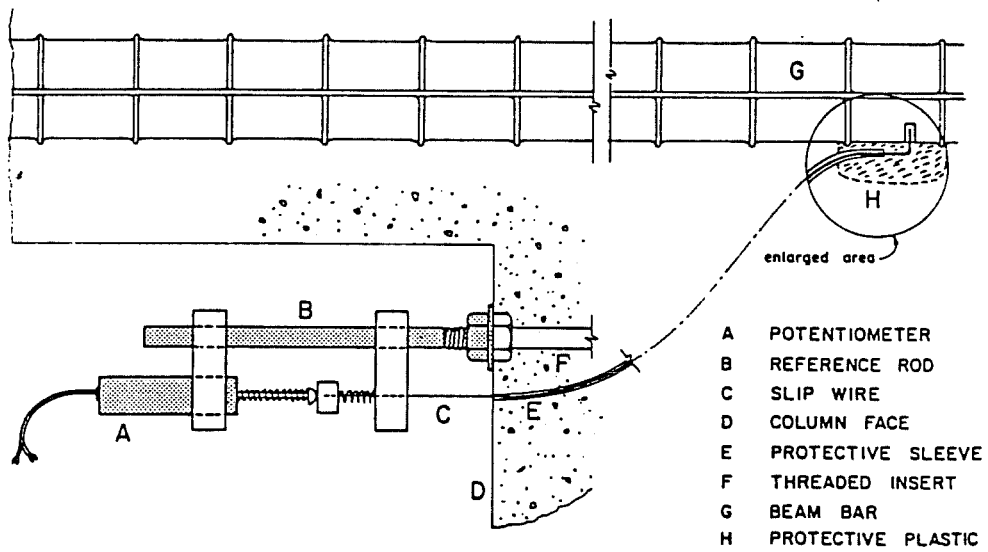
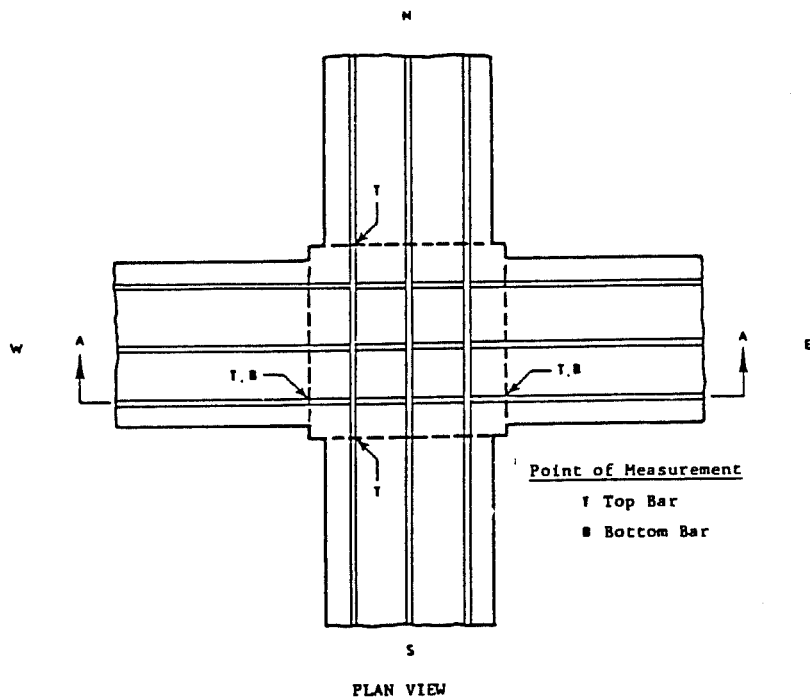


Figure 3-11: Slip-wire instrumentation

model the behavior of an actual structure it was decided to apply dead load to precrack the beams. Thus the first load stages consisted of first deflecting the tips of all beams downwards by 0.1 in. to simulate the effect of gravity loads, and then applying a cycle of racking loads to a peak deflection of 0.2 in. to precrack the beams top and bottom. This cycle will be referred to as the initial cracking cycle. Furthermore, a regular rather than random loading sequence was chosen to facilitate correlation between the analytical and experimental results, see Fig. 3-13. A regular sequence made it possible to better compare the results with those of other tests run with similar load histories, although the magnitude of the deflections is not always directly comparable.

After the initial cracking cycle was applied, the next peak deflection produced yielding of the negative beam reinforcement at a displacement of about 1.3 in. from the dead load position. Three cycles were imposed at this level since it was observed that little additional degradation of stiffness and strength occurred after the third cycle at a given deflection level was applied. The first three cycles correspond to a nominal ductility of 1.0. Three additional cycles at nominal ductilities of 2.0 and 3.0 were then applied. A nominal ductility of 1.0 as defined here corresponds to about a yield ductility of 2.5 to 3.0 if the latter is defined as the ratio of the total displacement at the peak of each cycle to the displacement where the initial slope of the curve intersects the yield load. The

beam tip deformations correspond to equivalent interstory drifts of 2%, 4%, and 6% if a story height of 12 ft. is assumed.

3.7 Summary

The test series described herein intends to clarify the effect of biaxial loading, framing member size, and slabs on beam-column joint behavior. The specimens were large-scale and well instrumented. The instrumentation was designed to help separate the contribution of different mechanisms to joint shear strength and deterioration. A severe load history was chosen to simulate the effects of a maximum credible earthquake on beam-column joint behavior.

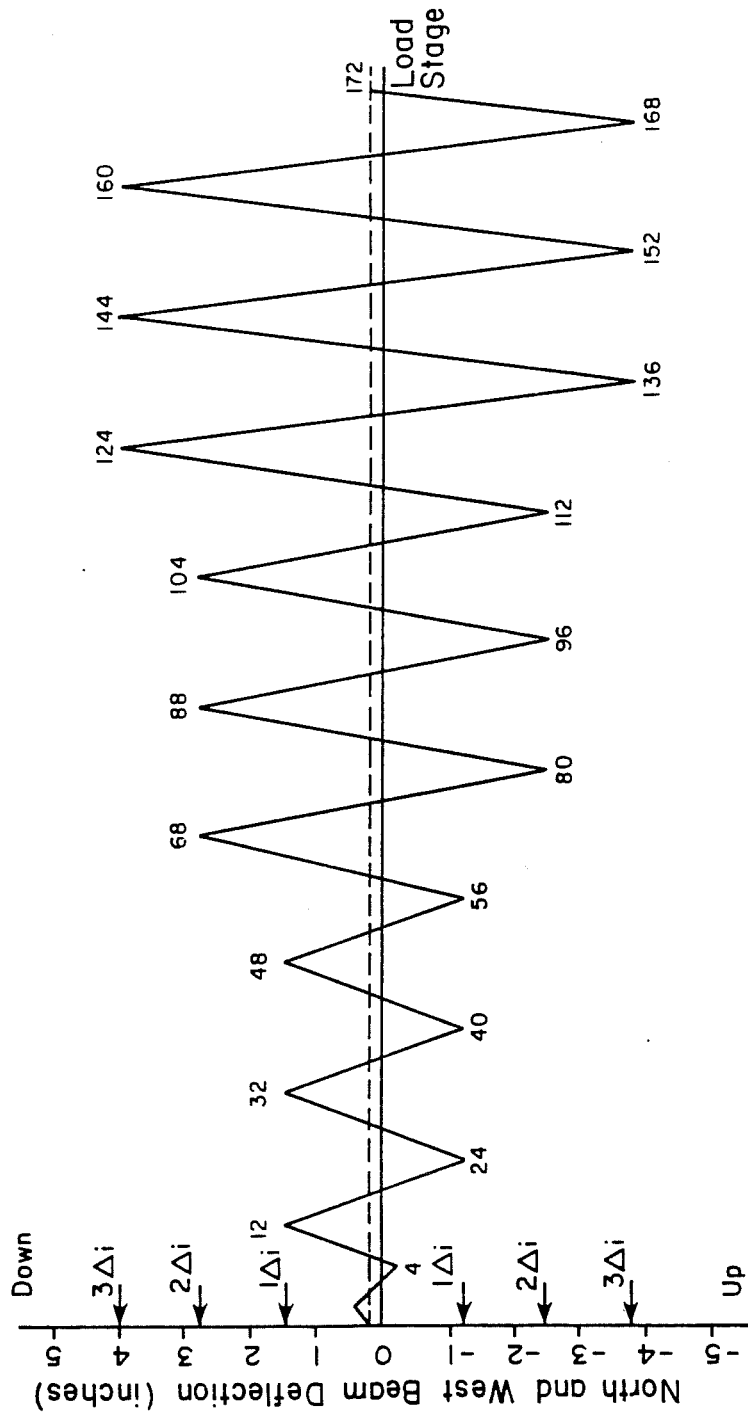


Figure 3-12: Load history applied.

Chapter 4

Experimental Results

4.1 General

The specimens used were heavily instrumented, and therefore the amount of data available for each test is very large. In order to limit the amount of detail presented it was decided to describe only one representative test, BCJ8, in detail. Data from other tests will be presented to amplify behavioral aspects discussed in Chapters 5 and 6. Other results for tests BCJ9 through BCJ14 will be found in Appendix D.

Test BCJ8, chosen for detailed discussion, was the control specimen for the tests with slabs. The geometry and reinforcement were the same as for BCJ5 except that BCJ8 carried no axial load. The details for this specimen are given in Table 3-1, and a schematic representation of the steel in the joint area is given in Fig. 4-1. It should be mentioned that the joint was more congested than the figure shows; the size of the bars was reduced in order to ease visualization. In the test specimen the column bars in each face and the top longitudinal beam bars are in contact. Note that only two

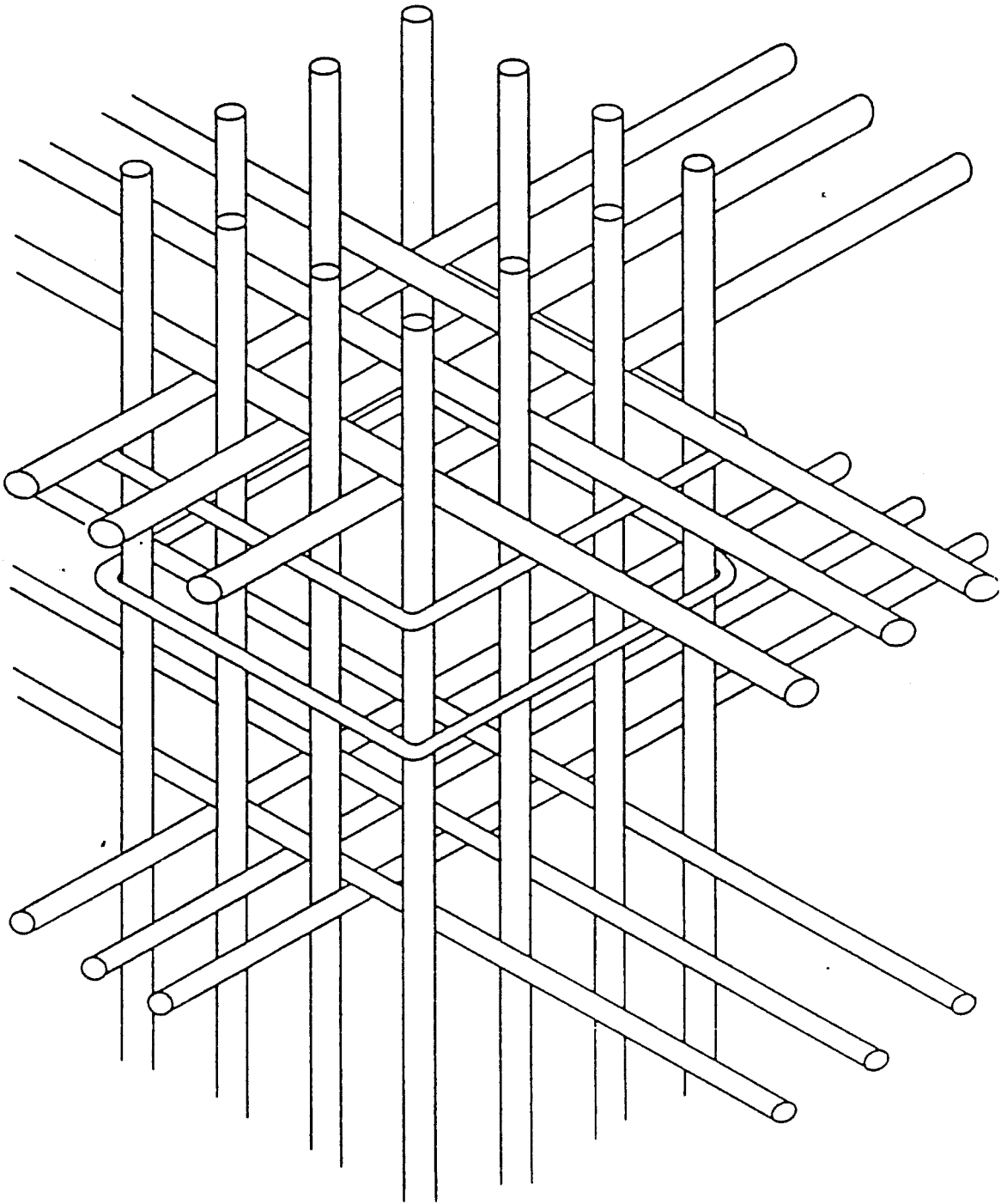


Figure 4-1 : Reinforcement in the joint area

joint ties are present, at a spacing of about 5. in., and that there are no ties between intermediate column bars either through the joint or in the column.

4.2 Load History

The specimen was subjected to the load history shown in Fig 3-11, which consisted of deflecting all beams 0.1 in. to simulate dead load and cycling from that deformed position. Ten cycles of load were imposed; the first was an initial cracking cycle, followed by three cycles at three different deflection levels, or ductilities, in the inelastic range. A total of 201 load increments, or load stages (LS), were applied; the first excursions at each deflection level consisted of 28 load stages in total, while the second and third consisted of 16 each. The last 20 load stages consisted of a cycle of loading at very large amplitudes on a plane at 90 degrees from that used for the first nine cycles. The load stage numbers are given in Fig. 4-2; thus load stage 12, or LS12, corresponds to the peak at the first downward deflection to 1.4 in. At this point in the load history the North and West beams were loaded downward, the strong direction, while the South and East beams were displaced upwards, the weak direction. In the text, the peaks will be referred as $+i\Delta_j$ or $-i\Delta_j$, where the sign indicates the direction of displacement (positive is downward), the i the deflection level, and the j the cycle at that particular level. Thus $+2\Delta_1$ refers to

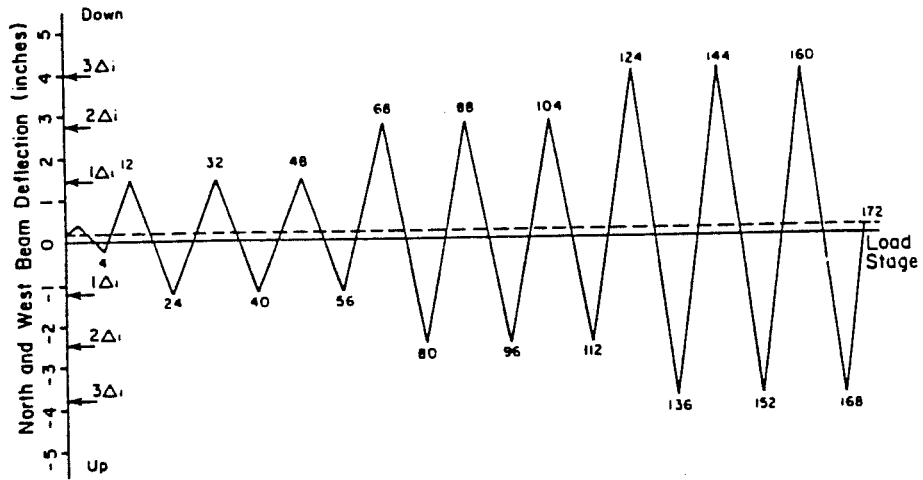


Figure 4-2: Load history for BCJ8

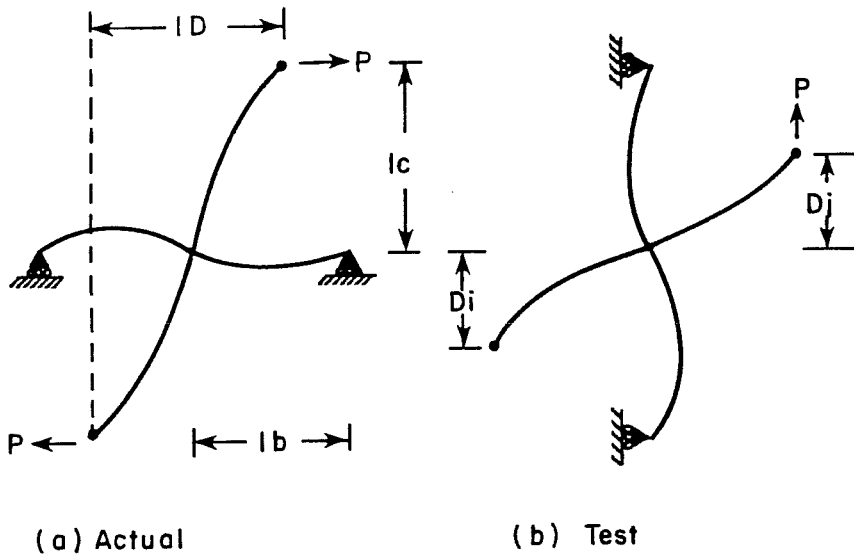


Figure 4-3: Equivalent interstory displacement

the first downward displacement at the second deflection , or to load stage 68.

The applied deflection levels were multiples of the deflection causing first yield in the beam longitudinal steel and thus correspond to nominal deflection ductilities of 1.0, 2.0, and 3.0 . Deflection at first yield was determined experimentally to be about 1.3 inches from the dead load position, a value considerably larger than the 0.3 to 0.4 inches predicted by analytical methods assuming the beam to be anchored in a rigid block. The discrepancy can be attributed to the high ratio of beam-to column stiffness , errors in the assumed cracked section properties, and the indeterminacy of the test setup. However, even accounting for these factors in the analysis the calculated beam end deflection at first yield did not exceed 0.9 in.

The beam end deflection can be easily translated into equivalent interstory displacements (ID) by multiplying the total beam end deflections by the ratio of the distances between the load points in the beams and the inflection points of the column, as shown in Fig. 4-3.

$$ID = [l_c/l_b] [D_i + D_j] \quad (4.1)$$

where i and j refer to the beam end deflections in either principal direction. Thus, the first deflection level produces an interstory

displacement of about 2.7 inches over a story height of 12.0 feet. This corresponds to about a 2.0% drift in each principal direction, and almost 3% in the resultant plane of loading 45 degrees from the main structural axis.

Although the imposed drifts are very large, it is important to recognize that the purpose of the tests was to introduce as large a shear into the joint as possible, as well as to ascertain if the shear strength could be maintained through several cycles. To accomplish this without complications of frame instability, the P-delta effect was excluded. Once the specimen becomes unstable the loads in the joint area, and consequently the shear strength demand, will decrease. In addition, it must be recognized that the test specimen was more flexible than design calculations indicated, necessitating large drifts to induce yielding in the beam steel. The best explanation for this flexibility is that the joint is not a rigid member as often idealized in analysis, when joint shear cracking is permitted.

4.3 Principal Load vs. Deformation Relationships

Two sets of force-displacement relationships for BCJ8 will be examined; first, measured beam load versus beam displacement, and second calculated joint shear versus joint shear strain. Both of these are stiffness-type plots; the first can be thought of as the

usual flexural stiffness of the system, while the second can be described as its shear stiffness.

4.3.1 Beam Load-Beam Displacement

The load-deformation curves for the North and South beams of BCJ8 are shown in Figs. 4-4 and 4-5. All beams seem to have reached flexural capacity by $+1\Delta_1$, the first peak. All curves seem to be following the envelope represented by the monotonic test conducted by Longwell on a similar specimen with axial load [60]. The initial secant stiffness, calculated from the readings taken after the application of the dead load deflection gave values of between 88 and 104 k/in. The stiffness decreased rapidly to about 20 to 25 kips/inch at a deflection of 0.7 to 0.8 in. Since it is hard to determine a single value which defines stiffness from a curve with a continuously changing slope, it was decided to arbitrarily define two types of stiffnesses. The first, called equivalent stiffness (K_e), is taken as the slope of the line joining the peak and the point where the line crosses the x-axis on its ascent to that peak as shown in Fig. 4-6. For this test, the equivalent stiffness for the first load cycle was about 24 kips/inch in the North beam (strong direction), and about 18 kips/inch in the South beam (weak direction). A summary of the equivalent stiffnesses for all cycles is given in Table 4-1. The second called peak-to-peak stiffness (K_p), or backbone stiffness, is given as the slope of the line

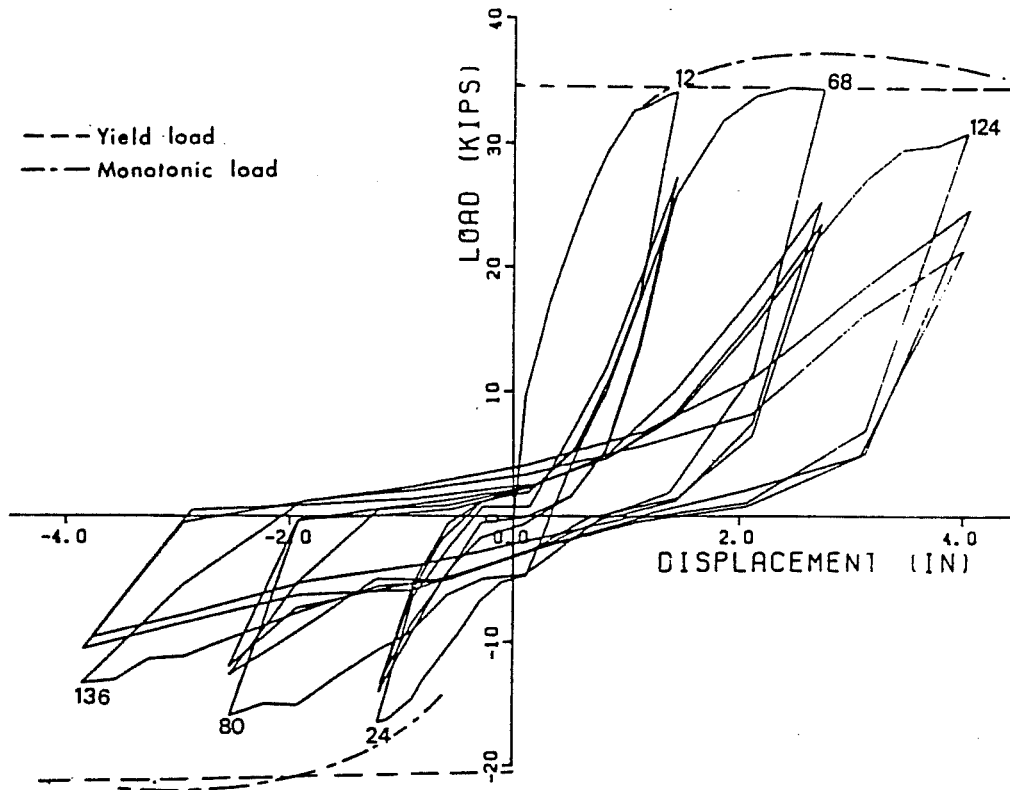


Figure 4-4: Load-deformation for North beam [BCJ8]

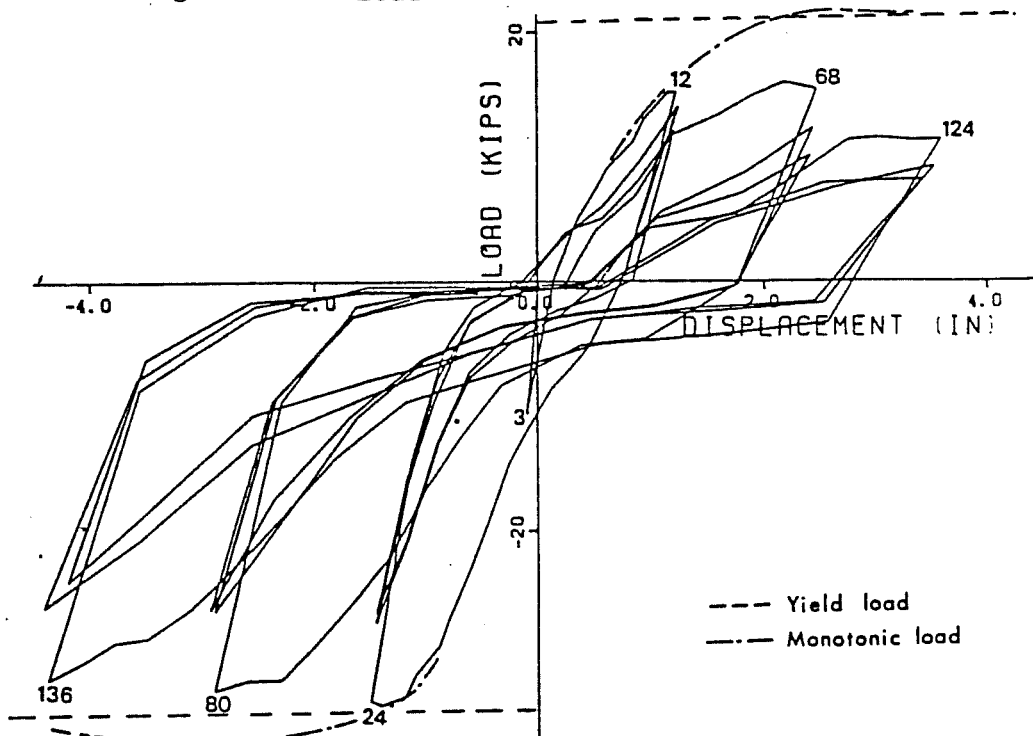


Figure 4-5: Load-deformation for South beam [BCJ8]

joining the positive and negative peaks at each load cycle. For this specimen, the peak-to-peak stiffnesses ranged from 17 kips/in to 19 kips/in. This second definition will be used in Chapter 6 to compare the behavior of different specimens.

Unloading from the first peak followed a line parallel to that of the initial load stage, and showed large residual deflections at zero load for the beam loaded in the weak direction. Upon loading to the first peak in the opposite direction, $-1\Delta_{-1}$, the first signs of degrading behavior became obvious. The North beam did not reach its calculated yield force before the curve began to flatten; the same is not true for the beam originally loaded in its weak direction, which reached calculated yield strength. The stiffnesses of the beams loaded originally in the strong direction degraded more rapidly than those loaded originally in the weak direction.

The degradation of stiffness and strength became very obvious in the second and third cycles at the first deflection level ($+1\Delta_{2,3}$ and $-1\Delta_{2,3}$). The loops were pinched at the origin, and the stiffness near the zero deflection point tended toward zero. If it is assumed that the energy dissipation capacity of the subassemblage is a function of the swept areas under the load deflection curve, then the loss from the first to the second cycle is on the order of 70%. In addition the equivalent stiffness dropped about 40% from the first to the second cycle. With cycling a strength loss of 20% to

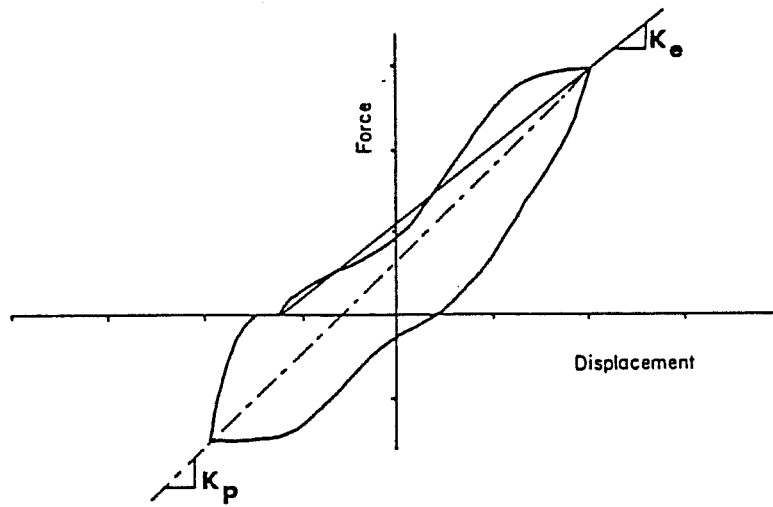


Figure 4-6 : Definition of equivalent stiffnesses

Deflection Level	Cycle	Equivalent stiffness (kip/in)	Peak-to-peak stiffness (kip/in)
1	1	24	19
	2	15	16
	3	14	15
2	1	11	10
	2	6	7
	3	6	7
3	1	5	7
	2	4	4
	3	3	4

Table 4-1: Equivalent stiffnesses

25% at equivalent deformations was also clear. It should be noted that most of the changes in response take place between the first and second cycles to any deflection level. The behavior at subsequent cycles at a particular deflection level was similar to that of the second cycle. A similar observation was made by Uzumeri [105] for exterior joints.

The second and third deflection levels ($2\Delta_j$, and $3\Delta_j$) showed similar behavior. The original strength may be regained if large deformations had been imposed, but the stiffness continues to deteriorate rapidly. The drop in strength from the first to second cycle seemed larger at the second deflection level. At the third level the descending portion of the envelope is reached.

The degradation of stiffness and strength with cycling, as will be discussed extensively later, is due mainly to the loss of bond through the joint caused by yield penetration and by slippage of the main reinforcement. A good idea of the magnitude of the forces being introduced into the joint can be gleaned from the plot of total shear vs. interstory displacement, shown in Fig 4-7. The total shear is the vectorial summation of the horizontal shears in the North-South and East-West directions, and thus represents a vector at approximately 45 degrees from the main structural axis. The positive sign indicates a direction to the Northwest, while a negative one indicates a direction to the Southeast corner of the joint. In this

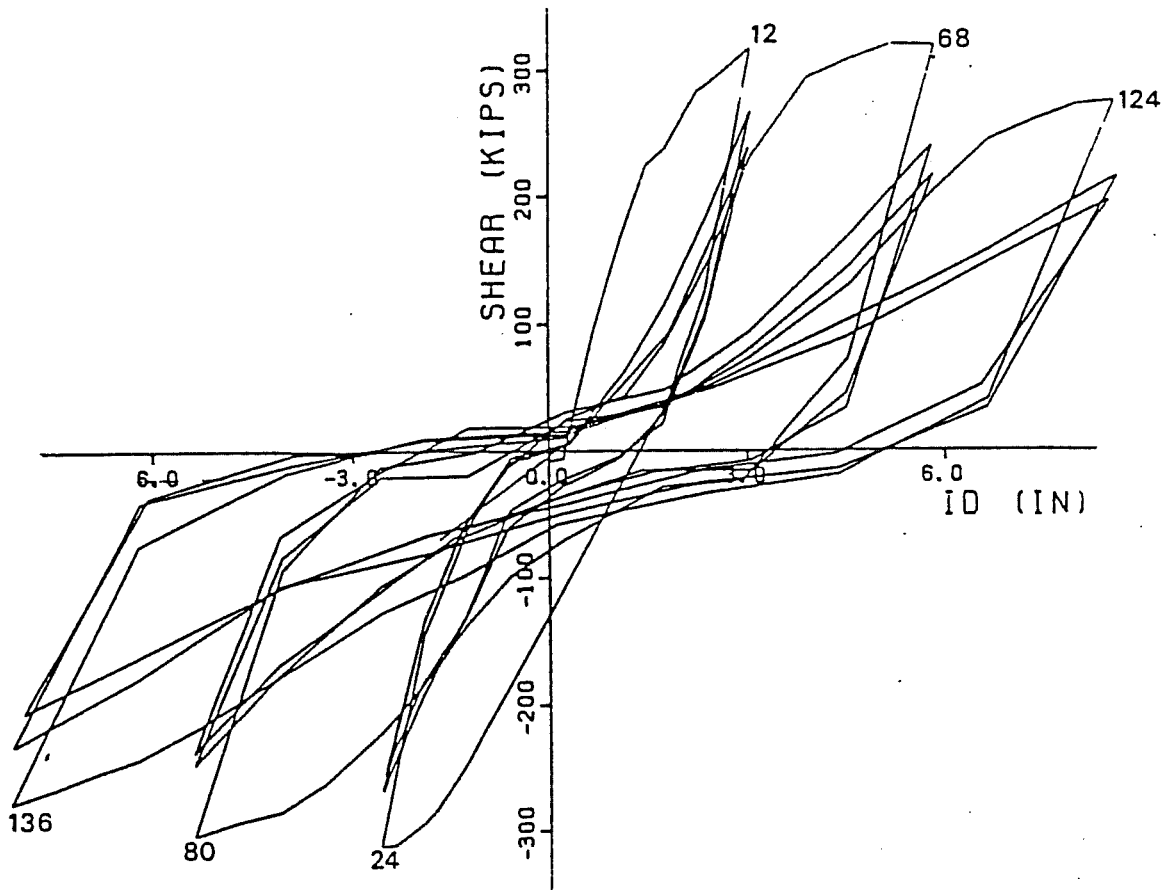


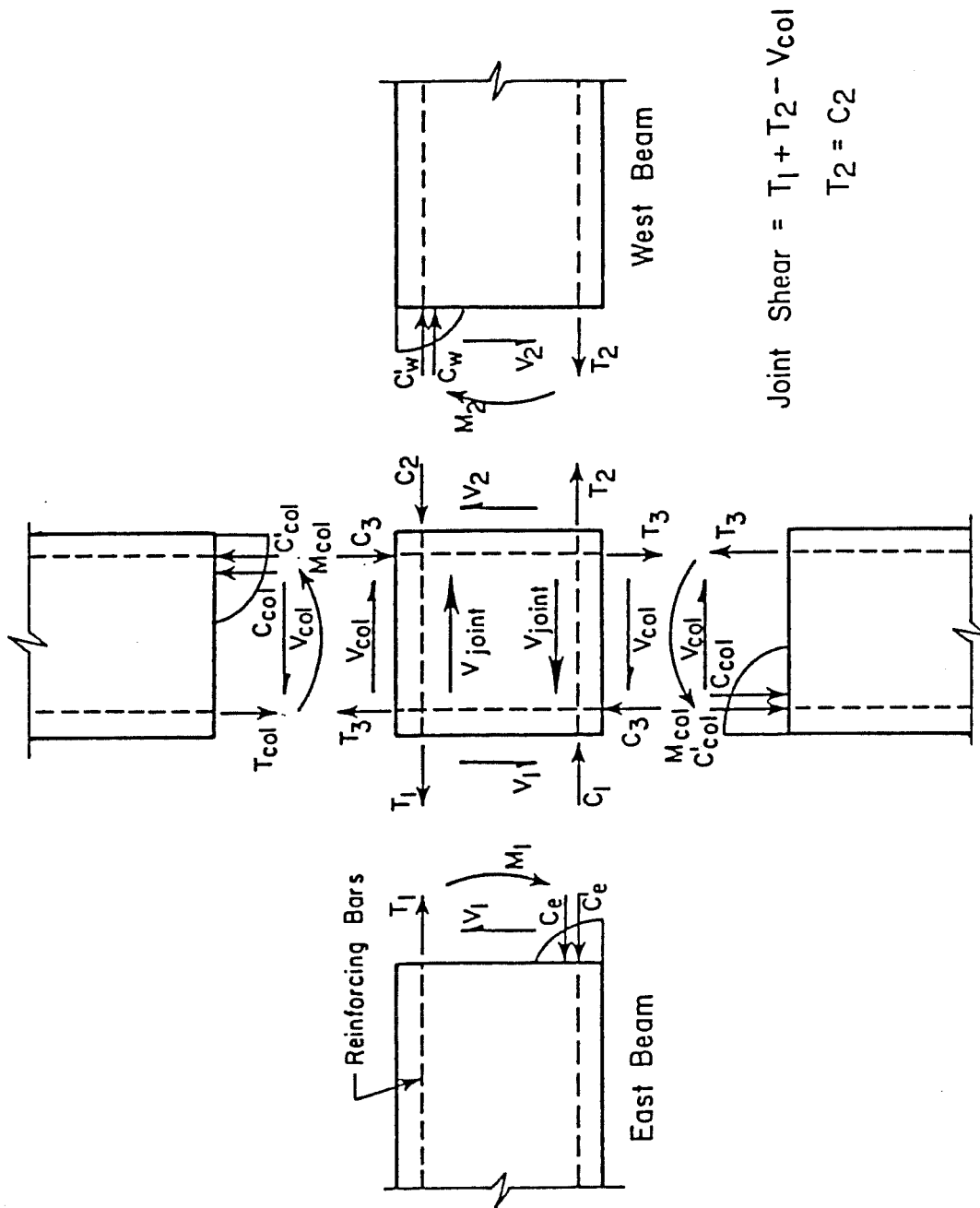
Figure 4-7 : Total joint shear vs. interstory displacement

plot the same trends with regard to stiffness and strength degradation present in the beam load-beam deformation plots can be seen. The maximum shear of 320 kips along the diagonal corresponds to about $28\sqrt{f'_c}$ nominal shear stress in the joint, a value higher than the $20\sqrt{f'_c}$ allowed by current design procedures.

4.3.2 Joint Shear - Joint Shear Strain

As previously discussed, an analysis of a typical joint will show that shear is the main parameter controlling design. Thus, it is more significant to look at the influence of shear rather than flexural forces on the joint. The total shear introduced in the joint can be estimated from equilibrium conditions, as shown in Fig. 4-8.

In the tests reported here, the compressive and tensile (C and T respectively) forces in the beams were not measured directly. To determine these forces the beam moments at the joint face were taken as the product of the beam end load times the distance from the load point. The depth of the compressive block was then assumed using ultimate strength design procedures, and the T and C forces backcalculated. The pertinent calculations are shown in Appendix B. The value for V_{col} was obtained from strain measurements at the top column struts; the values obtained experimentally at deflections of 0.5 inches or more showed a satisfactory correlation with those



$$\text{Joint Shear} = T_1 + T_2 - V_{col}$$

$$T_2 = C_2$$

Figure 4-8 : Calculation of shear in the joint area

derived from an analysis assuming an inflection point at about 12 inches from the bottom of the column.

Since shear is almost a linear function of beam loads, a plot of shear versus interstory displacement in each principal direction results in a graph of shape similar to that of Fig. 4-4, with the maximum ordinates changing from about 36 kips to about 230 kips. A more meaningful way of measuring the effect of shear is plotted in Figs. 4-9 and 4-10, in which total shear is shown graphed versus joint shear strain. The joint shear strain is measured directly using the instrumentation shown in Fig. 3-9, and is calculated as shown in Appendix C.

The most significant observation from these plots is the lack of symmetry about the y-axis. The joint appears to be much stiffer in shear when loaded to the first positive peak ($+1\Delta_1$) than when loaded to the first negative peak ($-1\Delta_1$). Almost twice as much joint shear strain occurred in the negative direction as in the positive one; the obvious explanation is that the joint shear cracking limit is exceeded in the first excursion to a peak, and when loaded in the opposite direction the joint had been considerably "softened". Once this softening has occurred the second and third cycles should exhibit a larger shear strain. However, the plots show almost equal amounts of joint shear strain for all cycles in each direction at given deflection level.

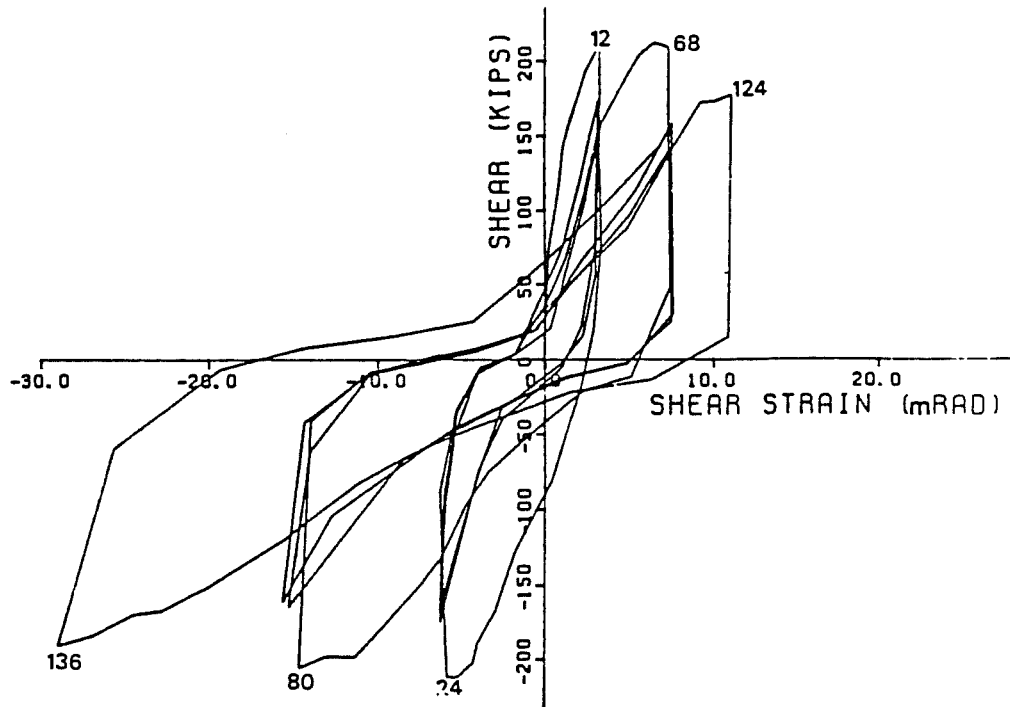


Figure 4-9: Joint shear vs. joint shear strain - NS - BCJ8

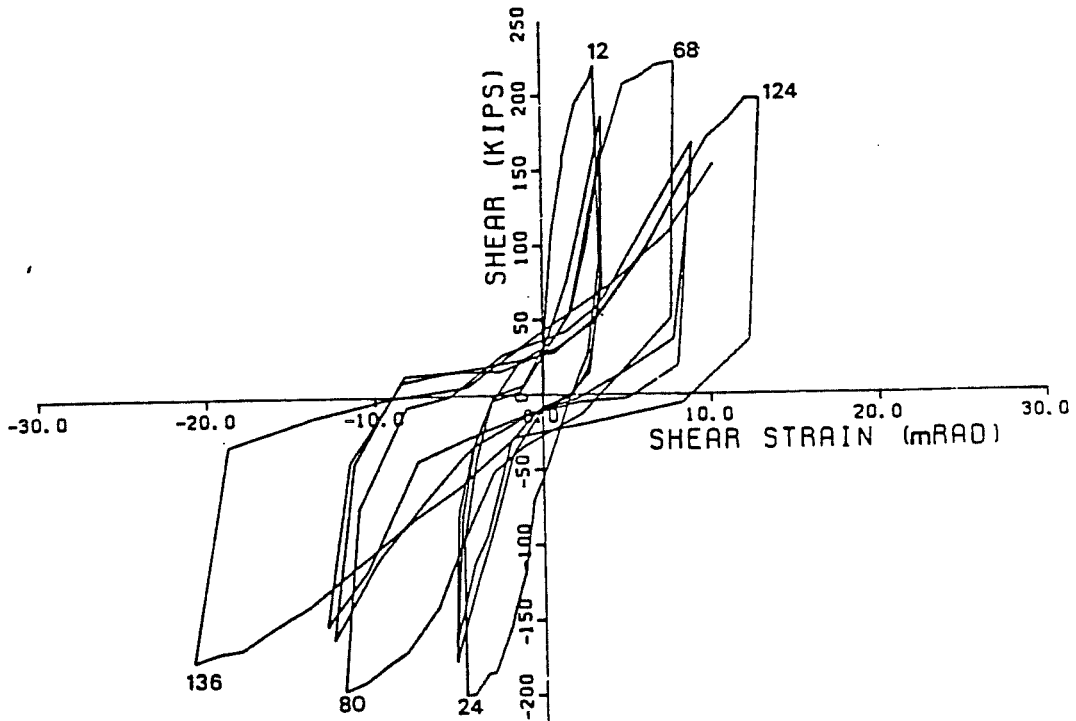


Figure 4-10: Joint shear vs. joint shear strain - EW - BCJ8 .

Two hypotheses can be advanced to explain this phenomenon. First, considering the peaks at the first cycle in each direction, it is clear that the curves flatten. The maximum shear is reached at this point because the beam steel has yielded and no additional force can be introduced into the joint. The linearity between nominal shear stress and shear strain is lost around a deflection of 0.8 in., when the joint first showed visible evidence of shear cracking. After this point the "shear stiffness" begins to decrease, and the behavior will be governed by the extent and orientation of the cracks. It must be noted that the shear stress decreases at the second and third cycles of any deflection level due to bar slip already mentioned. Thus, additional shear cracking in the joint is unlikely past the first cycle and the reduced shear stresses could explain the similar amounts of shear strain measured for all cycles at a given deflection level. Also it must be noted that the shear stiffness becomes very small near the origin after the first cycle, but at the first deflection level about 75% of its original value is regained near the peaks of the second and third cycles. This is not true for the second deflection level, where the drop in "shear stiffness" between the first and the remaining cycles is very large. As a matter of fact, this drop occurs almost immediately after the first yield deflection is exceeded during the loading to $+2\Delta_1$, and could signal the initiation of shear failure in the joint.

A second, more plausible explanation is that the shear

deformation is dependent on the forces acting and the size of the framing members. When loading to the first peak the joint will benefit from the confinement provided by uncracked compressive blocks on the beams (See Fig 4-11). When loading in the opposite direction, however, the tension cracks must close before any of this confinement can be developed. The cracks may be very wide due to the yielding of the bars and to slip. Although strain compatibility is usually assumed between the steel and the concrete, such compatibility is lost early in the load history leading to the equilibrium conditions shown in Fig. 4-12. The importance of strain incompatibility at the joint increases as cycling proceeds since the bars begin to increase in length due to yielding and to slip due to bond deterioration. The tension cracks at the beam-column joint become larger and thus more difficult to close, leading to flatter slopes for any load-deformation relationship. The confining effect of the framing members becomes noticeable near the peaks when the cracks have closed, and this hypothesis will be pursued fully in Chapter 6 when comparing the performance of test specimen with different size beams.

Several other observations must be made about Figs. 4-7 and 4-8. First, the initial slope is very steep. The joint shear strain shows a large jump (about 1.0 milliradian) between load stages 5 and 6, indicating the first significant shear cracking. The resultant shear at this point is about 167 kips (a nominal joint shear stress

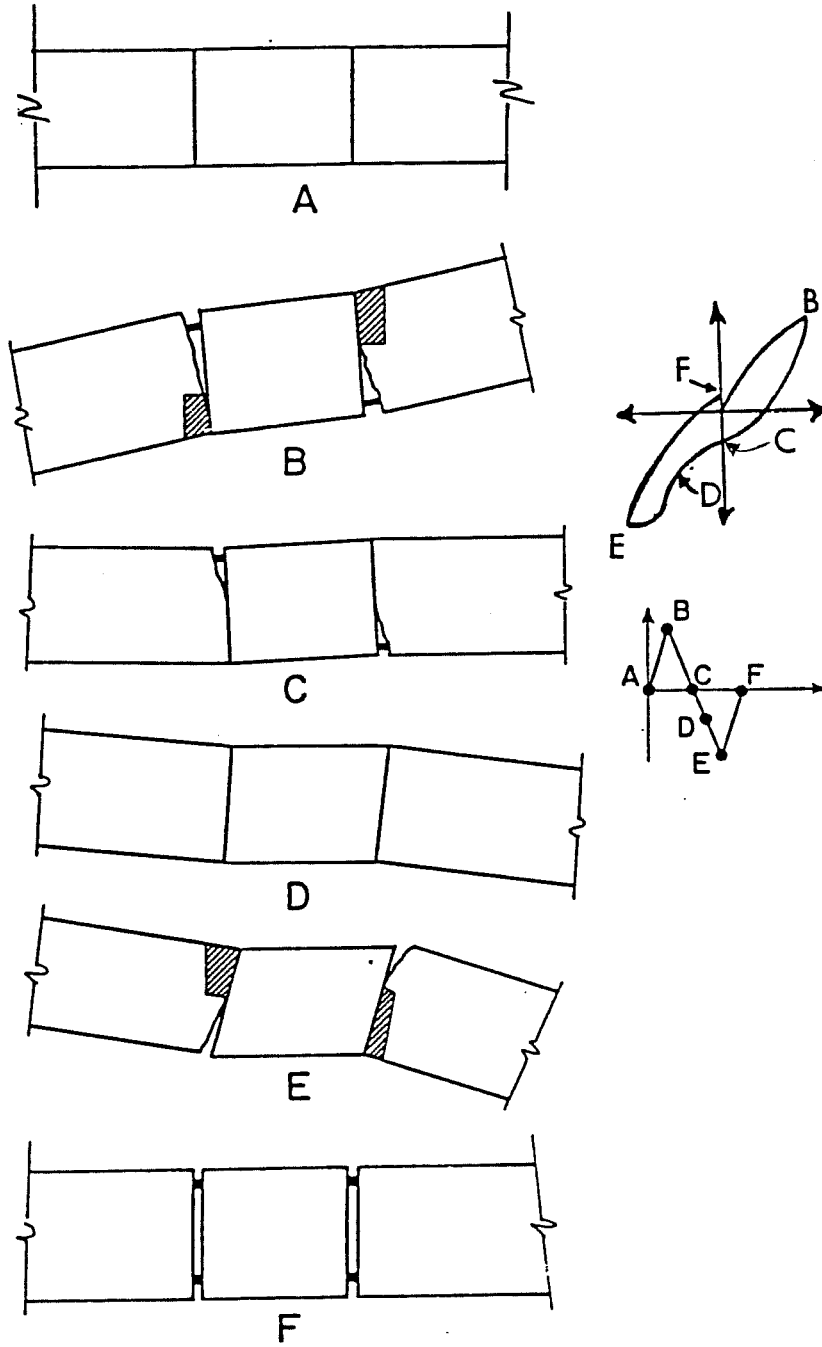
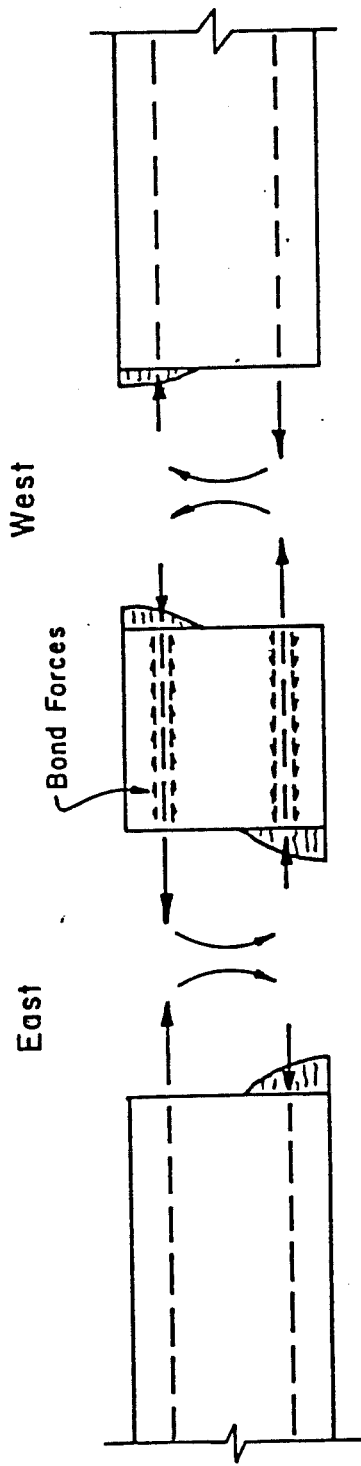
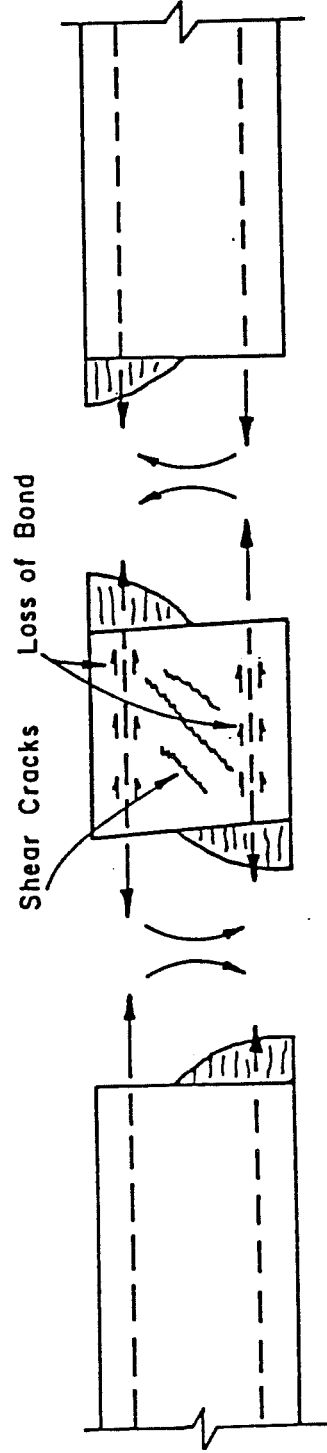


Figure 4-11: Effect of strain incompatibility on joint shear strain.



a) Force Equilibrium Required by Strain Compatibility



b) Force Equilibrium Because of Shear and Bond Failure

Figure 4-12 : Effect of strain incompatibility on joint forces

of about 900 psi) which is not much higher than the one calculated by the procedures for estimating first cracking suggested by Meinheit and Jirsa [50] and Sugano and Koreishi [97]. The second observation is that while the joint cracked, it continued to pick up shear. In fact the maximum shear strength was at least twice that necessary to crack the joint. Finally, the magnitude of the measured shear strains suggests that the joint is much less rigid than one would expect. Following the initial, linear portion of the curve (no shear cracks) will lead to a shear strain that will be only about a tenth of that measured at $1\Delta_1$. It would seem that most damage to the joint shear stiffness occurred during the first cycle at the second deflection level; after this cycle, the joint shear strength did not come close to its original values even if the deformations were substantially increased. If very large drifts are expected, therefore, it is unsafe in design to consider joints with geometric proportions similar to those tested as rigid members.

4.4 General Specimen Behavior

The observed behavior of all specimens will be described in detail because an idea of where and when cracking and spalling of critical sections occurred is essential to understanding the conclusions about column-to-beam moment ratios, shear stress levels and bond conditions developed in Chapter 6.

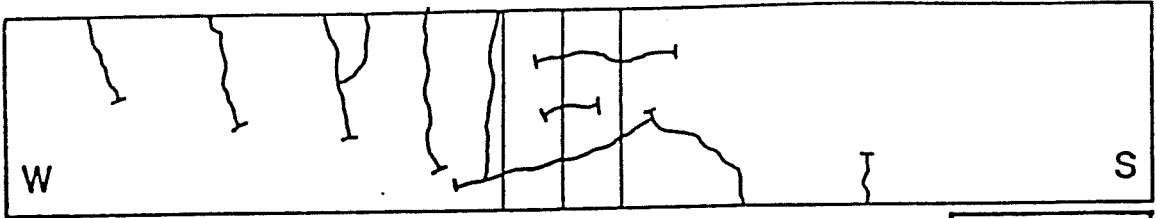
4.4.1 Dead Load and Initial Cracking Cycle

The application of dead load deflection to the specimen caused no observable distress, only elastic deformations of the beams and a small axial deformation in the column. The initial cracking cycle consisted of deflecting the beams an additional 0.2 inches from the dead load position and led to some flexural cracking of the beams near the joint. No shear cracking was observable at this point. This initial cycle precracked the beams in order to simulate the effects of both the service loads and any previous, minor lateral loads.

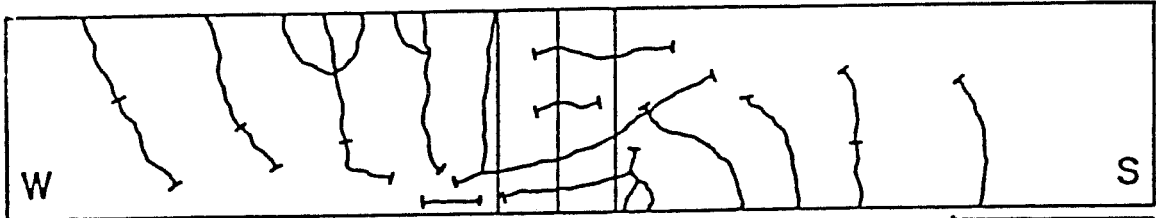
4.4.2 First Deflection Level

The first deflection level consisted of 3 cycles of load at about 1.3 inches in each direction from the dead load position. During the loading to the first peak, cracks were marked at three stages : first at LS 5 (0.2 inches), at LS 7 (0.5 in.), and at the peak of the cycle, LS 12 (1.3 in.). In Fig. 4-13 the progressive cracking of the West and South beams, as well as cracking across the SW joint corner can be seen. The dimensions of the joint corner are exaggerated to clarify the drawing, so that the cracks across this area are steeper than indicated on the sketches. The shadowed portion indicates spalling of the concrete cover.

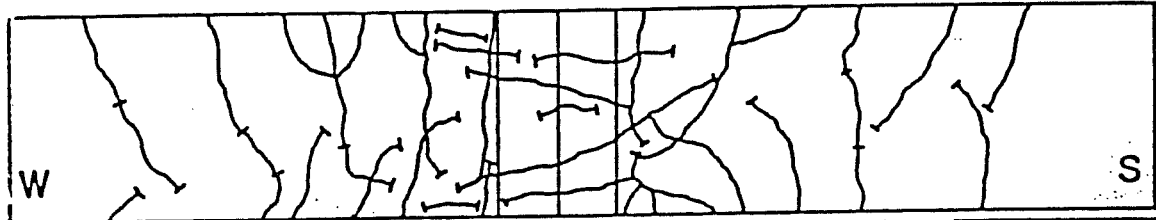
At LS 5, which was about equal to the maximum deflection



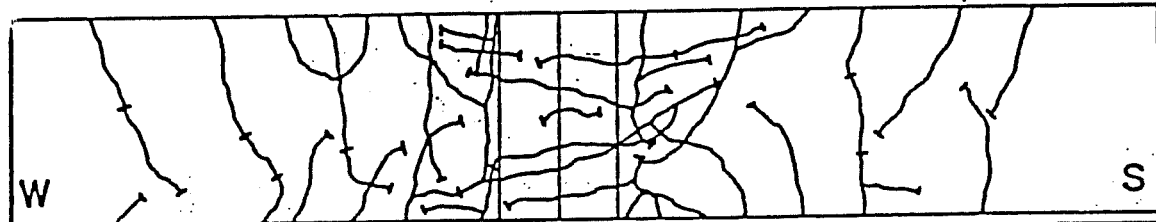
LS 7



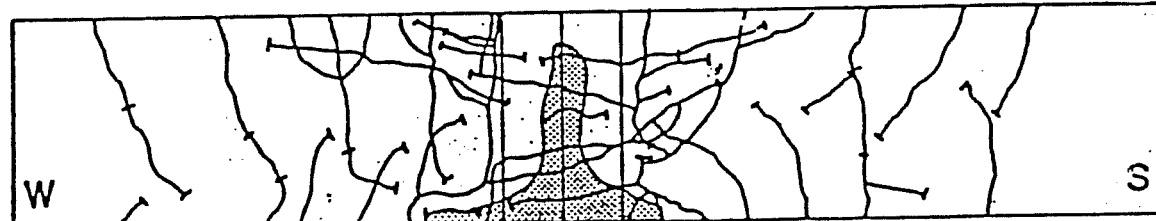
LS 12



LS 24



LS 68



LS 124

Figure 4-13: Cracking of the South and West Beams

imposed during the initial cracking cycle, the first flexural cracks began to open. These cracks were present not only in the tension side of the beams, but also in the column. Since no axial column was present, this cracking was expected although perhaps not this early in the loading history. At this stage, the North and West beams had already begun to separate from the joint, and the crack at the column face covered about 50% of the beam depth.

At LS 7, the first shear cracks began to form across the top of the SW and NE corners of the joint. The shear cracks were inclined at about 35 to 45 degrees, parallel to the line joining the top NW and bottom SE corners of the joint. This diagonal forms the centerline of the concrete strut that is probably carrying most of the shear at this stage. There was obvious separation of the beams from the column face at the West and North beams, as well as separation of the joint from the column at the top NW and bottom SE corners. The flexural cracks in the beams continued to extend and widen, while some shear cracks began to appear in the bottom of the South beam.

By LS 12, extensive cracking was present; it included flexural and shear-flexural cracking of the beams, the latter especially in the West beam, as well as shear cracking across the joint. Of particular importance, the column corners in compression began to crush, especially at the NW bottom corner of the joint.

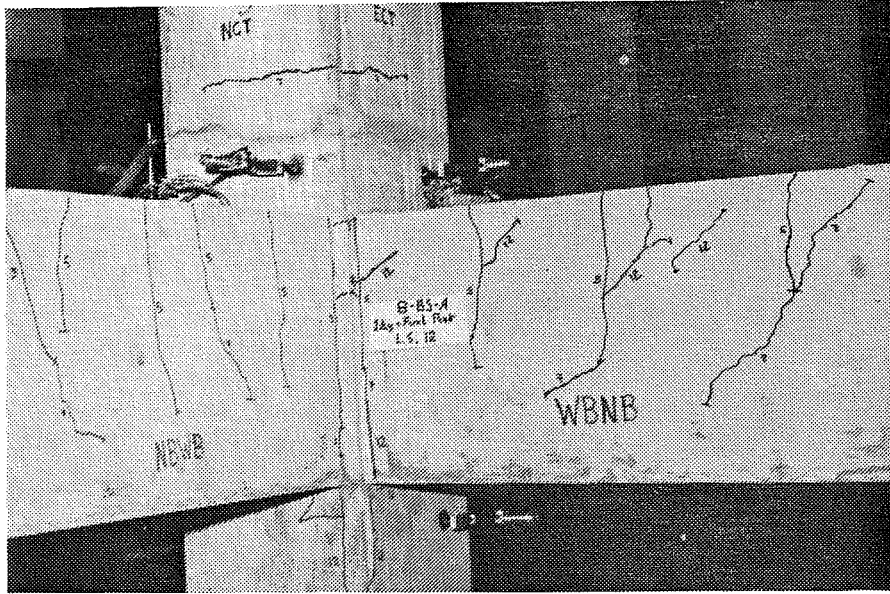


Figure 4-14 : Joint SW corner at LS 12

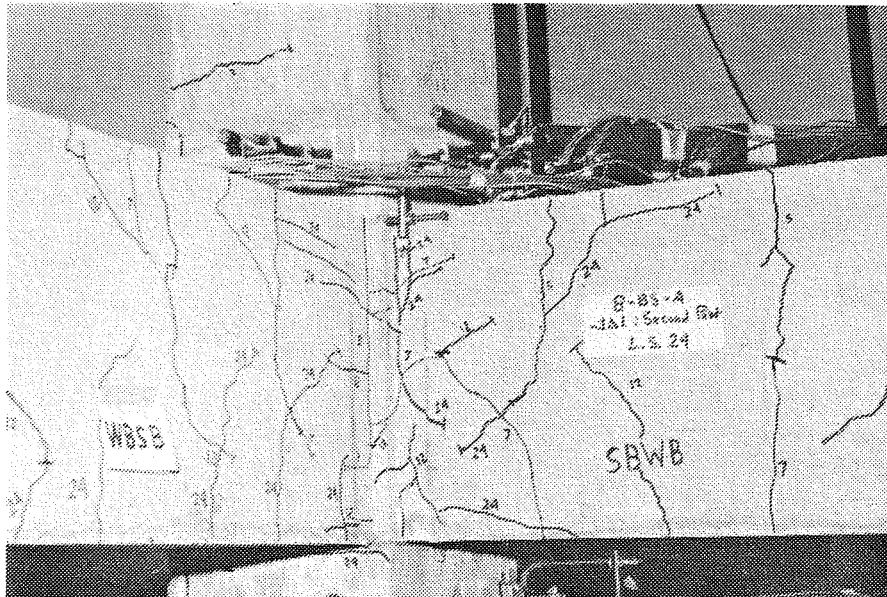


Figure 4-15 : Joint SW corner at LS 24

Meanwhile, flexural cracking of the column corner in tension progressed along the length of the column. The column never exhibited shear distress. The compressive blocks at the bottom of the North and West beams also showed some signs of crushing.

Upon reversal, to $-1\Delta_1$, the cracking described above began to take place in the opposite direction and resulted in a criss-crossing pattern of shear cracks near the joint. Flexural cracks extended across the beams. There was less flexural cracking when loading in this direction, but the cracks at the column face were wider. The column corners crushed at the top NW and bottom SE corners and the column tension cracks at the top SE and bottom NW corners were very wide. Both the beams and the column seemed to be yielding and forming plastic hinges at this stage. While the beam steel was yielding, the column steel was not. The large column rotation was a product of slippage of the longitudinal column bars due to cycling even before they yielded. According to the "weak-girder strong-column" design philosophy this type of behavior is to be avoided, since the columns are undergoing deformations beyond acceptable limits (2% drift). It should be emphasized that this did not seem to be a problem when the specimen was designed since the column had sufficient moment capacity to resist the biaxial flexural forces.

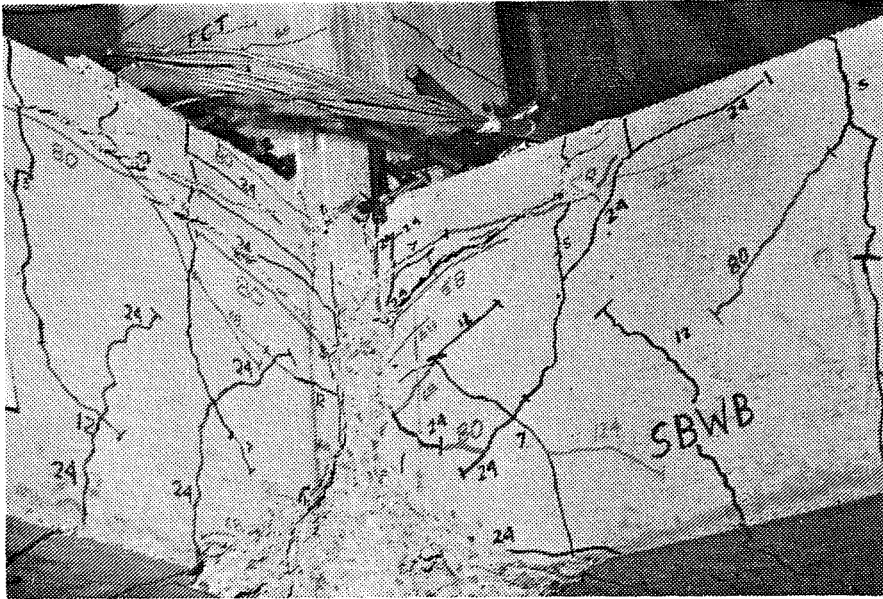


Figure 4-16 : Joint SW corner at LS 124

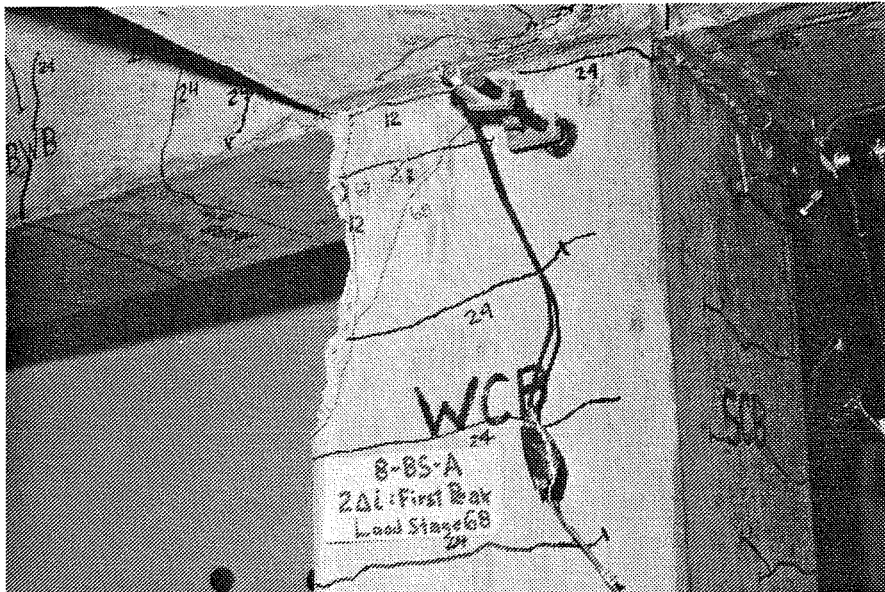


Figure 4-17 : NW bottom column corner

4.4.3 Second and Third Deflection Levels

Loading to the second deflection level, or about 2.7 inches from the dead load position, did not create any more significant flexural cracking in the beams. However, shear cracking near the joint became more pronounced and crushing of the compressive zones of the North and West beams was clear. Significant spalling took place in the column at the NW bottom corner of the joint; almost all the cover was lost at the column-joint plane and spalling extended downward about 12 in. as shown in Fig. 4-17. Moreover, the cracks at the column joint corners in tension became very wide, although still smaller than those at the beam-joint faces. Upon reversal, to $-2\Delta_1$, trends similar to those outlined above were observed. An interesting point was that splitting cracks along the top reinforcement of the South and East beam bars was observed near the joint at $+2\Delta_2$. At this stage the top bars of these beams were supposed to be in compression. The only possible explanation is that the bars were no longer anchored in the joint but on the beam on the opposite side. Under these conditions the tensile stresses produced by the bars in the compression zone could have generated the splitting cracks observed.

Loading to the third deflection level, or about 4.1 inches from the dead load position, resulted in little additional cracking. It must be pointed out that after the first excursion at the second

deflection level most of the cover had separated from the core in the critical regions near the joint and therefore crack patterns had little significance. However, spalling of the remaining column corners as well as crushing of the compressive blocks on all beams took place at the third deflection level.

It must also be noted that during the second and third deflection levels there were significant torsional forces in the beams. Although there were no measurements of these torsional forces, they were probably produced as a consequence of the very large deformations undergone by the specimens. The loading rams had spherical loading heads which allowed complete freedom of rotation in the plane of the applied load, and about 8 degrees in either direction in the out-of-plane direction. During the third deflection level the beams probably exceeded this value and the rams began to provide some torsional restraint to the beams.

A final important observation must be reported. It seemed that as cycling progressed, the size of the tension cracks at the beam-column faces varied from one side of the beam to another. Although no measurements were made, visual inspection at the latter load cycles clearly showed that the tension cracks were wider at the NE and SW corners of the beams than at the NW and SE corners. The latter coincide with the axis of loading, and indicate that the beams, due to both concrete crushing and spalling, were not confining

the joint evenly. At the peaks it seemed that the corners where the column was in compression offered better lateral restraint than the unloaded column corners.

4.5 Other Measures of Response

In this section a series of plots are developed to help understand the overall behavior of BCJ8. Joint shear strain, beam rotations, column rotations, and joint rotations are presented. The calculations necessary to derive these quantities from the measured displacements are shown in Appendix C.

4.5.1 Interstory Displacement vs. Joint Shear Strain

The plots of joint shear strain vs. interstory displacement for both principal directions are shown in Figs. 4-18 and 4-19. Both figures show an interesting feature of the joint shear strain; it is not strictly linear with lateral displacement as one would expect. At the top of each cycle, the strain stops increasing, and the curve becomes almost flat. This would seem to indicate that the shear deformation becomes "locked", and that the shear stiffness becomes very large. This increment in shear stiffness cannot be explained in terms of material properties since the shear resistance of the subassembly should decrease as the deflection, and therefore shear cracking increases. A better explanation is that as the beams (and perhaps the column) begin to yield, the plastic hinges become the

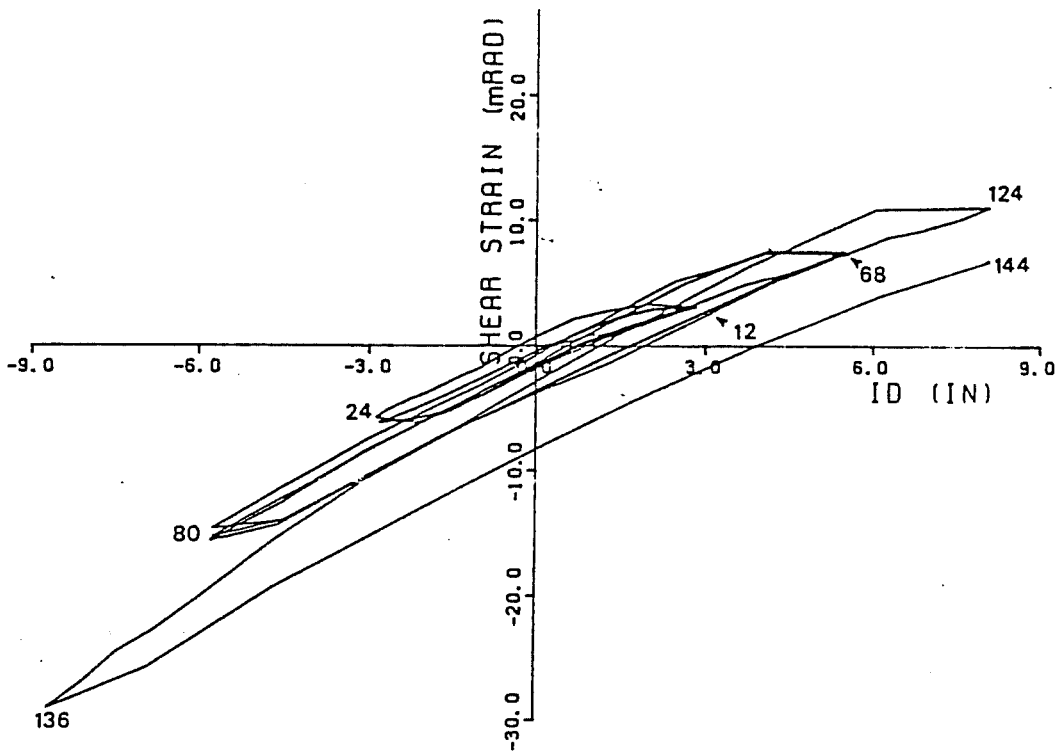


Figure 4-18: JSS vs. ID for North-South direction

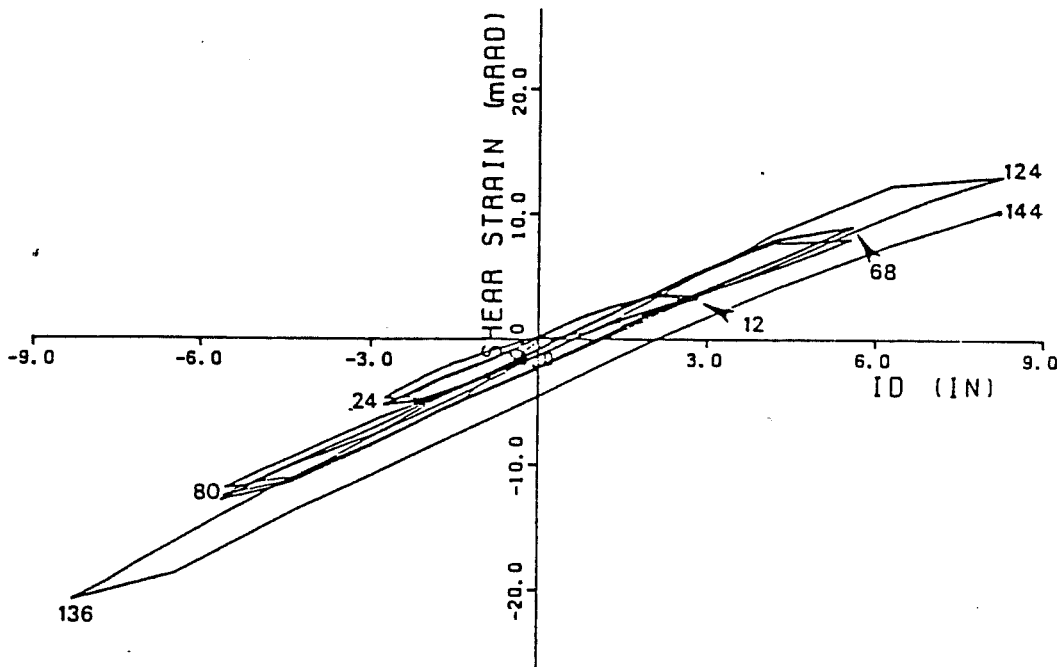


Figure 4-19: JSS vs. ID for East-West direction

main contributor to the beam end deflections. The deformation is thus taking the path of least resistance, and the shear strain remains constant until the peak is reached. The important point is that the shear strain is not linear with respect to either load or deflection, and that a certain amount of energy is being dissipated by shear strain deformations, as shown by Figs. 4.8 and 4.9 .

4.5.2 Joint Rotation vs. Interstory Displacement

An interesting comparison can be made between the plots discussed in the previous section and those for joint rotation vs. interstory displacement shown in Fig. 4-21. The overall joint rotation is linear with respect to displacement, and exhibits non-deteriorating behavior. Since the joint rotation includes the joint shear strain contribution, which is non linear near the peaks , the other components of joint rotation must also be non-linear in this area to compensate .

4.5.3 Column Rotation vs. Interstory Displacement

Since the elastic deformation of the column is proportional to the total beam end loads in the elastic range, the plot of elastic column deformation vs. interstory displacement is non-linear and very similar in shape to the curves in Figs. 4-4 and 4-5. The inelastic column rotation, shown in Fig 4-21, indicates that all the inelastic column rotation took place in the direction of initial loading. One

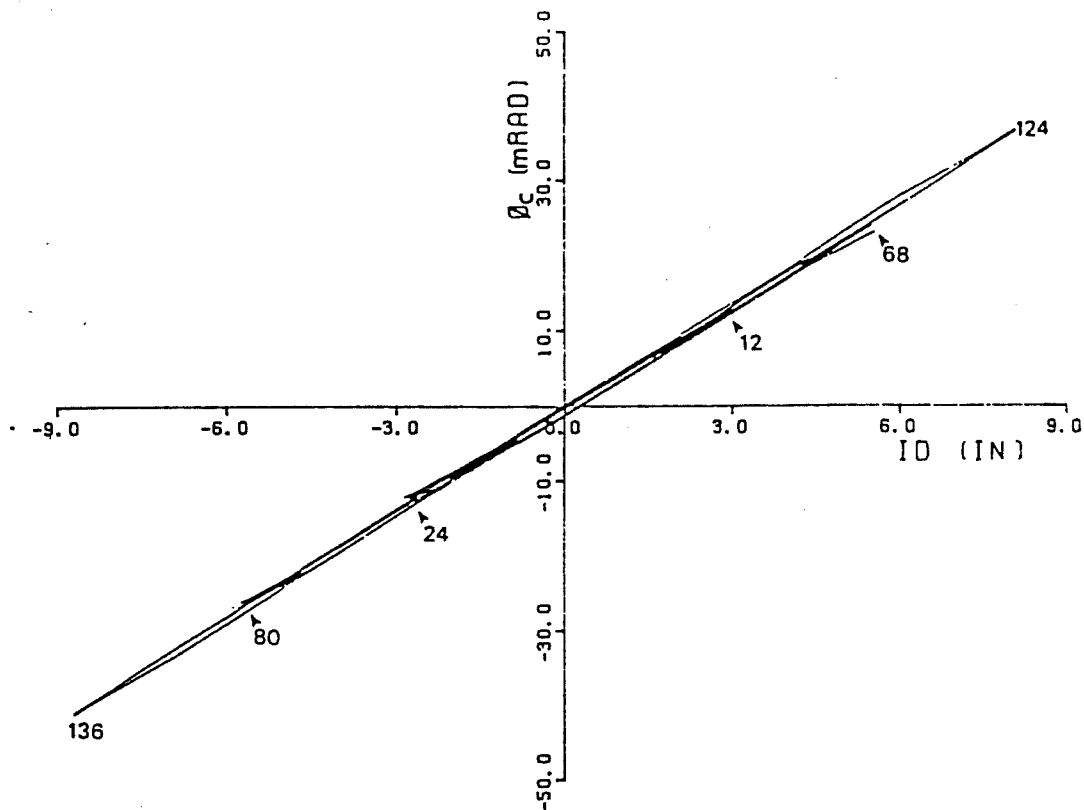


Figure 4-20: Joint rotation vs. interstory displacement.

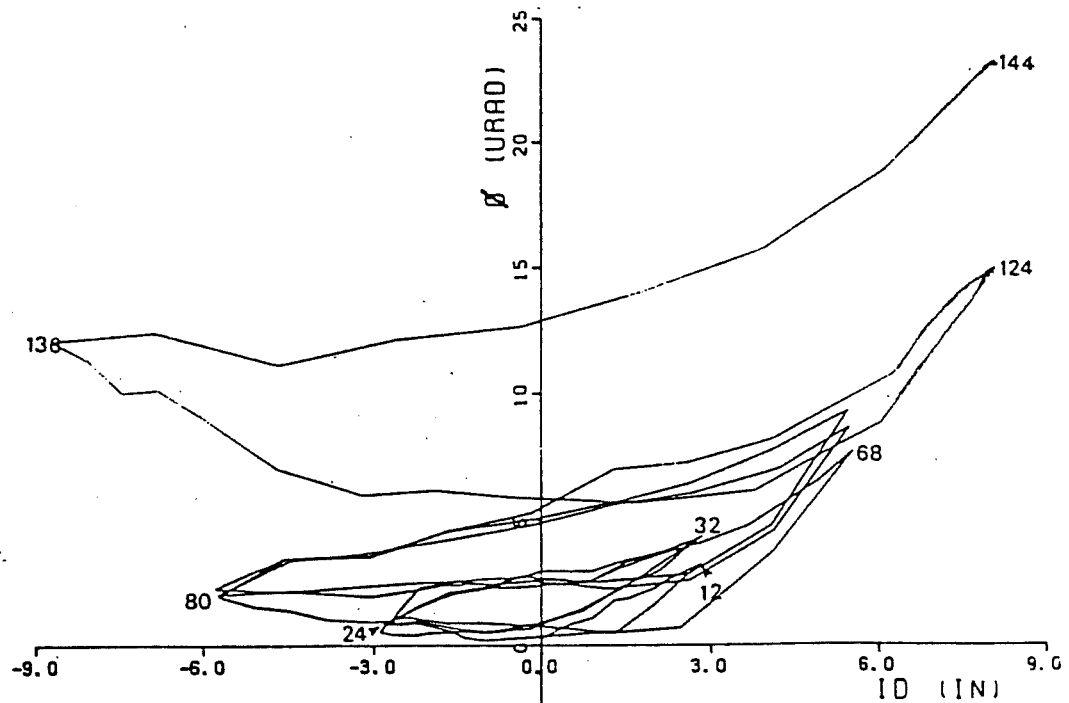


Figure 4-21: Inelastic column rotation vs. interstory displacement

must recognize that this does not mean that the column did not move in the opposite direction at all; it means that in the initial direction of loading, a large portion of the deflection was caused by this rotation. In the opposite direction, as shown in the previous section, most of the deflection was due to the large joint shear strains.

4.5.4 Beam Rotations vs. Interstory Displacement

The measured beam rotations, shown in Fig 4-22, are linear with respect to interstory displacement, indicating that the beams are not clearly developing plastic hinges as one would expect. If this were the case, an increasing slope with deflection should be evident as more and more of the deformation, and energy dissipation, is taken by the beams. Ideally the graph should show a bilinear trend, corresponding to the elastic and inelastic portions of the beam response.

4.5.5 Beam Longitudinal Displacement vs. Interstory Displacement

The mechanism proposed to account for the non-linear shear behavior implies that large cracks were opening at the beam-column interface and that the longitudinal beam bars were increasing in length. A measure of this phenomenon is given by Fig. 4-23, where the longitudinal displacement of the beam with respect to the joint is plotted. The longitudinal beam displacement is the average

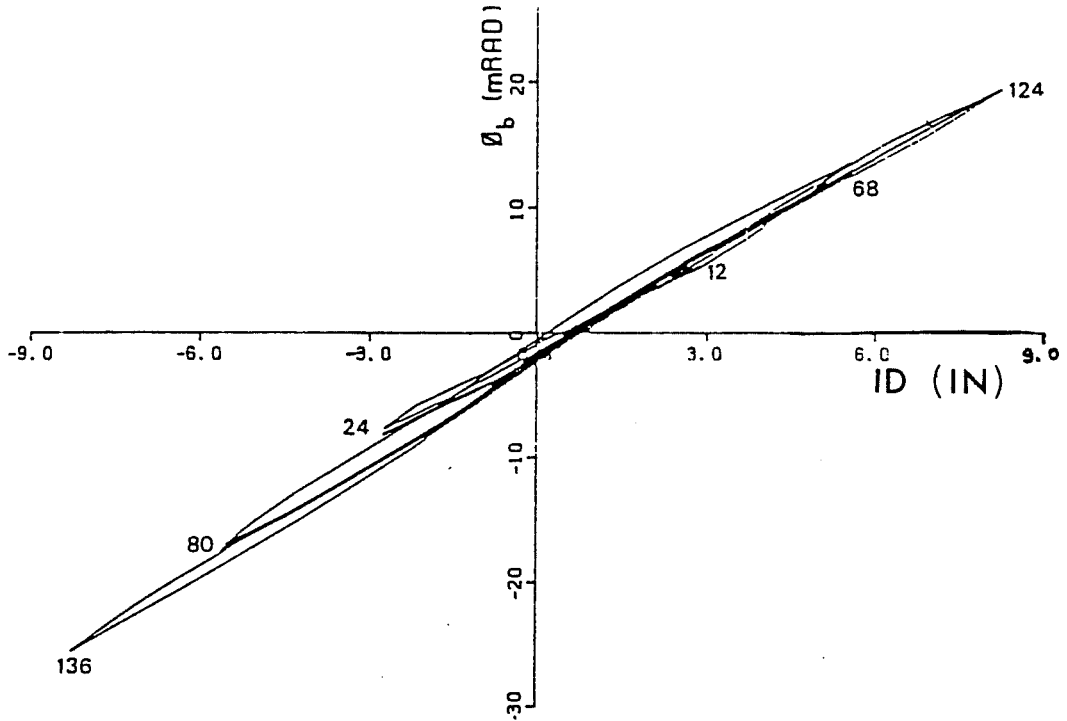


Figure 4-22 : Beam rotation vs. interstory displacement

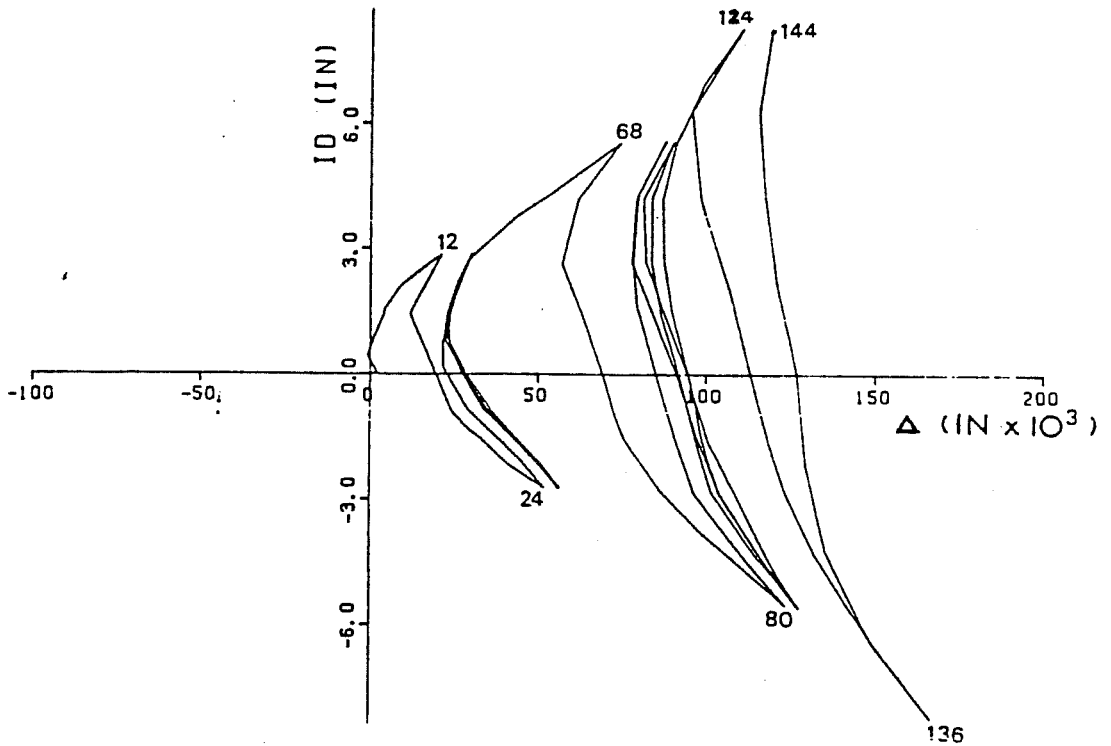


Figure 4-23 : Longitudinal beam displacement vs. interstory displacement

reading of the potentiometers measuring beam-to-column deformations. If this value is close to zero, it means that the beam is rotating rigidly about an axis at its mid depth; if the values are greater than zero, it means that the beam is moving away from the column face. As the plot shows, the beam moves away from the joint throughout the load history, and the residual deflections at the end of each cycle are essentially non-recoverable. The fact that similar behavior was observed in all beams indicates that the bars are not only slipping through the joint, but also increasing in length significantly due to yield penetration. It is problematic whether such increase in length would occur at all in joints in a continuous structure. In an isolated specimen the lack of continuity at the beam ends and slab boundaries makes such deformation more likely.

4.6 Reinforcing Bar Slip

Since it was anticipated that the longitudinal beam reinforcement might slip during reversed cycles to large deformations, the instrumentation shown in Fig. 3-11 was used to measure the longitudinal beam bar movement through the joint. The measurements obtained had to be corrected to account for joint and column rotations, as shown in Appendix C.

Slip were measured at the beam-joint face in three bars: the top longitudinal bars in the EW beam (South face) and NS beam (West

face), and the bottom longitudinal bar in the EW beam (South face). The slip measured at each side of the joint for the top EW beam bar is shown in Figs. 4-24 and 4-25. As can be seen, the magnitude of slip varies from about 0.06 inches at the first deflection level to 0.13 inches at the second and 0.20 inches at the third.

The measured slips indicate that the yield penetration and subsequent elongation of the bar caused the bars to slip away from the column face. The bars, moreover, never returned to their original position as cycling progressed. It became more and more difficult to close the cracks at the column face, as is evidenced by the pronounced losses of stiffness through the region near zero deflection as shown in Figs. 4-4 and 4-5.

For downward loading of the West beam ($+1\Delta_1$, $+2\Delta_1$, and $+3\Delta_1$), the amount of slip in the top bars on the West side of the joint was more than twice that measured on the East side. Based on the measured strains in the bars, the top bars in the East-West direction were in tension at both sides of the joint. At $+1\Delta_1$, the bar was yielding in the West side, and had a strain of about 0.005 on the East side. The bar had increased in length about 0.03 inches over the 15 in. column dimension, indicating an average strain of 0.002 across the joint. Although no gages were present on the bars within the joint itself, it is evident that yielding penetrated the joint very early in the load history, and contributed significantly to the loss of stiffness and strength.

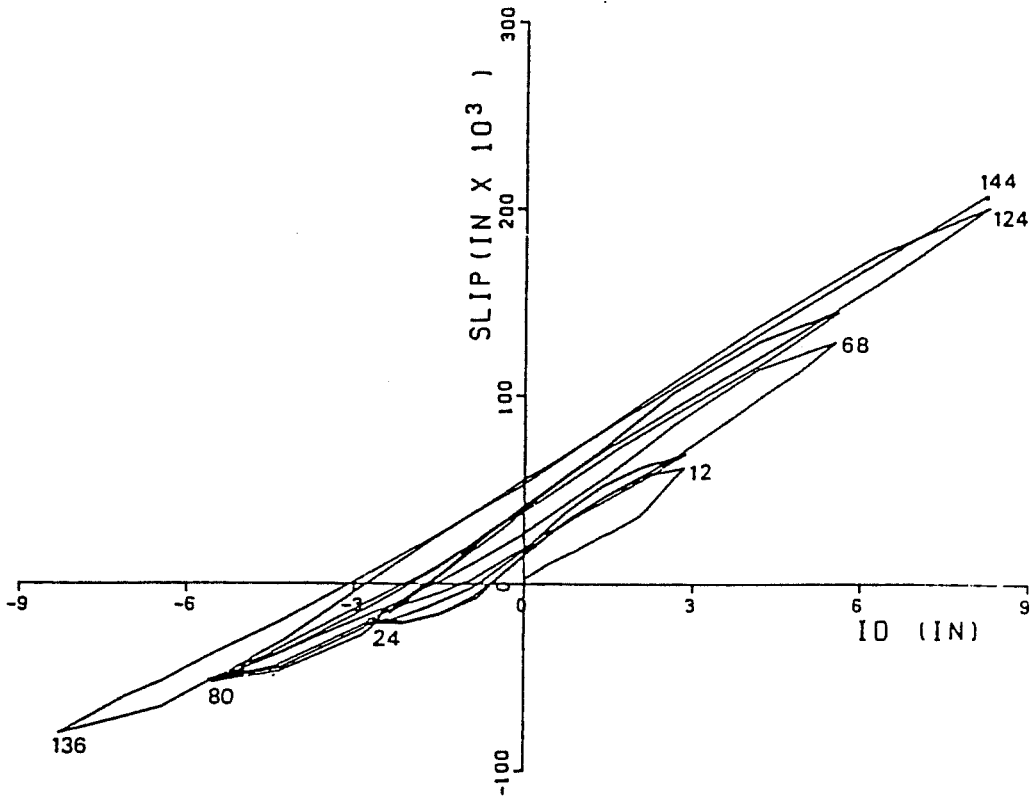


Figure 4-24: Slip vs. interstory displacement - Top bar, West

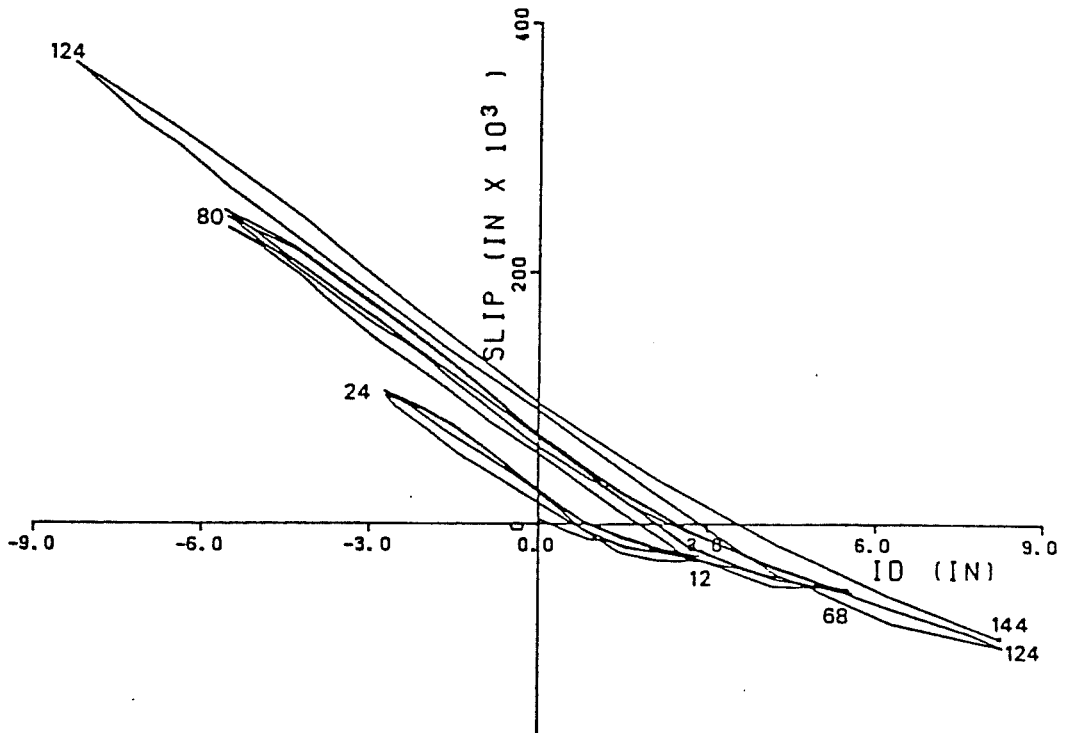


Figure 4-25: Slip vs. interstory displacement - Top bar, East

4.7 Reinforcing Bar Stresses and Strains

Strains in the bars and joint ties were measured using strain gages at the locations shown in Fig. 3-11. The stresses were obtained using a conversion program developed by Longwell [60] that utilizes Thompson's method for calculating steel stresses in bars subjected to cyclic, inelastic loading [104]. It must be pointed out that the measurements provided by the strain gages adjacent to the joint are suspect because of local effects; the joint distortion and beam inelastic rotation at this position might have created local bending in the bars, and thus masked the true measurements.

4.7.1 Beam Bars

The strain profiles along the longitudinal beam bars through the joint area for the first loading cycle are shown in Figs. 4-26 and 4-27. As can be seen, a fairly uniform increment in strain with increased deformation was observed when loading to $+1\Delta_1$ (or LS 12), with yielding occurring at LS 11 on the West face of the joint. The plot clearly shows that the steel across the joint was always in tension. Bond stresses reached values as high as 1000 to 1200 psi. The fact that the bars were in tension across the joint clearly show that compatibility was lost in this area. However, this compatibility was restored at the second gage (8 in. from the joint face), where the bar in the East side is again in compression. The bottom bar appeared to have yielded considerably more than the top

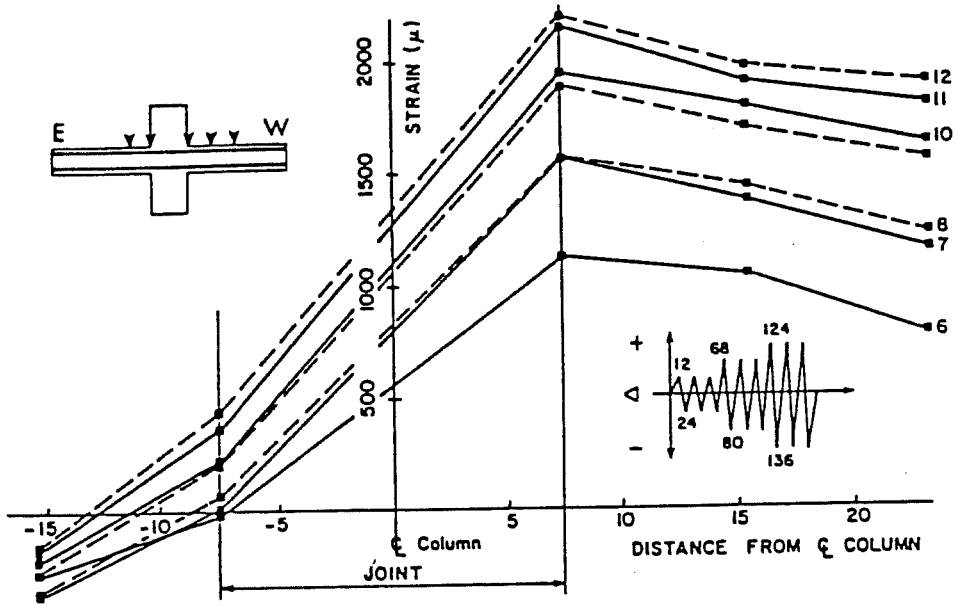


Figure 4-26: Strain profile - Top East-West bar

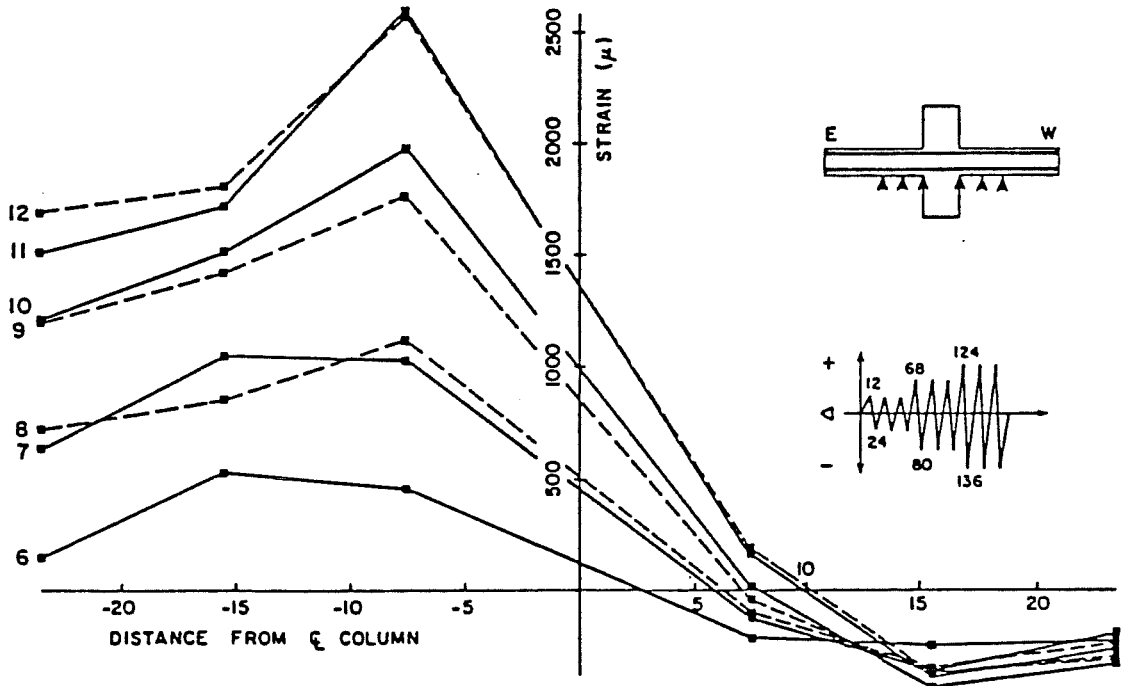


Figure 4-27: Strain profile - Bottom East-West bar

one, although yielding for both began at about the same interstory displacement. The bottom bar withstood cycling much better than the top one. This seems reasonable given the smaller diameter of the bar, and therefore the more favorable bond conditions. This level of performance was also probably influenced by the fact that through large parts of the load history the top bars in the East-West direction were not in the compression zone of the beam. The bars were centered about 3.375 in below the compression edge fiber, while the depth of an equivalent compression block at ultimate would be only about 1.80 in. below the compression edge fiber.

The stresses for the same top bar gages for the latter load stages are shown in Figs. 4-28 and 4-29. These plots clearly show the rapid breakdown of bond near and inside the joint. For the top bar on the EW beam, extensive yielding was evident in the West side at L.S. 12; when the opposite peak, L.S. 24, was reached the bar was in tension not only in the East side, but also for about 16 inches from the joint face in the West side.

A typical stress vs strain relationship is shown in Fig. 4-30, for a gage at the joint face in a bottom bar of the East beam. After a small amount of compression was recorded during the application of the dead load (LS 3), a stress reversal took place and the bar began to pick up tension as the East beam was deflected upwards. The beam reached yield at about LS 10, and entered the

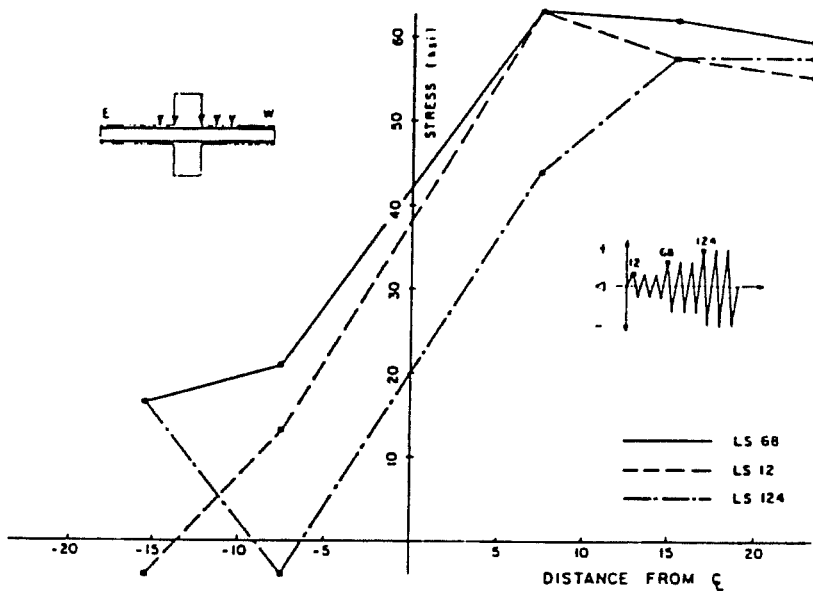


Figure 4-28 : Stress profiles - Top EW bar - Positive peaks

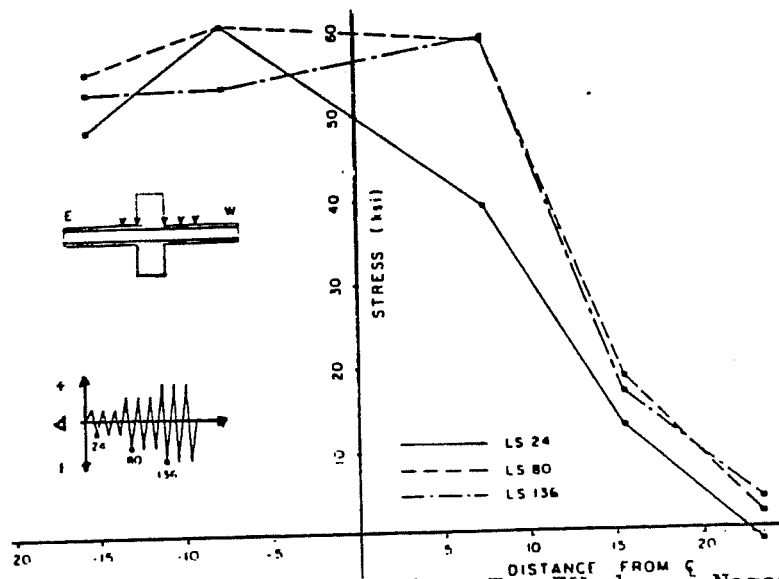


Figure 4-29 : Stress profile - Top EW bar - Negative peaks

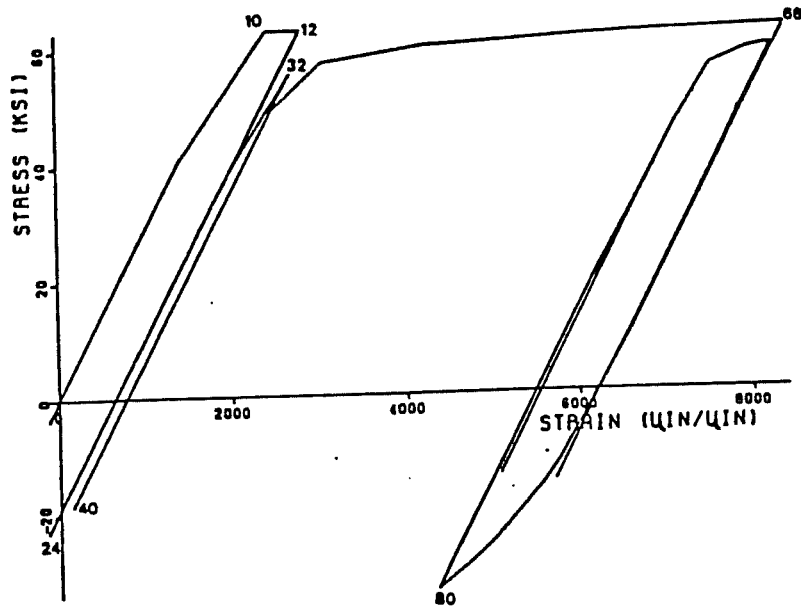


Figure 4-30: Stress vs. strain for BEBN .

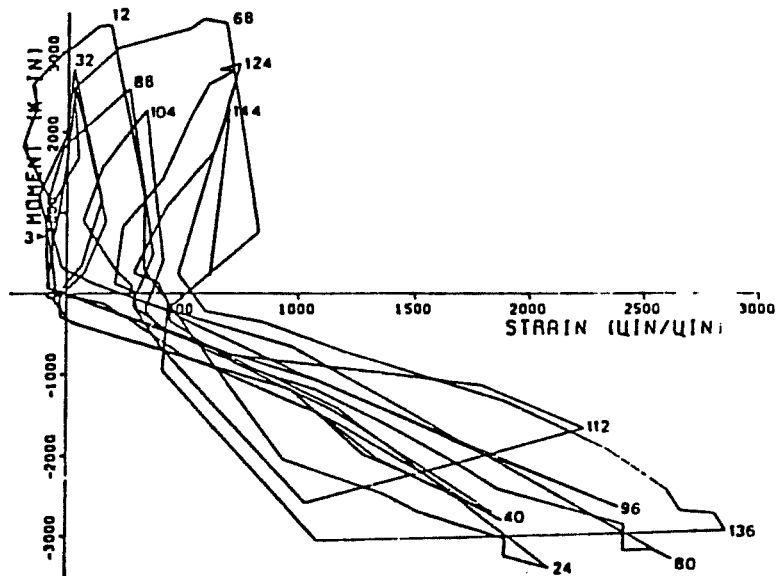


Figure 4-31: Moment vs strain curve for BWBN .

yield plateau. Upon reversals of load (to L.S. 24) bar went into compression, and additional cycling at the first deflection level resulted in slightly more yielding. Loading up to L.S. 68 caused considerable yielding; further cycling resulted in the formation of the typical stress-strain curve for steel subjected to cyclic loading. Note that because the conversion program uses a Ramberg-Osgood relationship, the stress does not quite reach the initial yield value after cycling.

In Fig. 4-31, a typical strain vs. moment curve is plotted. As can be seen the steel was under some initial compression due to application of the dead load. As the cycling began, the beam began to move downwards, and the bar picked up additional compression, although it is clear that the concrete was carrying most of the compressive force at this stage. As the first peak approached, the bar began to lose compression, as yield penetration from the other side of the joint began to create some tension. With further cycling the bond in this bar began to deteriorate and throughout the rest of the load history the bar was seldom in compression, except for some load stages near the zero deflection point. The slight compression was due to the fact that the cracks had not fully closed and the steel alone was acting as a couple to carry all the load.

4.7.2 Column Bars

The strains in the column bars were measured using resistance strain gages at the top and bottom joint-column face in the four corner bars; additionally, the NW corner bars were instrumented at 8 in. and 16 in. from the joint face. Unfortunately, because of the vibration required during casting, many of the column gages were destroyed. The plots of column bar strain versus moment resultant are shown in Figs. 4-32 and 4-33, for the NW corner bar.

The behavior of this bar, after the first load cycle, is very similar to that of the beam bars already examined. For the initial cycle, the bottom bars were in compression. A strain of 0.0005 (about 15 ksi compressive stress) in the steel would indicate that the extreme concrete fibers are highly strained, and thus the observed crushing in the corner at latter load stages was to be expected. After the first cycle, the portion of the bar below the joint appeared to loose compatibility, and showed a very slight compression only in the first cycle at each deflection level. The upper part of the bar was in tension, and came close to yielding during the first cycle. Under reversal of the load, this section of the bar went into a small amount of compression, a situation that was not repeated as cycling progresses.

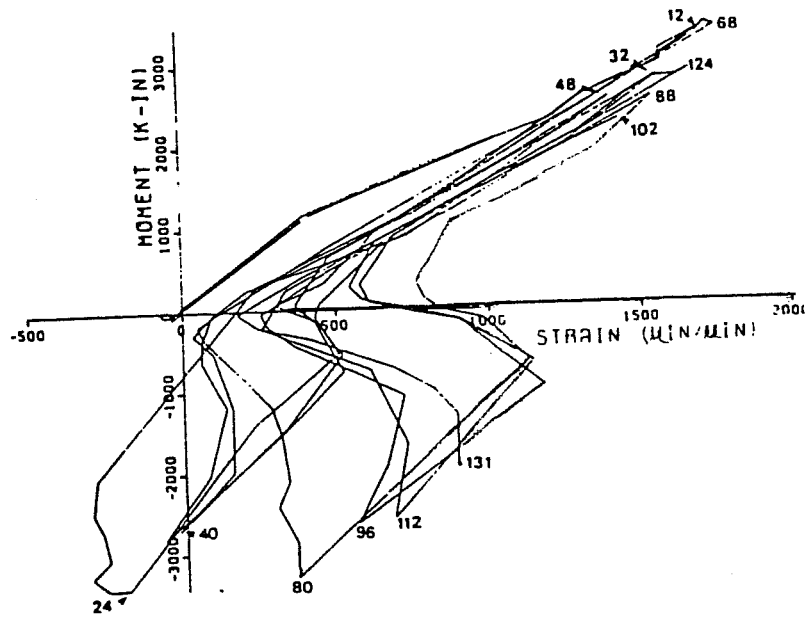


Figure 4-32: Stress vs. moment resultant- NW column bar top .

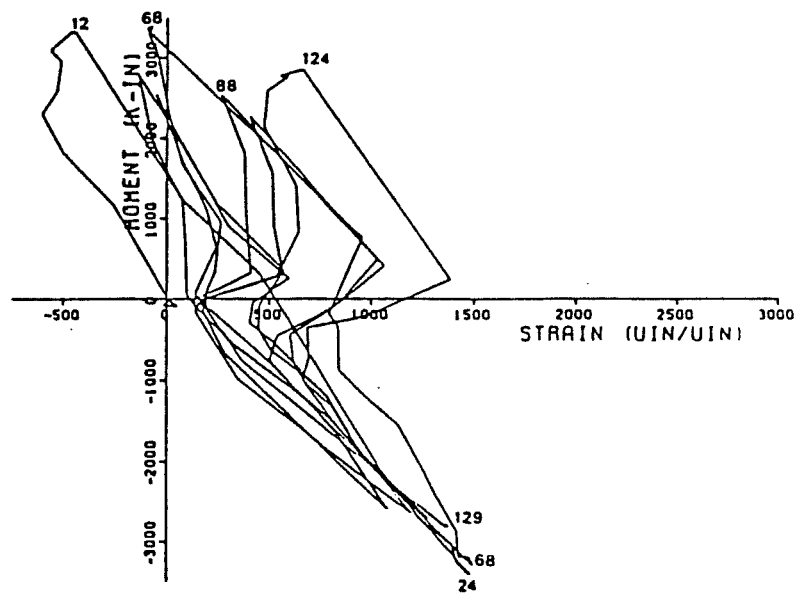


Figure 4-33: Stress vs. moment resultant- NW column bar bottom .

4.7.3 Joint Ties

Strain was measured by gages in each leg of the two ties present in the joint. The gages were located on the outside of the ties to prevent accidental destruction when the beam cages were placed into the column cage during construction and during concrete placement. Therefore it is impossible to determine what amount of the strain corresponds to elongation of the joint tie or to local bending because of the bulging of the joint core.

The initial shear cracking of the joint, from the measurements obtained, seems to have occurred between load stages 5 and 6 when a large jump in strain was observed. The plots for the stresses in the ties versus interstory displacement for the top and bottom legs on the North side of the joint are shown in Figs. 4-34 and 4-35.

During the first cycles of loading the tensile stresses of the ties remained locked in when the specimen was returned to the original position. A possible explanation is that cracks which had opened could not be closed immediately because small concrete particles lodged in the open cracks. However, as cycling continued, the amount of locked tensile stresses decreased, and eventually compressive stresses were achieved. It may be that as the cracks grew larger, inelastic elongation of the ties occurred. When the load was reversed some local compression was created by bending of the ties.

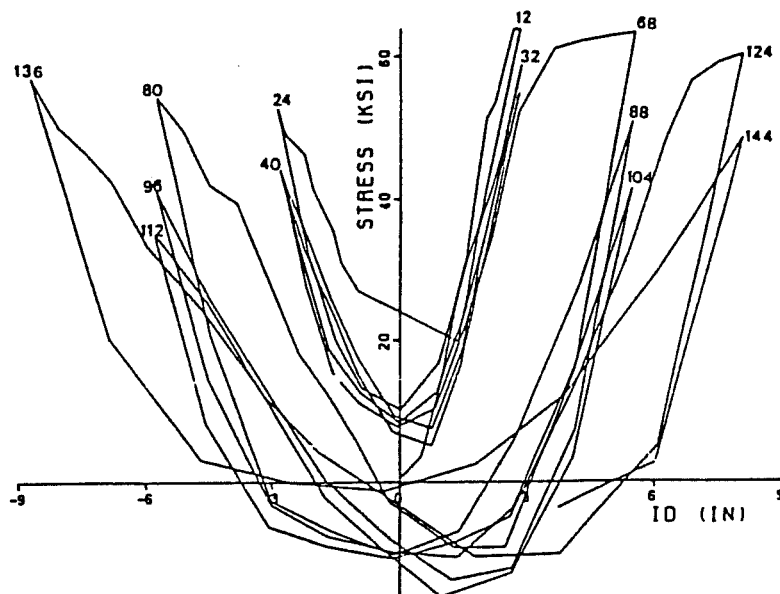


Figure 4-34: Stress vs. ID - Top tie, North

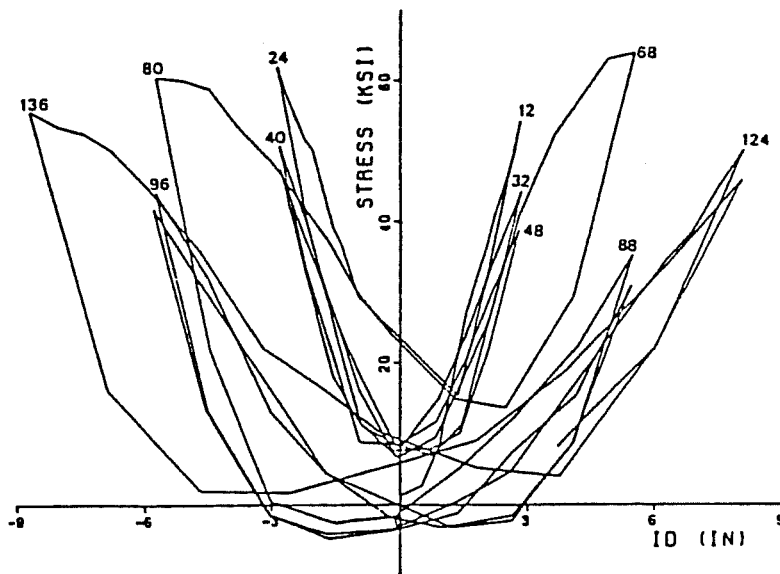


Figure 4-35: Stress vs. ID - Bottom tie North

4.8 Components of Displacement

At the beginning of the test series it was decided that investigating the stiffness behavior of the specimens would probably yield the most significant data. Therefore, it was decided to try to separate the amount of deflection that could be attributed to each of four mechanisms at each load stage. Appropriate instrumentation was designed and installed in the specimen to accomplish this task (See Appendix C). The mechanisms selected were flexural deformation, inelastic beam rotation, inelastic column rotation, and joint shear strain, as shown in Fig. 3-10. In this section the calculated data obtained for BCJ8 and its importance will be discussed.

4.8.1 Definitions of Components

Since the definitions given to each mechanism might differ from those commonly assumed, a complete definition of each will be given here :

- Total flexural deformations - refers to all the elastic flexural deformations in the subassemblage. It includes both beams and column, and is calculated from equilibrium conditions using the loads measured during the test.
- Inelastic beam measured rotation - refers to the measured rotation of the longitudinal beam with respect to the joint. It includes the elastic and inelastic deformations over a length of half the beam depth on each side of the joint. However, elastic deformations will be small over such a short distance.
- Inelastic column rotation - refers to inelastic deformations at the column-joint interface, and includes

yielding of the bars, slippage of the column bars and loss of section due to spalling and crushing. This quantity was not measured directly; it was determined from the measured and calculated deformations.

- Joint shear strain - this is a direct measurement, and refers exclusively to the deformation of the joint due to shear alone.

* The reader is cautioned that the importance of this data is more qualitative than quantitative. The data is useful to make comparisons between the relative contributions of the different mechanisms, and to give an idea of their magnitude. It should not be interpreted to represent an exact measurement of all the defined components, since the summation of all measured and calculated contributions fell between 0.85 and 1.15 times the measured beam end deflection for load stages near the peak of each load cycle.

4.8.2 Beam End Deflection Components

The first component calculations were done for the individual beam deflections as shown in Appendix C. The results, shown in Fig 4-36, are presented as ratios of calculated contribution of each mechanism versus measured end deflection.

Several trends are clear from this plot. The contribution of the flexural deformations decreased as the beam end deflections increased; this was logical since the elastic contributions were a function of the beam end loads. The maximum values of the loads are about constant at the peak deflections while the beam end deflections are increasing. Thus, the ratios of elastic to total deflection components must decrease.

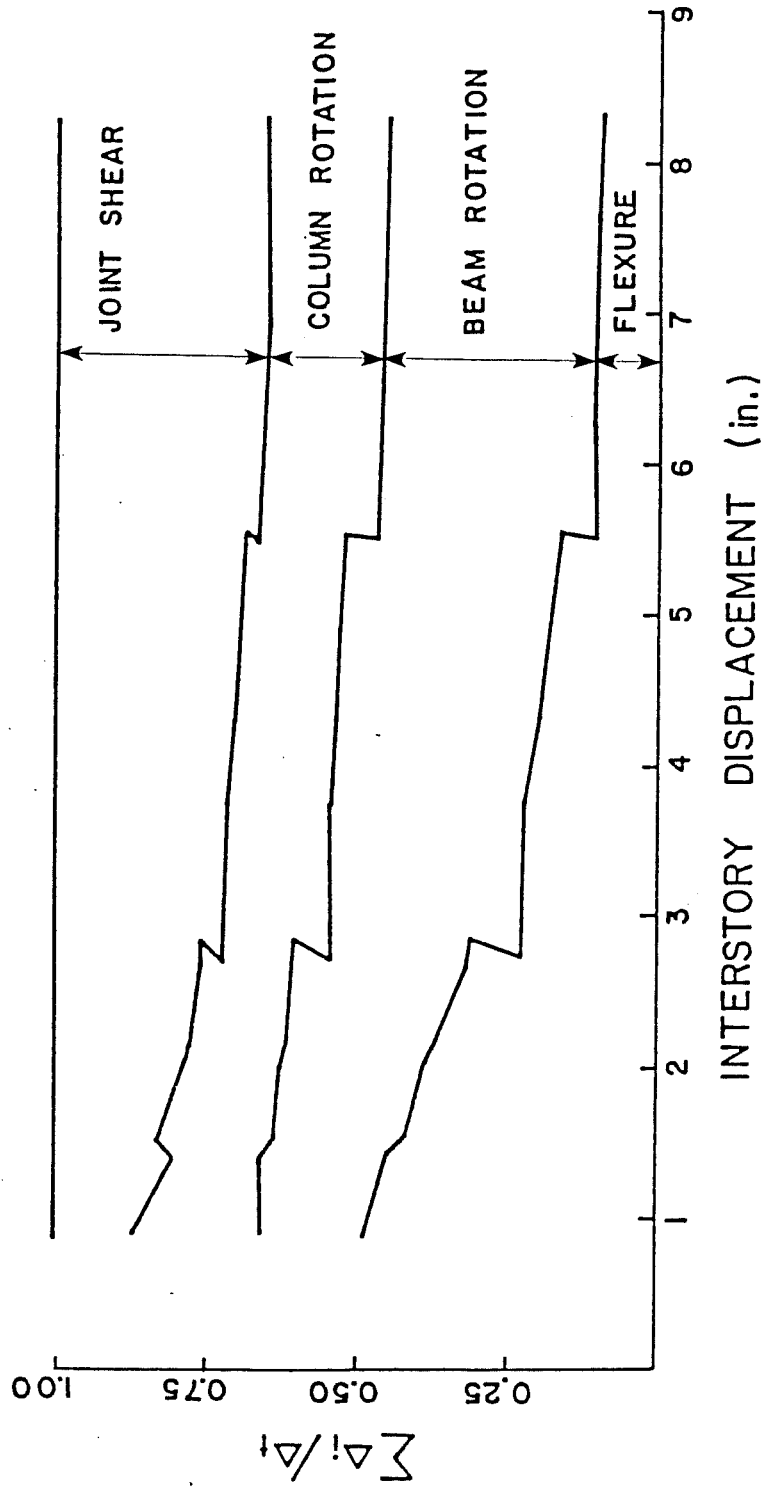


Figure 4-36: Contributions to East beam deflection (BCJ8)

The amount of inelastic beam rotation increased as the first peak was reached since the bars had begun to yield and plastic hinges were being formed. The contribution increased from about 18% at 0.5 inches to 30% at LS 12, to 36% at LS 68, and seemed to level off at about 35% for all the third deflection level (LS 120-172).

The contribution of column rotation was much larger than expected; it was between 18% and 25% for the first deflection level, and remained at that level for the rest of the load history.

The second largest contribution was that of joint shear strain. Its contribution increased steadily from about 15% at LS 7 to 35% at the end of the test. Thus the joint is progressively less rigid with cycling particularly after it cracked in shear.

4.8.3 Interstory Displacement Components

The contributions described in the preceding section referred to a single beam. The individual contributions to the interstory displacement were then calculated. For this purpose it was assumed that the contributions of shear strain and column rotations were the same for both beams in each direction, while the elastic deformations were calculated from the measured beam loads. Finally, since the beam rotations were measured only on one side of the joint, the difference between the summation of all computed deflections at this point and the total interstory displacement was ascribed to the beam

rotation in the negative direction. It should be noted that the interstory inelastic beam rotation arrived at by this scheme is about twice that of the single beam, and thus a reasonable quantity. To further simplify the results, it was decided to average the contributions over the first cycle, that is averaging the first positive and negative peaks.

The individual contributions are shown in Figs. 4-37 through 4-40, in which the computed values are shown for both the first and second cycles at each deflection level. These results are presented this way to highlight several important points; while the contributions of the elastic and inelastic beam rotations remained the same for both the positive and negative peak deflections, the column inelastic rotations and the joint shear strain showed dramatic differences. For the positive peak the column inelastic rotation always provided a positive contribution to the interstory deflection, for the negative peaks, past the first deflection level, it was mostly a negative contribution. This is not an unreasonable result if we recall that the column rotation is calculated by subtracting the elastic deformations and the joint shear strain from the total joint rotation. Moreover, it is supported by the fact that less serious cracking was observed in the column in the negative direction than in the positive one.

Perhaps as interesting are the observations to be derived

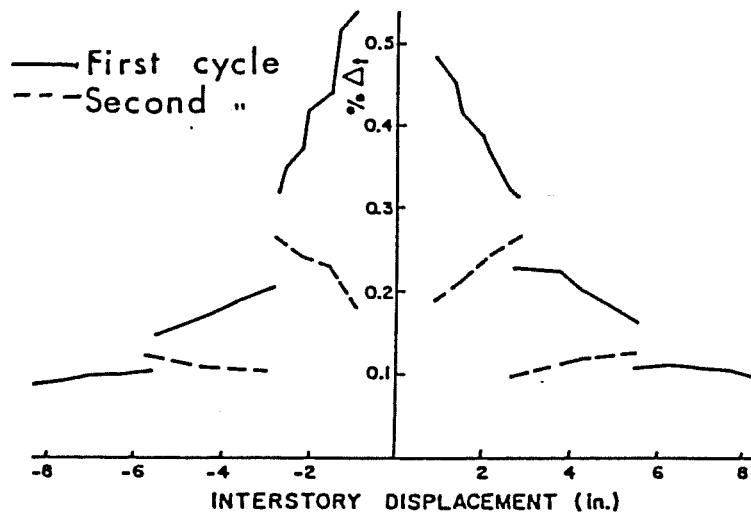


Figure 4-37: Contribution due to elastic deformation. .

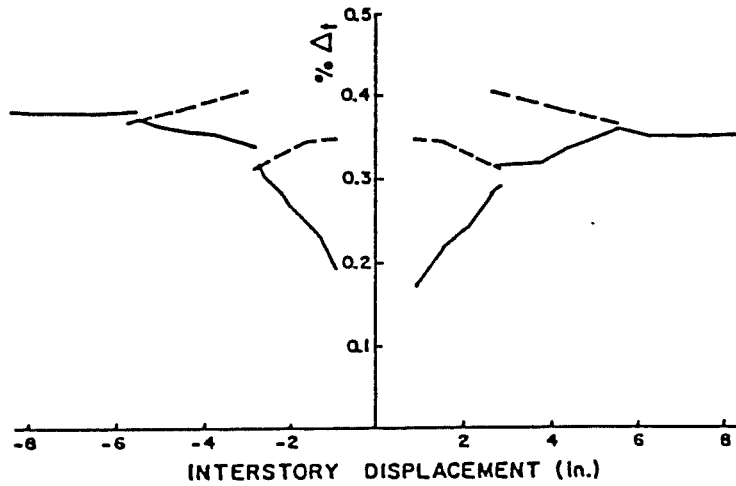


Figure 4-38: Contribution due to beam inelastic rotation. .

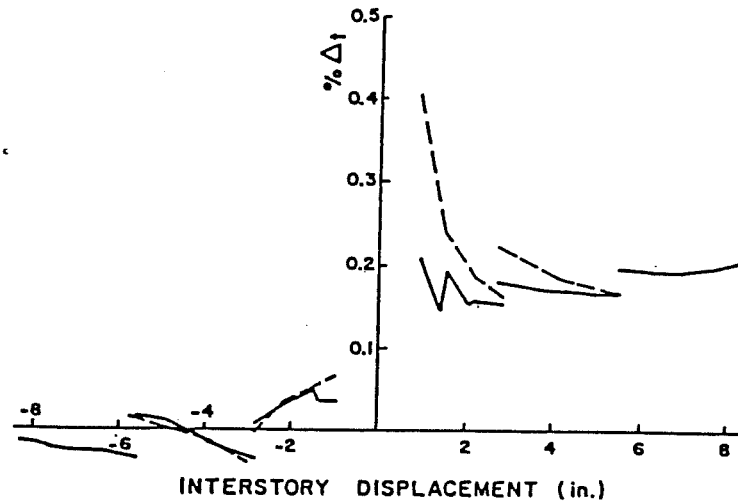


Figure 4-39: Contribution due to column inelastic rotation..

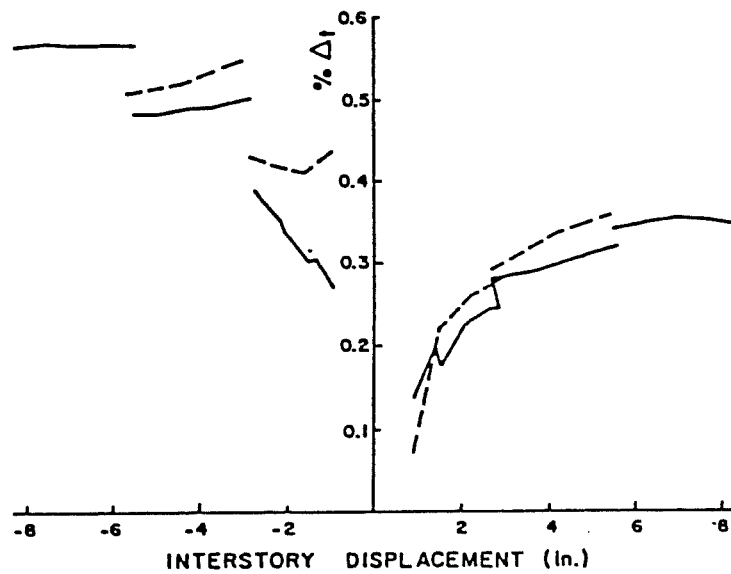


Figure 4-40: Contribution due to joint shear strain. .

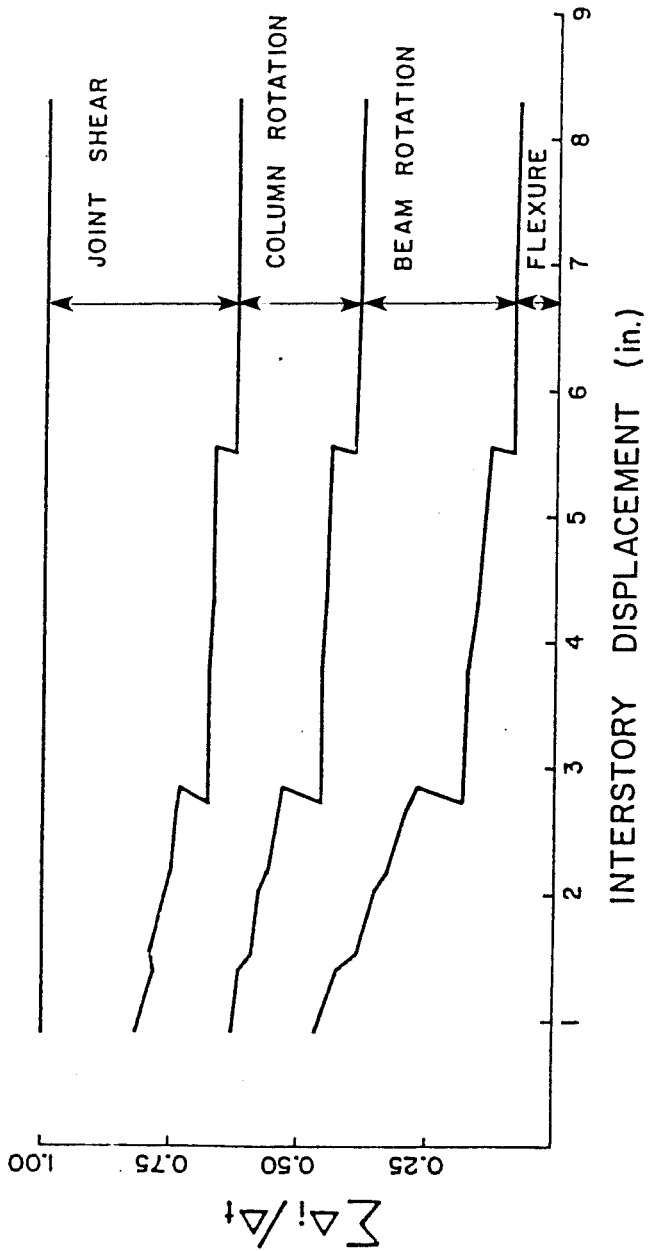


Figure 4-41 : Components of interstory displacement- East-West direction

from the contributions at the second peaks of each deflection levels. Due to the loss of strength between the first and second cycles, the elastic contribution at the peak decreases somewhat; the low values at the beginning of the reloading in each direction are a function of the loss of stiffness of the subassemblage. Most of the difference is then taken up by the inelastic beam rotation, especially at the beginning of each reloading cycle. The joint shear strain and the column rotation contributions do not change very much between the first and second cycles at each deflection level. The second cycle at the last deflection level is not plotted because the specimen was so damaged that the instrumentation was reflecting local effects more than overall behavior.

4.9 Summary

The experimental results for BCJ8 seem to divide the test into two phases. The first comprises the first deflection level, in which the specimen behaved well with respect to flexural and shear strength. The losses in stiffness and energy dissipation were significant, but the subassemblage was able to carry the loads without much visible distress. The second phase, when the uniaxial drifts exceeded 2%, indicates that the joint can be expected to achieve the necessary shear strength at even very large deformations but that the stiffness and energy dissipation capacities will likely have deteriorated beyond acceptable limits.

Chapter 5

Description of Other Tests

5.1 Introduction

In this chapter the behavior of the other specimens will be examined. The remaining tests can be divided into three series, according to the geometric parameters which were varied. The first series was aimed at clarifying the effect of the size of the framing beams, with the beams covering 60%, 86%, and over 100% of the joint face. The second series dealt with the influence of a slab the behavior of an interior beam-column joint, and consisted of two specimens with slab and one without a slab. The third series consisted of the two exterior joint specimens, one with and one without floor slabs.

All the specimens were subjected to the same load history as BCJ8, and had similar reinforcement details. Unfortunately, it was not possible to carry out all the tests with bars having the same bar deformation patterns or stress-strain behavior. After careful analysis of the data, however, it is clear that these variations did not lead to significant differences in behavior. Thus, it is possible to make meaningful comparisons among all tests conducted.

5.2 Effect of Beam Size

It has been hypothesized by several researchers [70, 71] that the size of the beam framing into a joint should have an impact on joint behavior. Tests on uniaxially loaded specimens with stub beams or unloaded perpendicular framing beams have shown better shear behavior than specimens without any structural side confinement. Moreover, the size of the member introducing the shear into the joint may have an impact on joint behavior especially if the beams have very different dimensions from those of the column.

In fact, in the ACI-ASCE Committee 352 recommendations, a decrease in shear capacity attributed to the joint is not necessary if the framing members cover more than 75% of the joint face. This ratio will be referred to as the area ratio. This specification was primarily based on engineering judgement and has never been fully verified with experimental data for the biaxial loading case. Three specimens were designed to cover as large a range of lateral beam sizes as possible. The control specimen had beams covering about 86% of the joint face, and was designated as BCJ5. The specimen designated as BCJ11 had narrow beams, covering slightly less than 60% of the joint face, while BCJ12 had beams whose width exceeded that of the column by 20%.

All the specimens in this series were tested with a column axial load of about 300 kips, a value very close to the balance point

axial load for the column. The effect of the axial load on the overall stability of the system (P-delta effect) was added mathematically after the test. Since the specimen was loaded by moving the beam ends and not the column, it was stable throughout the test.

5.2.1 BCJ5 - Control Specimen [Area Ratio = 86%]

5.2.1.1. Behavior of Test Specimen

The total moment vs. interstory displacement for BCJ5 is shown in Fig 5-1. This plot shows that there was a significant stiffness deterioration during the first cycle at any deformation level, just as observed in BCJ8. The second and third cycle at each deformation level were characterized by severe pinching of the hysteresis loops, which would indicate that joint shear distortion and/or reinforcing bar slip were a major influence on the behavior of the joint. If the additional moment due to the axial load (P-delta effect) is incorporated into the calculations (Fig 5-2), it is clear that deformations to the first deflection level would be sufficient to create stability problems if substantial axial loads were present.

Although there was degradation of stiffness under cycling at $1\Delta_1$, the beam loads did not reach their calculated ultimate loads until the beams were deformed to $2\Delta_1$ (see Fig. 5-3). At $3\Delta_1$, however, strength degradation was evident as the beam end loads were

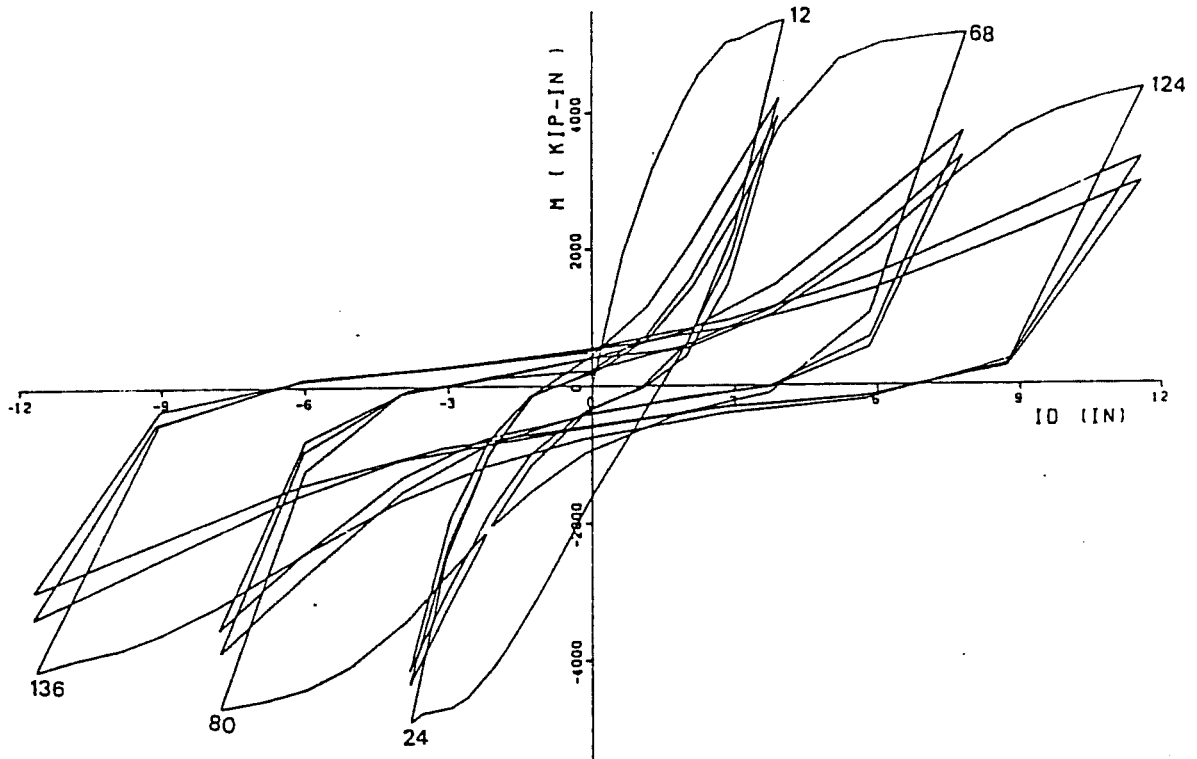


Figure 5-1 : Total moment vs. intersory displacement (BCJ5)

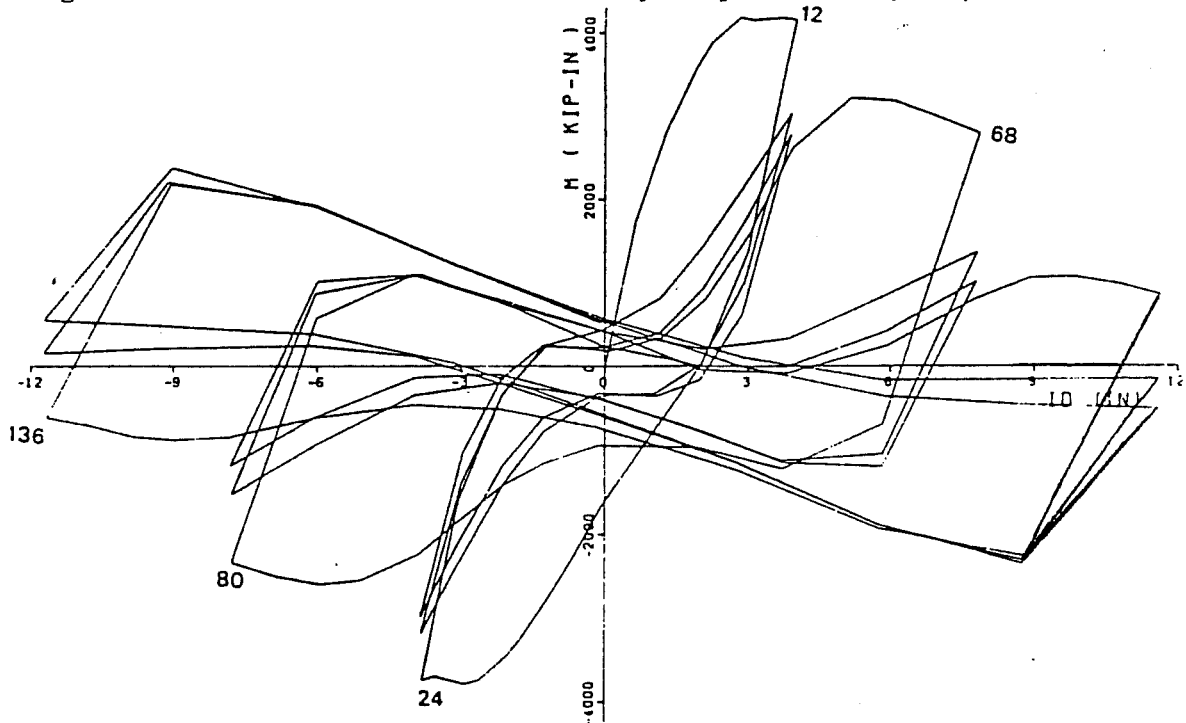


Figure 5-2 : P-delta correction for BCJ5

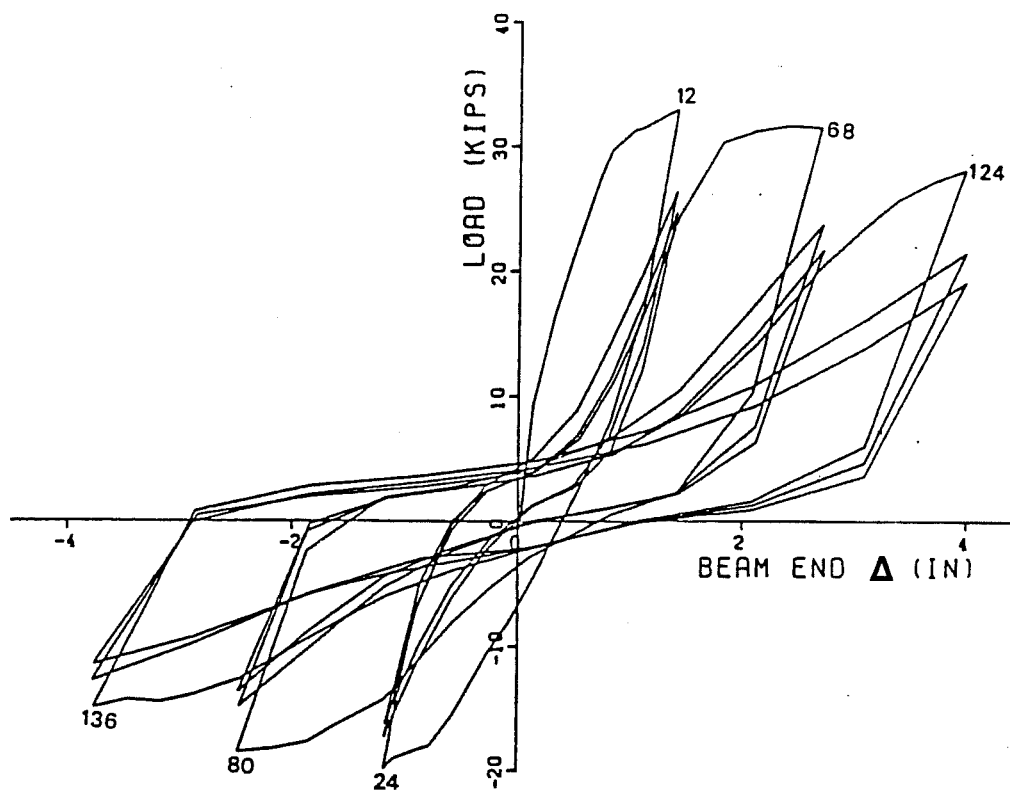


Figure 5-3 : Beam load vs. beam end deflection - West - BCJ5

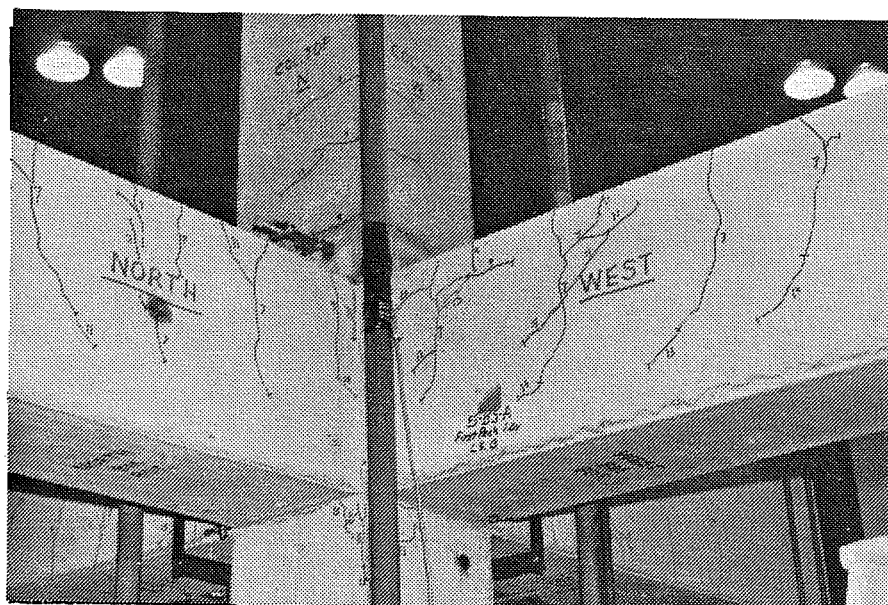


Figure 5-4 : Shear cracking at joint - LS 12 - BCJ5

well below their calculated strengths. The initial direction of loading influenced the strength of the beams when the loads were reversed. The beam loads were always less than the calculated strength at the first negative peak (LS 24, 80, and 136) at any given deformation level. This may be due to degradation of bond of the tensile reinforcement during the initial excursion, so that the reinforcement was not effective in compression when the load was reversed. A better explanation is that the degradation of the bond through the joint, as well as yield penetration, produce tensile stresses in the steel embedded in the compression zones of the beams. The result was that the moment arm, and thus the moment capacity, decreased. It also resulted in higher compressive stresses in the concrete and led to longitudinal cracks along the bars in the compressive blocks in the beams. Similar behavior can occur in the column, and may explain the unexpectedly high deformations observed in the column at the column-joint face.

The first shear cracks were observed at the NE and SW corners of the joint at LS 7 (See Fig 5-4), and crossing shear cracks appeared upon reversal of load to the first negative peak, LS 24. There was extensive flexural and flexural-shear cracking in the beams during cycling at the first deflection level, as shown in Fig. 5-5, but a well-defined beam hinge was not apparent. There was also some flexural cracking at the corners of the column which were in tension, and evidence of some crushing at the corners of the column which were initially loaded in compression.

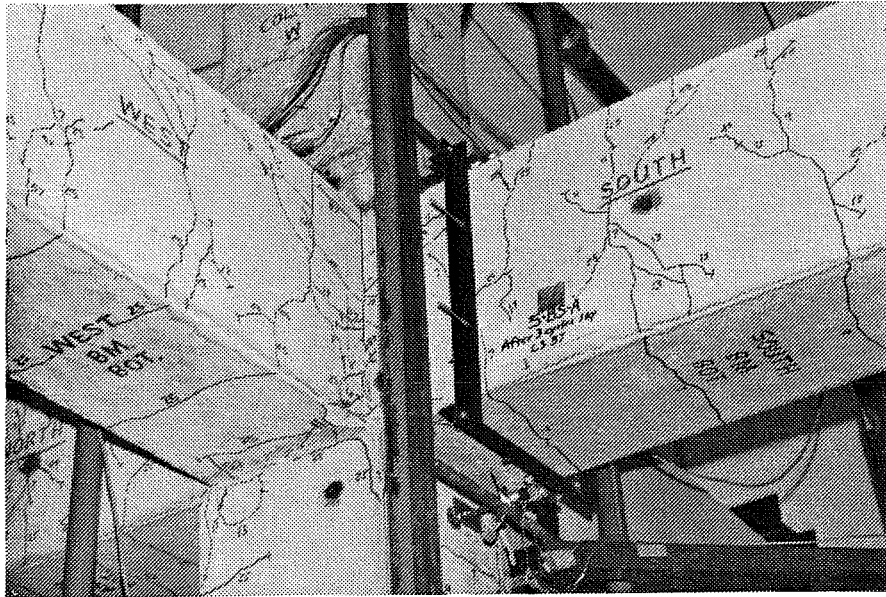


Figure 5-5 : BCJ5 at the end of first three cycles

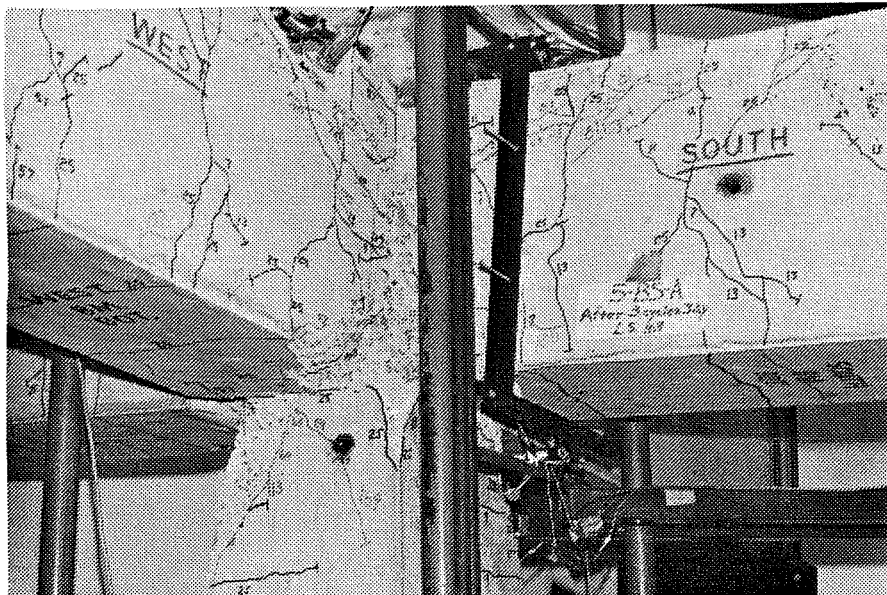


Figure 5-6 : BCJ5 at the end of the test

As cycling at higher deformation continued, the concrete cover at the column compression zones progressively deteriorated and some spalling occurred. With spalling there was a decrease in the biaxial moment capacity of the column. This decrease in column flexural capacity may help explain why the beams did not form a clearer beam hinge as the deformations increased. It was also observed that the cracks at the beam-joint face varied in width from one side to another. This indicated a slight change in geometry due to the addition of the two horizontal components of joint shear strain. The appearance of the specimen at the end of the test is shown in Fig. 5-6.

5.2.1.2. Deflection Measurements

The deflection components for the first positive cycle at each deflection level for the East beam of BCJ5, shown in Fig. 5-7, were calculated as described for BCJ8 (See Section 4.8). It is interesting to note the increase in the contribution of joint shear strain and the decrease of column inelastic rotation during the first two deflection levels. It should be noted that for the South beam, loaded in a similar manner, the contribution of joint shear strain during the first deflection level was almost twice that of the East beam, with the corresponding decrease of the inelastic column contribution. This point is important because the calculations shown in these plots are intended to be interpreted qualitatively rather than quantitatively. Of all the tests, the example of the joint

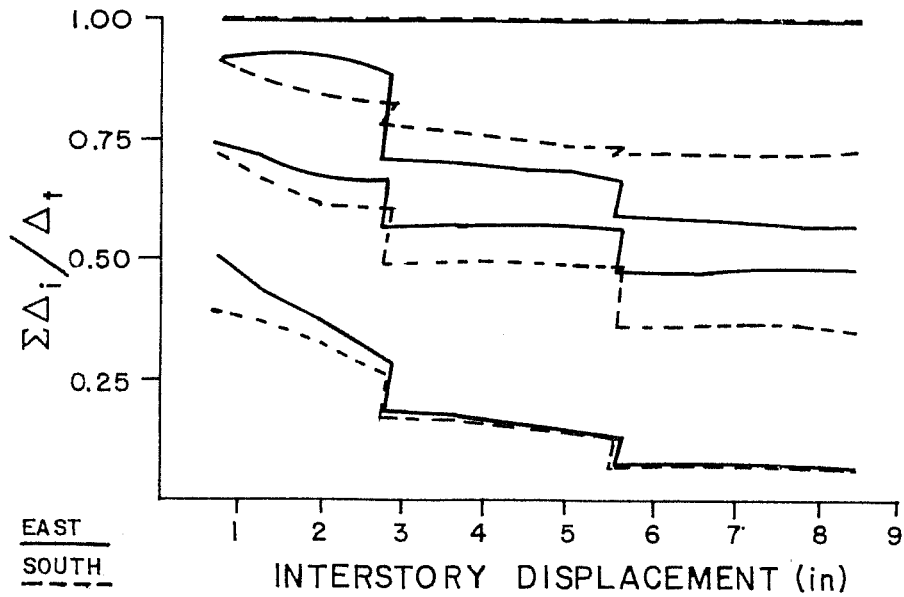


Figure 5-7 : Contributions to total deformation for East and South beams at first peak - BCJ5

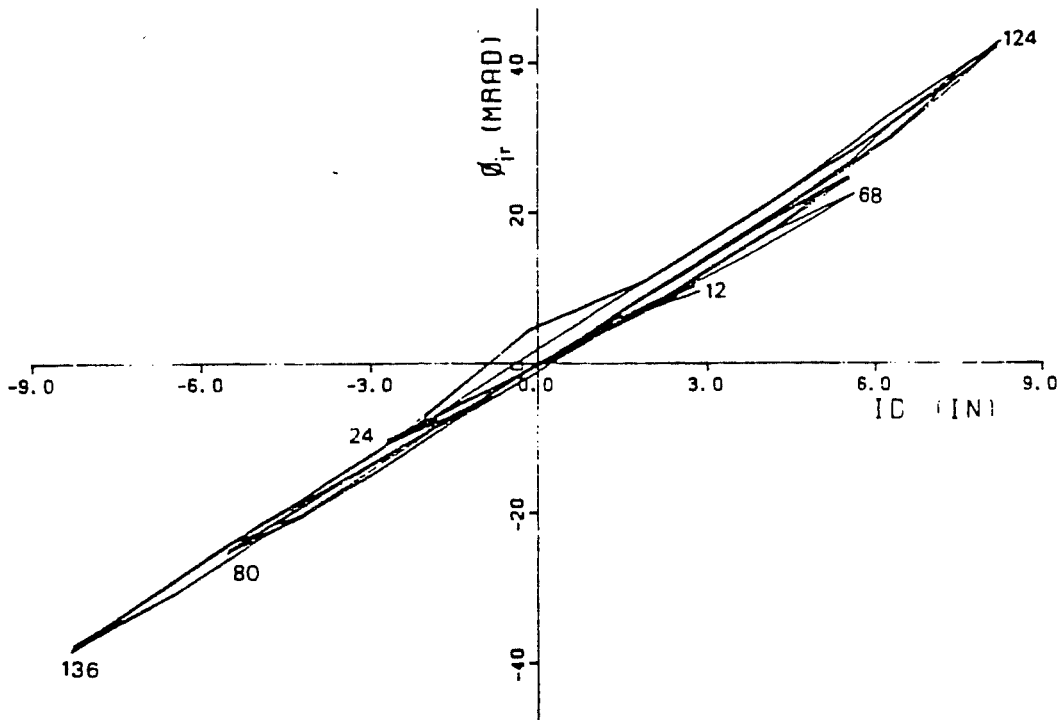


Figure 5-8 : Joint rotation vs. interstory displacement - BCJ5

shear strain at the first deflection level for BCJ5 represents the highest differential found between the two directions of loading. A good index of the possible differences is the transition zone between the first and second deflection levels; abrupt changes in this area indicate that large differences were measured in the two directions of loading, since examination of the data for tests were both directions were measured reliably indicate very ~~little~~ differences after the first deflection level, *in shear strain.*

Under cycling at the first deflection level the joint shear stiffness is reduced considerably, although not as much as for BCJ8 (See Fig. 5-8). The performance of BCJ5 was slightly better than that of BCJ8 because the column rotations and joint shear strain were smaller. These two parameters, however, still account for almost 40% of the total deformation. This should be considered unacceptable in a moment-resisting frame where hinging in the column or excessive joint deformations are to be avoided. The slight difference in behavior previously described can be explained in terms of the benefit provided by the axial load present in BCJ5. The axial load should have a beneficial effect on joint strength because as the axial load is increased from zero the balance load, the moment capacity of the section increases; if the column capacity increases, the column-to-beam flexural capacity ratio also increases. As this ratio increases the likelihood of column hinging is decreased. The beneficial effects of the axial load present in BCJ5 are not

pronounced, probably due to the low compressive stresses in the column (about 1300 psi nominal axial stress). Other researchers [9] have observed more striking differences in behavior when the axial load is above one half of the ultimate axial capacity.

5.2.2 Steel Strains

The strains measured in the reinforcing bars of BCJ5 did not indicate any qualitative difference in behavior from BCJ8. The top bars in the North and West beams yielded near LS 9, and did not show any substantial compressive stresses until very late in the load history (See Fig. 5-9). As the beams were unloaded from the first peak, LS 12, the steel stresses decreased; however, as soon as the beams passed the dead load position the top bars began to pick up tensile stresses again, indicating a deterioration of bond through the joint. Similar behavior was observed in the column bars (See Fig 5-10), where appreciable compressive strains were measured as the beams passed through the dead load position (LS 16) upon unloading from $+1\Delta_1$, but bar slippage occurred as soon as loading in the opposite direction began. This behavior was typical of most bars at the joint-beam or joint-column section, and occurred regardless of whether the steel had yielded or not. The bond stresses across the joint were calculated to be about 1000 to 1200 psi, which are higher than the values generally associated with the onset of bond deterioration.

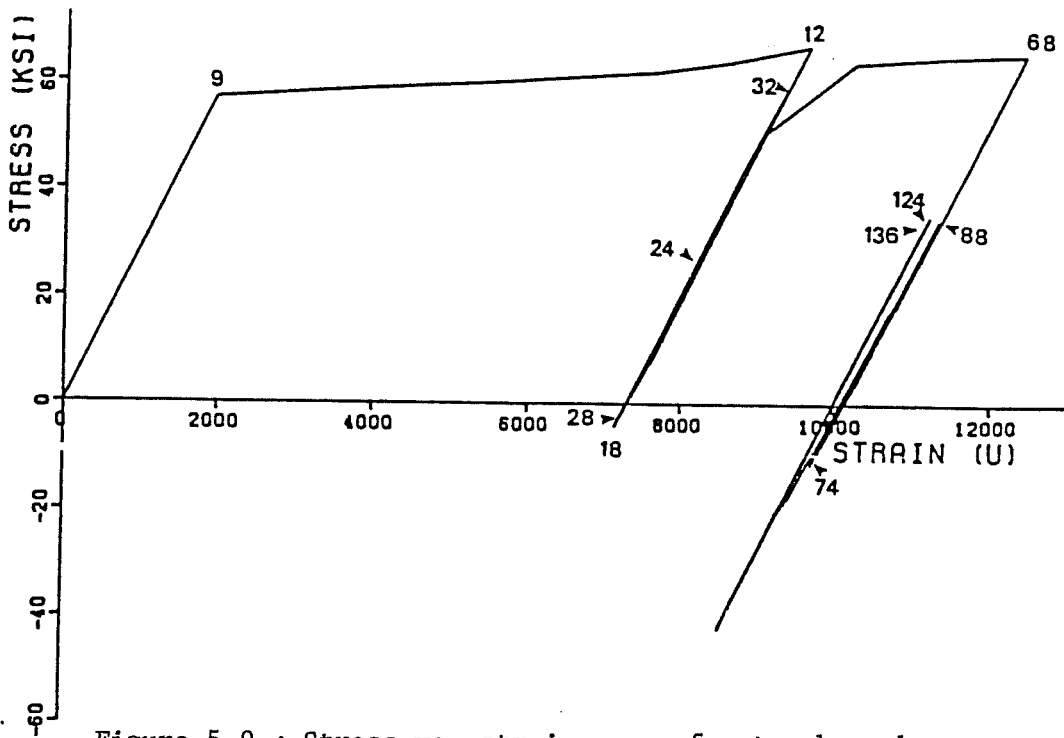


Figure 5-9 : Stress vs. strain curve for top beam bar at joint face - BCJ5

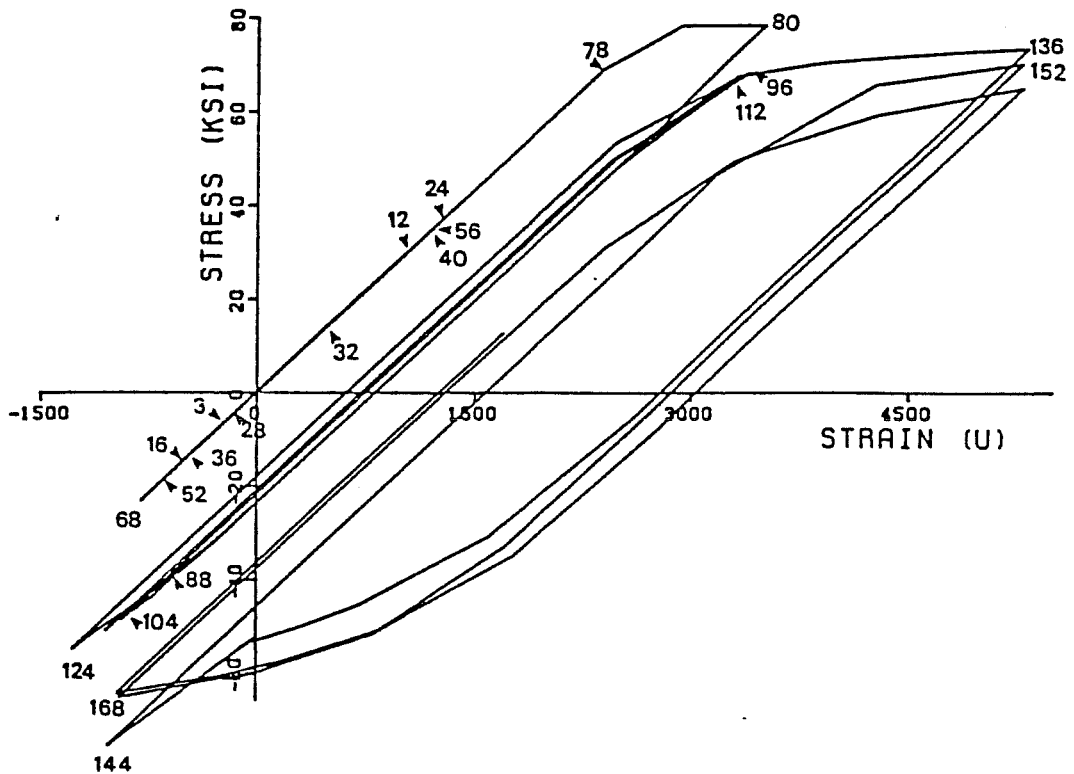


Figure 5-10 : Stress vs. strain curve for column bar

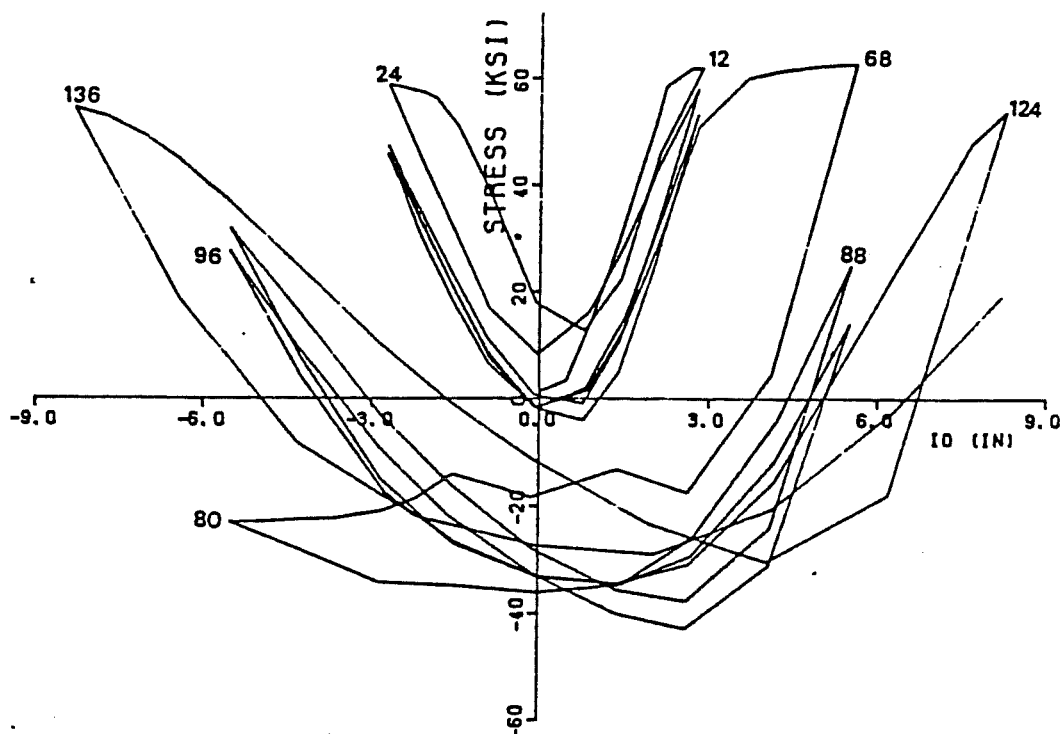


Figure 5-11 : Top joint tie stress vs. interstory displacement - BCJ5

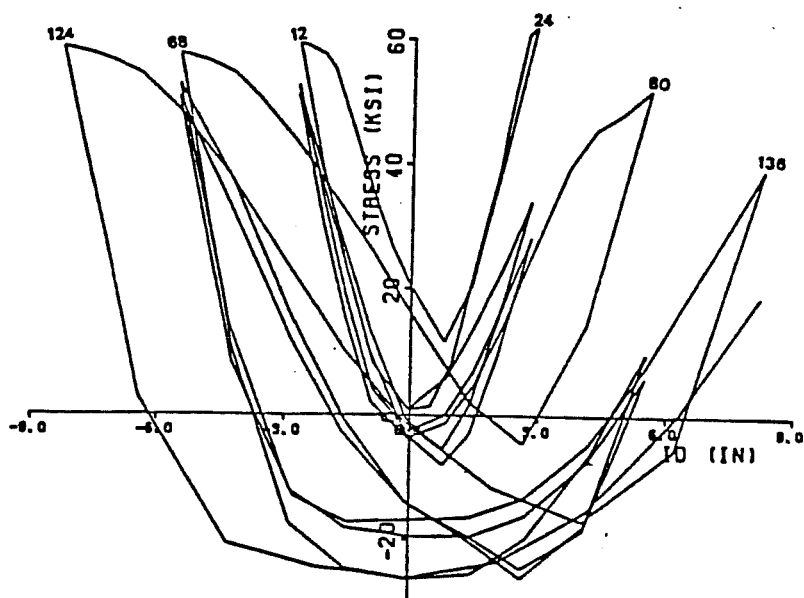


Figure 5-12 : Bottom joint tie stress vs. interstory displacement - BCJ5

The strains in the joint ties showed that the upper tie had consistently larger strains than the bottom one in the positive direction of deflection, and that the opposite was true in the negative direction, as a comparison of Figs. 5-11 and 5-12 clearly shows. These plots correspond to averages of the strains measured in all sides of the joint ties, and indicate that the confining action required of the ties depends on the size of the longitudinal beam bar closest to the ties. Thus, the upper tie, closer to the # 8 top beam bars was required to provide more confinement the joint core than the bottom tie, which is closer to the bottom # 6 longitudinal beam bars. When loaded in the opposite direction the bottom tie receives more strain because the tension cracks need to close before the compressive blocks in the beams begin to help in confining the joint core. Thus, it could be said that the difference in measured strains between the top and bottom ties is more an effect of original direction of loading and crack size than beam bar size.

The bar slips measured ranged from 0.05 in. at small deformations to 0.30 in. at large deformations, and varied nearly linearly with beam end deformation. The effect of cycling, as previously noted, was to shift the neutral position of the reference point in the bar away from the column face, a direct result of the elongation of the bar due to yield penetration.

5.2.2.1. Evaluation of Performance

Although BCJ5 did not exhibit shear or flexural failure in the joint area, behavior was controlled by slippage of the bars across the joint as well as yield penetration into that region as in BCJ8 . The specimen was able to withstand deformations much larger than expected from a moderate to large earthquake, although there was some degradation of stiffness and strength. In summary, the behavior of BCJ5 can be described as acceptable for the range of deformations realistically expected.

5.2.3 BCJ11 - Narrow Beams [Area Ratio =58%]

The narrow beam specimen designated as BCJ11 had different beam longitudinal reinforcement. Because the beam was narrow, 2 #10 bars at the top and 2 #8 bars at the bottom were used instead of 3 #8 at the top and 3 #6 at the bottom as in the rest of the specimens tested. This allowed the beam's width to be reduced to about 8.75 in without appreciably changing the moment capacity of the beams, and therefore the shear forces in the joint region. The column reinforcement was altered also, from 12 #9 bars to 8 # 11 bars to accommodate the new beam bar arrangement. This resulted in a moment capacity of the columns about equal to that of the beams. In designing the specimen it was anticipated that the column in BCJ11 would show more distress than columns in other tests.

5.2.3.1. Behavior of Test Specimen

The load-deflection behavior of BCJ11A is illustrated in Fig. 5-13. It obviously exhibits very poor hysteretic behavior, as well as a rather pronounced loss of strength with cycling, see Fig. 5-14, as well as a rapid loss of stiffness. While the behavior during the first three cycles was similar to that of BCJ5, a rather sudden failure in the joint area occurred during the first cycle at $2\Delta_1$. The loss of stiffness and strength between the first two cycles at this deflection level, combined with the lack of recovery of strength when the deformations were increased to $3\Delta_1$, indicate that the specimen was seriously damaged.

Specimen BCJ11 began to crack significantly even during the application of the dead load and initial cracking cycle. Several large flexural and flexural-shear cracks were observed in the beams during the initial loading stages, and may account for the loss of stiffness apparent in a comparison of the first cycle of load for BCJ11 and BCJ5, shown in Fig. 5-14. The pronounced loss of stiffness can be explained in terms of the decrease in section properties of the narrower beams; under the same deflections the narrower sections of BCJ11 were cracked more than those of BCJ5.

The first significant cracks in the joint area did not appear until LS 7, with some inclined cracks appearing in the SW and NE corners. By this stage there was a large crack at all the beam-joint

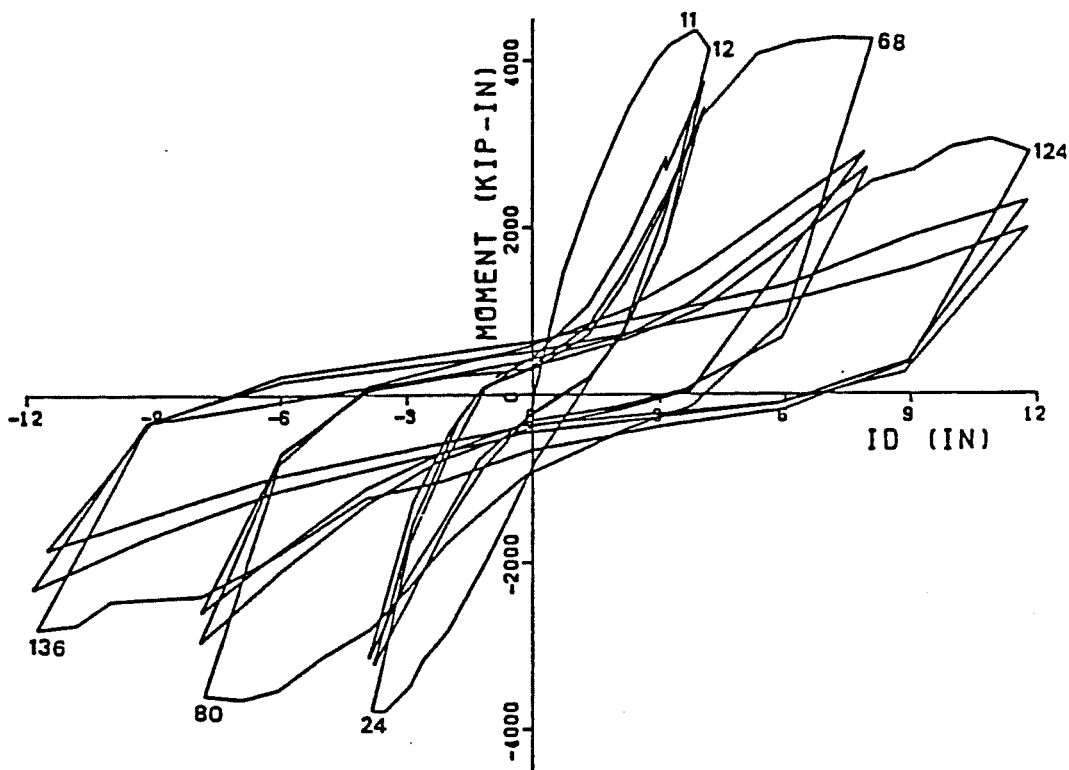


Figure 5-13 : Total moment vs. interstory displacement - BCJ11

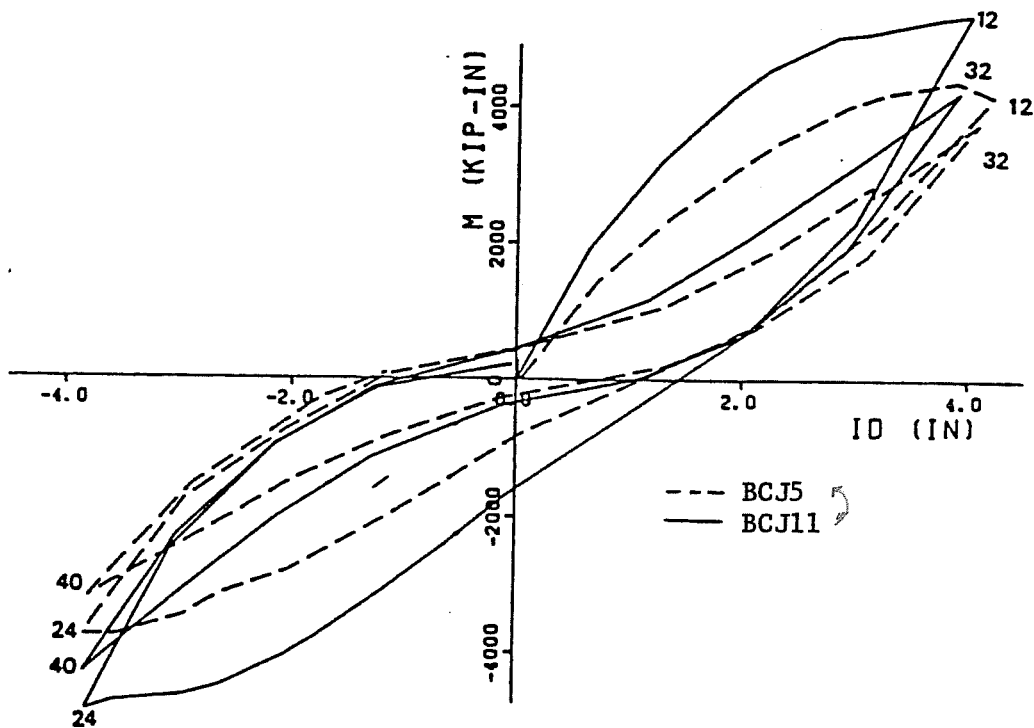


Figure 5 -14 : Comparison for first cycle for BCJ5 and BCJ11

interfaces, with the cracks covering as much as 75% of the beam depth in the West beam. The column did not show any distress at this load stage, with only some minor flexural cracking in the bottom SE corner. When loading continued to the peak of the first cycle, LS 12, more shear cracks began to appear in the joint area, and there was some evidence of concrete crushing in the West corner of the North beam. There was also crushing in the NW corner of the column at the bottom of the joint, although the flexural cracks in the column did not lengthen appreciably. The load-deflection curve, which began to drop before reaching maximum deflection, shows that at the peak of this cycle the strength of the specimen was already deteriorating. If the specimen had been loaded by displacing the column ends it is likely that it would have been unstable at this load stage. As cycling progressed at this deflection level, it became clear that the unprotected corners of the joint were separating from the joint core, and could not provide any strength to the section. Under loading to $+2\Delta_1$, see Fig. 5-15, the column was no longer providing adequate strength. The beams showed only minor additional shear cracking from the previous deflection level; the column, on the other hand, showed extensive crushing at the NW bottom and SE top corners of the joint. Crushing resulted in the complete separation of the NW corner of the joint from the joint core, reducing by almost 30% the effective section of the column in the biaxial direction, see Fig. 5-16. The column bar in the NW corner of the column was visible, and most of the concrete surrounding it

was reduced to powder. As cycling at this deflection level progressed, it was easy to observe the NW corner column bar slipping through the joint. The last four cycles of load imposed showed that the specimen had softened considerably, and that it could not sustain comparable amounts of load to those carried by the other specimens.

5.2.3.2. Deflection Measurements

The calculated deflection components for BCJ11, shown in Fig. 5-17, help explain the behavior of the specimen as the deformation increased. In the first deflection level, the contributions of the elastic and beam inelastic deformation were very similar to those in BCJ5; the shear deformations, however, were smaller, while the column rotation picked up a much larger proportion of the deformation. It must be recalled that these results represent an average of the contributions to both the first positive and negative peaks; thus, in the case of column rotation, the contribution to the positive deflection was in the neighborhood of 45%, while in the negative, after the column had been damaged significantly in the direction of initial loading, it was of the order of 5% to 10%. As loading progressed into the second deflection level, the failure in the joint area began to increase the contribution of the joint shear strain, until it accounted for more than 30% of the total deflection. The computed ratios for the third deflection level, not shown in the figure, indicate a shear strain contribution of the order of 50%, indicating that the joint area had failed. The contribution of the



Figure 5-15 : BCJ11 at LS 68

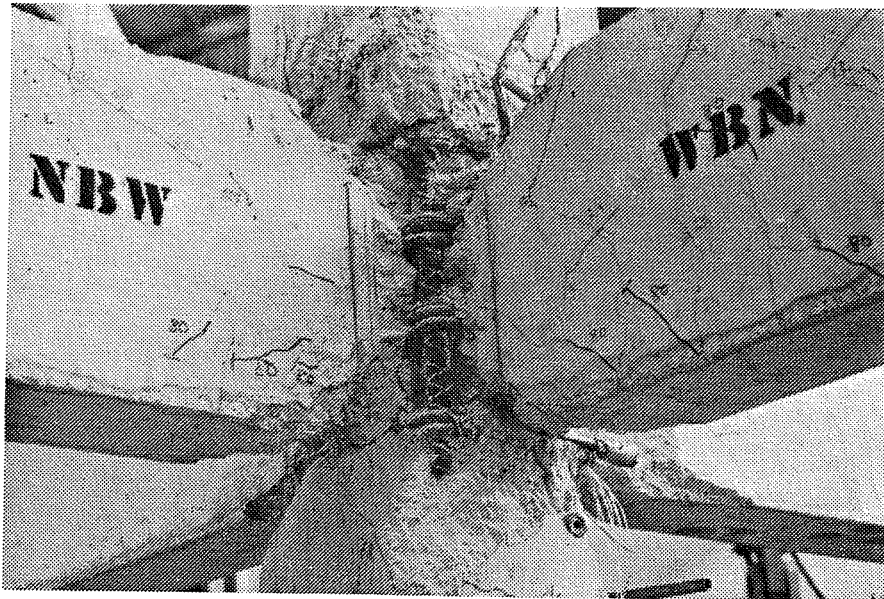


Figure 5-16 : BCJ11 at end of test

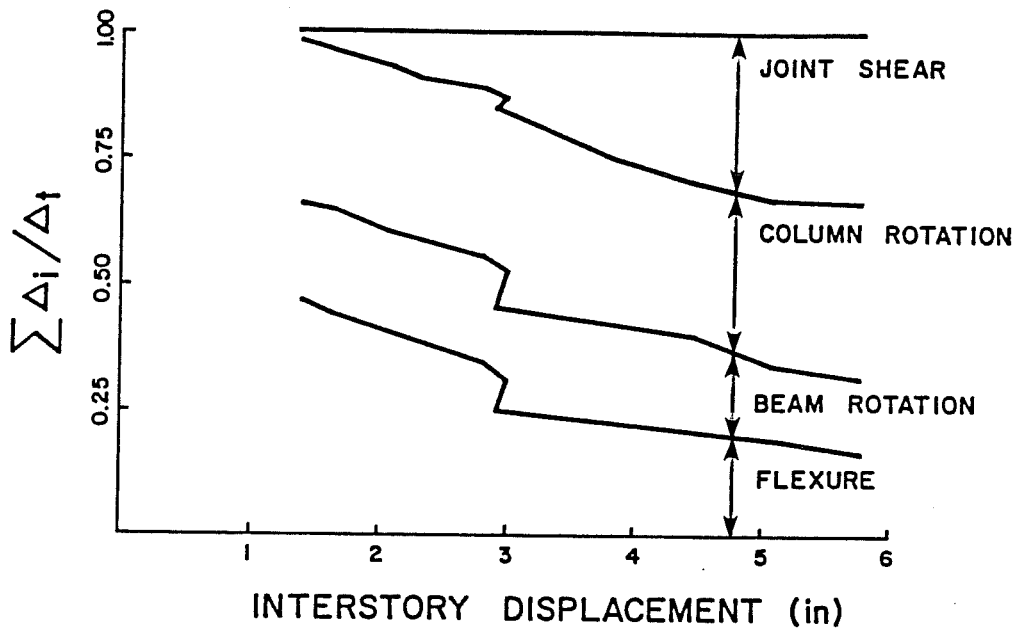


Figure 5-17 : Deflection components for BCJ11

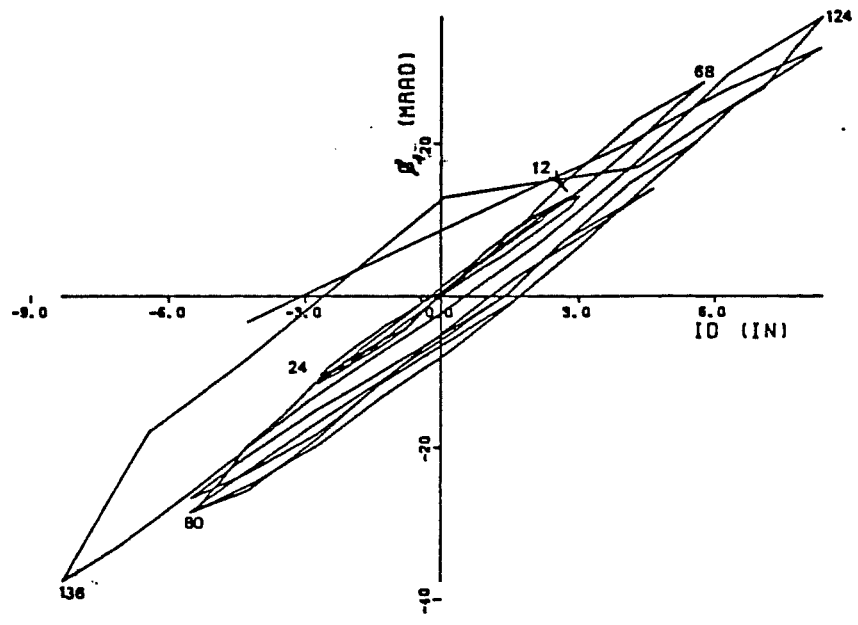


Figure 5-18 : Joint rotations for BCJ11

inelastic beam rotation decreased slightly as loading progressed, also indicating a continuous loss of strength of the column with respect to the beams.

5.2.3.3. Steel Strains

The steel strains measured for this specimen showed that the steel in the column did not yield at any time in the load history. The slippage of the bar is clearly shown by the stress history of the gage at the top SE corner the joint. As shown in Fig 5-19, the strains are compressive at LS 8, and continue to increase in that direction until LS 12; at this point the load is reversed, the bar slips though the joint, and the stresses become tensile at the column face . This explains the loss of strength observed in the load deflection curves between LS 11 and LS 12. The strains at this location also indicate that significant tensile stresses were developed as far as 16 in. from the joint face during the loading to the first negative peak. The 35 ksi stresses at LS 24 for BCJ11 can be compared to 12 to 15 ksi at the same location for specimen BCJ5 under similar loading.

The strains measured in the beam longitudinal steel do not show any appreciable yielding until the second deflection level; thus, the full flexural capacity of the specimen was not mobilized during the first three cycles. The strains measured in the legs of the joint hoops also did not indicate any yielding until the second

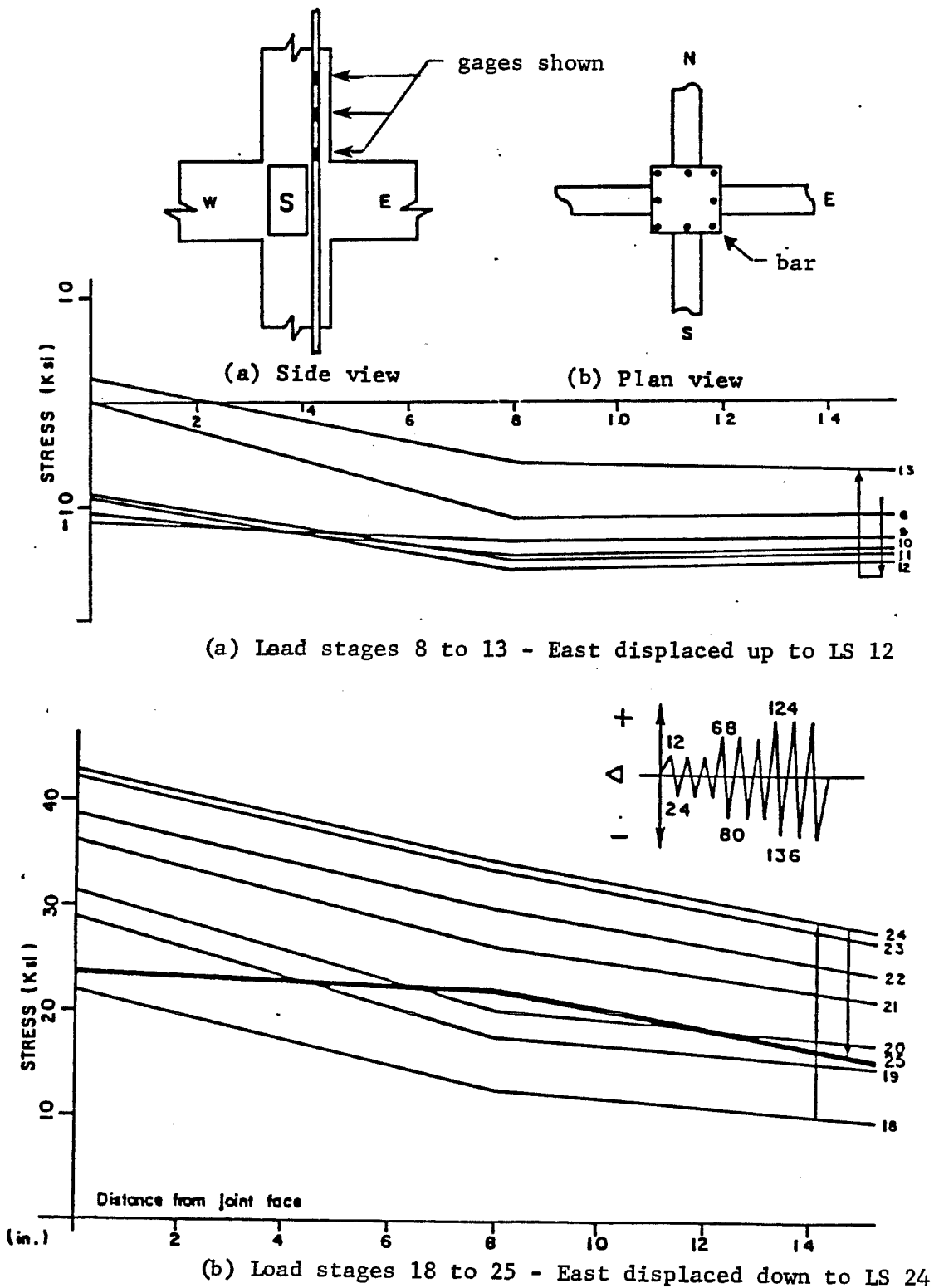


Figure 5-19 : Stress profile for top column SE corner bar - BCJ11

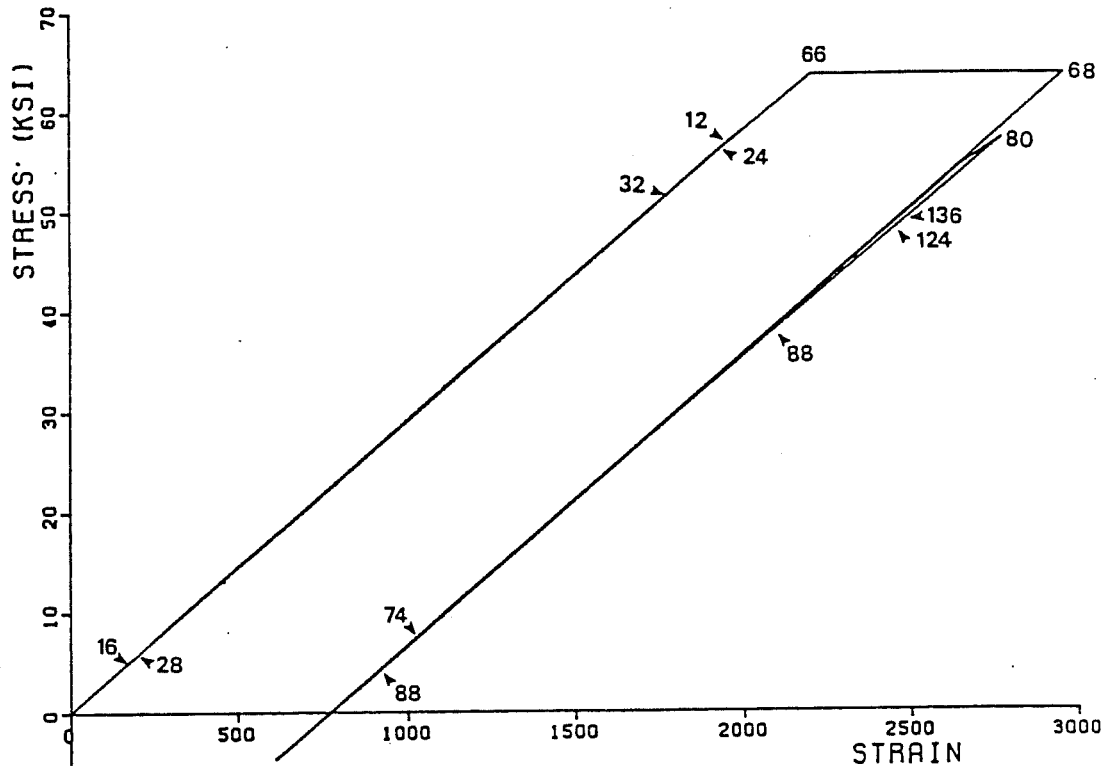


Figure 5-20 : Stress vs. strain for joint tie - BCJ11

deflection level. There was no evidence of serious distress in the joint core until the sudden failure while loading to $+2\Delta_1$.

5.2.3.4. Evaluation of Performance

The performance of BCJ11 was unacceptable. The lack of confinement in the corners of the joint due to the small width of the framing beam led to crushing and spalling of the critical sections and undesirable behavior in the column. The loss of stiffness and strength that took place between the first two cycles at the second deflection level indicates that the joint failed in shear, since little or none of the stiffness and strength was recovered when the deformations were increased.

5.2.4 BCJ12 - Wide Beams [Area Ratio = 120%]

Specimen BCJ12 was designed with beams having a width (18 in.) greater than that of the column (15 in.). The reinforcement was identical to BCJ5 except that the outside longitudinal bars in the beams no longer passed through the joint core. The wide beams were intended to provide good confinement to the joint, but there was concern regarding the influence of such wide beams on the potential hinging of the column.

5.2.4.1. Behavior of Test Specimen

The load-deflection curve for this specimen is shown in Fig. 5-21. The hysteretic behavior is better than that of BCJ11 (narrow beams), and similar to that of BCJ5 (control specimen). The specimen was able to mobilize the full strength of the beam members for the first two deflection levels, and only a slight strength decrease was apparent in the third one. The loss of strength between the first and second cycles was also less pronounced than in the specimen with narrow beams. The energy dissipation capacity during the first cycle of each deflection level was excellent. As expected, BCJ12 was slightly stronger flexurally than BCJ5 because the change in beam width only produced a slight increase in the internal moment arm of the beam section at ultimate conditions.

The cracking behavior of BCJ12 was markedly different from that of BCJ11. Very few flexural cracks were observed during the dead load and initial cracking cycle portions of the load history. At LS 7, there was extensive flexural and flexural-shear cracking of the beams, with the main flexural crack at the joint face extending for about 70% of the depth in the West and North beams. Although the joint was masked by the beams, some shear cracking at the interface between perpendicular beams indicated that shear cracking had developed in the joint. There were a number of flexural cracks in the bottom SE corner of the column, and only a few cracks in the top

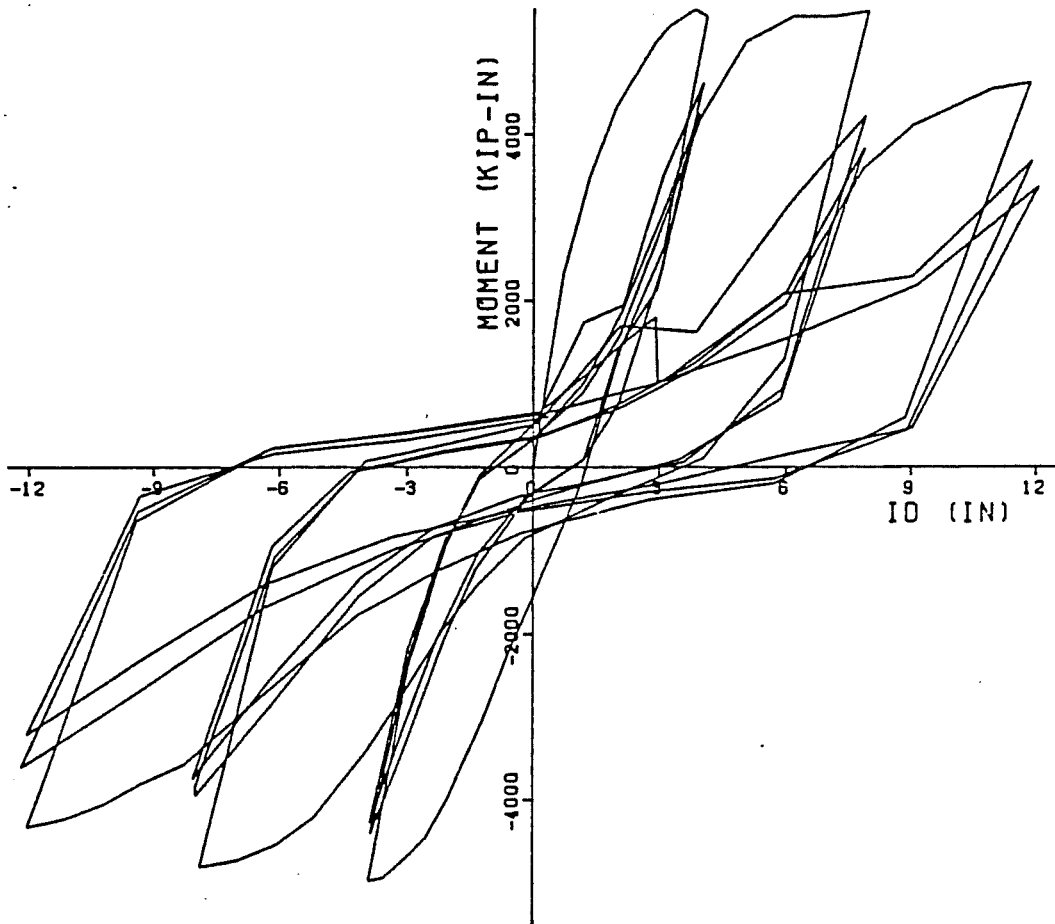


Figure 5-21 : Total moment vs. interstory displacement - BCJ12

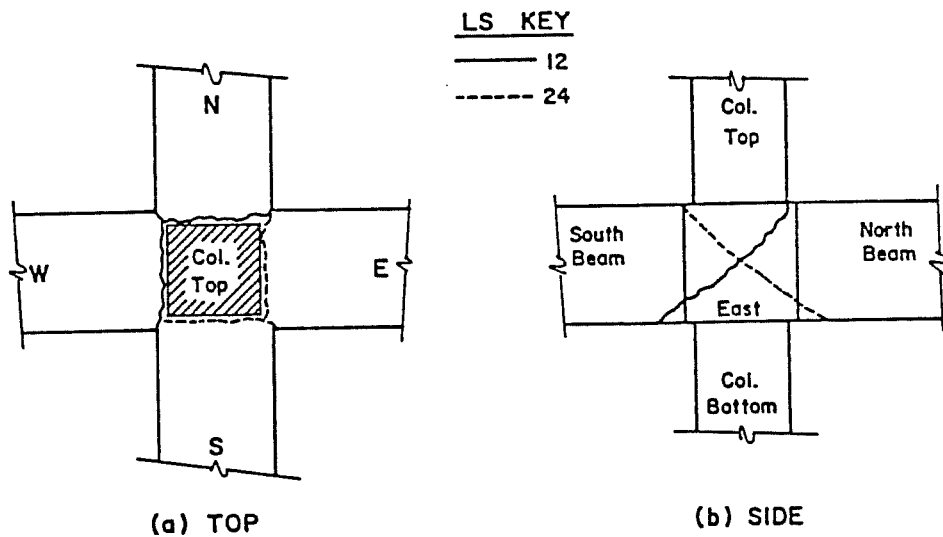


Figure 5-22 : Cracking in the joint area - BCJ12

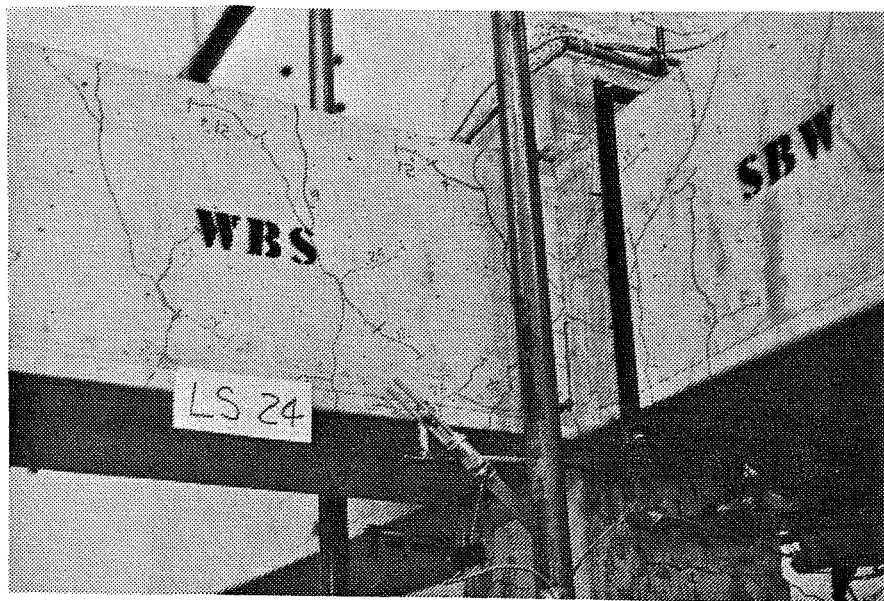


Figure 5-23 : BCJ12 at LS 12

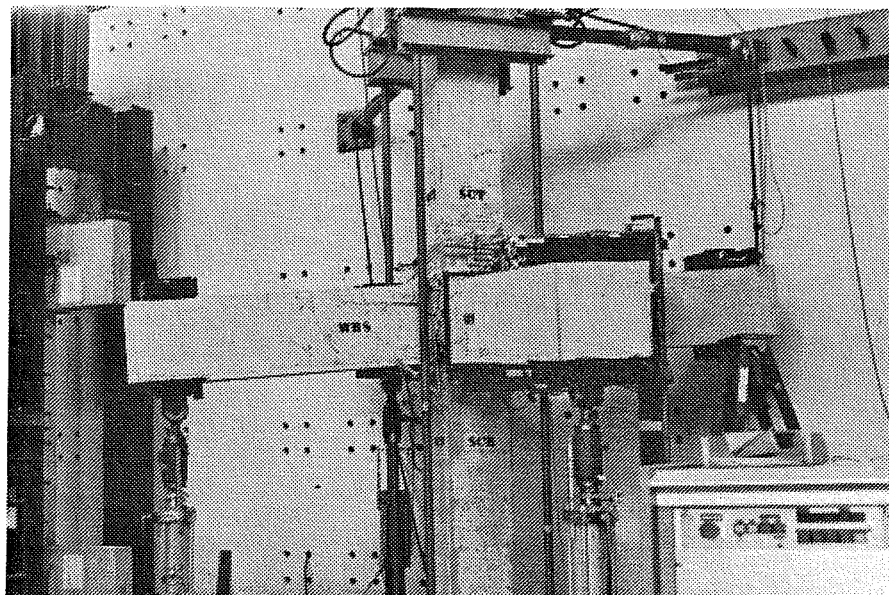


Figure 5-24: BCJ12 at LS 124

NW corner. By LS 12, the beams had completely separated from the column; the separation cracks started at the corner where the beams met, progressed to the corner of the column, and along its side as shown in Fig 5-22. Similar cracking occurred at the bottom of the South and East beams, although the pattern was less clear. It is interesting to note that the cracks seemed to be inclined at an angle of 45 degrees to the principal horizontal axes and downward, from the corner where the beams met toward the nearest corner of the top joint hoop, as shown in Fig. 5-22. There was evidence of crushing in the compression zones of the North and West beam at the NW corner. The spalling that later took place in these corners indicated a possible interaction between the joint shear and the forces in the compressive blocks of the beams. The top SE and bottom NW corners of the column were crushed, although the crushing seemed to be confined to about one half of the cover concrete only. Reversing the load to LS 24 caused some crossing shear cracks at the SW and NE corners, as well as a complete separation of the beams from the column at the top of the joint. The cracks in this area were very wide, about 1/16 in., indicating that the top longitudinal steel was either yielding and elongating considerably or that the bars were slipping. By the end of the second deflection level, the top and bottom SE and NW corner of the columns showed extensive crushing. In order for the beams to develop almost their full strength at the third deflection level, the column had to be relatively undamaged. This is a surprising result, since one would expect the larger beams (with larger strength) of

BCJ12 to shift the hinging from the beams to the columns earlier in the load history than in other tests.

5.2.4.2. Deflection Measurements

The deflection measurements for BCJ12 are shown in Fig 5-25. The calculated deformations for this test were not as reliable as for the preceding ones, primarily because the joint shear strain instrumentation recorded smaller values than for previous tests. The fact that the joint was surrounded by such large beams would make this plausible, since the shear deformations seem to be dependent on the amount of lateral confinement. The contribution of elastic deformation and beam rotation decreased rapidly, from about 70% at the beginning of the test to about 50% at the end of the first deflection level and 40% at the end of the second. The column rotation picked up a significant portion of the remaining deformation at each load stage, while the joint shear strain did not contribute appreciably until the second deflection level. While the steel in the beams yielded as predicted, the contribution of the beam rotations was low because the beam-to-column stiffness ratio changed as well. As cracking increased the stiffness ratio tended to decrease, and thus more deformations were forced into the column.

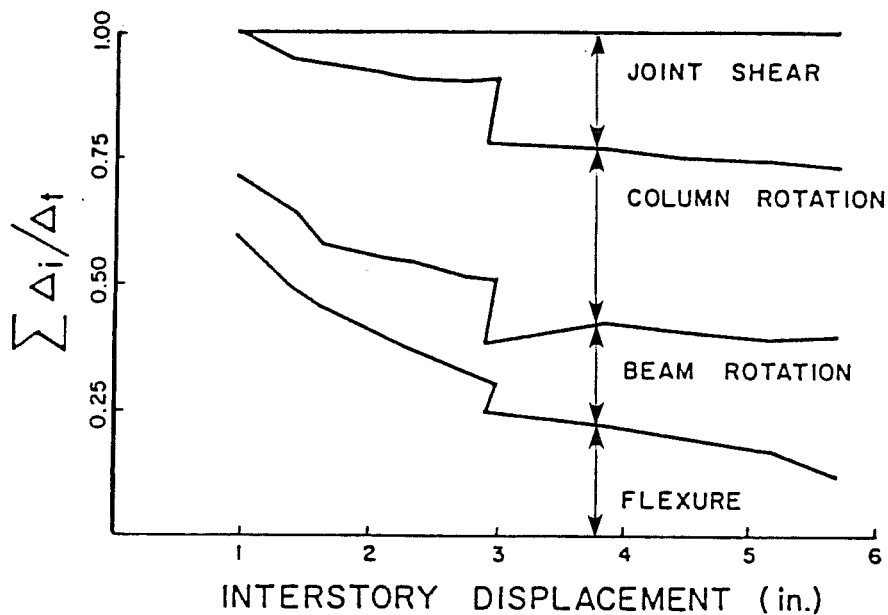


Figure 5-25 : Deflection components for BCJ12

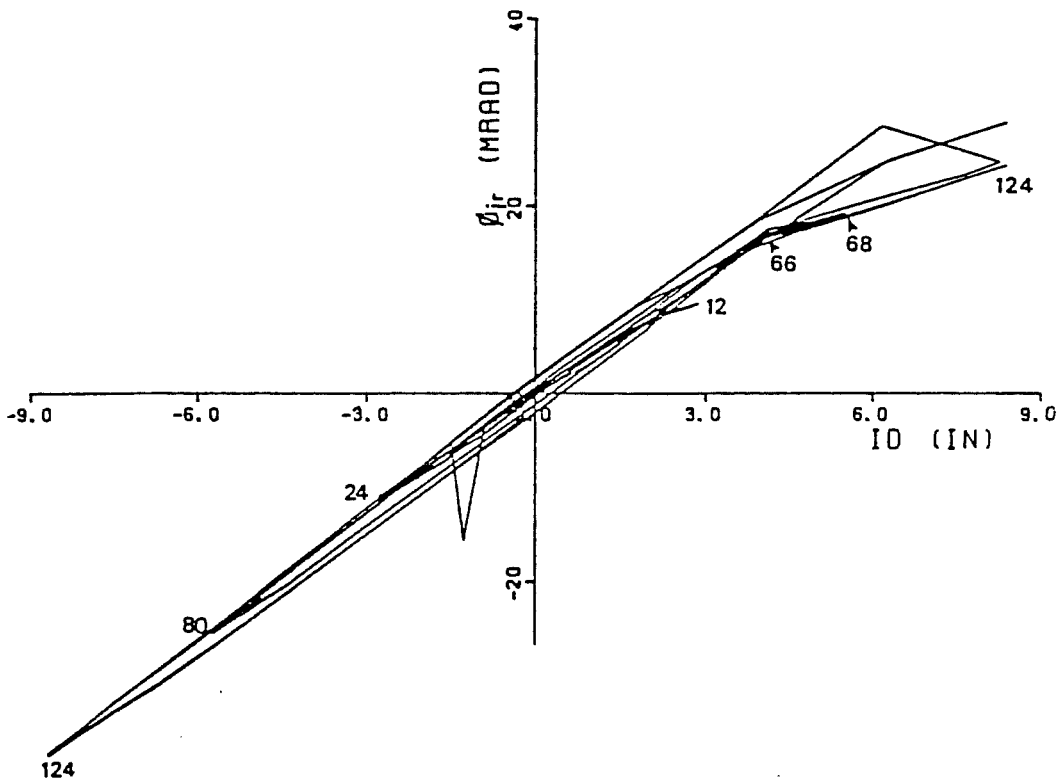


Figure 5-26 : Joint rotations vs. interstory displacement - BCJ12

5.2.4.3. Steel Strains

The steel strains for BCJ12 clearly indicate that the full capacity of the specimen was mobilized as early as the first cycle of inelastic loading. Yielding began in the top longitudinal bars of the North beam during LS 9, with ones in West beam following shortly afterwards. Tensile stresses as high as 25 ksi were measured in the beam steel as far away as 16 in. from the joint. The column steel also showed some yielding in the SE corner of the joint. The measured strains indicated that the SE column bar did not slip until the first negative peak, LS 24, was reached. The gage at the NW bottom corner of the joint indicated that the NW column bar maintained its compatibility in the bottom section through most of the load history, and did not yield at all. The gage in this same bar at the NW top of the joint showed that bond degradation, and thus slip, began to occur at LS 24; this part of the bar remained in tension throughout the test and yielded around LS 80. The joint hoops showed similar behavior to those of BCJ5, with yielding beginning at LS 9 in the top East leg. The bottom hop showed yielding in the same leg at LS 12, and the West leg of the top hoop yielded upon reversal to LS 24.

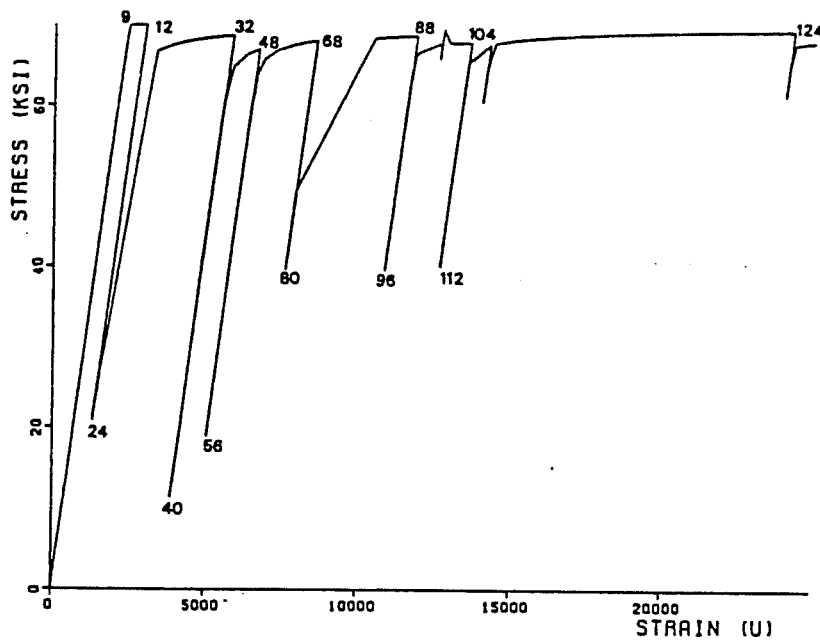


Figure 5-27 : Stress vs. interstory displacement for the gage at the bottom of the SE column bar.

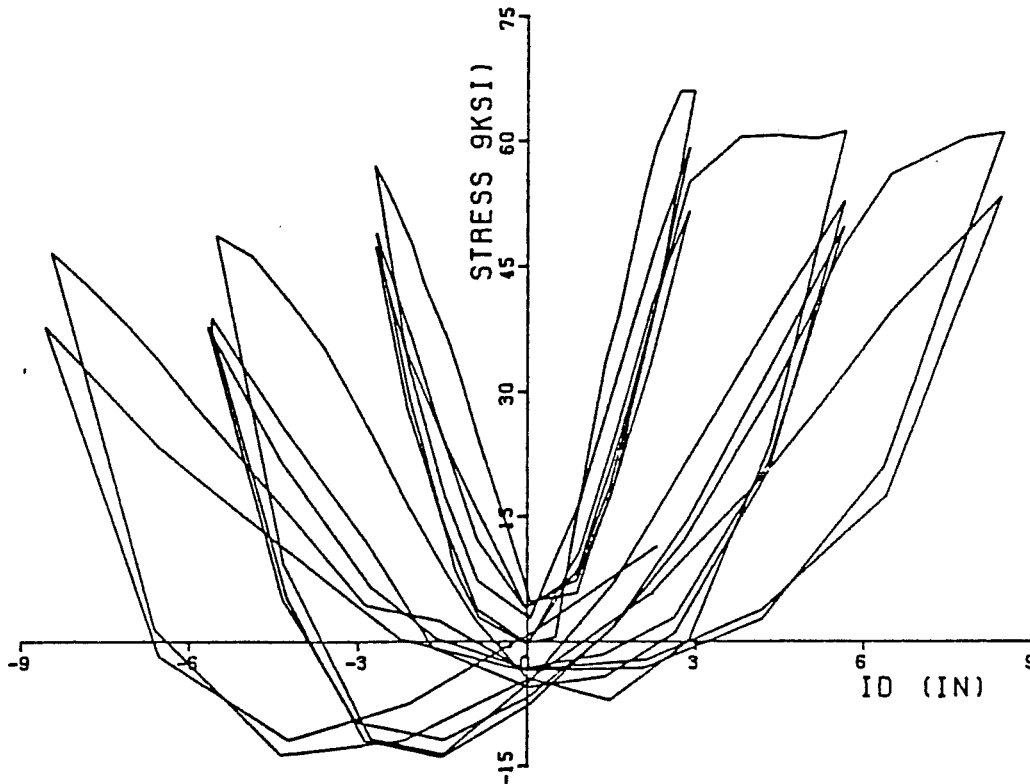


Figure 5-28 : Joint tie stress vs. interstory displacement - BCJ12

5.2.4.4. Evaluation of Performance

The behavior of BCJ12 was acceptable, especially in light of the current philosophies for seismic design which discourage the use of beam sections larger than the column. The overall behavior of this specimen was very similar to that of BCJ5, and the results support the conclusion that joint confinement provided by lateral beams improves performance. However, it is not possible to extrapolate these results to joints with beams larger than those used here.

5.3 BCJ10 - Wide Beam [Area Ratio =120% , $f_c = 2800$ psi]

Specimen BCJ10 was a replica of BCJ12, except that the concrete compressive strength achieved by this specimen was only 2800 psi, as opposed to 4500 psi for BCJ12. Because of an error in the zeroing of the load cells at the beginning of the test, the load measurements for this tests were taken from the plots actually generated during testing rather than from the digital data recorded by the VIDAR suystem.

5.4 Behavior of Specimen

The load-deformation curves for BCJ10 are very similar to those shown by BCJ12, except that the peak beam end loads were about 10% lower in the North-South direction and 15% lower in the East-West one. This decrease is due both to difference in steel strength and

to shifting of the moment arms due to the lower concrete strength. The loops at the second and third deflection level were more pinched and showed about a 5% larger strength loss than those for BCJ12. The more pronounced pinching might indicate that the bond conditions in the joint deteriorated faster due to the poorer anchorage conditions. The steel yielded as expected, although at load stages closer to the peak (L.S. 11) than BCJ12. The measured steel strains showed no significant differences in magnitude or trends from those of BCJ12.

The observed cracking behavior of both specimens with wide beams was essentially the same, except for the fact that the flexural cracking did not extend as far below the joint in BCJ10 as it did in BCJ12. The crushing and spalling occurred in the same areas, but typically at earlier load stages for BCJ10. The crack patterns differed only in that BCJ10 had less shear cracking near the joint and less flexural-shear cracks in the beams. The crack at the beam-column face seemed larger for BCJ10, but no measurements of crack widths were taken. The concrete that spalled was very powdery, indicating that perhaps the mix did not contain the appropriate amount of cement. This lack of cement is also evidenced by the very white color of the specimen, in contrast to the gray appearance of the other specimens.

The components of deflection for BCJ10 were similar to those of BCJ12, except for the lower contributions of the elastic

components. The difference was made up by an slight increase of the joint shear strain and column rotation. This difference was in the order of 5% for the first deflection level, and smaller for the second and third deflection level.

The fact that this specimen did not show significant differences form BCJ12 in either observed or measured behavior would indicate that the concrete compressive strength is not as important a parameter as previously thought. For the purpose of comparing beam size effects the results of BCJ10 will be disregarded and only those of BCJ12 will be used.

5.5 Effect of Slab

In typical reinforced concrete monolithic construction, the floor slabs are cast as a unit with the beams and columns. Thus, the slab is an integral part of the structural system and its effect on the strength and stiffness of the joint should be considered in design. The specimens designed to examine the effect of the slab were similar to BCJ8, except that a slab 3.75 in. thick was added around the joint as shown in Fig. 5-29. The slab had only one top layer of steel consisting of #3 bars spaced at 12 in on center, and beginning at about 6 in. from the column face. The intent was to determine the effect of a slab irrespective of the amount and detailing of the steel.

5.5.1 BCJ8 - Control Test

The control specimen for the specimens with slab tests was BCJ8, which was extensively discussed in the previous chapter. BCJ8 was a replica of BCJ5 except that it carried no axial load.

5.5.2 BCJ9 and BCJ9A - Specimens with Slab

Two similar specimens with slabs were tested. The two tests, labelled as BCJ9 and BCJ9A, gave very similar results and will be discussed together. Two identical specimens with slab were tested because a failure of the hydraulic system midway through the testing of BCJ9A may have resulted in severe premature damage to the specimen. Since no data was available for joints with slabs loaded bidirectionally, a second test was carried out to insure reliable data.

5.5.2.1. Behavior of Test Specimen

The load-deflection behavior for BCJ9 is shown in Fig. 5-30. The hysteretic behavior of this specimen was not very different from that of BCJ8. The strengths achieved are higher due to the added moment capacity provided by the slab. The deterioration of strength and stiffness followed the same patterns as BCJ8. During the first three cycles, the slab provided the flanges to the beams producing a T-section as long as the shear cracks at the beam-slab interface remained small. As soon as the specimen was taken to the second

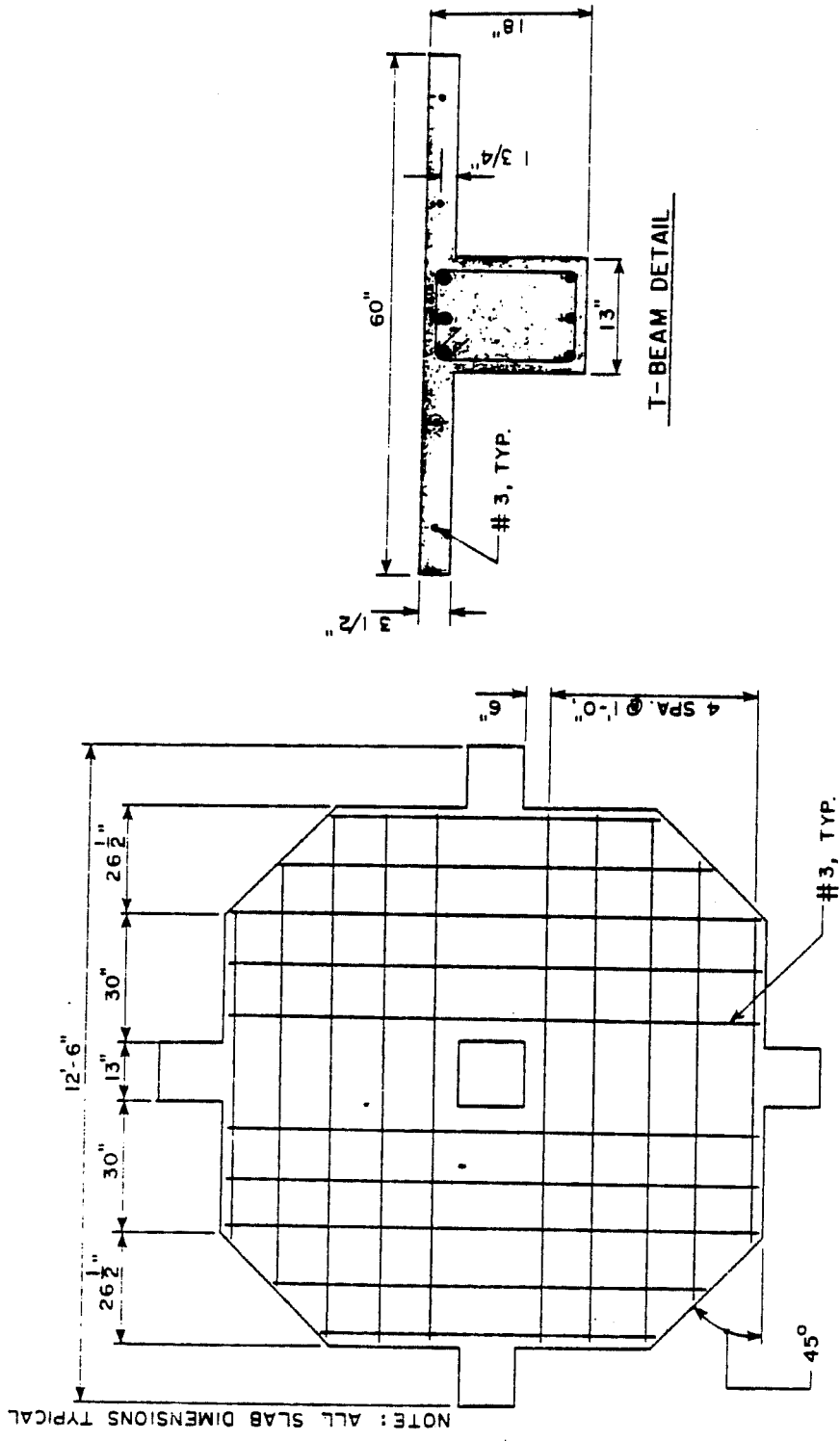


Figure 5-29 : BCJ9 - Specimen with a slab - Slab details

SLAB DETAILS

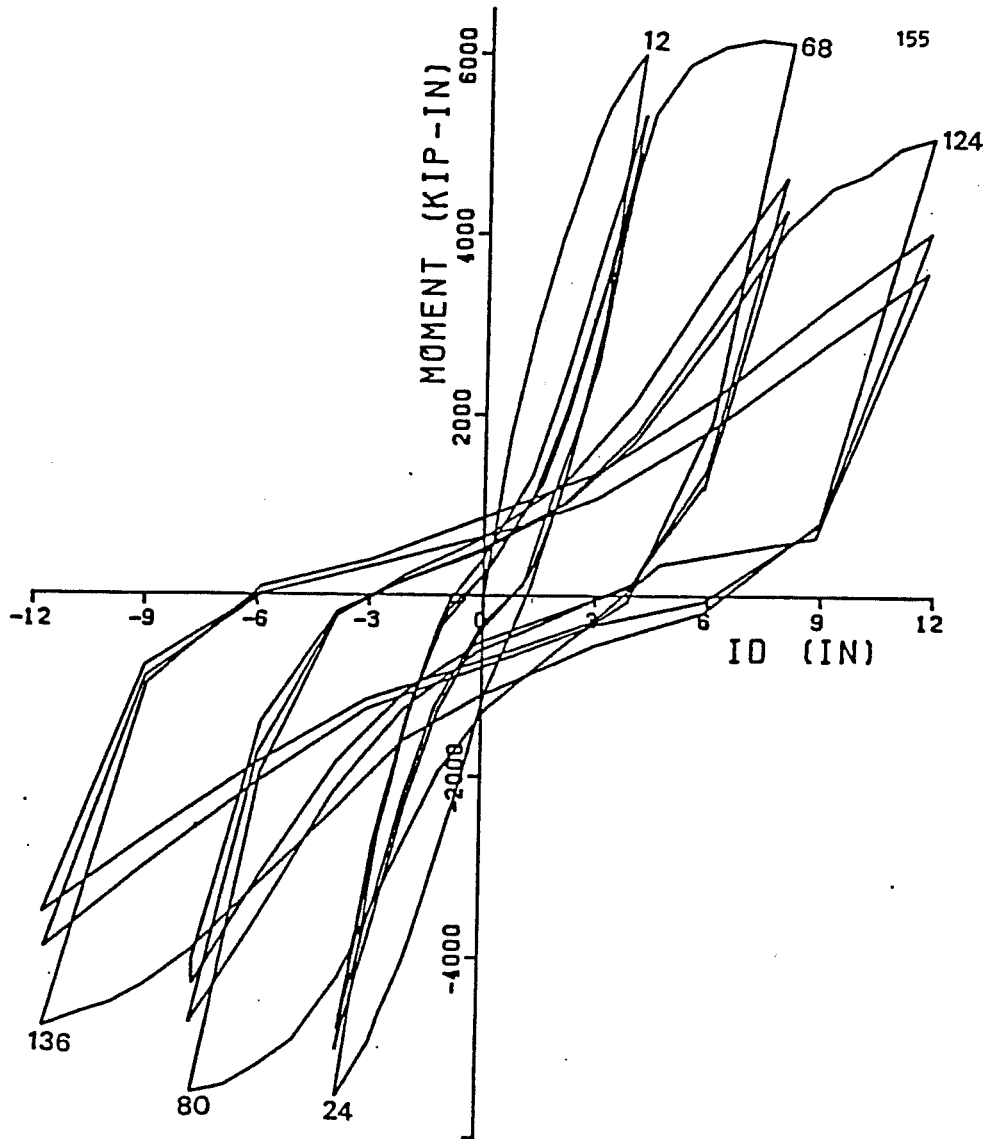


Figure 5-30: Load-deflection for BCJ9

deflection level, the cracks between the slab and the beams became large. The slab had little influence on the shear strength and stiffness of the joint throughout the remaining load history. In fact, the large moments generated in the floor may have increased the shear action in the joint.

The first flexural cracks in the beams and shear cracks in the joint were observed at LS 7. The patterns were very similar to those in BCJ8, except that the inclined cracks at the top of the North and west beams extended into the slab. At this stage the beams and slab had begun to separate from the column, and some radial cracking was observed near the loading points in the slab. By LS 12, see Fig. 5-31, the cracking in the beams was extensive, and several shear cracks were evident at the NE and SW corners of the joint. There was extensive flexural cracking of the column at this stage, primarily due to the absence of an axial load. Cracks in the column extended throughout the height of the column, and were evidence of the decrease of the column to beam moment ratio created by the addition of the slab.

During the second deflection level, few new cracks formed. Shear cracks at the bottom of the North and South beams were very wide, and crushing and spalling occurred in the compressive zones of these beams. Significant crushing of the compression blocks in the column also took place at this deflection level; specimen BCJ8^a, on

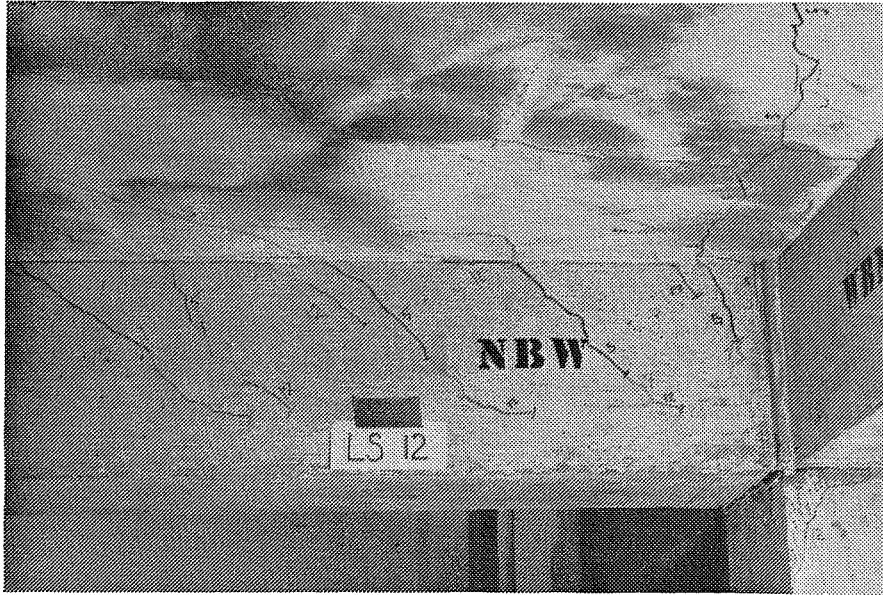


Figure 5-31 : BCJ9 at LS 12

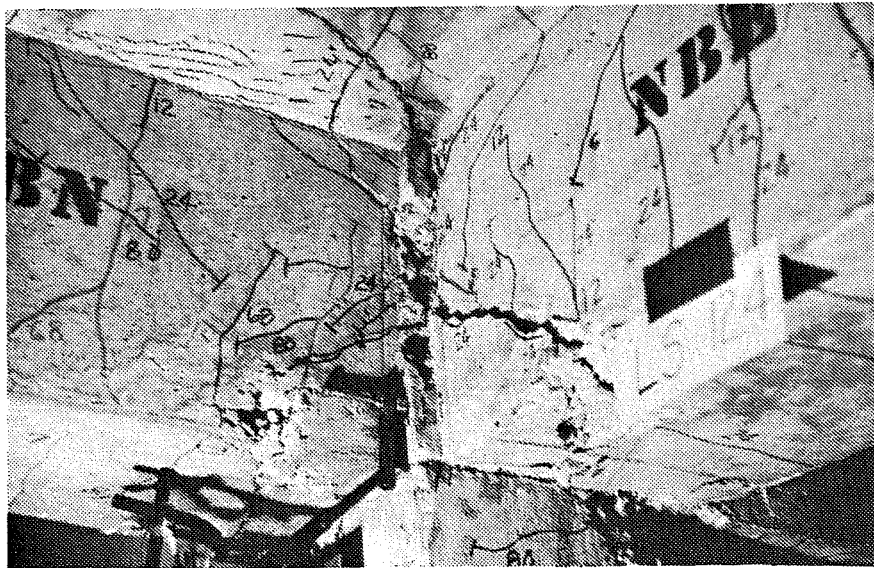


Figure 5-32 : BCJ9 at LS 124

the other hand, exhibited very little if any crushing at all in the column (see Fig. 5-32). At the third deflection level, more crushing of the compression zones in the beams and column was evident, as well as crushing of the slab at the beam-slab interface. The beams separated totally from the column, and the only slab contribution at this stage was that of the small amount of steel reinforcement still acting as tensile reinforcement.

5.5.2.2. Deflection Measurements

The deflection components for BCJ9, shown in Fig 5-33, exhibited trends similar to those of BCJ8, except for the higher values of column rotation in the first deflection level. The small additional decrease in elastic contribution due to the slab is balanced by a increase of inelastic beam deformation. The ratio of inelastic beam/column contribution also decreased slightly, an unexpected result, since the beam-slab assembly is much stiffer than that of the beams alone. The joint rotations, as shown in Fig. 5-34, are very similar for the two specimens, and prove that the slab did have a significant effect on the behavior at large displacements (LS 136) since the joint rotations were about 30% to 40% higher. It should be noted that comparisons of stiffness between BCJ8 and BCJ9 showed that the slab specimen was about 30% stiffer at the first deflection level, and that this difference narrowed to about 20% at the second deflection level, and finally to 15% during the third level. In the specimen with the slab a hinge seemed to have formed

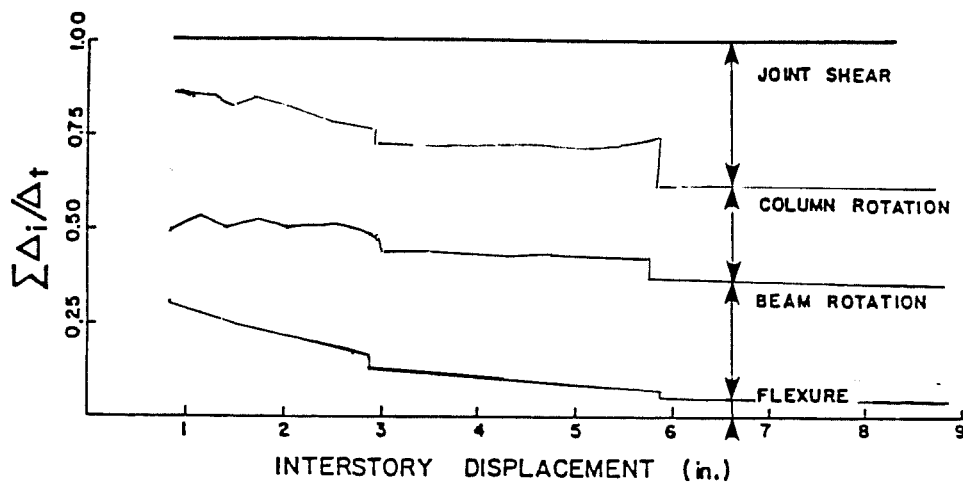
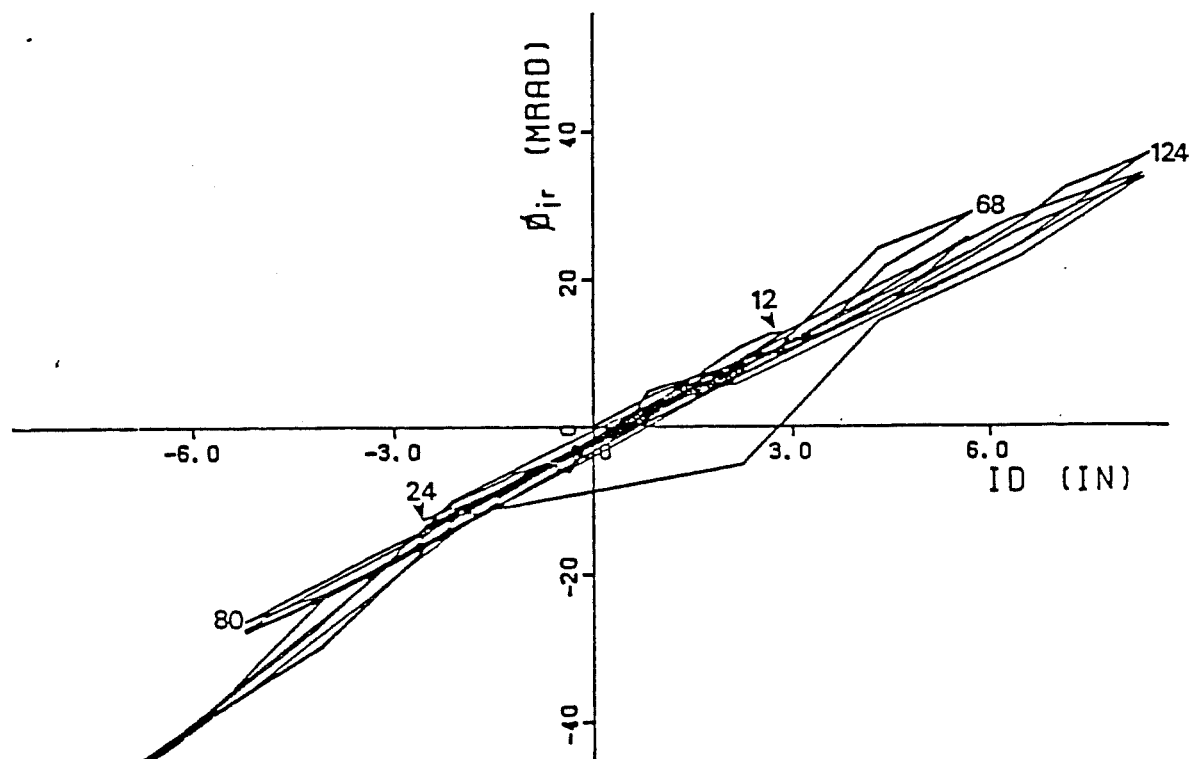


Figure 5-33 : Deflection components for BCJ9



136 Figure 5-34 : Joint rotations for BCJ9

in the joint area, as shown in Fig. 5-35. No appreciable inelastic column deformations were apparent outside the joint, and no clear hinges in the beams were apparent either.

Finally, the addition of the slab decreased sharply the torsional deformations of the beam ends that had been observed in the specimens without slabs. The increase in torsional stiffness provided by a slab resulted in a decrease in the amount of cracking in the beams away from the joint. The deformations in the beams were concentrated near or inside the joint.

5.5.2.3. Steel Strains

The strains measured for this test indicated that the NW corner column bar began to yield above the joint at LS 10, while that at the SE corner below the joint did not yield until LS 36. Unfortunately, many of the column gages were damaged by the vibration during casting, and thus only a limited number were operational during the test.

The longitudinal steel began to yield at LS 9 for the North beam and LS 11 for the West beam, indicating that the full strength of the beams was mobilized in this first load cycle. As for all previous tests, the bottom bars yielded around LS 9, and began to slip through the joint quite early in the load history. The strains measured in these bars near the joint are shown in Figs. 5-37 and

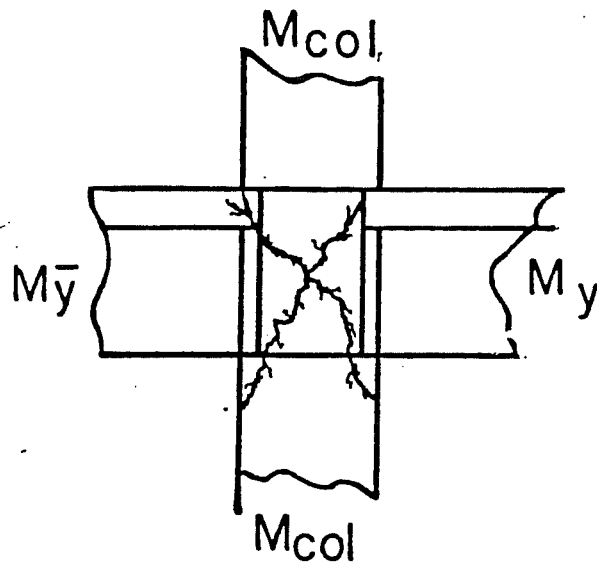


Figure 5-35 : Cracks in the joint area - BCJ9

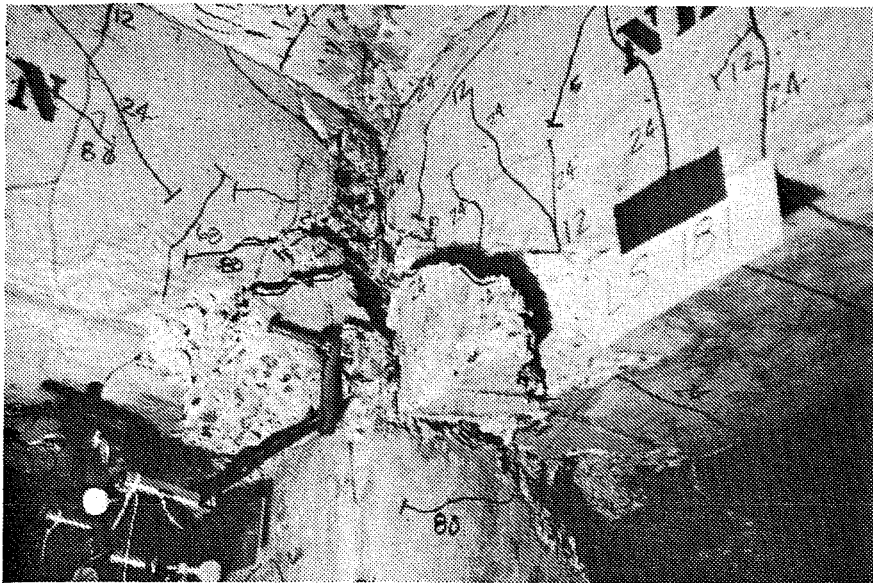


Figure 5-36 : BCJ9 at the end of the test

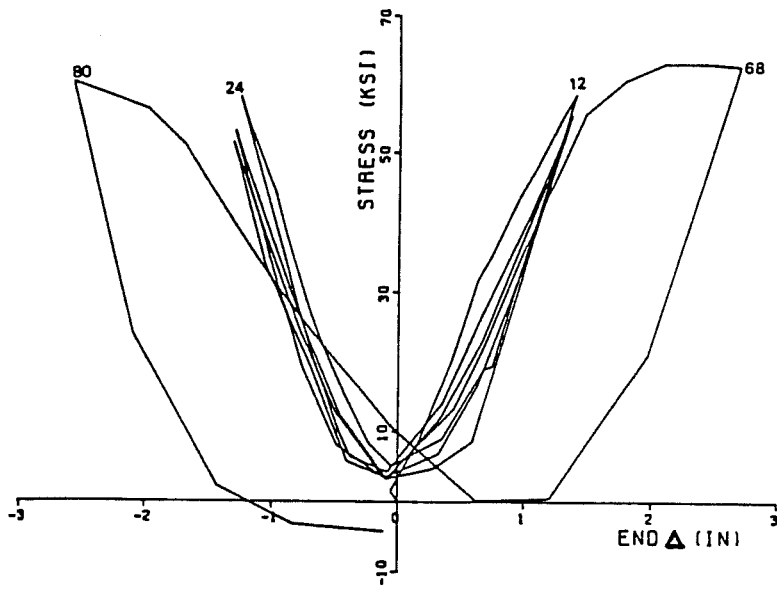


Figure 5-37 : Stress vs. ID for top East top tie leg

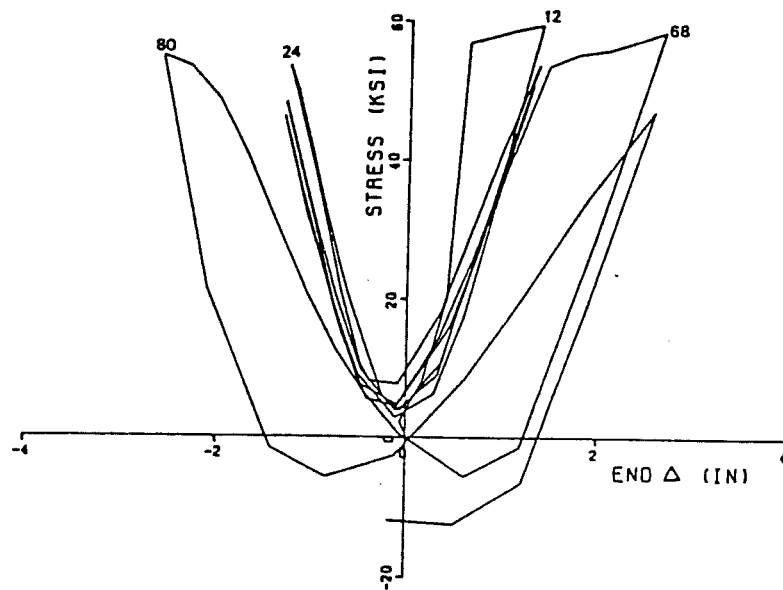


Figure 5-38 : Stress vs. ID for bottom East tie leg

5-38, and indicate that very large tensile stresses were present as far away as 16 in. from the joint face due to the breakdown of the bond . The strains measured in the joint hoops indicated that yielding began around LS 11, and that much more yielding than in previous specimens was occurring in the bottom hoops during the initial load stages.

5.5.2.4. Evaluation of Performance

The performance of BCJ9 and BCJ9A can be considered satisfactory in so far as strength and stiffness is concerned. The specimen was able to withstand very large shear stresses, but at large drifts the damage to the joint was excessive. The effect of the slab was to create a T-beam during the initial deflection level; this effect disappeared as the deformations increased. The effect of the slab should be taken into account in the design process since it will lead to lower ratios of the column-to-beam flexural capacity, and thus cannot be neglected safely .

5.6 Exterior vs. Interior Joints

Although a large number of tests has been carried out on exterior specimens with slabs, none has been subjected to bidirectional loading. In general, an exterior connection is more difficult to design because of the need to provide adequate anchorage for the beam bars in a restricted area. Thus, an exterior connection designed for cyclic loads usually exhibits severe steel congestion

and fabrication problems. Transverse steel requirements, such as those in the ACI-ASCE Joint Committee 352 Recommendations, are often difficult to apply in practice.

In order to make comparisons between exterior and interior connections, the geometry and reinforcement of the specimens was left unchanged. Development lengths for the top bars in the exterior joint specimens were only 75% of those required by the new Appendix A of ACI 318-83 when the design material properties were used. Utilizing the actual material properties, BCJ13 had 88% and BCJ14 had 96% of the required development lengths. The tail extension of the top and bottom beam bars created a "steel wall" in the exterior part of the joint. This is shown in Fig. 5-39. The two exterior specimens (BCJ13 and BCJ14) were tested without axial loads, and were similar except for the presence of a 3.75 in. slab on BCJ14.

5.6.1 BCJ13 - Exterior without Slab

5.6.1.1. Behavior of Test Specimen

The load deflection behavior of BCJ13 is shown in Figs 5-40 and 5-41. In the NS direction, parallel to the edge of the specimen, the behavior of BCJ13 was similar to that of BCJ8, its control specimen. With beams on both sides of the column, the calculated yield loads were reached only in the positive direction of loading. In the negative direction, the beams reached only 70% the

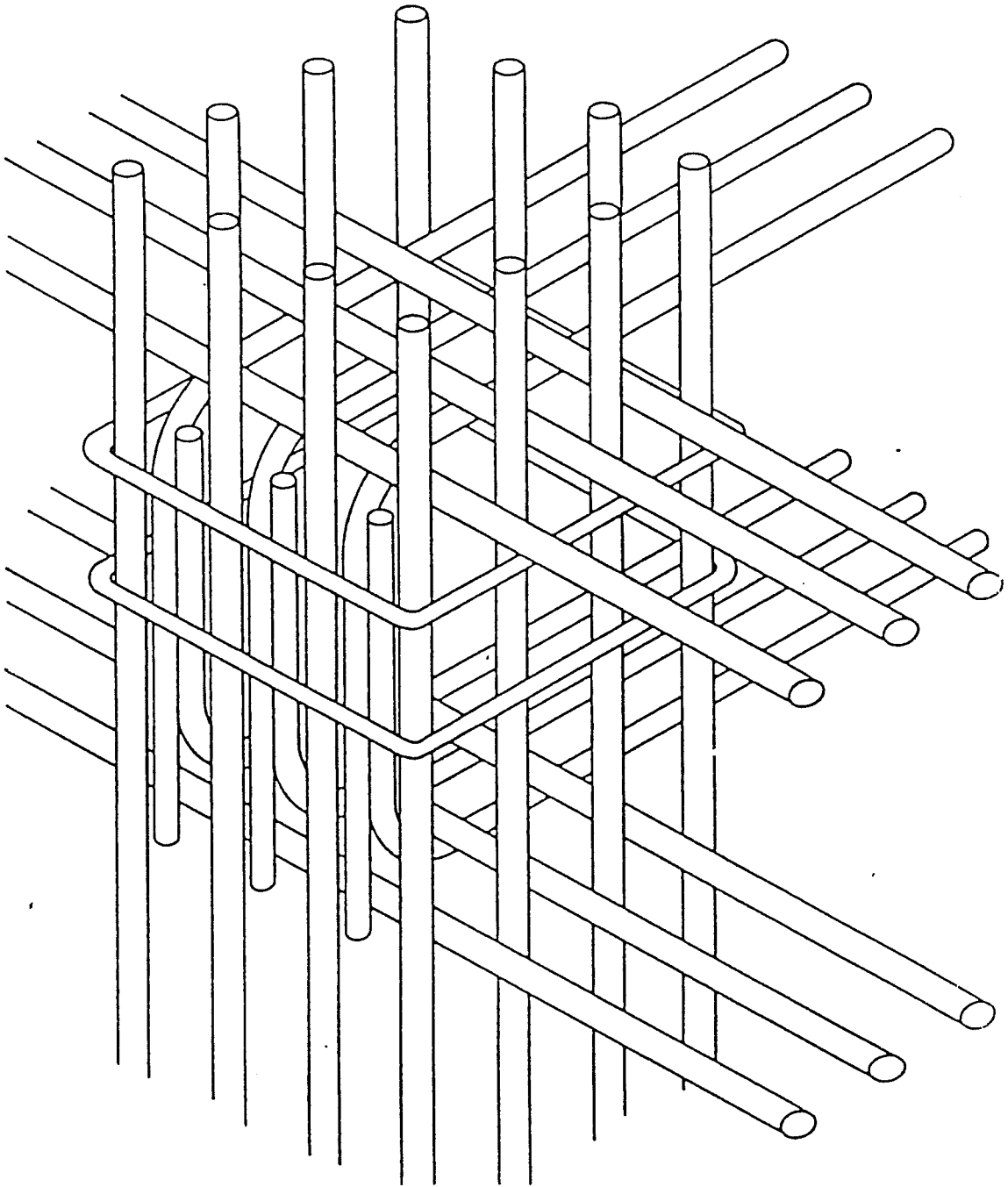


Figure 5-39 : Steel in the joint area for exterior joints

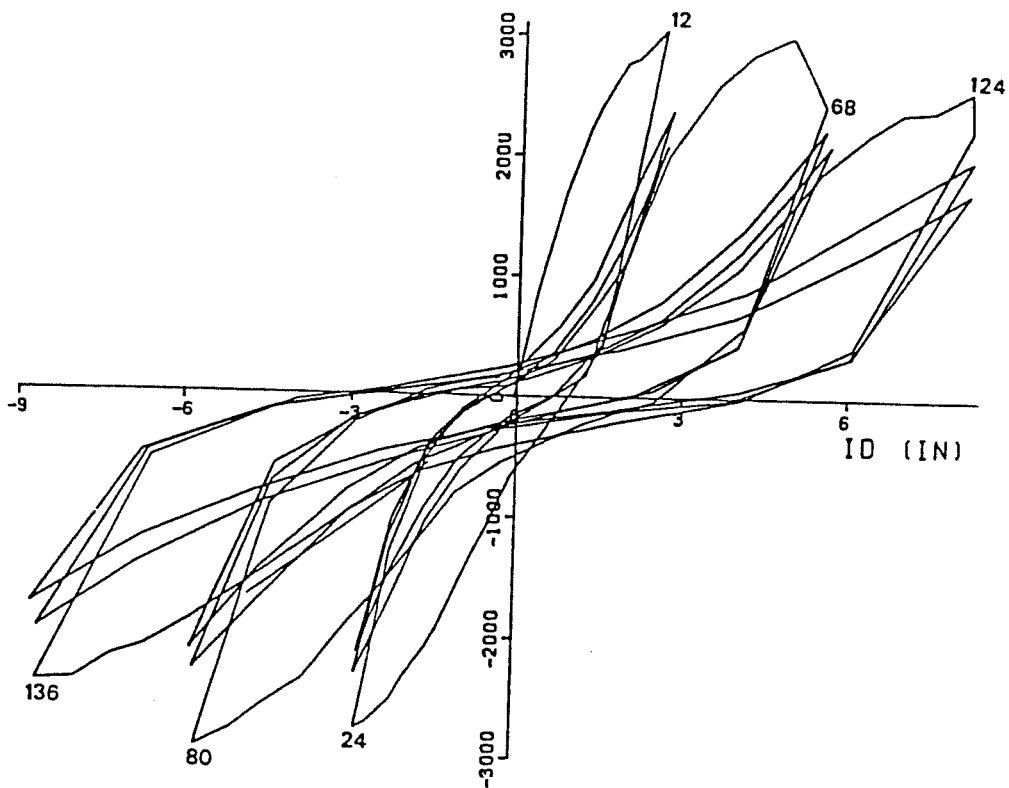


Figure 5-40: Load-deflection for BCJ13 NS

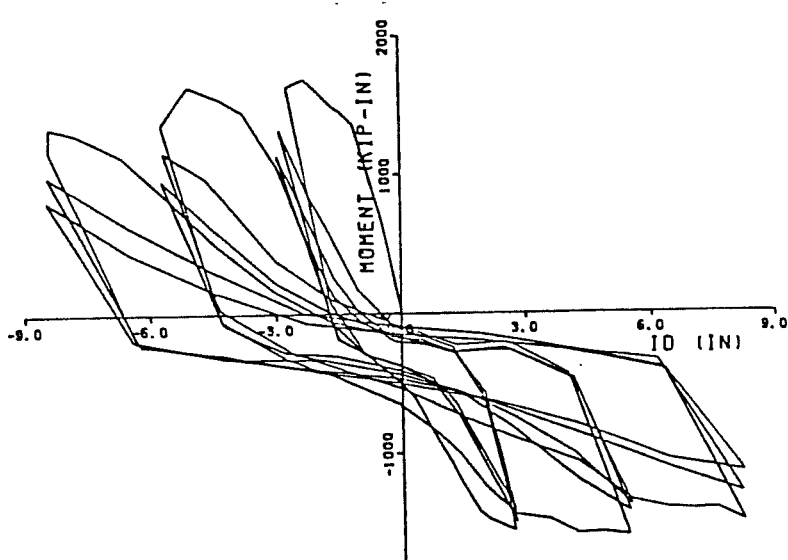


Figure 5-41: Load-deflection for BCJ13 EW

yield load because the onset bond deterioration in the joint area caused the reduction of the moment arm.. In the EW direction, normal to the edge, the beams never reached their calculated yield loads because inadequate anchorage of the hooked top hooked bars resulted in an early bond failure.

It was possible to observe the cracking across the joint, since there was no framing beam on the East side. By LS 7, a major inclined crack had formed in the joint face at an angle of about 45 degrees, as shown in Fig. 5-44. The beams showed the usual flexural and flexural-shear cracking at this load stage, while only minor flexural cracking was evident in the bottom SE corner of the column. By LS 12, much more shear cracking was present in the joint area, and there was some evidence that the joint cover in the East face had begun to separate from the steel in the column. This separation began in the top SE corner, and comprised the triangle shadowed in Fig. 5-42. Loading to the opposite peak, LS 24, resulted in a crisscrossing pattern of cracks in the exposed joint face, but by this time the cover had completely separated from the steel. The East legs of the joint hoops were bent outwards by the prying forces from the tail extensions of the 90 degree hook on the beam West beam bars. Prying caused the concrete cover to separate from the joint core. The column showed some flexural cracking at both top and bottom at this stage, while the beams had only flexural cracking in the tension faces. By LS 68, as shown in Fig. 5-43 , , the cover on

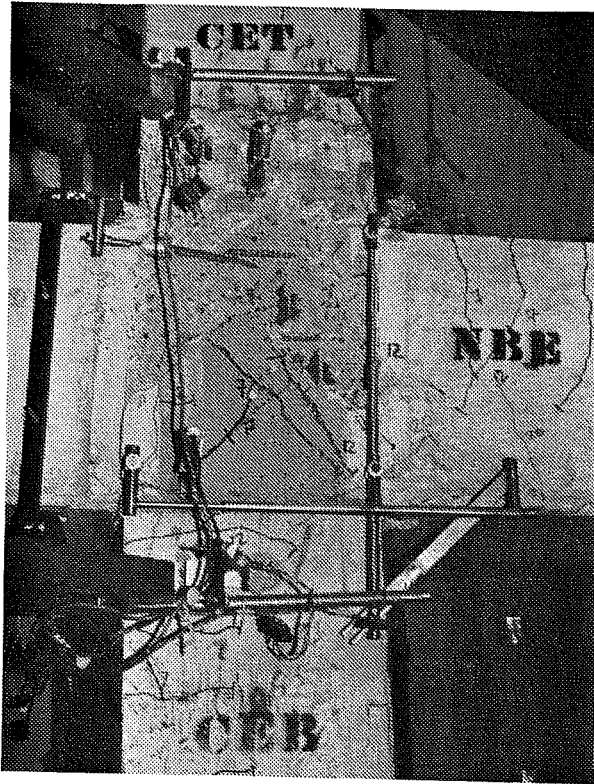


Figure 5-42 : BCJ13 at LS 24

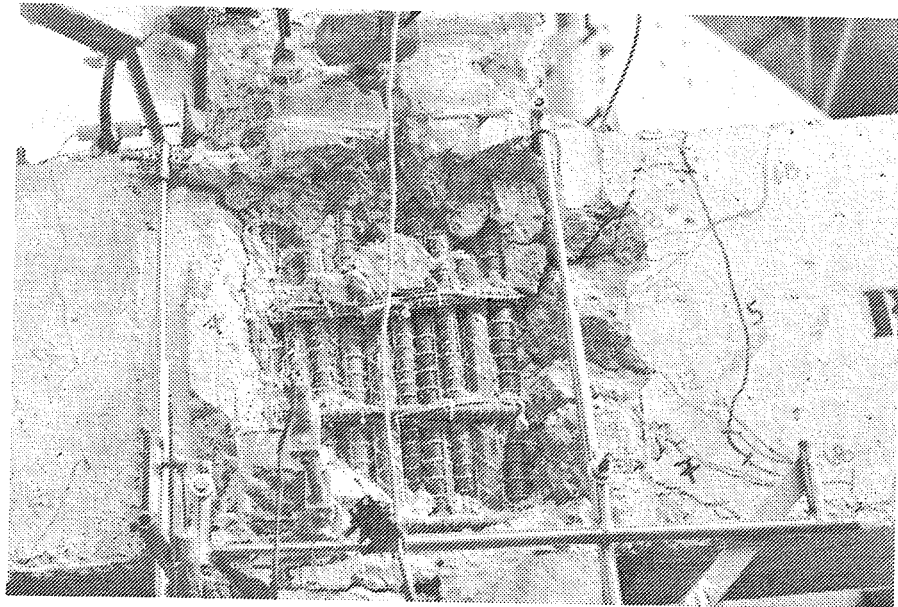


Figure 5-43 : BCJ13 at LS 68

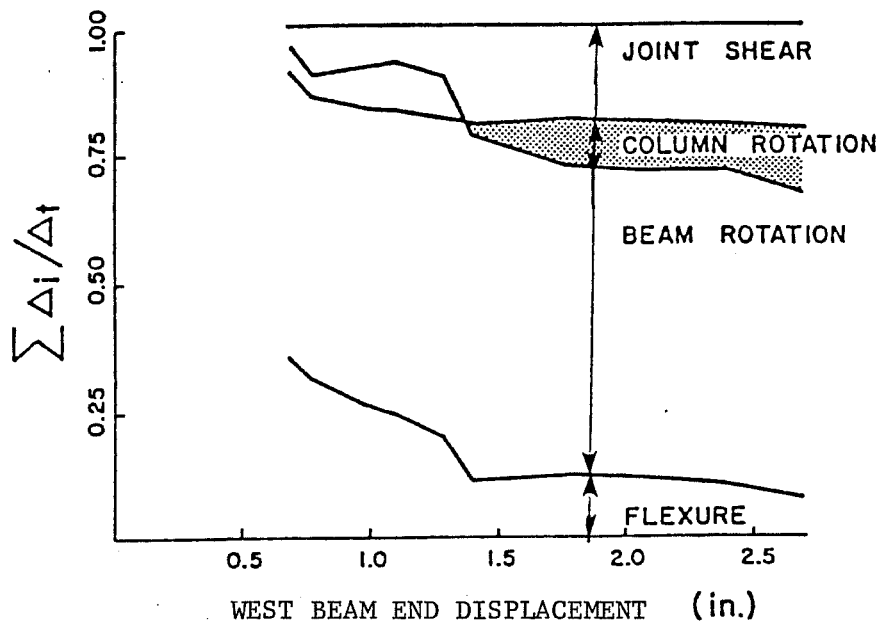


Figure 5-44 : Deflection components for BCJ13

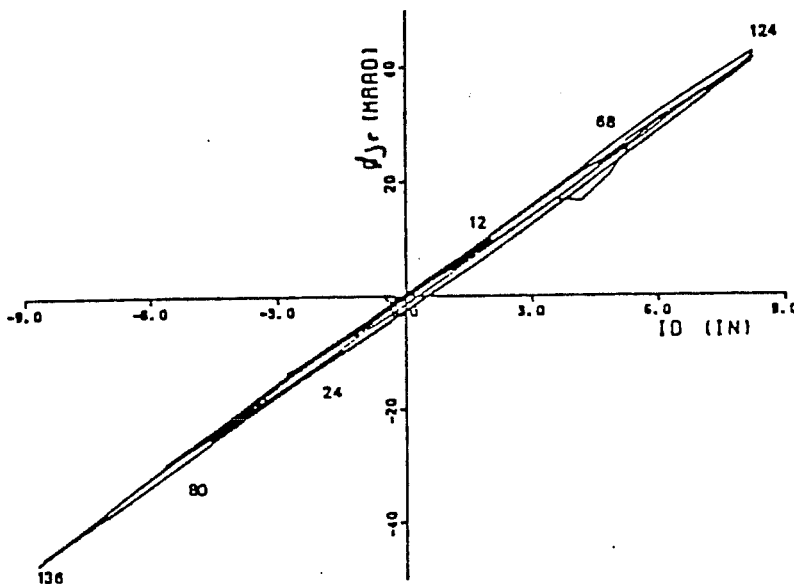


Figure 5-45 : Joint rotations for BCJ13

the upper NW corner of the East face of the joint was clearly separated from the joint core and was removed. The removal of this concrete showed that the top longitudinal bars in the West beam had pulled out about 0.25 in. from their original position, and the East leg of the top joint hoop was bent outwards by about 0.2 in. The tendency to continue to pull out the hooked bars increased as the load history progressed, with the additional pullout of the bottom bars of the West beam around LS 80. The top bar hooks pulled out from their original position by about 0.5 to 0.6 in., while the bottom hooks pulled out slightly more at LS 136. The whole face of the joint separated by LS 124, significantly decreasing the column capacity and thus severely impairing the strength of the subassembly. Little cracking was observed in the second and third deflection levels, as the deformations concentrated in the joint area.

5.6.1.2. Deflection Measurements

The calculated deflection components for the North-South direction were similar from those of BCJ8. For the East-West direction the slippage of the top longitudinal bars resulted in poor correlation of measured to calculated components. As shown in Fig. 5-44, the contributions of the beam rotations were very high throughout the load history. At the second deflection level the contribution of the column rotation, shadowed in the figure, was negative. Since the plotted values refer only to the first peak at each deflection level and do not represent an average, this would

indicate that large slippage of large bars cannot be easily accounted for in the proposed deflection calculations.

5.6.1.3. Steel Strains

The measured steel strains show that while the top longitudinal steel in the North beam yielded during the first cycle, the steel in the West beam did not. Measurements at the beginning of the hook on the west top middle bar indicate that the steel in the hook began to yield around LS 6. This gage continued to show yielding as the deformations increased, but those about 7.0 in away, at the joint face, never reached yield. This confirms the visual observation that the hooks probably began to slip as early as LS 7. The bottom bars in the West beam did yield when the load was reversed the first time, but began to slip when the load was reversed at the second deflection level.

The strain gages in the column did not show any yielding, although slippage occurred in the SE corner bar at LS 12. With cycling, this deterioration continued, until the bond breakdown extended as far as 8 in. into the column by LS 144. The joint hoops began to yield in the East face around LS 7, the product of the prying action of the hooked bars already discussed. The other legs of the joint hoops did not yield until LS 66, with almost all of them yielding simultaneously.

5.6.1.4. Evaluation of Performance

The behavior of BCJ13 was unsatisfactory. The West beam never achieved its calculated strength due an anchorage failure which resulted in extensive spalling and crushing in the joint area. The results of BCJ13 point out that detailing of the anchorage in an exterior joint is probably the key to satisfactory behavior.

5.6.2 BCJ14 - Exterior with Slab

5.6.2.1. Behavior of Test Specimen

The load-deflection diagrams for BCJ14 , shown in Figs. 5-46 and 5-47, clearly demonstrates that the West beam performed much better in in BCJ14 than on BCJ13, the specimen without a slab. The EW beam reached its calculated capacity without the longitudinal bars failing at their anchorage. The additional flexural capacity provided by the slab steel is the best explanation for the difference in behavior In the early stages of the load history, the strains in the hooked bars for BCJ14 were smaller than those of BCJ13 because the slab steel helped to keep the stresses low by redistributing them to the slab along the NS edge. Obviously some of the moment is being transferred to the column as torsional forces through the edge beam. The West beam also reached its yield strength in the opposite direction, and showed a less pronounced loss of strength with cycling than any other test. The behavior of the North-South direction (parallel to the edge beam) was less satisfactory, and it follows the

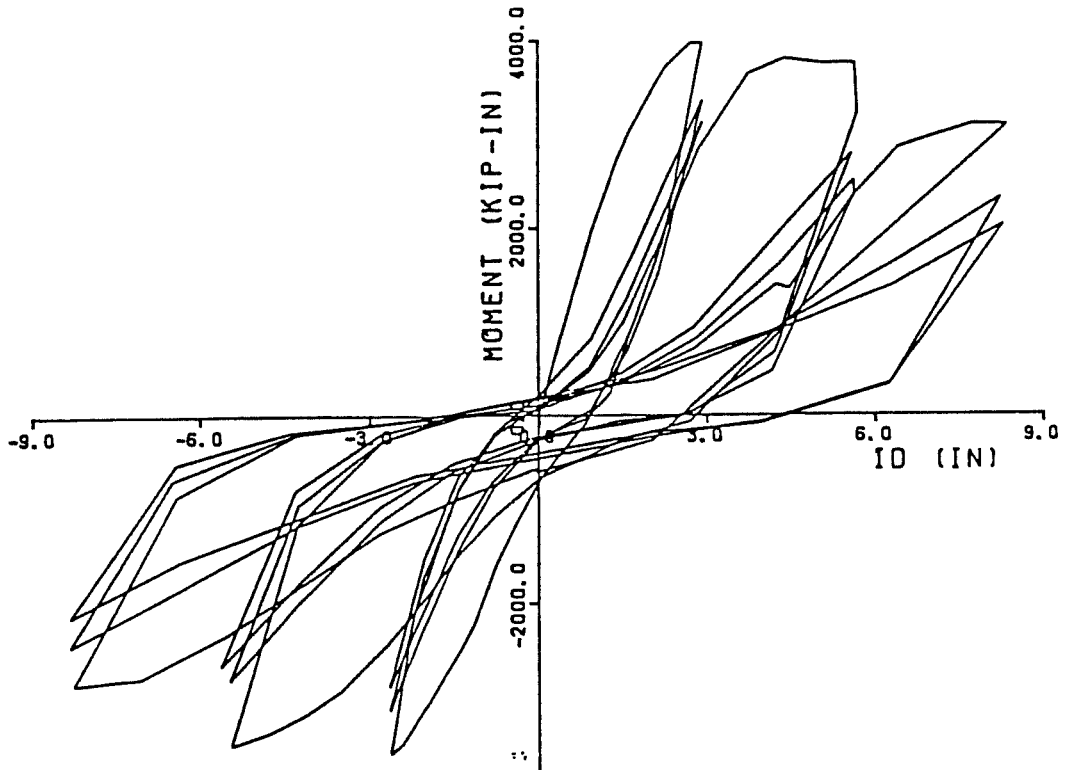


Figure 5-46 : Load-deflection curve for NS direction - BCJ14

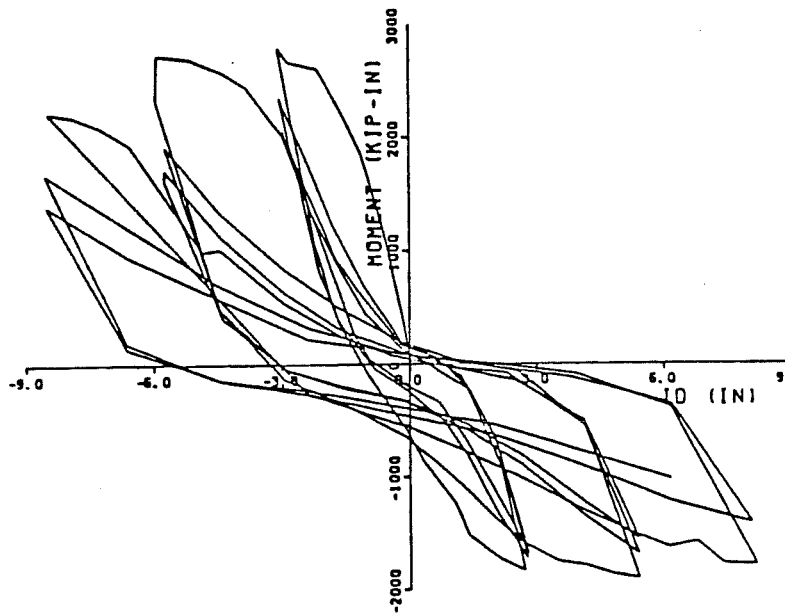


Figure 5-47 : Load-deflection curve for EW direction - BCJ14

patterns already described for tests with beams on both sides of the joint. The NS direction showed severe losses of strength between the first and second cycles at higher deflection levels and more significant pinching of the hysteresis loops near the zero deflection position in the larger deflection levels.

The observed behavior of BCJ14 did not differ substantially from that of BCJ13, except that the separation of the East face cover of the joint was delayed until the second deflection level. At LS 7, the joint showed some large inclined cracks, as shown in Fig. 5-48. Since the cover remained intact for much longer than in BCJ13, it is possible to see the crossing crack pattern formed by the load reversal to LS 24. The slab began to crack at LS 5, with cracks propagating into the slab from flexural cracks in the beam. The cracks formed perpendicular to the beams for a distance about equal to one beam width during the first deflection level, as shown in Fig. 6-6. At greater deformations, the cracks radiated away from the joint as shown in the same figure. Most of the initial cracking was confined to the top of the North and West beams, while no flexural cracking was evident at the bottom of the South beam. At LS 12, the beams had separated from the joint for about 50% of their depth, while extensive flexural cracking began to appear in the column corners in tension. Some compressive crushing was apparent at the bottom of the North and West beams, but not in the column corners. Loading to higher load stages created some more shear cracking in the

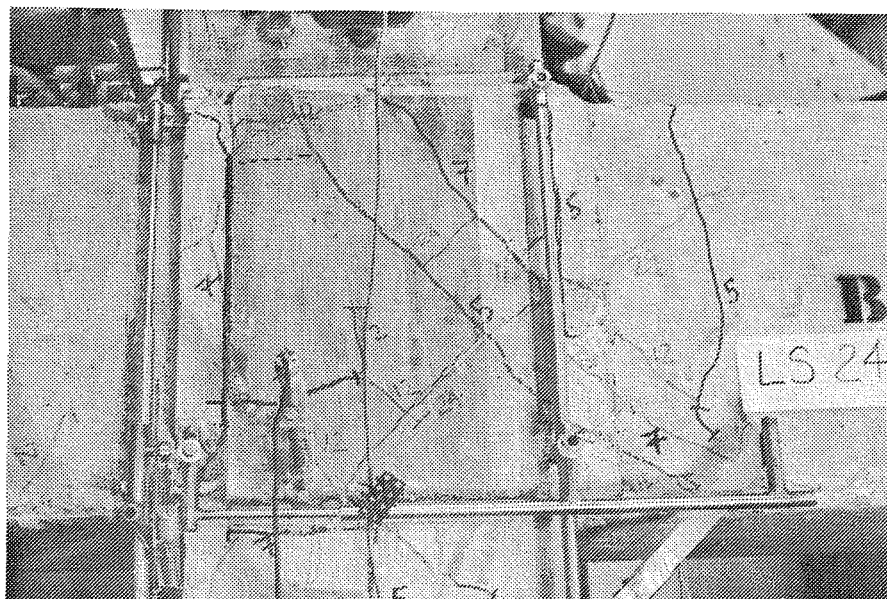


Figure 5-48 : BCJ14 at LS 24

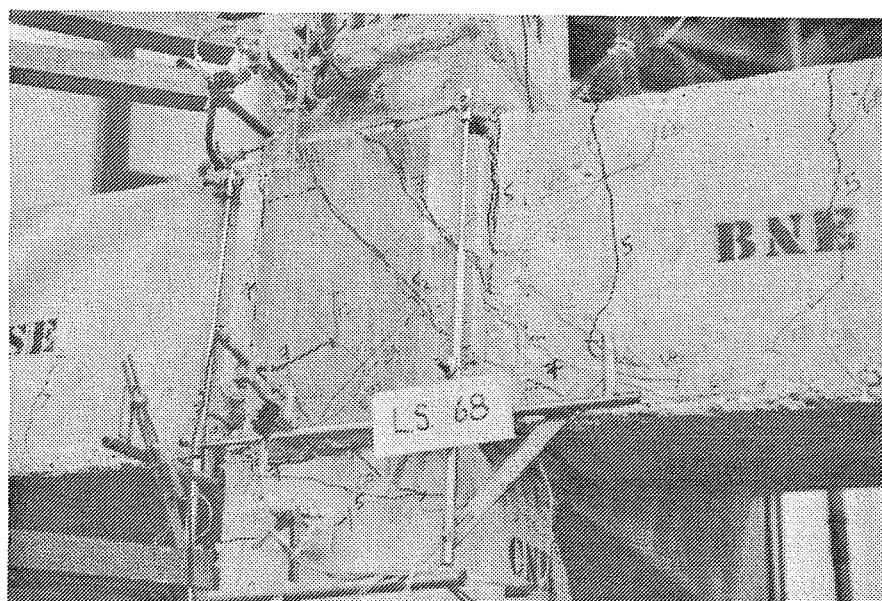


Figure 5-49 : BCJ14 at LS 68

East joint face, until the concrete separated near LS 124. The bar slips observed in this specimen were about one half of those of BCJ13 and gave another indirect indication of superior performance.

5.6.2.2. Deflection Measurements

The observations made for BCJ13 in terms of the calculated beam deflection components are also valid for BCJ14 (see Fig. 5-50). The contribution of the beam rotations beginning at the second deflection level, when the bars began to slip, are uncertain, but probably larger than those measured in other specimens. The measured joint shear strain were very similar to those of BCJ13, while the joint rotations were slightly smaller in the East-West direction.

5.6.2.3. Steel Strains

The steel strains measured for BCJ14 confirmed that the top longitudinal bars had indeed yielded during the first cycle, and continued to do so at the first peak for the next two deflection levels (See Figs. 5-52 and 5-53). The strains measured at the hooks of these bars, surprisingly, showed no yielding until LS 68, and confirmed that no slippage at the anchorage occurred during the first deflection level. The top reinforcement in the North beam yielded at LS 11, while the bottom reinforcement in the South beam yielded at LS 10, and slip occurred before that.

The column reinforcement showed some yielding at the SE top

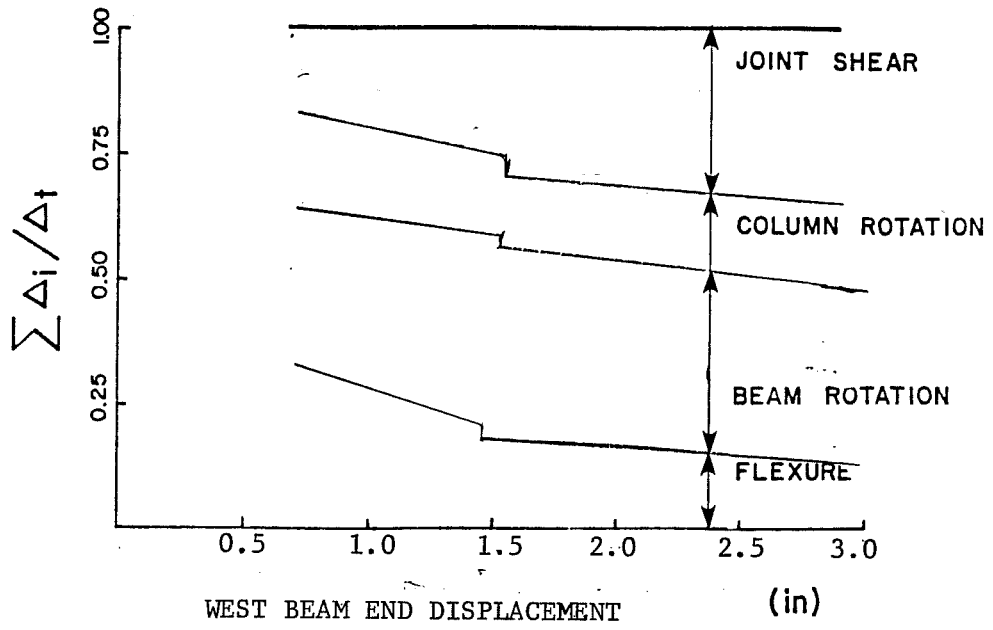


Figure 5-50 : Deflection components for BCJ14 (estimated)

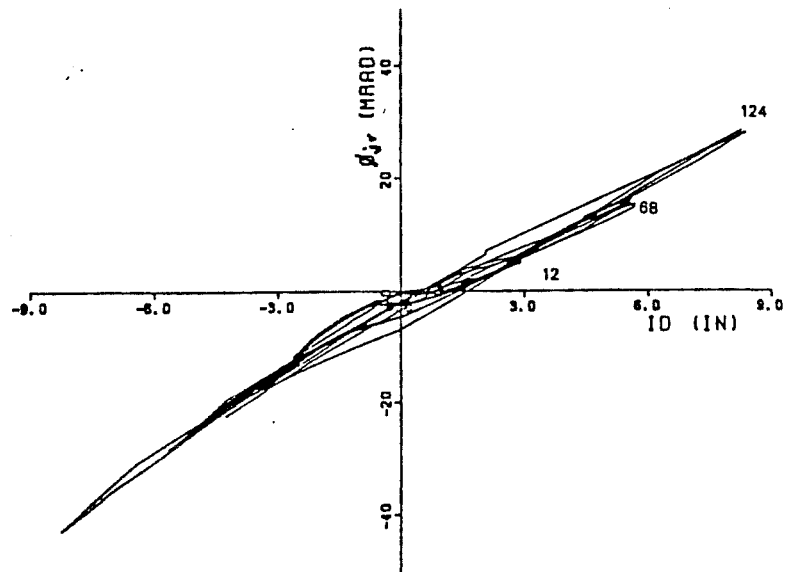


Figure 5-51 : Joint rotations for BCJ14

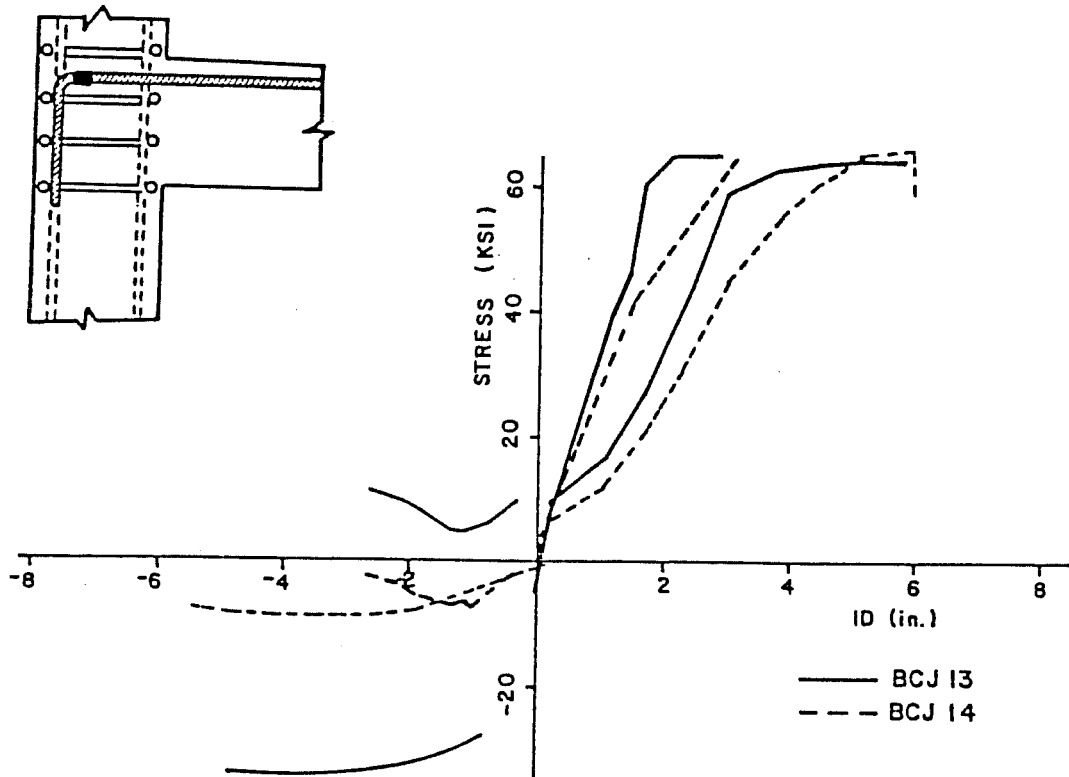


Figure 5-54 : Stresses at hook for exterior joint specimens

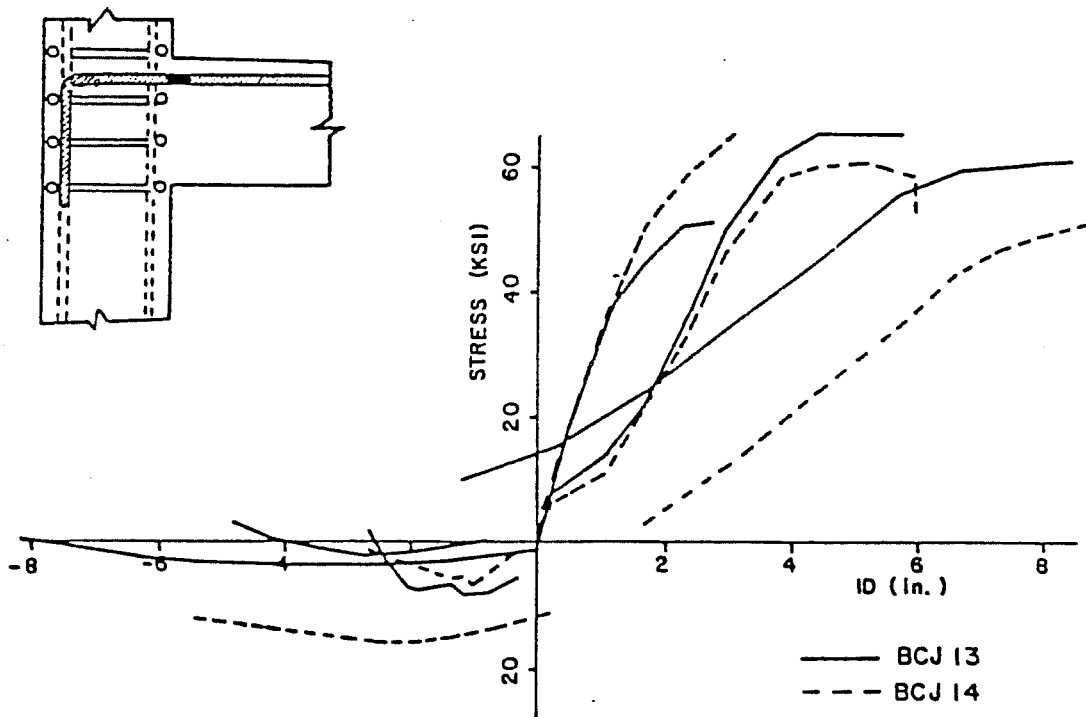


Figure 5-53 : Stresses at column face for exterior joint specimens

corner at LS 12, but the bar did not slip until LS 80. The column bar strains for this BCJ14 were larger than for BCJ13, but the column did not seem to lose capacity as fast, probably because the loss of section due to the separation of the East joint cover did not take place until the second deflection level. The ties showed some yielding in the Et leg during the first cycle but yielding for the remaining legs did not occur until the first positive peak at the second deflection level.

5.6.2.4. Evaluation of Performance

Specimen BCJ14 (with slab) showed much better behavior than BCJ13 (without slab) in terms of hysteretic response and ability to maintain strength. The anchorage details for both specimens were identical, so the improvement in behavior is likely due to the presence of a slab. The slab reinforcement delayed slip of the longitudinal bar of the West beam by providing an alternate path for the load to go from the slab into the column. The load was transferred as a torsional force through the North-South beams to the column, rather than as a flexural force through the hooked bars.

5.7 Conclusions

In Chapters 4 and 5, the behavior of specimens BCJ5 through BCJ14 was reviewed. It is clear that bar slippage and yield penetration rather than shear strength are the controlling mechanisms for the beam-column geometries tested. Only two of the specimens,

BCJ11 and BCJ15 can be said to have performed unsatisfactorily. BCJ11 failed early due to the lack of lateral restraint provided by the small framing beams. BCJ1 failed early due to the anchorage failure of the hooked bars. The rest of the specimens performed well during the first displacement level (2% drift), and only deteriorated when the drifts became unrealistically large (4% to 6% drifts).

The data collected in this test series indicates that the current design procedures, based on permissible shear stresses, are probably conservative. However, it is clear that joint design should take into account not only shear stresses, but also bond conditions and framing beam size. In the next chapter the behavior of the specimens tested will be summarized with respect to stiffness, shear strength and bond deterioration. A review of the joint capacities given by different design methods is also included, and a preliminary design procedure is suggested in Chapter 7.

Chapter 6

Evaluation of Experimental Data

6.1 Introduction

In this chapter the performance of the tests described in Chapters 4 and 5 will be examined in greater detail. The shear strengths predicted by current design procedures will be compared with the experimental values. The hysteretic response and the influence of bond on the performance of these subassemblages will be analyzed. Finally, the effect of the lateral restraint provided by the floor system will be discussed. In Chapter 7 design guidelines for beam-column joints are presented. The guidelines evolve from the evaluation of test results presented in this Chapter.

The behavior of six of the eight tested specimens will be used for this discussion. Specimens BCJ9 and BCJ9A, with slabs, will be treated as a single specimen since no significant differences were observed. Specimens BCJ10 and BCJ12, with wide beams, exhibited nearly identical behavior, although the concrete strengths were very different. For purposes of comparing the effect of framing beam size, the specimens with the most similar properties were used.

Therefore, BCJ12 will be considered as the typical specimen with wide beams.

6.2 Shear Strength

The forces acting on a beam-column joint in a frame subjected to seismic loading produce large horizontal and vertical shear forces in the joint area. The amount of horizontal shear in a joint is proportional to the sum of the positive and negative steel present in the beams at the joint face. For example, if it is assumed that the beams and columns have about the same cross-sectional area, and that the sum of the positive and negative reinforcement ratios is about 1.6%, shear stresses between $18\sqrt{f'_c}$ and $22\sqrt{f'_c}$ will be developed, as shown in Fig. 6-1.

Since concrete is weak in tension it has always been assumed that the shear force producing diagonal tension will be the controlling parameter in joint design. It is clear that shear is not transmitted through joints by the same mechanisms as in beams, and therefore the shear strengths obtained from beam-column joint tests are not comparable to those from beam specimens. This difference is recognized in design procedures by allowing much higher nominal shear stresses (up to $24\sqrt{f'_c}$) for joints than for beams and columns (up to $8\sqrt{f'_c}$). However, these design procedures apportion the shear strength between the steel and the concrete in various manners. In

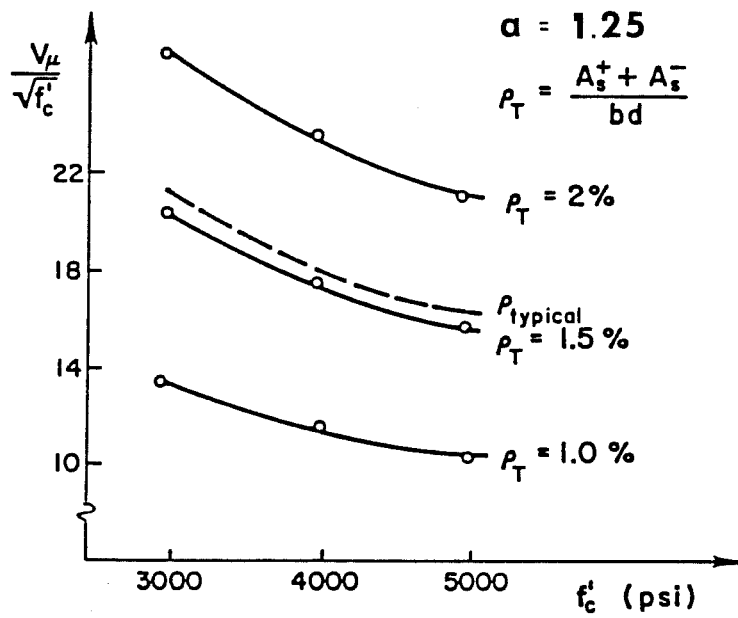


Figure 6-1 : Shear demand on typical joint

some design procedures , joints may be allowed to carry very large shear forces. To accomplish this, however, there may be congestion produced by the excessive amounts of transverse shear reinforcement required.

The beam-column joint series reported herein shows that specimens with insufficient transverse joint shear reinforcement (according to current design practices) nevertheless resisted and maintained very high shear stresses. As can be seen from Table 6-1, maximum nominal shear stresses in the test specimens were very large. In this table the data for all tests is shown to indicate that the maximum shears attained were not significantly different from those expected (See Appendix B), unless an early failure occurred (BCJ3, BCJ11, and BCJ13). The maximum shears shown in this table refer to the vectorial sum of the shears in the two principal horizontal directions (See Fig. 6-2(a)). The shear stresses are based on a nominal area of 185 in.^2 . Note that the normalized shear is very sensitive to the shear area assumed . The gross area of the column is 225 in.^2 , while the core area is only 144 in.^2 . The shear area used corresponds to the width and effective depth for the case of uniaxial loading. The width was equal to 15 in. and the depth to 12.3 in. In general, the shear in the two principal horizontal directions did not differ by more than 10% at the peaks, so the resultant can be considered to be oriented at 45 degrees from the axis of the beams for the interior joints, and about 30 degrees from the spandrel for the exterior joints.

Specimen Number	Max. Shear (1) (kips)	Max. Shear (2) (psi)	Max. Shear (3) Normalized
BCJ1	359.7	1940	28.0
BCJ2	396.7	2132	33.3
BCJ3	338.3	1819	27.6
BCJ4	346.4	1862	29.1
BCJ5 °	332.0	1794	27.7
BCJ6	317.1	1705	25.8
BCJ7	328.5	1766	25.5
BCJ8 °	305.0	1648	25.1
BCJ9 °	379.0	2048	30.5
BCJ9A	365.4	1972	28.5
BCJ10	295.0*	1594	30.1
BCJ11 °	264.0	1427	21.3
BCJ12 °	339.0	1837	27.3
BCJ13 °	206.0	1135	16.4
BCJ14 °	290.0	1567	21.7

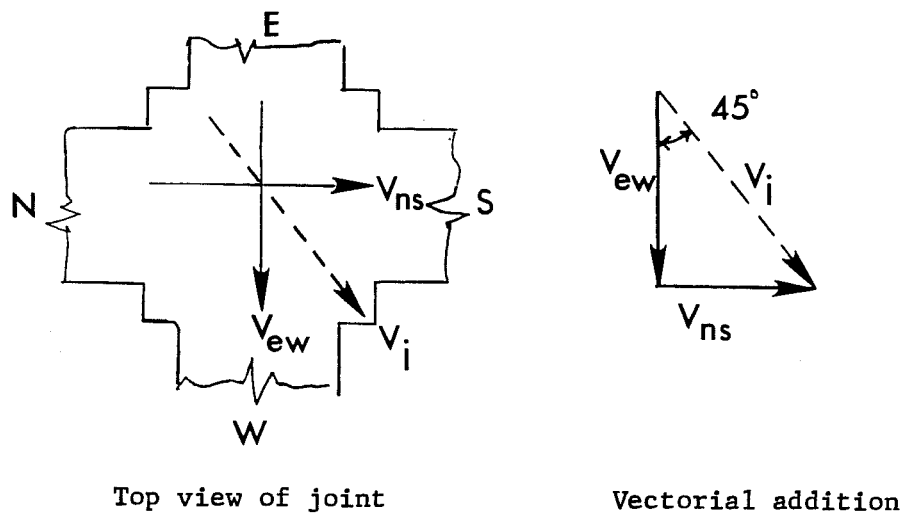
(1) Maximum shear is the vectorial addition of the North-South and East-West shear forces. The resultant acts at about 45 degrees from the main structural axis.

(2) Effective area assumed to be 185 in.² for all cases, as shown in Fig. 6.1

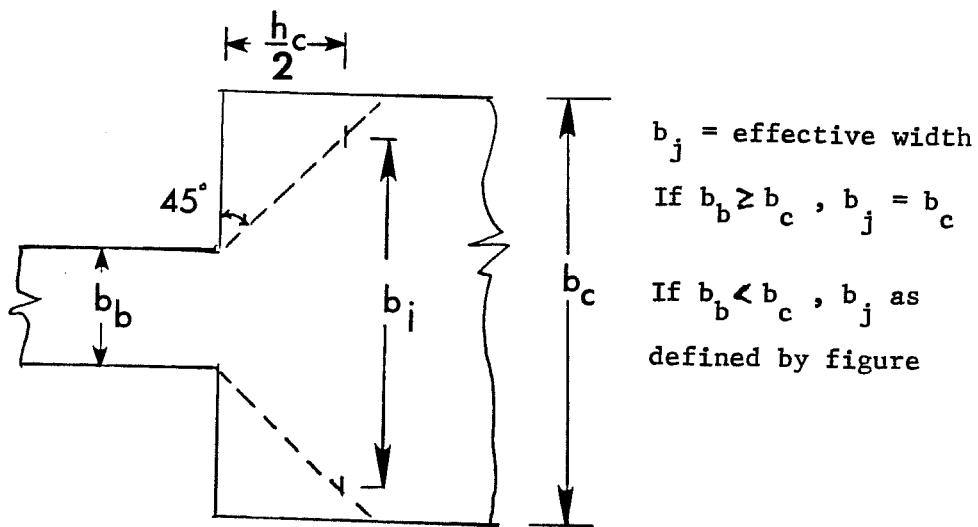
(3) Maximum shear stress divided by $\sqrt{f'_c}$

(*) Estimated

Table 6.1: Summary of shear strengths



(a) Calculation of joint shear in the joint



(b) Definition of effective joint width. (Ref. 7)

Figure 6-2 : Calculation for joint shear

The maximum shear stresses shown in Table 6-1 correspond to the maximum shear that could be introduced into the joint by the beam reinforcement. The exceptions are BCJ3 in which a hinge formed in the column, BCJ11 in which a combination of bond, flexure and shear failure occurred, and BCJ15 where the anchorage of the hooked bars failed. Thus, the values shown are not the actual shear strengths at failure but rather the maxima attained during the tests. The average values for the normalized shear strength are $26.5\sqrt{f'_c}$ for all specimens and $27.6\sqrt{f'_c}$ for the specimens that did not show an early failure (all except BCJ3, BCJ11, and BCJ13). This would correspond to about $18\sqrt{f'_c}$ in the uniaxial case, a value very close to the maximum allowed by most design procedures.

Table 6-2 shows the values of maximum horizontal joint shear at the positive and negative peaks. It is clear that the maximum shears attained for the first positive peaks are in general higher than those of the negative ones by about 5 to 10% for the first deflection level, and 10 to 15% for the second one. This difference disappears in the second and third cycles at each deflection level, where the values tend to equalize. It is interesting to note that the values at the first peak of the first and second deflection level are not very different, while that for the first peak at the third deflection level reflects the fact that the descending portion of the shear strength envelope has been reached. It is clear that the shear strength is regained as the deflections increase from the first to

TABLE 6.2 MAXIMUM RESULTANT SHEARS--POSITIVE PEAKS¹ (NEGATIVE PEAKS²)

Specimen Number	First Deflection Level			Second Deflection Level			Third Deflection Level		
	1	2	3	1	2	3	1	2	3
BCJ5	332 (304)	261 (269)	245 (257)	320 (290)	230 (240)	208 (219)	270 (255)	206 (209)	184 (184)
BCJ8	305 (291)	254 (249)	227 (237)	305 (284)	230 (231)	209 (222)	264 (259)	209 (218)	190 (194)
BCJ11	257 (234)	232 (200)	213 (195)	264 (223)	180 (183)	168 (161)	180 (173)	144 (144)	123 (115)
BCJ12	335 (309)	285 (273)	263 (265)	339 (299)	261 (238)	237 (233)	286 (268)	228 (224)	209 (200)
BCJ9	372 (345)	330 (313)	304 (299)	379 (343)	287 (295)	264 (252)	315 (297)	249 (243)	222 (219)
BCJ14	206 (189)	162 (164)	142 (153)	166 (199)	150 (168) ³	137 (151)	172 (160) ³	133 (140)	114 (125)
BCJ15	290 (241)	245 (213)	223 (199)	276 (237)	201 (196)	169 (183)	227 (201)	171 (169)	147 (148)

¹ Refers to North and West beams going down (LS 12, 32, 48, 68, 88, 104, 124, 144, 160).
² Refers to South and East beams going down (LS 24, 40, 56, 80, 96, 112, 136, 152, 168).
³ Estimated

the second deflection level, but that by the time the third cycle at the second deflection level is reached the shear strength is degrading rapidly. It should be recalled that a moment resisting frame is not likely to undergo such a severe load history even during a major earthquake, unless P-Delta effects become important. Therefore the extreme degradation of shear strength observed in these tests is not likely to be reached in practice.

It would be conservative to assume in design a value of shear strength for the cyclic loading case equal to the average of the second and third cycles at the first deflection level. With the exception of BCJ11 and BCJ15, the average reduction in shear strength with cycling for the first deflection level was 14% to 25% for the positive peaks and 11% to 17% for the negative peaks. Comparisons of this type for all the tests (See figures in Appendix D), showed that a reduction factor of 0.70 for cyclic loading seems reasonable.

A comparison of the allowable uniaxial shear strengths given by the different design procedures described in Chapter 3 are shown in Table 6-3. The individual contributions of steel and concrete are shown in Table 6-4. It must be noted that all these design procedures are not applicable to all BCJ specimens. For the exterior joints and the very wide or narrow beams, the most optimistic assumptions were made in order to obtain the maximum allowable shear stress values. The biaxial values shown refer to the vectorial addition of the unidirectional capacities along a 45 degree plane.

Table 6.3 Uniaxial Predicted Shear Strengths

Specimen	ACI 352	Japan	New Zealand	Meinheit & Jirsa	Flexure (3)	Measured
BCJ5	169	187	97	233	225	234
BCJ8	116	187	45	233	225	215
BCJ11	137	187	97	233	253	186
BCJ12	169	187	97	233	235	239
BCJ9	116	187	45	233	253	267
¹³ BCJ14(1)	116	187	45	233	235	187
BCJ14(2)	100	187	45	233	150	100
¹⁴ BCJ15(1)	116	187	45	233	253	237
BCJ15(2)	100	187	45	233	150	166

(1) North-South direction (two beams)

(2) East-West direction (one beam)

(3) Calculated using actual material properties and ultimate strength analysis

Table 6.4 Contributions of Steel and Concrete to Predicted Shear Strength (kips)

Specimen Number	ACI-ASCE 352 Committee			Sugano & Koreishi (Japan)			New Zealand standard			
	V_c	V_s	V_{uni}	V_c	V_s	V_{uni}	V_c	V_s	V_{uni}	
BCJ5	110	59	169	154	34	187	264	45	99	160
BCJ8	57	59	116	154	34	187	264	45	45	83
BCJ11	78	59	137	154	34	187	264	45	99	160
BCJ12	110	59	169	154	34	187	264	45	99	160
BCJ9	57	59	116	154	34	187	264	45	45	83
BCJ15(1)	57	59	116	154	34	187	264	45	45	83
BCJ15(2)	41	59	100	154	34	187	264	45	45	83
BCJ16(1)	57	59	116	154	34	187	264	45	45	83
BCJ16(2)	41	59	100	154	34	187	264	45	45	83

(1) North-South direction (two beams)

(2) East-West direction (one beam)

The reason for calculating the highest allowable rather than a minimum shear is clear from Table 6-5. In this table the ratios of the predicted to the measured capacity are shown. Most of the procedures underestimate the strength of the joint significantly, particularly in the case of the New Zealand provisions which allocate shear capacity to the concrete only when a column axial load is present. It must be recalled that the New Zealand recommendations were derived with the truss mechanism in mind. The situation in these tests is very different, since large bar slips and bond deterioration occurred. Thus, large discrepancies in the predicted and measured strengths should be expected. The ACI-ASCE 352 Committee recommendations also underestimate the strength significantly, although this procedure allocates about twice as much shear to the concrete as to the steel in most cases. The Sugano and Koreishi procedure assigns most shear (about 80%) to the concrete, and in most cases correlated well with the measured strengths. The Sugano and Koreishi procedure is not intended for exterior joints, but the results even for that case are very good. The Meinheit and Jirsa procedure, which was used to design the specimens in this test series, gives excellent correlation with the measured shear strengths, except for exterior joints for which no specific guidelines are given. The last column in Table 6-5 refers to the maximum shear strength that could be introduced into the joint assuming that the beam steel was yielding, an $\alpha = 1.1$, a maximum top column shear of 30 kips, and assuming the known material properties. This value is

an estimate of the maximum shear expected to be introduced in the joint area during each test. Thus, if this value is close to 1.00, the specimen reached the flexural strength of the beams and the shear strength obtained represent a maximum measured quantity rather than a failure value. If this value is less than 0.90 then probably some mechanism other than beam yielding governed the behavior of the specimen.

The values from the table indicate a very large scatter in calculated shear strength. Since the design procedures are based on different assumptions scatter is to be expected. It must be pointed out that most procedures are to be used in design to provide a safe lower bound to shear strength, and are not intended to predict actual shear strength by analysis. However, it is clear that there is no method currently available that accurately predicts the shear strength of all types of joints.

The values from the table also show that the contribution of the concrete to the shear strength, while hard to quantify, may be very large. The shear capacity provided by the 2 #4 ties present in the joint is only 45 kips in each direction. The difference between this and the measured shear force must be carried by the concrete. The concrete had to carry, at the peaks, a shear force of 175 kips in each direction, which would be equivalent to about a 945 psi shear stress. It is not likely that the concrete can carry such a stress

Table 6.5. Normalized Uniaxial Shear Strengths (1)

Specimen Number	ACI 352	Japan	New Zealand	M&J	Flexure
BCJ5	0.72	0.80	0.42	1.00	0.96
BCJ8	0.53	0.87	0.21	1.08	1.04
BCJ11	0.74	1.00	0.52	1.25	0.73
BCJ12	0.71	0.79	0.41	0.98	0.98
BCJ9	0.43	0.70	0.18	0.87	0.95
Interior					
x =	0.63	0.83	0.35	1.04	0.93
σ =	0.14	0.11	0.15	0.14	0.12
BCJ14(2)	0.62	1.00	0.24	1.24	0.79
BCJ14(3)	1.00	1.87	0.19	2.23	0.66
BCJ15(2)	0.49	0.79	0.19	0.98	0.93
BCJ15(3)	0.60	1.13	0.27	1.40	0.90
All					
x =	0.65	0.99	0.29	1.26	0.88
σ =	0.17	0.35	0.13	0.14	0.13

(1) Predicted shear strength by each method divided by measured one.

(2) North-South direction (two beams)

(3) East-West direction (one beam)

through a diagonal tension mechanism. Such a load could only be carried by a large concrete strut acting between opposite corners of the joint. A strut with an area of 80 in.² and with stresses of about 75% of the concrete compressive strength would be required to carry this 175 kips of horizontal shear. The size of the framing member will obviously influence the size of the strut. Thus it is likely that for the specimen with narrow beams the strut area was small and the compressive stress high, while the opposite would be true for the wide beam specimens.

For the case of biaxial loading, given the extensive cracking observed at the joint corners, a single large strut is not realistic. On the other hand, series of smaller struts whose required end restraints are provided by the beam and column compressive blocks rather than by the joint shear reinforcement, are quite possible. The important difference between this and the mechanism already discussed in Chapter 2 is that all the framing members are required to be present and loaded to confine the joint. This mechanism will be more fully discussed in Section 6.5, where the effect of framing member geometry on joint performance will be treated.

In conclusion, the shear strength of joints is probably very high compared to the shear values generally associated with reinforced concrete. The primary reason is the presence of framing members which confine the joint and allow very large forces to be

transmitted by several inclined concrete struts. Any design procedure for joints in monolithic reinforced concrete structures must take geometric effects into account to reflect observed behavior.

6.3 Hysteretic Behavior

To withstand moderate earthquakes without much structural damage and survive major earthquakes without collapsing, structures must be provided with certain stiffness, strength and energy-dissipation capacity. The stiffness is provided by the member sizes and material properties, while the energy dissipation is essentially a function of the location and detailing of those critical sections where most energy must be dissipated. In the case of moment-resisting frames, the beam ends and bottom story columns must be provided with large rotational capacities, while the beam-column joints and the remaining columns must be made as strong as possible.

In general the energy dissipation capacity of a section is related to its hysteretic behavior. It is assumed that if a particular section shows large, non-deteriorating hysteretic loops its behavior under seismic loads will be satisfactory. Tests show that such behavior may be difficult to obtain in reinforced concrete structures because of cracking, shear distortion, and deterioration of bond through the joint.

In Fig. 6-3 the typical hysteretic behavior for a reinforced concrete member is shown. In Fig 6-4 the main mechanisms contributing to this type of behavior are outlined. To obtain satisfactory behavior from a reinforced concrete section shear failures and bond deterioration must be avoided or delayed.

The hysteretic behavior can also give a measure of the stiffness of the system, since the slopes of the hysteretic loops correspond to the stiffness of the system. The importance of stiffness in moment-resisting frames resides in the need to limit interstory drifts to control both the damage under a moderate earthquake and the secondary moments under a large earthquake. A compromise between stiffness, strength, and energy dissipation capacity must be reached in design since all three can rarely be achieved simultaneously given practical and economical considerations. Stiffness requires large sections and high strength materials, while energy dissipation requires deformable sections and ductile materials.

The hysteretic behavior of the BCJ test series was described in the previous chapters. In general, the hysteretic curves shown would be characterized as poor since large losses in stiffness and strength were present. The equivalent peak-to-peak stiffnesses and the area of the loops for these tests are summarized in Table 6-6 and 6-7.

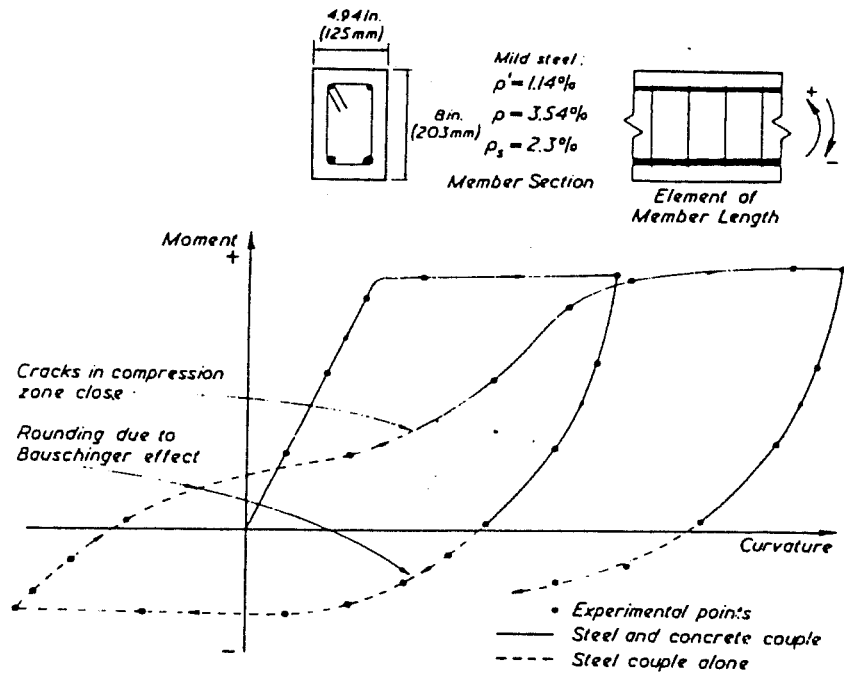


Figure 6-3 : Hysteretic behavior of reinforced concrete (Ref. 85)

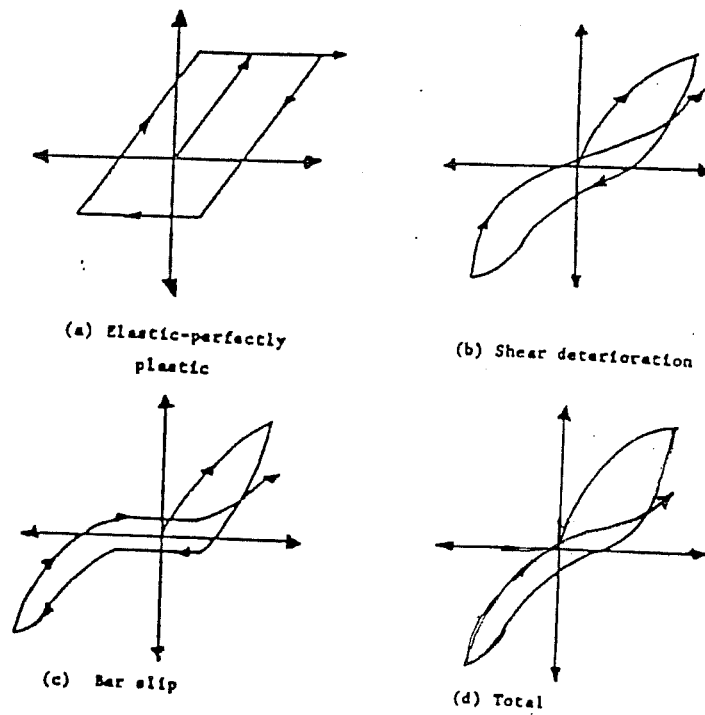


Figure 6-4 : Types of hysteretic behavior

TABLE 6.6 EQUIVALENT PEAK-TO-PEAK STIFFNESSES (KIPS/IN)
NORTH BEAM (N), SOUTH BEAM (S)

Specimen Number	First Deflection Level			Second Deflection Level			Third Deflection Level			
	1	2	3	1	2	3	1	2	3	
BCJ5	N	20.4	17.0	16.0	9.9	7.4	6.7	5.7	4.4	3.9
	S	20.4	17.7	16.9	9.9	7.8	7.0	5.7	4.5	4.0
BCJ8	N	19.1	15.6	14.9	9.5	7.2	6.7	5.6	4.4	4.0
	S	17.8	15.2	14.5	8.9	7.2	6.8	5.4	4.4	4.2
BCJ11	N	15.7	14.0	13.0	7.9	5.5	5.3	3.7	3.1	2.5
	S	15.6	14.2	13.4	7.9	5.0	5.3	3.8	3.1	2.5
BCJ12	N	19.9	17.1	16.5	10.1	7.7	7.3	6.0	4.9	4.5
	S	19.7	17.6	16.3	9.9	7.8	7.4	5.9	4.6	4.2
BCJ9	N	23.5	20.8	19.8	11.8	9.5	8.5	6.9	5.7	5.0
	S	22.8	20.0	19.1	11.3	9.2	8.0	6.1	5.6	4.2
BCJ14	N	17.1	13.5	12.4	8.0	6.6	6.1	5.0	4.0	3.5
	S	16.3	12.7	11.8	7.0	5.9	5.4	4.2	3.3	4.4
BCJ16	N	21.3	18.1	16.8	10.3	7.9	6.9	5.9	4.6	4.0
	S	21.4	18.3	17.0	10.0	8.0	7.0	5.3	4.4	3.9

The peak-to-peak stiffnesses for the North and South beams (Table 6-6) do not show a significant effect for the original direction of loading. The values for the North beams were almost always higher, but only by 2% to 5%. It is interesting to note that the stiffnesses for the first cycle are about one fifth to one fourth those found in the uncracked state. Moreover, because of the drop in strength with cycling, the peak-to-peak stiffness decreases by 15% to 20%. Although the stiffness continues to decrease between the second and third cycles, the decline is not as pronounced.

The stiffnesses decreased roughly by one half from one deflection level to the next. Between the first and second levels this is due mainly to doubling the displacement, while between the second and third some significant strength losses result in changes in stiffness larger than the 33% caused by the increase in deflection. It is clear that the decrease in stiffness is not too large in the first deflection level, while during the second and third levels the stiffnesses reach values unacceptable in actual design. It must be emphasized that one would not expect all beams in a structure to be yielding simultaneously unless a very large earthquake occurs. Thus, although large changes in stiffness can be anticipated, one must be careful in extrapolating the changes in stiffness for an individual beam to the overall stiffness of the structure.

The areas of the loops under the hysteretic curves for the North beams in all the tests are shown in Table 6-7. Three values are given in the table for each cycle of loading. The first is the actual area of the loop in kip-in. The second is the area of the loop normalized with respect to the largest loop in that test. The third value is the area of the loop normalized by the area of the largest loop of all the tests (first cycle at the third deflection level for BCJ19).

As previously discussed, these areas are a measure of the energy dissipation capacity. For the case of an elastic-perfectly plastic system, and given the calculated member strengths, the area under a single loop would be in the order of 130 kip-in. during the first cycle. The best performance, by BCJ12, achieved only about 30% of this value. Large losses were noted between the first two cycles at the first deflection level. These losses were typically on the order of 60% to 70%. The results indicate that the specimens had unsatisfactory hysteretic characteristics when the lateral drifts approach 2%. The performance was marginally better at the second deflection level. If it is assumed on the basis of an elasto-plastic model that the energy dissipation capacity for this case should be about twice that of the first deflection level, in most cases the first cycle at the second deflection level equalled or exceeded twice the value for the first. Perhaps as important, the deterioration between cycles was not as large with values varying between 35% and

TABLE 6-7 AREAS OF HYSTERESIS LOOPS FOR NORTH BEAMS

Specimen	First Deflection Level	Second Deflection Level	Third Deflection Level
BCJ5	36.7	67.5	77.2
	0.47 ¹	0.87	1.00
BCJ8	0.34 ²	0.63	0.72
	29.1	62.0	68.2
BCJ11	0.43	0.92	1.00
	0.27	0.59	0.64
BCJ12	34.5	56.9	66.6
	0.37	0.86	1.00
BCJ9	0.23	0.54	0.62
	37.2	75.6	95.3
BCJ15	0.39	0.80	1.00
	0.35	0.71	0.89
BCJ16	27.6	79.3	106.8
	0.26	0.74	1.00
BCJ5	0.26	0.74	1.00
	24.9	54.1	66.3
BCJ16	0.33	0.72	1.00
	0.23	0.50	0.62
BCJ16	28.0	71.6	68.0 ³
	0.40	1.00	0.96
BCJ16	0.26	0.67	0.66

¹ Normalized with respect to the maximum area for every specimen.

² Normalized with respect to the largest cycle obtained in all tests; first cycle at third

³ Estimated.

55% in most cases. For the third deflection level the situation is reversed; the specimens were so damaged at this stage that only the specimen with a slab (BCJ9) was able to obtain a value close to three times that of the first deflection level. In general, it can be said that the energy dissipation performance of these specimens was poor. The deterioration of bond, bar slip, and crushing of the compression areas are the main contributors to this unsatisfactory behavior. Comparison of these test results with those of other investigators shows that the amount of deterioration will decrease as more realistic ranges of column reinforcement and larger amounts of joint reinforcement are utilized. Thus actual beam-column joints designed according to the recommendations of the ACI-ASCE 352 Joint Committee will certainly show better behavior than that evidenced by the BCJ specimens.

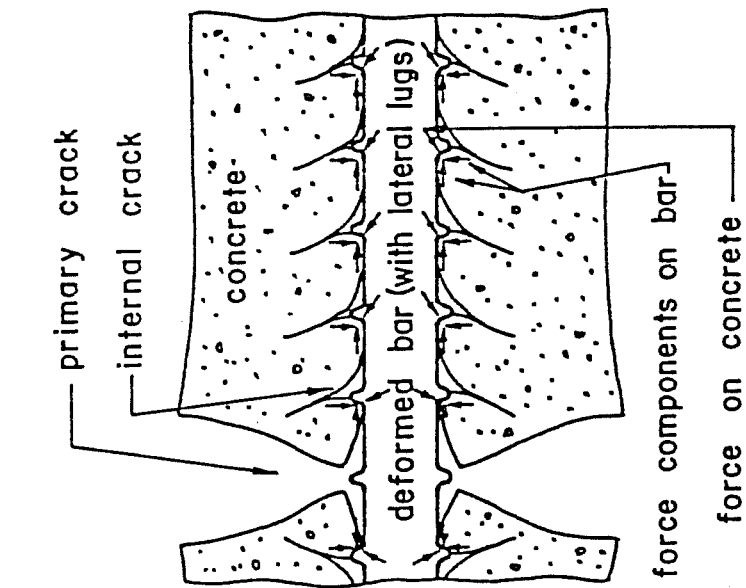
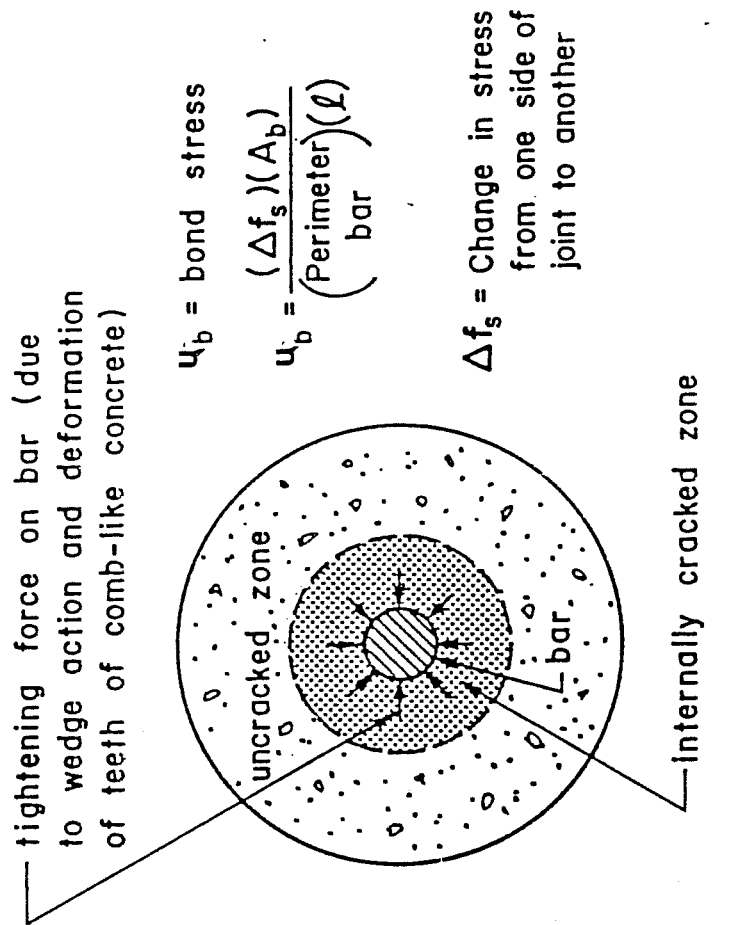
Although it is difficult to compare the energy dissipation capacity of different specimens, some conclusions can be drawn from Table 6-7. The specimens with the best confinement, BCJ12 (wide beams) and BCJ9 (slab), showed the best overall behavior. The specimen with the worst confinement, BCJ11, and those without axial loads, BCJ8 and BCJ15, showed the least satisfactory behavior.

The main reason for the unsatisfactory hysteretic behavior of the specimens in this series can be traced to the low ratio of column flexural capacity and the high shear stress levels. The typical

moment ratios for these tests were in the order of 1.25, with a minimum of 1.13 for test BCJ11 (See Appendix B). The shear stresses in the joint were in the range of 20 to $30 \sqrt{f'_c}$ for most peaks, considerably exceeding the cracking limit. Due to the small percentage of joint reinforcement extensive shear cracking of the joint, and the consequent deterioration in behavior, could not be prevented. The drop in stiffness and energy dissipation capacity can also be explained by the large amount of inelastic action apparent in the columns, particularly in the latter loading cycles. The low ratio of column to beam flexural capacity used in this test series is the result of one of the main objective of the study, i.e., the desire to introduce very large shears in the joint area. Thus, one would not expect the members in well-detailed moment-resisting frames to have such a low ratio of column to beam capacity. The tests confirmed that adding column longitudinal steel, rather than increasing the area of the column, is not a satisfactory solution to increase the column moment capacity. Tests and experience have shown that beam-column joint subassemblages with column-to-beam capacities less than 1.20 perform poorly, while those with ratios higher than 1.80 perform very well.

6.4 Bond Conditions and Bar Slip

The problem of anchoring longitudinal bars through beam-column joints is well known. As shown in Fig. 6-5, the bond stresses through the joint are directly proportional to bar diameter and inversely proportional to the depth of the column. In order for a joint to perform satisfactorily the bond stresses must be kept low, particularly if the bars are going to be cycled through several inelastic load reversals. While a particular upper limit for bond stress in the joint has not been defined, tests have shown that bond stresses higher than 800 psi bars result in unacceptable deterioration with cycling. By fixing the value for a maximum allowable bond stress, the size of the beams and columns would need to be proportioned to the diameter of the largest bar anchored in that member. For example, for an allowable bond stress of 800 psi and a total bar stress change of 60 ksi across the joint, the minimum column depth would need to be about 18 times the diameter of the beam bar. Since the design philosophy for ductile moment resisting frames requires yielding at one side and some compression at the other in order for the to satisfy strain compatibility, the minimum column depth should be about 24 times the maximum bar diameter. It is important to recognize that this requirement extends to the column bars also; they need to be anchored through a distance given by the beam depth. Since the column will not be required to yield, this requirement could be relaxed if we can assure that the level of



CROSS SECTION

LONGITUDINAL SECTION OF AXIALLY LOADED SPECIMEN

Figure 6- 5: Bond stresses in a bar anchored in a concrete block (Ref. 108)

stress in the column bars will be below yield. However, these tests as well as those by Ehsani [31] and Durrani [29] show that bond deterioration can occur even if the level of bar stress is well below yield; thus an equivalent requirement for column bars would have to take into account the amount of cracking to be expected due to shear and bond stresses as well as geometric considerations involving the lateral restraint of the column corners by framing members

For the series of tests reported herein, the measured bond stresses for the negative moment reinforcement should have been considerably above the 800 psi limit discussed above. In theory, assuming the bar to be yielding on one side of the joint and carrying some compression on the other, the resulting average bond stress through the joint would be about 1300 psi. It is recognized that the bond stresses are not equally distributed along the bar. Therefore the bond stress near the yielding end must have been higher [108].

In practice, large bond stresses through the joint were not achieved. Figures 6-6 and 6-7 show the bar stresses versus interstory displacement for a longitudinal bar at the column face of the East-West beams. From the strain gage in the East side of the joint, see Fig. 6-14, a tensile stress of about 14 ksi was reached during the application of the dead load (0.10 in. downwards). As soon as the direction of loading was reversed, the bar was unloaded, reaching the zero stress level when it had deflected about 0.3 in.

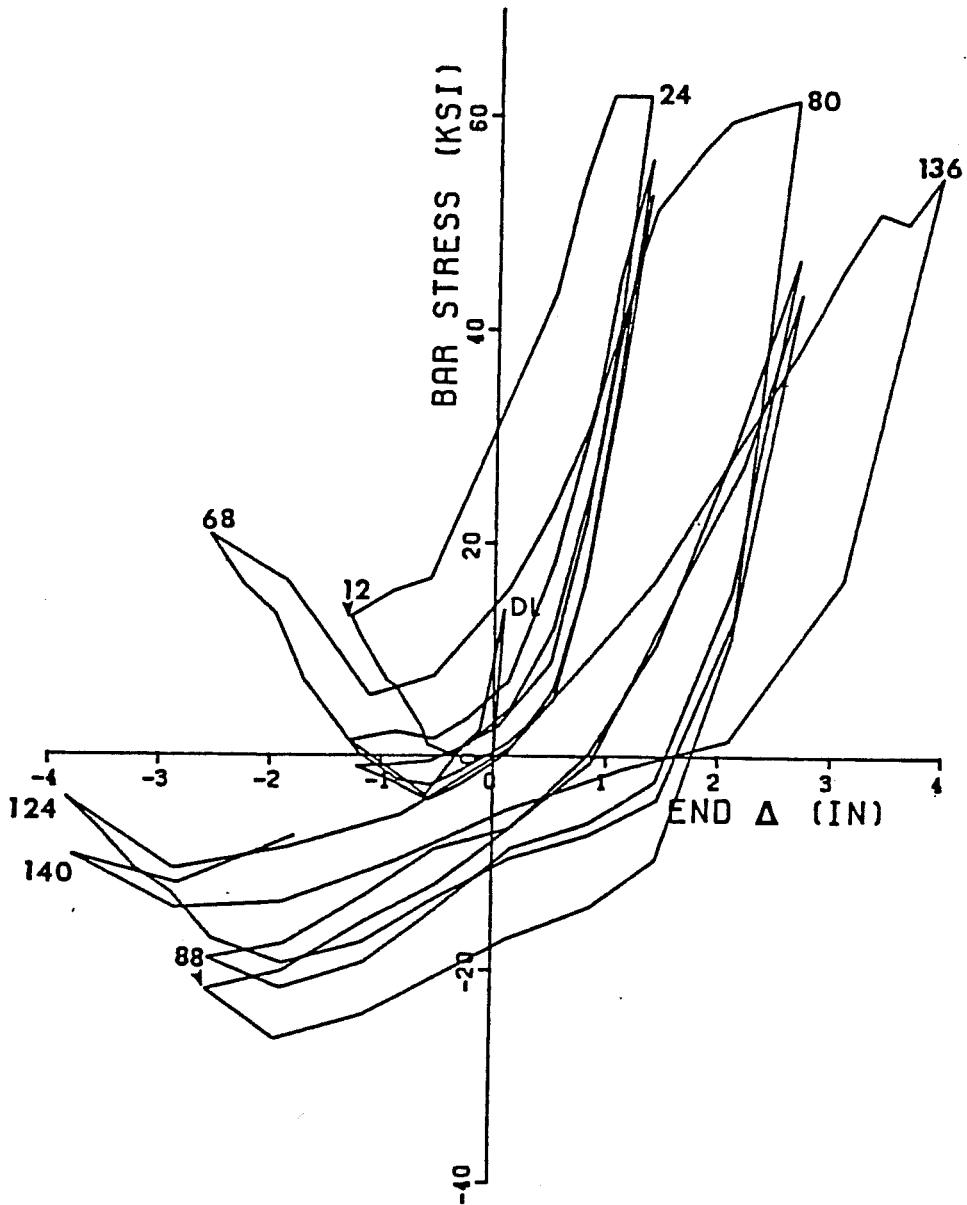


Figure 6-6 : Stress vs. beam end displacement history for top East gage at column face (BCJ8)

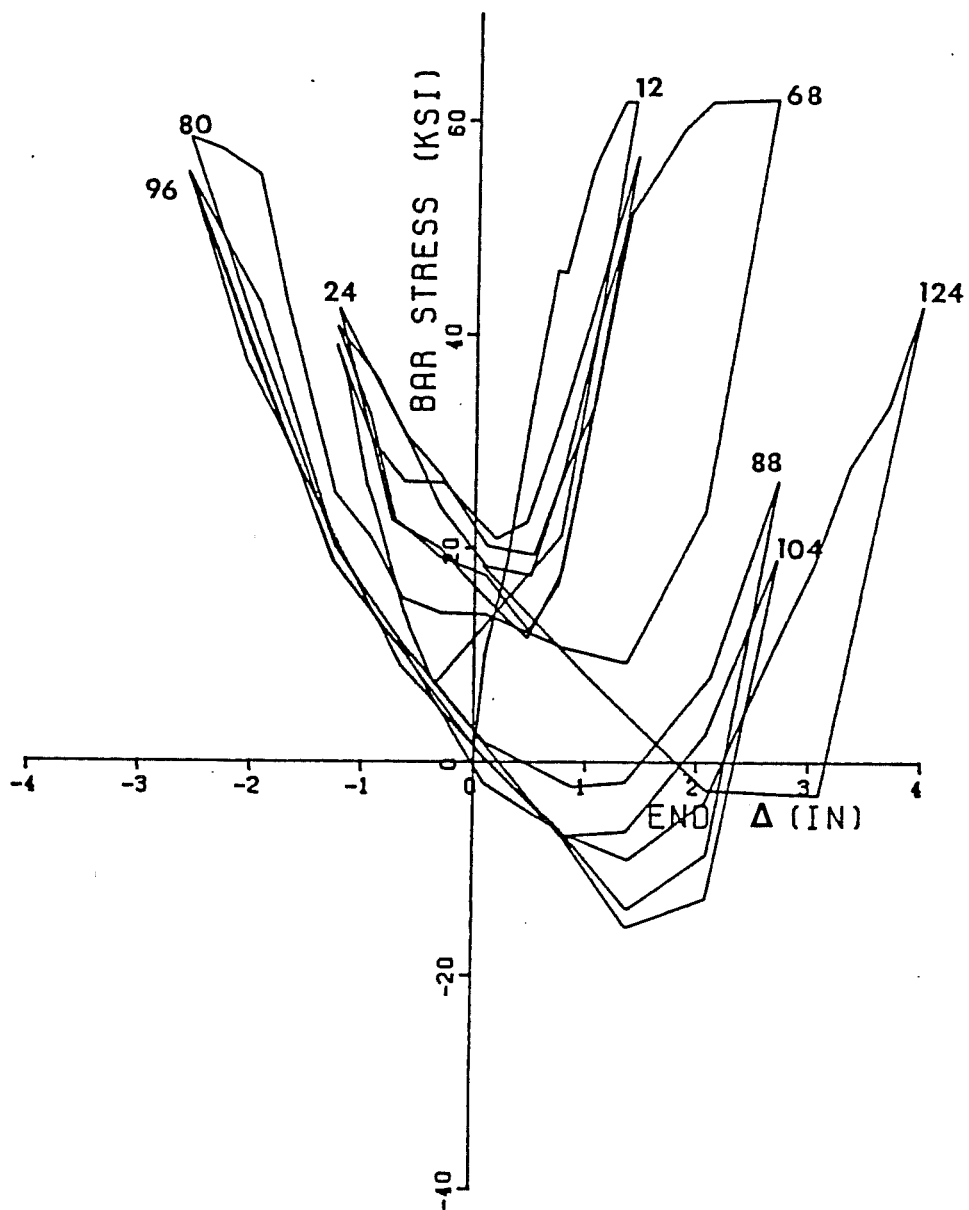


Figure 6-7 : Stress vs. beam end displacement history
for top West gage at joint face (BCJ8)

upwards. As the deflection was increased in the same direction, however, the bar did not continue to pick up compression as expected. After reaching about a 5 ksi compressive stress at L.S. 5, the bond across the joint began to deteriorate and the gage began to show tensile stresses. By the time the first peak was reached (L.S. 12), the tensile stresses were around 14 ksi. Surprisingly, these stresses did not decrease as the load direction was reversed. The stresses appeared to be "locked in" and the bar kept picking up tension as the beam moved back to the unloaded position. As the beam began to be loaded downwards, the gage began to show substantial amounts of tension, and yielded near L.S. 22 .

The second and third cycles at this deflection level indicated very little if any tension when the beam was loaded upwards (L.S. 32 and 48), and no evidence of yielding when loaded downwards (L.S. 40 and 56). When loaded to the second deflection level, the bar showed the same type of behavior as in the first cycle of the first deflection level. The only differences were that the bar did unload lightly when the load was reversed at L.S. 68, and that substantially more yielding was observed at the second negative peak (L.S. 80). Cycling at the second and third deflection levels resulted in more substantial compressive stresses when loaded upwards (L.S. 88, 104, 124, and 140) and no yielding when loaded downwards (L.S. 96, 112, and 136) Thus, the onset of bond deterioration can be traced to the top of the first cycle, but the bar was transferring some stress to the concrete throughout most of the load history.

By contrast, the stresses measured by the gage at the other side of the joint show significant early deterioration. At the West face tensile stresses of about 11 ksi were recorded at the dead load position, and continued to increase as expected as the beam was loaded downward to LS 12, the first peak. The bar yielded near L.S. 10 and when the load was reversed, it never showed compressive stresses. In fact, by the time the first negative peak was reached (L.S. 24) the bar again had very large (35 ksi) tensile stresses. This behavior continued throughout the first and second deflection levels, and indicated severe bond deterioration and yield penetration into the joint. By comparison, a gage at 8 in. away from the joint (Fig. 6-8) and one 16 in. away (Fig. 6-9), showed much better behavior, although the second gage in the West beam did show yielding during the second and third deflection level.

The average bond stresses through the joint for this bar are shown in Fig 6-10. The highest stress achieved was about 920 psi during the second cycle at the first deflection level; similar values were achieved for the first four positive peaks. For the peaks in the negative direction, comparable bond stresses were present only on the first cycle. This is due to bond deterioration, yield penetration, and bar slip of the bar at the West side of the joint (See Fig. 6-7). The West side of the bar behaved very poorly, and by LS 88 (+2 Δ ₂), it had slipped through the joint. This change is indicated by the fact that this curve is "out-of-phase" with respect

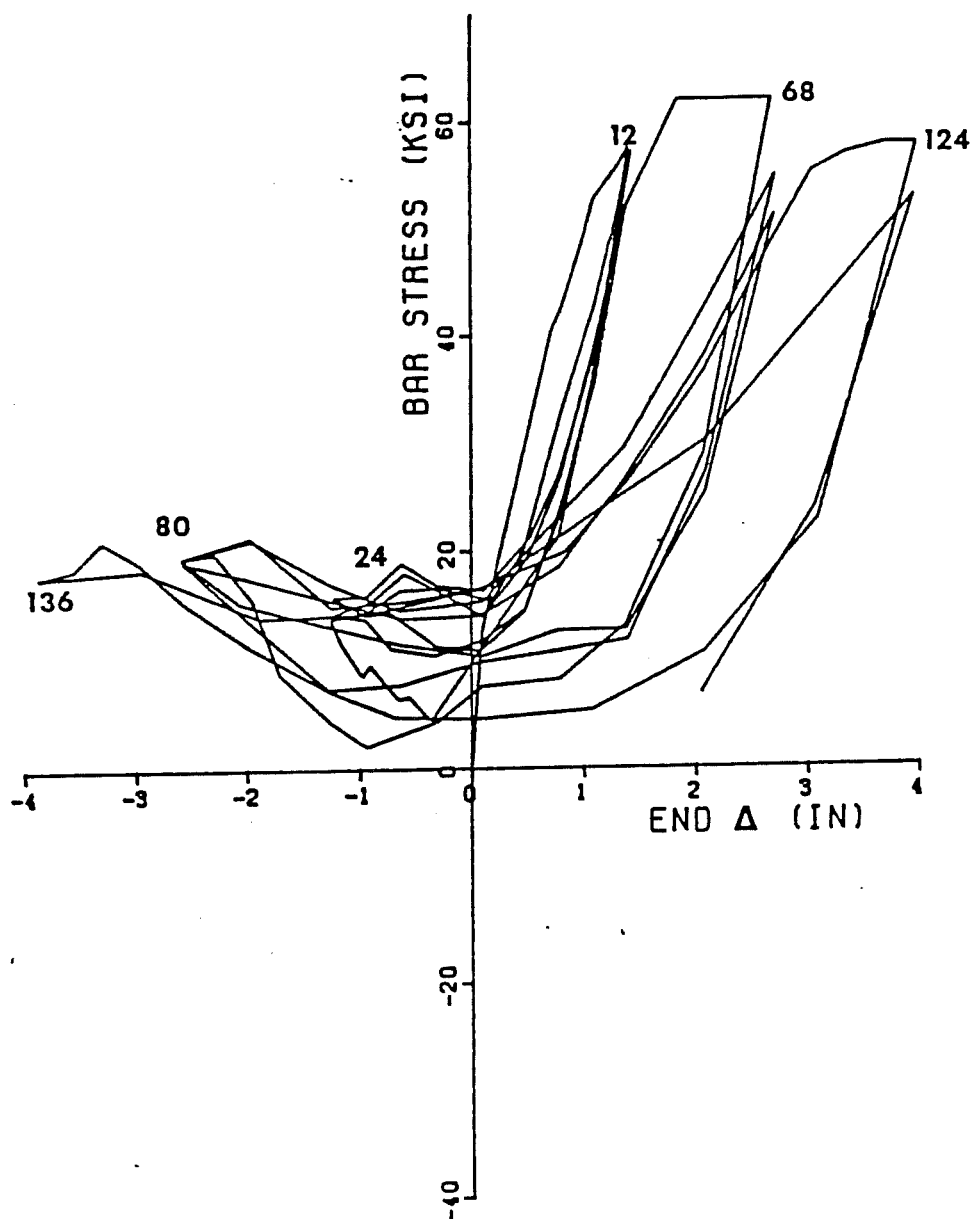


Figure 6-8 : Stress vs. beam end displacement history
for top West gage at 8 in. from column
face (BCJ8)

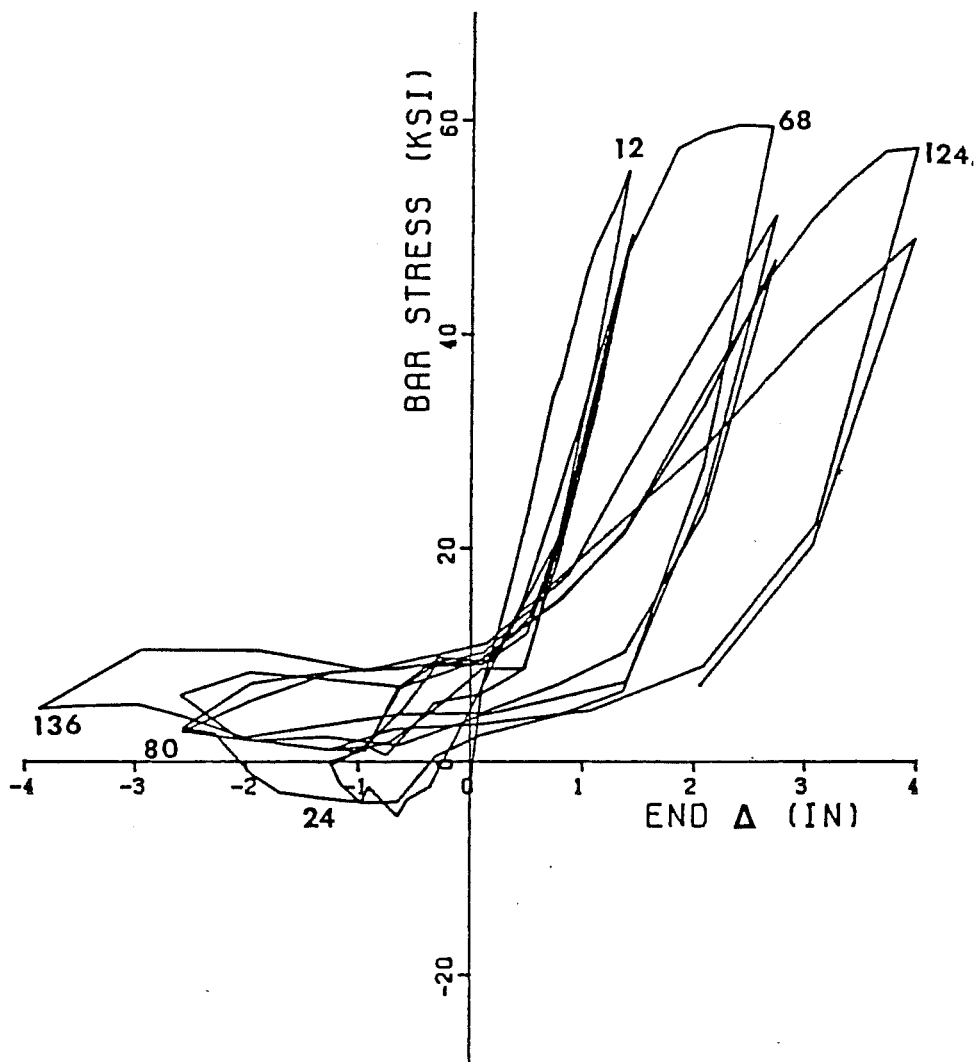


Figure 6-9 : Stress vs. beam end displacement history for top West gage at 16 in. from column face (BCJ8)

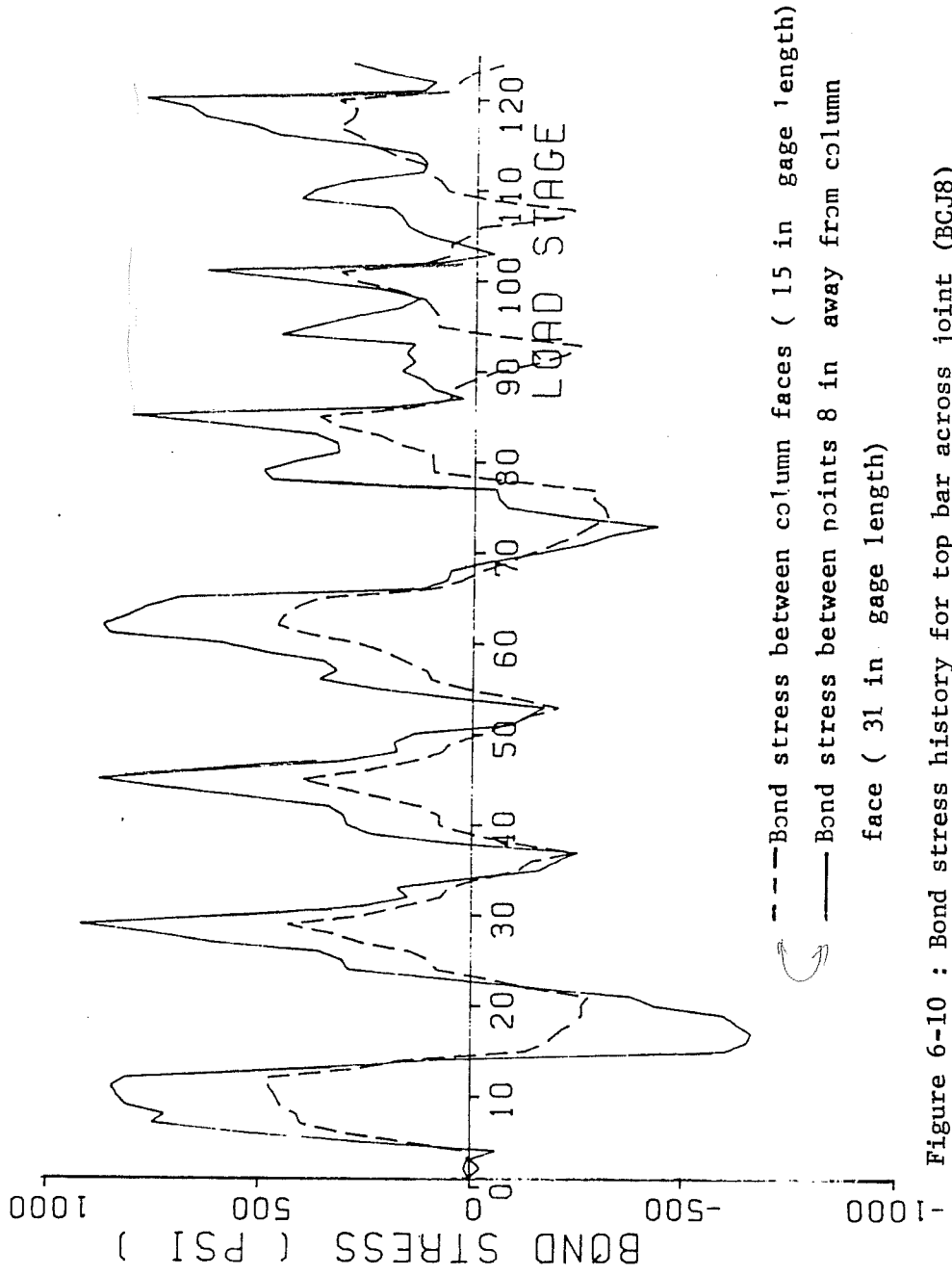
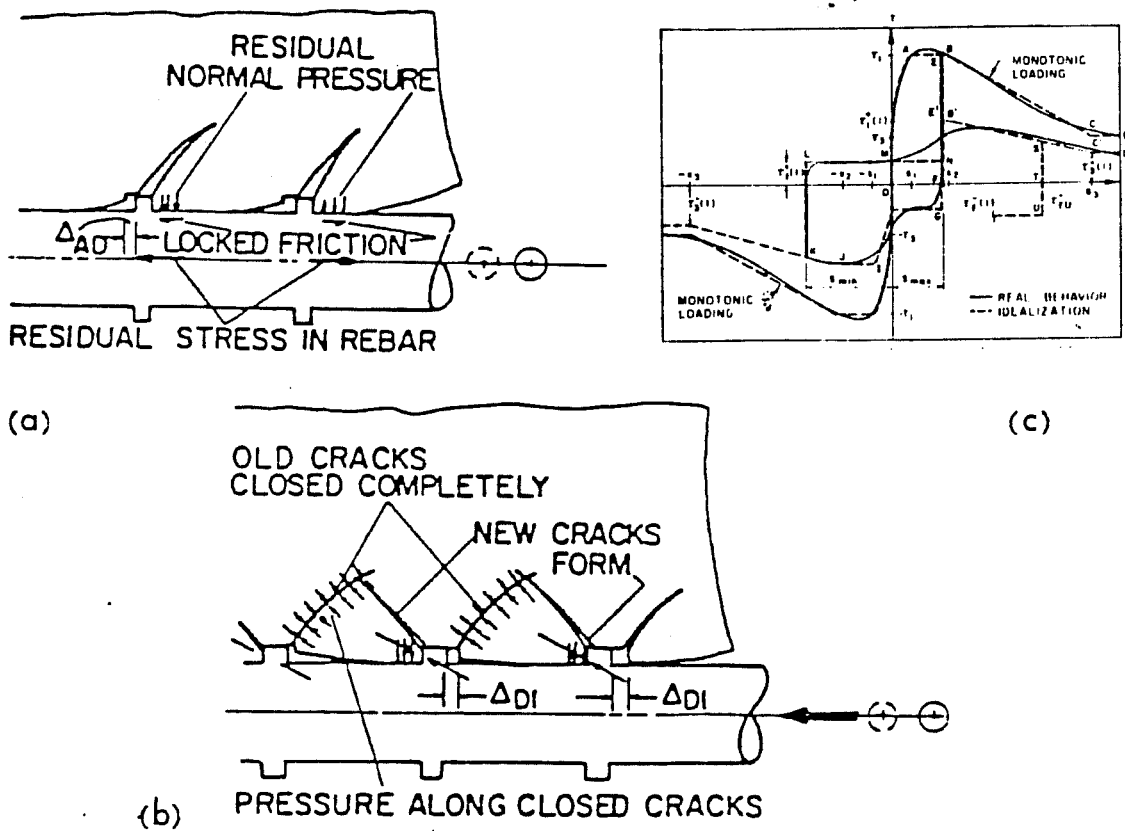


Figure 6-10 : Bond stress history for top bar across joint (BCJ8)

to that measuring the bond stresses between points 8 in. away from the column face. The latter, showed by the dotted line, indicates better behavior over this distance by its better symmetry about the x-axis. The "out-of-phase" curve, after LS 88, indicates that the bar is anchored in the beam at the opposite side of the joint instead of in the joint itself.

As shown in Chapter 4, there was substantial slip of the beam longitudinal reinforcement throughout the load history. Bar slip is evidence of the poor behavior outlined above. Although the bar slip versus strain behavior under severe cyclic loading has not been clearly established, several models have been proposed. The most complete and recent model stems from the work of Eligahausen, Fillippou, Bertero and Popov [32, 35, 26], and is shown in Fig. 6-11.

The slip vs. strain behavior for the top longitudinal bar at the column face of the East-west beams is shown in Fig. 6-12. The slip and bar strains were measured at points about 0.25 in. apart longitudinally. The slip was nearly linear with beam end displacement through most of the load history, so it is not surprising that this plot has a shape similar to that of Fig. 6-11. The plot of the slip of the same bar measured at the at the West side of the joint is shown in Fig. 6-13. Although the general shape of the plots is similar to the proposed Berkeley model, some differences were observed. First, slip did not occur in the first cycle (LS 1 to



Mechanism of Force Transfer from a Deformed Reinforcing Bar to Concrete at Two Stages of Cyclic Loading: (a) Unloaded Bar After an Inelastic Half-Cycle, and (b) Closure of Initial Cracks and Development of New Cracks on Loading the Bar in the Opposite Direction. (c) Hysteretic Loop Associated With the Illustrated Cycling Process [12].

Figure 6-11 : Bar slip versus strain model (Ref. 108)

28) even though the slip limit had been exceeded; the curves for the first cycle follow the monotonic curves rather than the cyclic ones. Second, as the bar slips became larger, the slip did not take place suddenly, as a horizontal line would indicate, but rather as at a constant rate. Finally, the good correlation found for the first deflection level could not be matched as the deflections became very large and substantial slips were measured.

From the two graphs it is possible to obtain an idea of the bar elongation with cycling. Bar elongation is important because it can be used to estimate the inelastic beam rotation at the beam-column face. At L.S. 12 the bar showed a slip of 0.050 in. at the West face of the joint, while the East side had a slip of only 0.025 in. The difference between the two measurements is made up of elastic and inelastic deformations. The inelastic deformation represents permanent bar elongation and can be related to the amount of slip necessary for the bar to begin picking up significant amounts of stress when load reversal occurs. It also represents increases in joint width due to unclosed shear cracks. Assuming a linear variation of stresses in the bar through the joint, the total inelastic deformation is about 60% of the measured difference in slip, or about 0.015 in. (See Fig. 6-14). As cycling progresses, the elongations increase, causing the cracks at the beam-column interface to become very large. Thus more slip is required before the bars become effective upon load reversal, resulting in the very flat

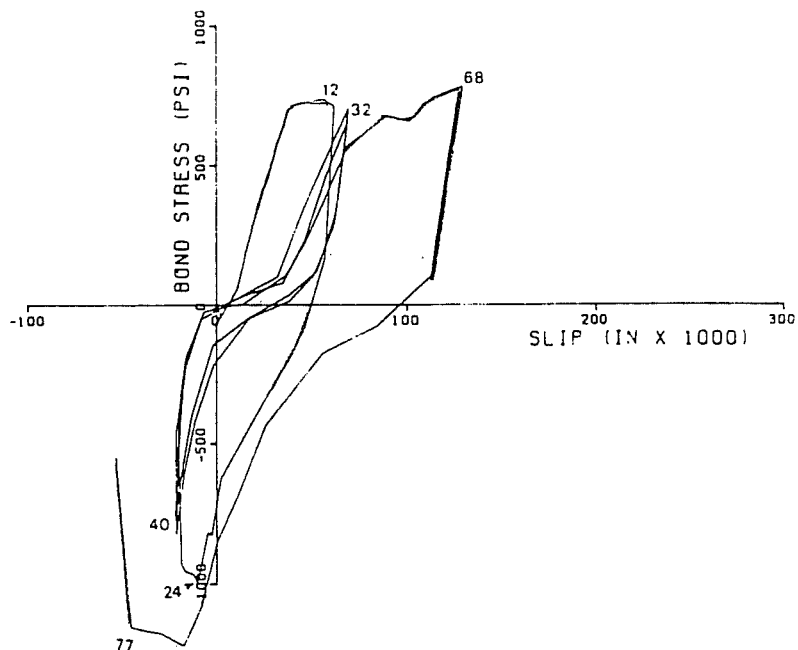


Figure 6-12 : Slip vs. bond stress history for the top East face of the joint (BCJ8)

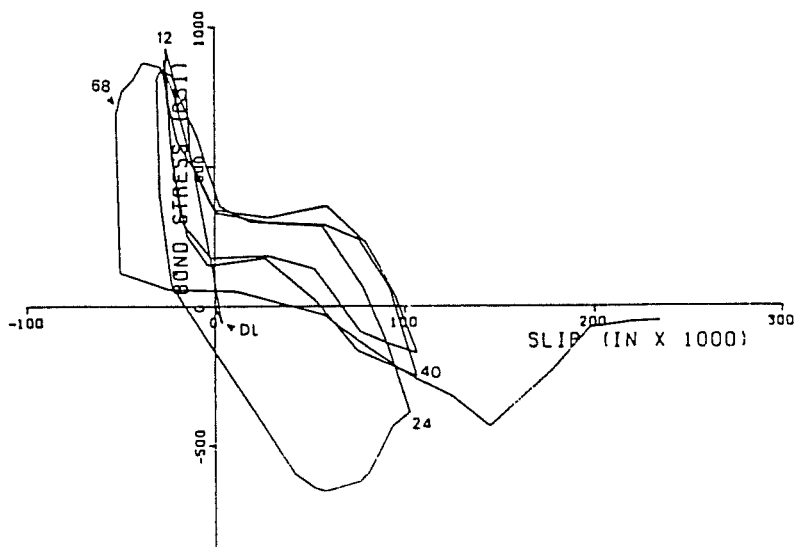
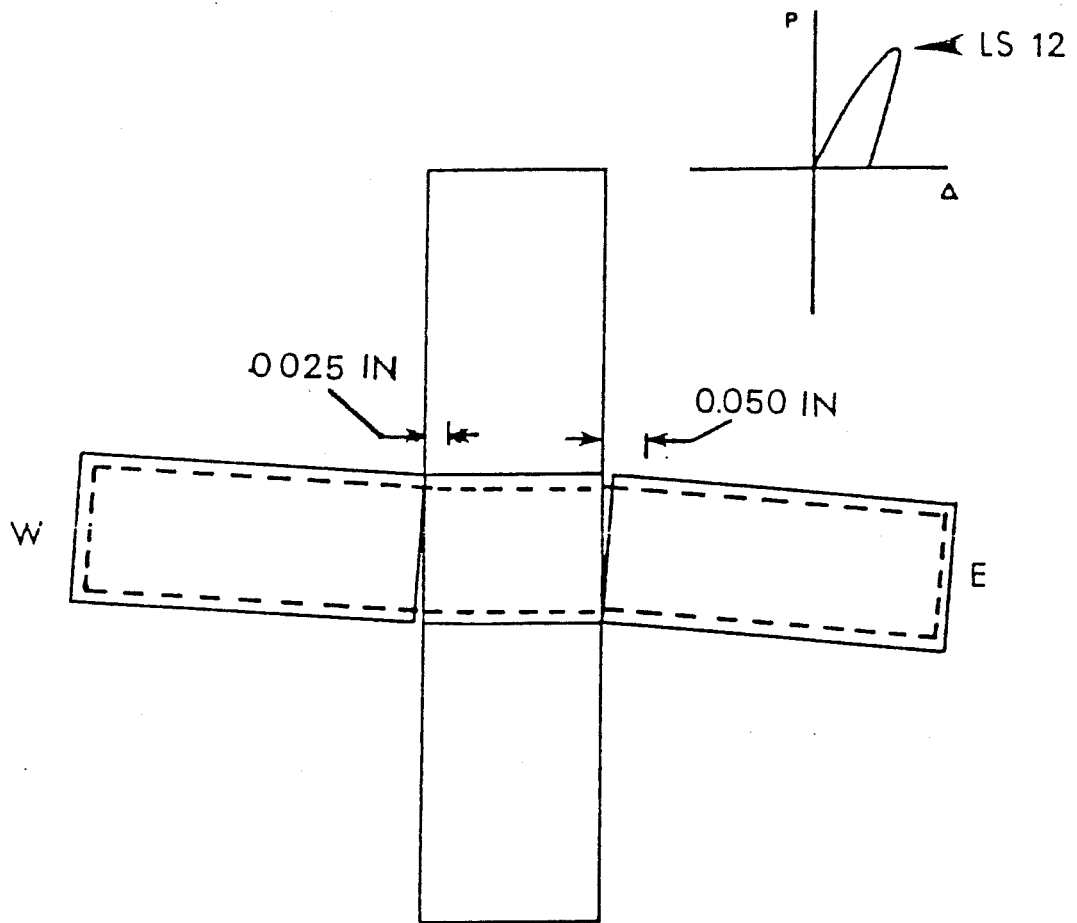
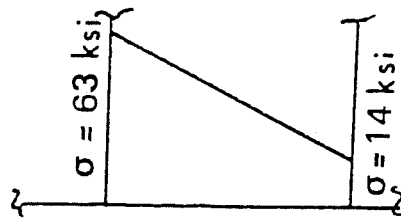


Figure 6-13 : Slip vs. bond stress history for the top West face of the joint (BCJ8)



$\Delta = 0.025 \text{ IN}$

(a) Measured slips at L, S 12 (first peak)



(b) Stress distribution in bar across the joint

Figure 6-14 : Calculations of slip and elongation (BCJ8)

slopes of the hysteresis loops already discussed. Very large slips at the second and third deflection levels indicate that bond conditions along the bar have deteriorated beyond acceptable limits.

The discussion above can be extended to almost any top longitudinal bar in the test series. Although the exact load stage at which the bond deteriorated sufficiently to produce a "bond failure" varied somewhat, it was generally reached between the first and second cycles at the second deflection level for all tests except BCJ11 and BCJ14. For BCJ11, the top longitudinal bars were # 10, and thus the bond stress required for the bars to yield was about 1600 psi. This value could not be achieved, and the specimen failed due to bond deterioration before the maximum expected shear in the joint could be achieved. In the case of BCJ14, the hooked bars from the West beam failed in anchorage before the yield was reached.

The behavior of the bottom # 6 longitudinal bars was better than that of the top bars. This was expected since the bond stress demands for the # 6 bars were in the vicinity of 650 psi. The corresponding results for the bottom bars are shown in Figs. 6-15 through 6-17.

The East bottom gage, in particular, shows excellent behavior. A compressive stress of 14 ksi was reached during the negative peak at the first deflection level, and this value increased

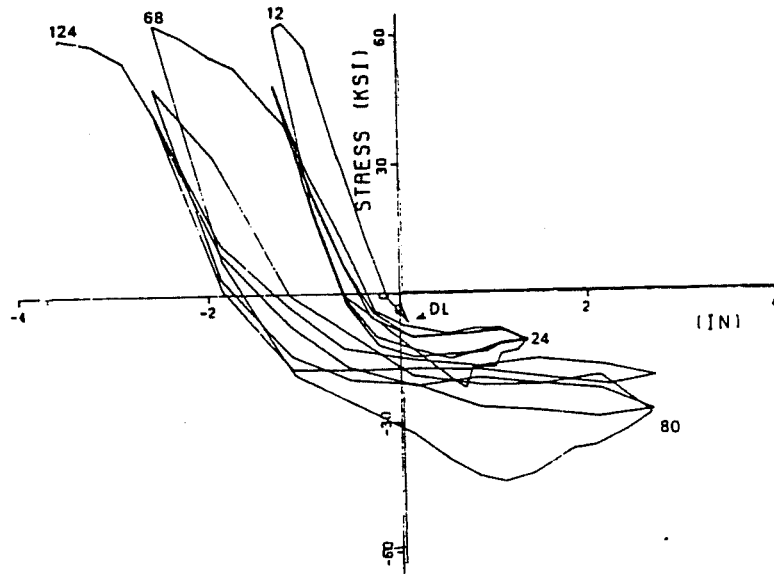


Figure 6-15 : Stress vs. beam end displacement history for bottom East gage (BCJ8)

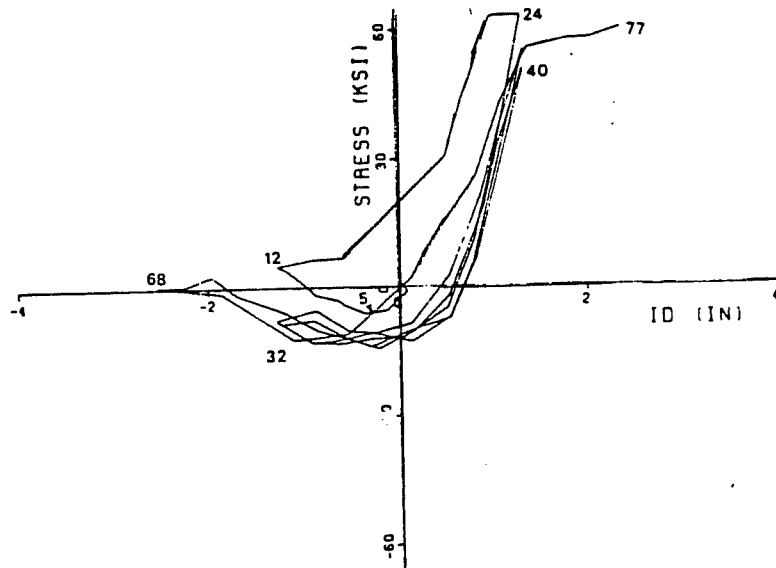


Figure 6-16 : Stress vs. beam end displacement history for bottom West gage (BCJ8)

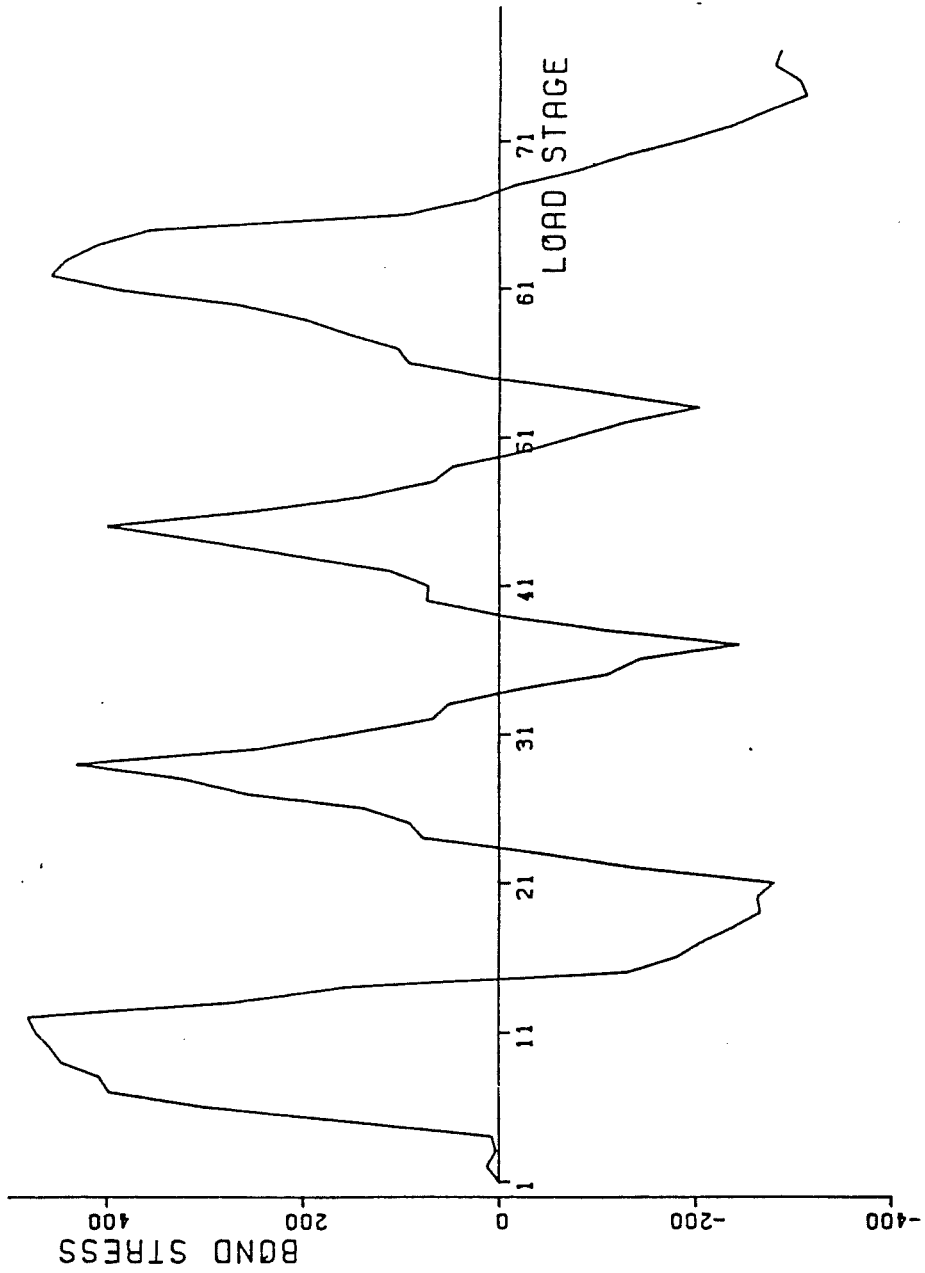


Figure 6 16 Bond stress history for bottom bar East West

to about 25 to 30 ksi for the second deflection level. A partial explanation for this large amount of compression is that the cracks at the beam-column section were very wide, and the steel, due to the yield elongation, was forced to transmit quite a bit of the compressive force in the beams.

The specimens in this test series were specifically designed to fail in shear. However, the behavior of most of the specimens was controlled by bond deterioration. If bar slip and bond deterioration are to be avoided, bond conditions should be incorporated into design codes to prevent early failures such as those observed in these tests.

6.5 Effect of Framing Member Size

As pointed out in Section 6.2, for the test series reported herein the concrete in the joint must carry a significant portion of the shear. In order to carry all this shear, one or more large compressive struts must form through the joint. For these struts to act effectively, adequate confinement of the concrete is imperative. In members subjected to axial and flexural forces, it is generally assumed that ties or spiral steel reinforcement are needed to provide proper confinement to core areas. In the case of biaxially loaded joints, however, the members framing into the joint are carrying flexural forces that result in the force system shown in Fig. 6-18.

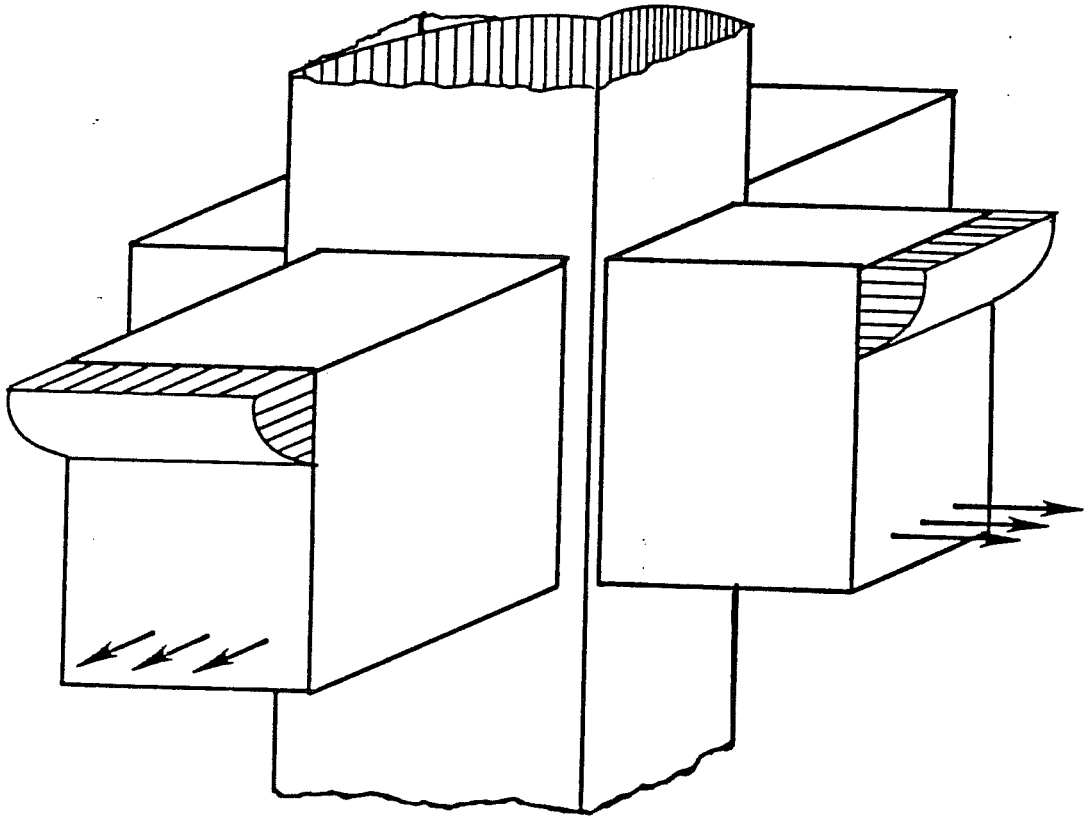


Figure 6-18: Forces on biaxially loaded joint

The lateral members therefore must provide significant restraint to the joint.

It is clear that the framing members cannot provide the joint with uniform lateral restraint. The compressive stress blocks in the beams and column are present at opposite corners of the joint, and act effectively only as the stresses increase. Thus the members provide lateral restraint, but act effectively biaxially only when high shear forces are applied simultaneously.

For subassemblages loaded as in this test series the shear demand on the joint did not increase until the stiffness of the system was regained, i.e., when the cracks closed and the compressive stress blocks of the beams were in contact with the joint. At this stage of the loading history, which corresponded to about the upper half of each loading cycle, the shear was being carried by a combination of strut and truss mechanism. The end conditions for the truss are provided by the transverse steel in the joint, while that of the strut is provided by the compressive blocks of the column and beams. Given the small amount of steel reinforcement present and its location, it is unlikely that the "interior" truss mechanism, formed by the transverse joint hoops and intermediate column bars, could have carried more than 20% of the total shear. The contribution of the "exterior" truss mechanism, formed by the main longitudinal reinforcement from the beams and column, is probably important but

impossible to quantify. It must be recalled that for such an "exterior" truss to perform well, the bond between the steel and the concrete must remain intact. Since substantial bond deterioration occurred with cycling, this contribution probably decreased as the test progressed.

As a lower bound for test BCJ8 for example, it could be assumed that the contribution of the "exterior" truss is small and therefore negligible during the second and third cycles at the second deflection levels (See Fig. 4.7). Thus the shear at this stages is taken by the "interior" truss and the concrete strut. The "interior" truss can carry only about 63 kips out of the 225 kips of biaxial shear present; thus the concrete strut must carry about 162 kips of horizontal force. This represents about 70% of the shear at this stage and about 50% of that at the first peak for the same deflection level (total shear at L.S. 68 was about 320 kips).

This type of separation of the contributions of the steel and the concrete has been attempted by researchers in New Zealand [9]. Their results indicate that while the truss mechanism becomes effective after the first cracking of the joint, it is not efficient enough to carry the total shear. On the average, the contribution of the concrete is about 40% and does not seem to deteriorate significantly with cycling, as shown in Fig 6-19. In light of these results, and the ones from this test series as outlined in Section

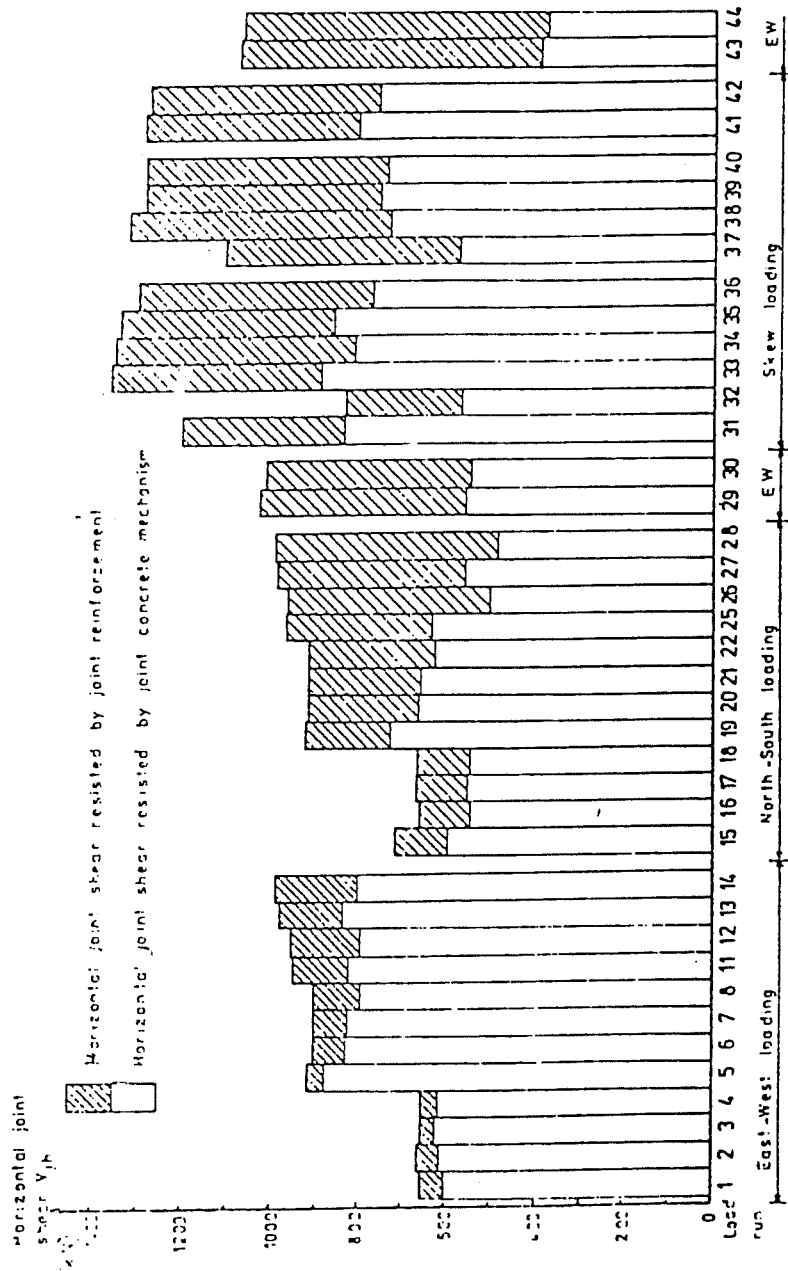
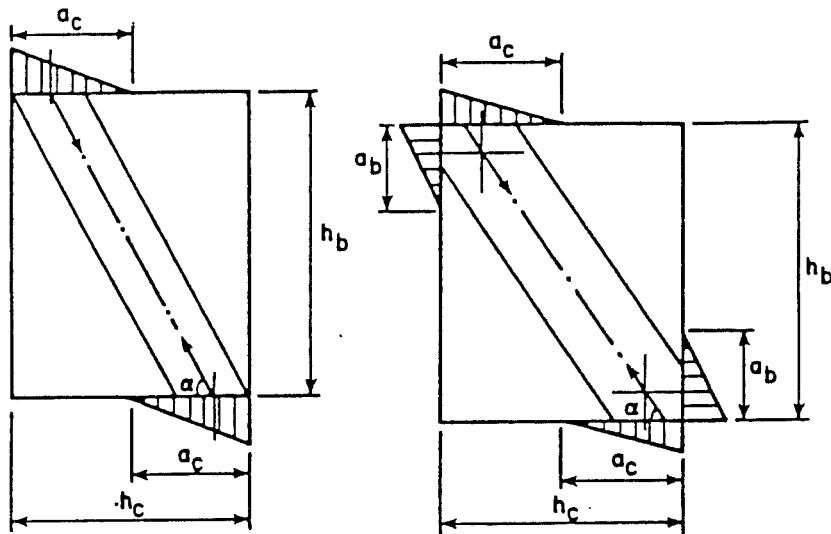


Figure 6-19 : Contribution of steel and concrete to joint strength - N.Z. (Ref. 9)

6.2, the concrete strut appears to be the main mechanism of joint shear transfer.

Of course, the contribution of the transverse shear reinforcement remains critical. The main function of the transverse steel may not be to carry the shear but to preserve the integrity of the confined concrete. Thus, shear reinforcement in the joint area is necessary, but its effectiveness in resisting shear is limited. This may help explain why volumetric reinforcement ratios larger than 2% in the joint area do not result in large increases in joint capacity.

If the transverse steel in the joint cannot be counted to develop an efficient truss mechanism, the forces in the confining members must provide the end conditions necessary for the strut to form. While the strain distribution across the strut is not uniform, an equivalent strut with a stress close to that of the compressive strength of the concrete can be calculated as proposed by Zhang and Jirsa [113]. This model is outlined in Fig. 6-20. The model is based on finding the compressive force that an equivalent strut can carry, and modifying this capacity to account for lateral beams, amount of joint reinforcement, and concrete strength. The physical interpretation of the strut mechanism in biaxially loaded joints is shown in Fig 6-22. It is clear that in a member loaded biaxially the area of the strut can be increased by about 1.4 times that of the uniaxial case .



For joints not hinging at joint,

$$Q_c = \eta K \zeta \gamma f'_c b_c \cos \alpha \sqrt{a_c^2 + a_b^2}$$

For joints hinging at joint,

$$Q_c = \eta K \zeta \gamma f'_c b_c \cos \alpha a_c$$

where,

Q_c = shear strength under cyclic loading

$$\eta = 1 - 0.4 (\Delta/L)$$

Δ = maximum beam end deflection, in.

$$K = 1.2 - 0.1 f'_c$$

$$\zeta = 0.95 + 4.5 \rho_s$$

ρ_s = transverse volumetric joint reinforcement, %

$$\gamma = 0.85 + 0.3 (w_L/h_c)$$

w_L = beam width, in.

h_c = column width, in.

Figure 6-20 : Zhang and Jirsa's model (Ref. 115)

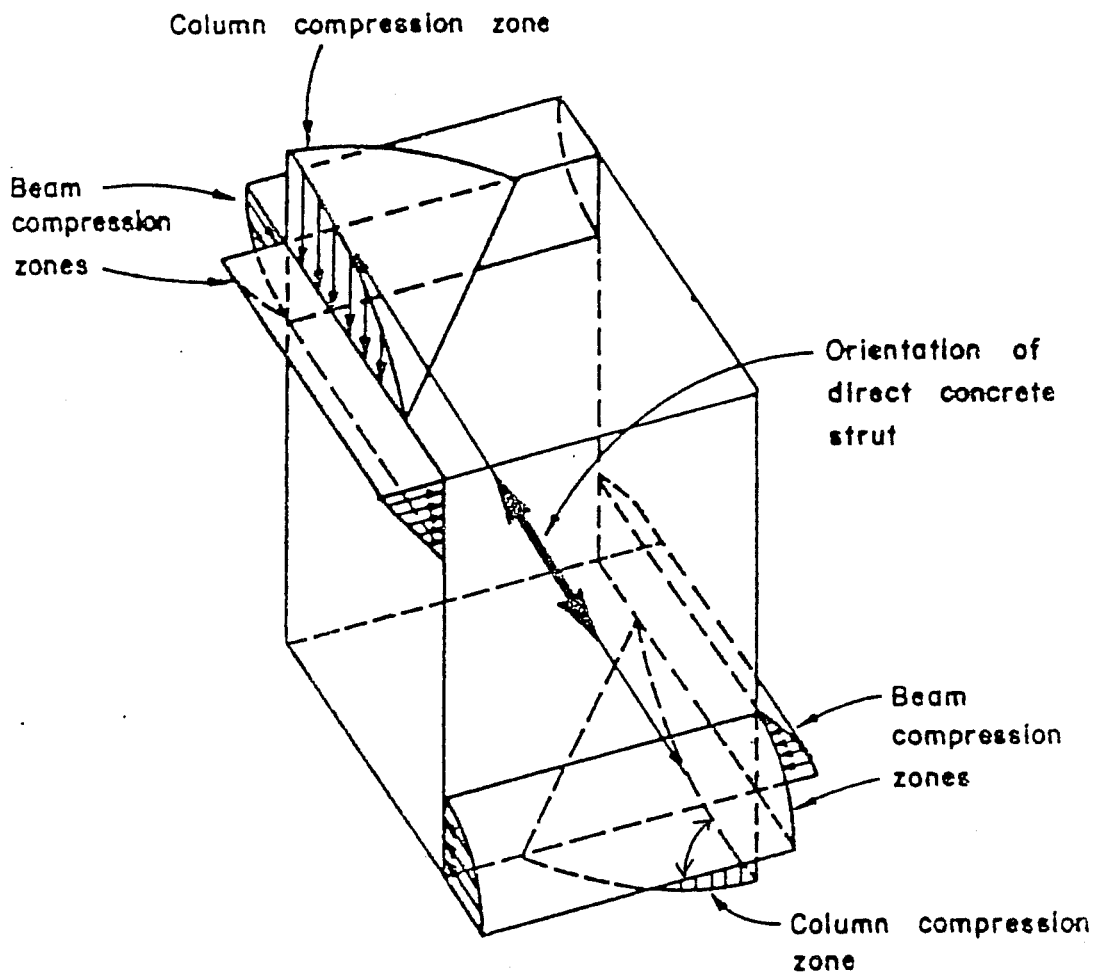


Figure 6-21 : Biaxially loaded joint - strut mechanism
(Ref. 9)

The effects of framing members can be separated into two categories. The first, or passive category, refers to unloaded framing members. The second, or active category, refers to loaded framing members. The discussion will be limited to this latter case. From the data obtained in the BCJ series, it is possible to make some conclusion about the effect of beam size, of the presence of a slab, and of the amount of force in the members on the equivalent strut .

6.5.1 Framing Beam Size

To define the area of the strut, the size of the compressive blocks in the beams and columns are critical. From the observations made during the tests, it seemed that the strains were not uniform across the compressive blocks of the beams. Thus, an assessment of the forces needed to provide the end conditions for the strut will give a distribution similar to that shown in Fig. 6-22. The extension of Zhang and Jirsa's strut model from uniaxially to biaxially loaded joints is a matter of determining the appropriate geometric parameters to fit the assumed stress distribution. Assuming a triangular shape for the column compressive block, and a rectangular one for those of the beams (deeper and narrower than those given by ultimate strength analysis), the resultant diagonal strut is shown in Fig. 6-23. The resultant strut has an octagonal shape, the product of several planes limiting the size of said strut. Obviously, in an uncracked joint, the distributions will not be

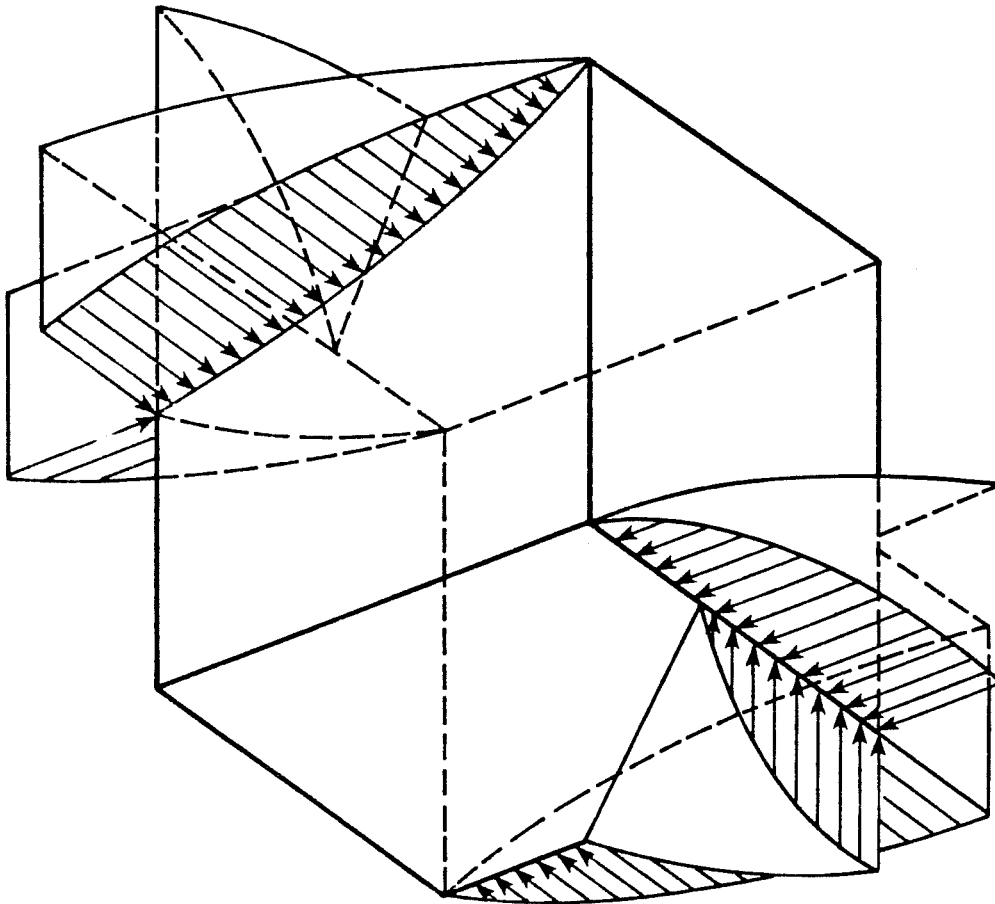


Figure 6-22 : Distribution of stresses near the joint

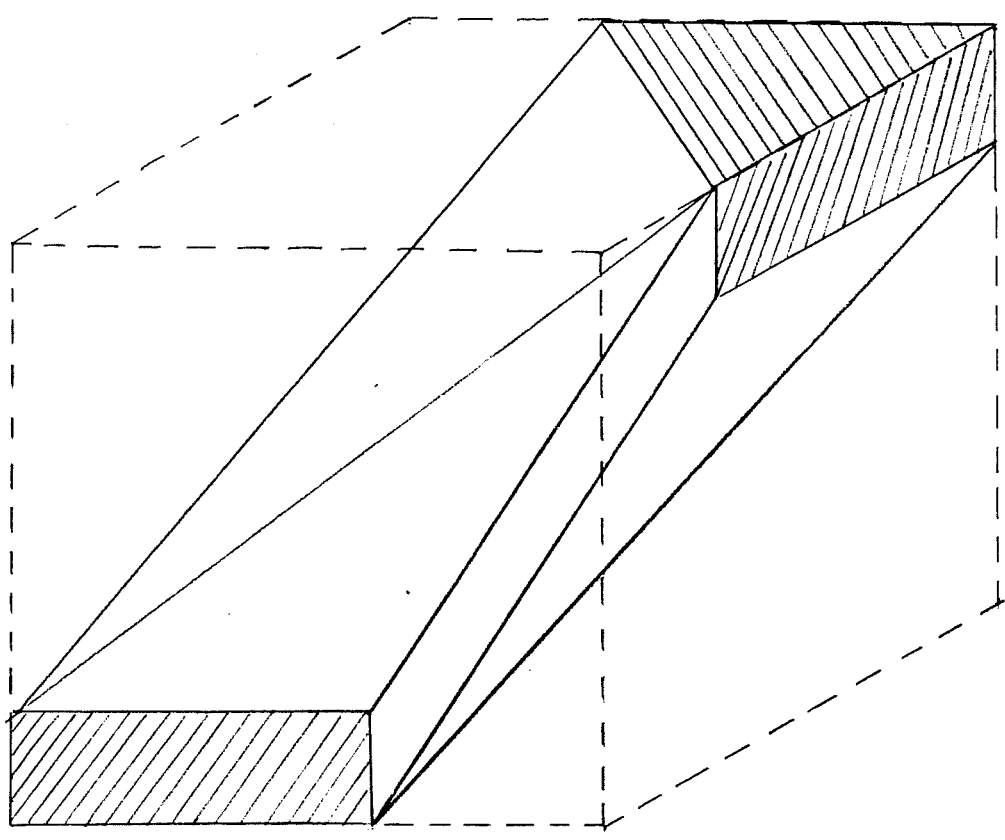


Figure 6-23 : Planes bounding diagonal strut

linear; in a cracked one, the distribution will depend on the orientation of the cracks. Thus it is likely that this strut will bulge and become elliptical near the middle.

As in the case of uniaxially loaded joints, the width of the framing beams can be considered as a linear factor affecting strut size and therefore shear strength. It can be hypothesized that the narrower the framing beams, the more independent the two directions of loading become. For the case of BCJ11, where the framing beam width was about 60% of the column width, two almost separate struts, as shown in Fig. 6-24 probably were present. For the case of BCJ12, where the framing beam width was about 120% of the column width, a single large strut, as shown in Fig. 6-25 was present. For the intermediate case of BCJ5, where the beam width was about 90% of the column width, a strut similar but smaller than the one for BCJ12 probably was present.

An effort was made to verify the size of the strut necessary to carry the horizontal shear forces calculated to be present in the joints tested (See Table 6-8). Assuming that the joint ties are yielding, and that therefore a truss mechanism is present, a minimum area for a strut was calculated; the intent was to check whether the strut could carry the required axial load. A minimum strut size given by planes bounding the compressive blocks of the beams and column was hypothesized, as shown in Fig. 6-23, and its area at the midsection computed.

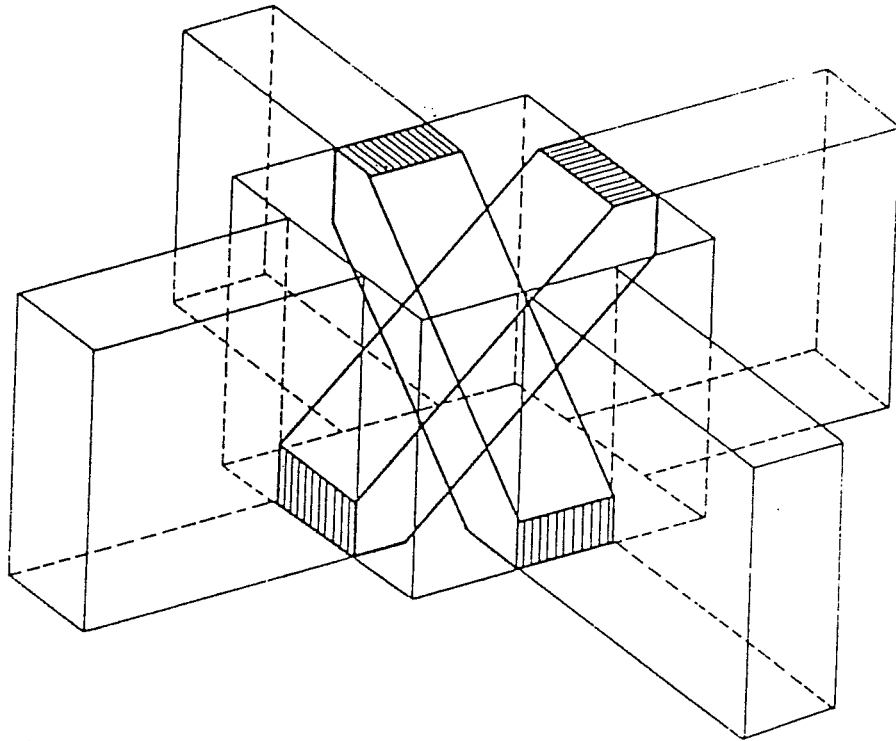


Figure 6-24 : Strut for BCJ11 - Narrow beam specimen

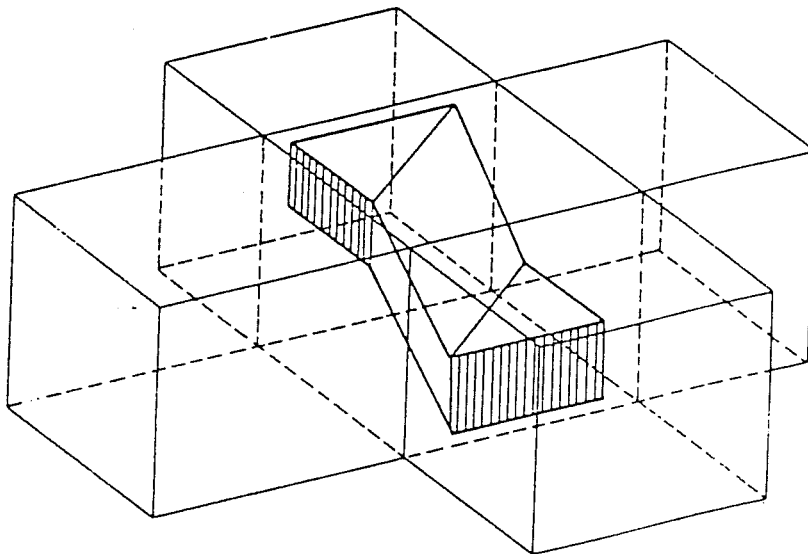


Figure 6-25 : Strut for BCJ12 - Wide beam specimen

For the case of BCJ11, the joint was assumed to have two independent, perpendicular struts. The total horizontal force on the struts was about 145 kips in each direction once the contribution of the truss mechanism was subtracted. The struts, inclined at an angle of 50 degrees, were required to carry about 226 kips of axial load. Utilizing Jirsa and Zhang's equations, it was determined that the required projection of the depth of the compressive blocks on the diagonal between opposite joint corners was about 64 in^2 , see Table 6-8. Assuming that the effective width of the strut was equal to the average of the beam and the column widths (11.88 in.), the resulting strut depth needs to be only 5.5 in. From ultimate strength analysis this probably can be provided by the column alone, since the neutral axis for this case lies about 10.4 in. from the extreme fiber in compression. Thus, it is unlikely that BCJ11 failed because of a strut compression failure; if the flexural capacity of the column had not deteriorated due to spalling, it is likely that the shear forces from the beams could have been carried without significant problems.

For the medium-size beams test (13" by 18"), a similar analysis was conducted, except that the strut was now assumed to be a single strut between opposite corners of the joint. It was found that an area of about 125 in^2 was necessary to carry the 263 kips of shear present in test BCJ5 if the stress level predicted by Zhang and Jirsa was used. This area could be provided in two manners; first, by the compressive blocks assumed in the ACI ultimate strength

Test	BCJ5	BCJ12	BCJ10	BCJ11 (*)
Case	Bi-ax.	Bi-ax.	Bi-ax.	Uni-ax.
d_{NA}	10.4"	10.4"	10.6"	$a_c = 5.31"$
a_b	3.24"	2.18"	3.42"	$a_b = 4.71$
s_1	10.4"	10.4"	10.6"	$K = 0.75$
s_2	6.99"	6.85"	7.10"	$\zeta = 1.01$
s_3	9.20"	8.39"	9.34"	$\alpha = 50.2^\circ$
Area (in ²)	145	134	148	$b_c = 11.9$ $\swarrow A = 68 \text{ in.}^2$
Shear cap. provided (kips)	364	346	292	188
Shear cap. required (kips)	263	274	230	145

(*) Following Zhang and Jirsa for uniaxial case.

Definitions :

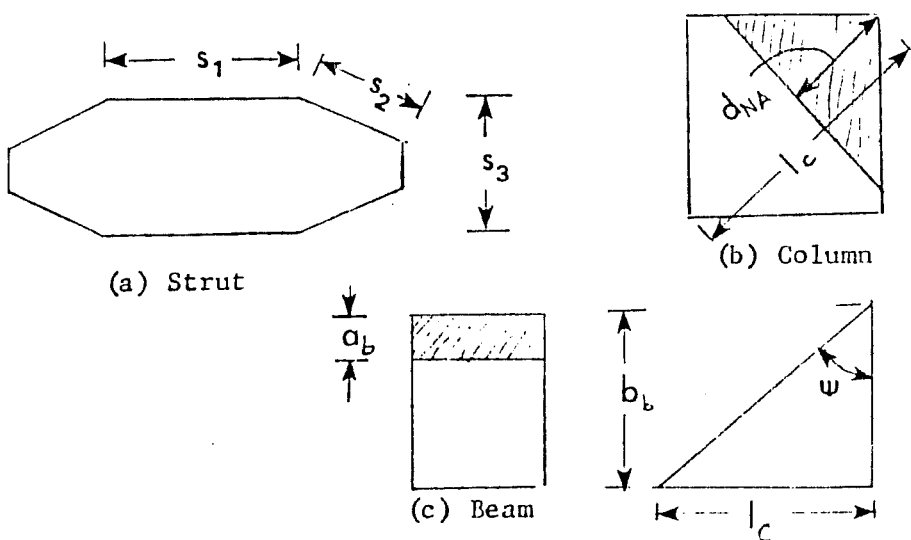


Table 6-8 : Strut size calculations.

design, resulting in a wide and narrow octagonal strut with an area of about 130 in^2 . Second, by a deeper and narrower set of compressive blocks (depth = 4.5 in, width = 9.0 in) modelled on the strain distribution shown in Fig. 6-21, and giving an area of about 135 in^2 . Both of these will provide the necessary end conditions given the assumed stress level. The actual computed area of the strut (144 in^2 .) exceeded the required area. It must be noted that these calculations have to be based on some assumption about the level axial stress in the strut. The Zhang and Jirsa procedure, derived for uniaxially loaded joints indicates a stress of about 75% of the concrete compressive strength. In the case of the medium-size beams, the strut is well confined and its ends are in a state of triaxial compression, this level could probably be increased. Thus it is very likely that the concrete strut can carry the entire shear force present for this loading case.

For the wide beam tests (18" by 18"), a similar analysis results in a shallower strut with a hexagonal cross-section. For the case of BCJ12, the computed area was about 134 in^2 , slightly lower than for the medium-size beam case. This is due to the fact that the strut could only increase in width slightly before the column corners were reached, while the depth of the compressive blocks decreased substantially. The strut, again, could have carried more than the required shear strength if the stress values of Zhang and Jirsa are assumed. For the case of BCJ10, where the weak concrete created a

much deeper compressive block in the beams, the computed area was about 148 in². ; this would allow the strut to carry the shear force present even given the low compressive strength.

The strut areas calculated are considered minimum areas. Even so, the strut mechanism was able to carry all of the shear present in the joint, including that which originally had been assigned to the truss mechanism. It is likely that the compressive stresses in the strut could be higher than those given by the Zhang and Jirsa equation. The state of triaxial stress near the ends, and the probable bulging of the strut near its middle could probably combine to carry even higher loads. Thus the strut mechanism could probably carry all the shear present in the joints tested. This would reduce the steel in the joint area to a confinement function only.

It is clear, however, that the compressive strength of the concrete would have become a limit if much higher shear forces were present. No indication of a strut compressive failure could be found in any of the tests, including BCJ10 where the concrete compressive strength was very low. While the geometry of the strut is very complex, and does not lend itself to a simplified solution, the author believes that a conservative approximation to the strut size can be given by :

$$A_{\text{strut}} = [1.3 \times l_c \times a_b / \cos \psi]$$

where the terms are defined in Table 6-8. It is intended to apply to joints with square columns and beam depths not to exceed 1.5 times the column width.

Zhang and Jirsa have proposed a factor to account for lateral unloaded members in uniaxially loaded joints. This factor gamma, a multiplier of the total strut capacity is given by the equation,

$$\gamma = 0.85 + 0.30 [w_L / h_c]$$

where w_L is the width of the beam and h_c is the size of the column perpendicular to the framing member. This equation was based on the statistical analysis of almost 250 specimens of beam-column joints loaded uniaxially, and where lateral beams, if present, were unloaded. For the case of biaxial loading a similar equation could be developed. There is, however, insufficient information about biaxially loaded joints to be able to derive such an expression from experimental data. Zhang and Jirsa's equation could be extended to the biaxial case if some conservative modifications are made. First of all, for joints with framing beams less than 70% of the column width, the allowable shear stress in the joint should be diminished by a factor of 0.66 to avoid the type of failure observed in BCJ11. If the beams are very small with respect to the column, the corners of the column must be protected to prevent spalling of the cover concrete and the subsequent poor bond conditions for the column bars. The observations made during the two tests with beams wider than the

column did not indicate any particular problem with this type of geometry. However, the tests do not provide enough data to indicate that the shear strength can be increased for the case of wide beams. Moreover, the effective width of the beam should not exceed that of the column by more than 25% since no data is available for that range. The main problem is that with very wide beams it may be nearly impossible to prevent a column hinge or column distress above and below the floor framing system.

Thus the equation proposed by Zhang could be modified to account for the effect of wider beams by increasing the factor of 0.30 to 0.35. This will result in an equation :

$$\gamma = 0.85 + 0.35 [w_L / h_c]$$

with allowable values of gamma between 0.85 and 1.20 . This equation is applicable only to the case where all the framing members are loaded.

6.5.2 Effect of a Slab

The effect of a slab on the joint shear strength is very hard to quantify for two reasons. The first is the lack of data on which to draw meaningful comparisons. The second is that the slab improves confinement in only the upper corner of the strut, while the other end of the strut does not receives any beneficial confinement. It is clear from tests BCJ9, BCJ9A, and BCJ15 that the slab had a beneficial

effect on joint confinement. The typical crack patterns for these tests are shown in Figs. 6-26 and 6-27. The cracks radiating from the joint, as well as the cracks radiating along the beam sides indicate that the slab steel carried significant forces and helped transfer forces away from the critical areas. Since the increased moment capacity due to the slab results in better confinement for the joint it is probable that the overall effect of the slab is to increase the capacity of the strut. Thus a factor to account for the presence of a slab could be included. A multiplier of about 1.20 on the shear strength equation would be included when the summation of the moment capacity of the beams, including the slab, was less than 70% of the moment capacity of the column.

The effect of framing members on exterior joints could be treated similarly. The demands on exterior joints, however, are smaller due to the lack of the moment added by the positive reinforcement on the far side of the joint.

6.5.3 Effect of Column Axial Load

In discussing the effects of framing members on joint shear capacity, the effect of column axial loads cannot be ignored. It is clear that a large axial load on the column will substantially improve the behavior of the joint. Unfortunately the level of axial loads present in columns during earthquakes is highly variable.

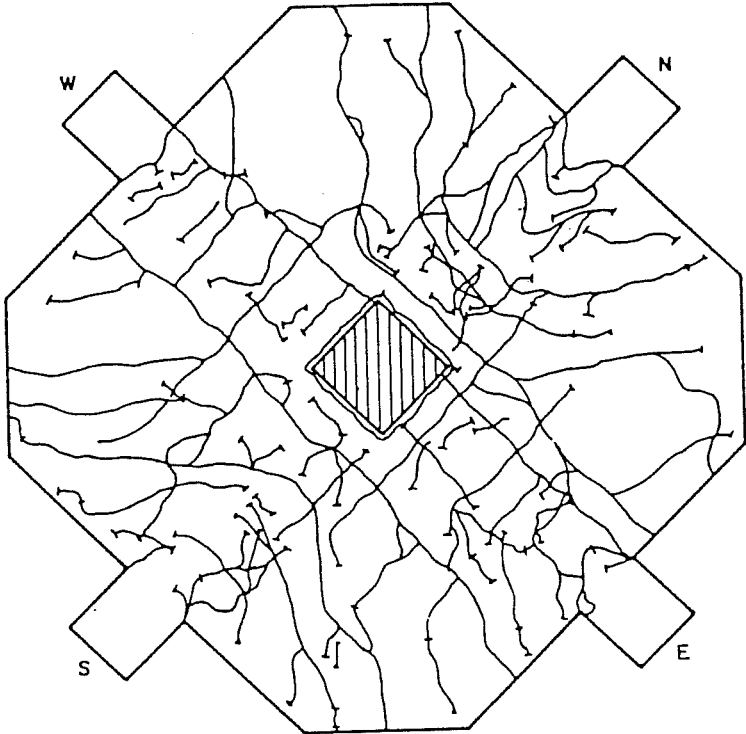


Figure 6-28 : Crack pattern for interior joint.

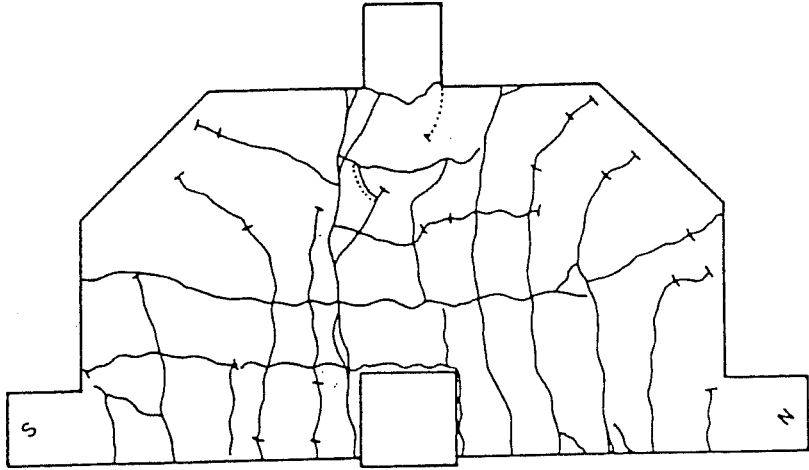


Figure 6-29 : Crack pattern for exterior joint

Compressive working stresses are generally low, in the order of 500 to 1000 psi for low buildings, and probably not more than 1500 to 2000 psi for tall buildings. If this is the case, the current practice of ignoring the axial load is conservative, and there is no reason to advocate a change in the manner column axial loads are treated in joint design. The axial load, of course, must be taken into account when the P-Delta effects become significant. The secondary moments must be added to those produced by the lateral load to give a satisfactory approximation to the required moment capacity for the columns and beams.

6.6 Conclusions

6.6.1 Lateral Restraint

The lateral restraint provided by the floor members, i.e. beams and slab, has a significant effect on joint behavior, especially when biaxial effects are considered. Joints with narrow beams did not provide the column corners with adequate passive restraint. This resulted in spalling and loss of section in the column that led to a premature column flexural failure even though the moment ratio for this specimen was well above one. While specimens with beams 20% larger than the column showed good performance at drifts up to 2%, the specimens showed degrading behavior and a shift of hinging from the beams to the column as the

deformations were increased and losses of column corner sections occurred. It is not advisable to extrapolate these results to cases of joints with larger framing beams until more experimental data is available. The effect of a floor slab was

to increase the negative moment capacity of the beams due to T-beam action; if this effect is not taken into account when calculating the required moment capacity for the column, hinging again may be shifted from the beams to the column. The biaxial loading history imposed on specimens with varying beam widths emphasize the need for a substantial flexural overstrength of the column with respect to the floor members.

6.6.2 Nominal Shear Stress Levels

The joints tested indicated that the joint shear strength of beam-column joints is very large. The nominal shear stresses attained in this study were on the order of 20 to 30 $\sqrt{f'_c}$ at the first peaks, and 12 to 25 $\sqrt{f'_c}$ at successive cycles to drifts of 2%. These were substantially higher than the 8 to 10 $\sqrt{f'_c}$ nominal shear stresses required to crack the joint in shear. If some inelasticity is allowed in the joint, these and other tests indicate that acceptable joint performance can be achieved with moderate levels (12 to 15 $\sqrt{f'_c}$) of joint shear stress. This would allow a large concrete strut as those postulated in this chapter to form and carry a

substantial amount of shear. By reducing the cracking in the joint, this would also lead to less joint shear stiffness deterioration, and better overall behavior. The need to keep nominal shear stresses within these limits indicates that the column sizes will need to be increased

6.6.3 Bond Conditions

The anchorage lengths provided in the joint for the longitudinal bars were clearly insufficient. The top bars, with an anchorage length of 15 times their bar diameter, showed large slips and bond deterioration from the first cycle of loading. The bottom bars, with an anchorage length of 20 bar diameters through the column, performed better initially but bond deterioration and slip occurred with cycling. This and other test series [55] indicate that an anchorage length of 24 bar diameters is the least required for bar to show acceptable bond behavior when subjected to large cyclic loads. Since the stiffness of the subassembly may be severely impaired by bond deterioration and bar slip, large anchorage lengths, and therefore large columns, are required to provide satisfactory bond behavior.

6.6.4 Transverse Joint Shear Reinforcement

The amount of joint reinforcement required in an interior beam-column joint is closely tied to the joint shear stiffness deterioration to be permitted. Transverse joint shear reinforcement helps to control shear cracking in the joint after the cracking limit is exceeded, and thus limits shear stiffness losses. If the joint shear stress levels are kept moderate, however, it is likely that the only the steel necessary to properly confine the joint is required for satisfactory performance. To reach the range of shear stresses associated with low amounts of transverse steel and good performance, the column size would need to be increased.

Chapter 7

Preliminary Design Approach for Beam-Column Joints in Moment Resisting Frames in Seismic Regions

7.1 Introduction

In this chapter a design approach for proportioning beam-column joints is developed. The approach is based on the results of experimental studies which have shown that many of the variables which govern joint behavior are controlled directly or indirectly by the column. If the size and strength of the column were sufficient, and if an adequate amount of transverse shear reinforcement were placed in the joint, the specimens tested developed adequate energy-dissipation capacity. On the basis of this and other test series [107, 73, 74, 29] the approach will ^{be to} use capacity design principles [75, Park75] to find limits on the reinforcement ratios of beams and columns.

In developing the design approach, it is recognized that shear and bond requirements for the joint may be satisfied if the column is large enough. Therefore, joint shear and bond requirements are introduced at the time initial proportioning of the main

structural members is made. Limits for the column and beam reinforcement are then obtained for a particular joint geometry. Numerical examples are worked out and discussed.

The emphasis is on unifying the flexure, shear, and bond requirements for beam-column joints in moment-resisting frames into a single design approach, and to incorporate them as early as possible in the frame design process.

7.2 Evaluation of Parameters Governing Design

The design of structures in seismic areas is governed by limit states. The three most commonly accepted limit states in earthquake design are:

1. A structure must survive a moderate earthquake with no structural damage and only limited non-structural damage.
2. A structure must survive a large earthquake with little and repairable structural damage, while the non-structural damage can be substantial.
3. A structure must survive the maximum credible earthquake at the site without collapsing. The building may be unusable after the earthquake, but no loss of life must occur due to structural failures.

The collapse mechanism for a moment resisting frame can be predicted by plastic design procedures [75]. If the local mechanisms of failure (shear and bond) are avoided, then the collapse load is a function of the flexural strength and plastic rotational capacity

(detailing) of the flexural members. If it is assumed that in moment resisting frames the dissipation of energy, and thus the seismic performance, is a function of the ability of the structure to form plastic hinges in the proper locations (beams adjacent to the joint and lower story columns), then proper seismic performance depends on satisfying the following equation at every joint:

$$\Sigma M_{\text{column}} > \Sigma M_{\text{beams}} \quad (7.1)$$

where ΣM_{column} is the sum of the flexural moment capacities of the column above and below the joint, and ΣM_{beams} is the sum of the flexural capacities of the beams framing into the joint when the subassemblage is subjected to lateral loads. It must be clearly understood that this is valid only if shear and bond failures can be prevented. Thus, merely satisfying equation (7.1) will not insure adequate seismic performance. The magnitude of shear and bond stresses must also be kept low so that mechanisms involving shear and bond do not have a significant effect on structural performance. It must also be recognized that there are limits, both structural and economic, to the means by which shear and bond deterioration mechanisms can be prevented. Sufficient deformations can always be applied to a structure or subassemblage to produce such deterioration. However, measures can be adopted which will delay or decrease the influence of such mechanisms within the range of deformations anticipated for a particular limit state.

A rational design for joints in moment resisting frames must therefore include the following restrictions:

1. Low shear stresses to avoid a sudden, brittle failure of the structure.
2. Low bond stresses in the beam bars through the joint to prevent large losses of stiffnesses and instability of the structure.
3. Moment capacity ratios large enough to insure that the hinging occurs in the beams and no significant inelasticity is shifted to the columns and joints.

It is clear that all these restrictions are not independent of one another. The parameters involve geometric considerations found to be important in the experimental work described in the previous chapters. Thus it should be possible to unify all these requirements into a single design approach.

7.3 Selection of Governing Parameter

It has been shown by this study that the geometry of the joint can have a significant effect on joint behavior. Other tests [73, 106, 31] have shown that very different levels of joint performance can be obtained when moment ratios are changed. Such knowledge can be used to develop a design approach that satisfies all the requirements outlined in Section 7.2.

7.3.1 The Moment Ratio

The moment ratio criteria described by equation (7.1) can be rewritten as:

$$[\Sigma M_c / \Sigma M_b] > 1.0 \quad (7.2)$$

While satisfying this equation for static loads presents no problems, the situation under dynamic loads is very different in reinforced concrete buildings. Large ductility demands and load reversals such as those produced by a major earthquake are associated with extensive flexural cracking of the beams and columns, shear cracking of the beams and joint, bond deterioration and yield penetration through the joint area, and possibly spalling and crushing of the cover of the structural members. Thus, as a building deforms during an earthquake the values of the flexural capacities of its members change. The designer's task is to insure that even under the maximum credible earthquake the moment ratio does not fall below 1.0.

The easiest way of insuring adequate behavior under an uncertain set of loads such as those produced by an earthquake is to assume a factor of safety (" β " = the moment ratio). Applying this to (7.2), and recalling that for a typical joint the column must be stronger than the beams, we obtain :

$$[>M_c / > M_b] > \beta \quad (7.3)$$

To satisfy this equation as the moment ratio is increased the

designer has three options. The first is to maintain the column size and increase the column reinforcement ratio. The second is to increase the column size and keep or decrease the column reinforcement ratio. The third, and most common solution, is to use a combination of the first two. Recalling that for ductility considerations the column reinforcement ratio should be kept low, it is likely that most designers will choose to increase the column size over the reinforcement ratio. The effect of increasing the moment ratio on construction costs and structural behavior are briefly reviewed next.

7.3.1.1. Effect on Construction Costs

The effects of increasing the moment ratio on construction costs are not clear. Increasing the column and beam sizes obviously increases the concrete but decreases the steel requirements, which may tend to compensate. The initial cost of formwork will obviously increase, but the reusability of the forms might limit the impact of form costs. On the other hand larger joints are less congested, and therefore easier to fabricate and to cast. The saving in field labor thus obtained may more than offset the increased cost of materials. It must be recalled that the overall cost of materials in a large project probably does not exceed 10% to 15% of the cost of the structure. Changing the material quantities slightly will not result in significantly more expensive structures.

7.3.1.2. Structural Effects

The effect on structural behavior of imposing a moment ratio are twofold. First, it reduces the likelihood of a column failure. Second, and perhaps more important, it decreases the possibility of local failures in or near the joint. By increasing the column size, the average shear stress in the joint will be reduced and the bond conditions improved. Increasing the moment ratio meets all the requirements established for selecting a parameter on which to base a design procedure. Selection of appropriate values of the moment ratio is described next.

7.4 Determination of the Beta Factor

7.4.1 Experimental Data

The determination of a numerical value for the moment ratio is not a simple task. The results of past research, summarized in Table 7-1, indicate that sufficient data is available for moment ratios between 1.0 and 2.0. The data presented in this table refers to interior beam-column connections with beams bars having an anchorage length at least equal to 15 bar diameters and with columns of at least 12 in. minimum dimension. These two limits were imposed to insure that bond conditions and scale effects would not influence the data. Bars anchored in interior joints need at least 15 bar diameters to withstand several cycles of inelastic loading; anchorage

Table 7-1 (cont.)

Ref.	Label	Column Size	Beam Size	M.R.(1)	(%)	P/P _u	V _j (2)	Performance
Japan								
Bessho	J1	15.8 x 15.8	14.8 x 10.8	1.12	4.0	0.08	20.9	A
	J2	"	"	1.12	4.0	0.08	20.9	A
	J3	"	"	1.12	4.0	0.08	21.6	E
Nakada	1	31.5 x 21.7	23.6 x 15.8	1.40	2.0	0.24	19.2	E
	2	"	21.7 x 15.8	1.34	2.0	0.24	18.3	E
Ishibashi	1	26 x 26	23.6 x 15.8	1.95	1.7	0.24	16.0	E
	2	"	"	1.33	3.4	0.22	17.9	P
	3	"	23.6 x 23.6	1.28	1.7	0.18	21.8	A
	4	"	"	1.28	3.4	0.19	22.4	A
New Zealand								
Park, Paulay, Beckingsale	B11	18 x 18	24 x 14	1.16 (*)	4.3	0.05	9.0	E
	B12	"	"	1.16	4.3	0.05	9.7	E
	B13A	"	"	1.35	3.1	0.44	9.7	E
	B13B	"	"	1.31	3.1	0.22	9.7	E
Birss	1	18 x 18	24 x 14	1.14 (*)	2.2	0.04	12.5	P
	2	"	"	1.07	0.6	0.44	11.8	P

Table 7-1 (cont.)

Ref.	Label	Column Size	Beam Size	M.R. (1)	(%)	P/P _u	V _j (2)	Performance
New Zealand (cont.)								
	Milburn	16 x 12	18 x 9	1.55(*)	3.7	0.10	14.8	E
	2	"	"	1.64	1.7	0.10	13.8	E
	Gagerty	16 x 12	18 x 9	1.18(*)	2.3	0.24	16.2	P
(U. of Canterbury)								

(1) The moment ratio was computed using the values provided by the authors(*), or if missing from the cross section dimensions and reinforcement given by the author and utilizing ACI-318 formulas with $\phi = 1.0$.

(2) This is the nominal shear stress divided by the f'_c

$$V_j = \frac{\text{Total Shear}}{\sqrt{f'_c} (A_g) \text{ column}}$$

(3) Reinforcement ratios for the joints are calculated as per Zhang and Jirsa (Ref. 115) It is defined as :

$$= \frac{(b^* + h^*) n A_t}{h^* b^* s}$$

where b^* and h^* are the confined widths and depth of the column, n is the number of ties at each level, A_t is the area of the tie leg, and s is the spacing.

lengths smaller than these will lead to premature bond failures or large bar slips. When the columns become smaller than 12 in., the specimens tested generally represented one-half to one-third scale models; the bond conditions in these test depend heavily of the details of the bar lugs, on the bar diameter, on the concrete properties, etc. Tests on very small specimens tend to show better behavior and more scatter than larger specimens do; it was decided to ignore such tests so that the data would represent more realistic, more severe bond conditions.

In Fig. 7-1 the moment ratio is plotted against the volumetric reinforcement in the joint for 39 beam-column joint tests. The performance of each specimen is classified as poor, acceptable, or excellent (See last column of Table 7.1) The criteria used to classify these test was based on the performance of the joint at the second loading cycle at an interstory drifts of about 2%. The specimens classified as poor showed some strength loss, large stiffness loss, and evidence of bond distress at this stage. Typical load deformation curves for these tests are shown in Fig 7-3.

Those classified as acceptable showed some degree of deterioration insofar as stiffness and strength were concerned, but showed little or no bond deterioration. Those classified as excellent showed non-deteriorating hysteretic behavior, and withstood drifts of 4% without failing. Obviously the scale is subjective, but

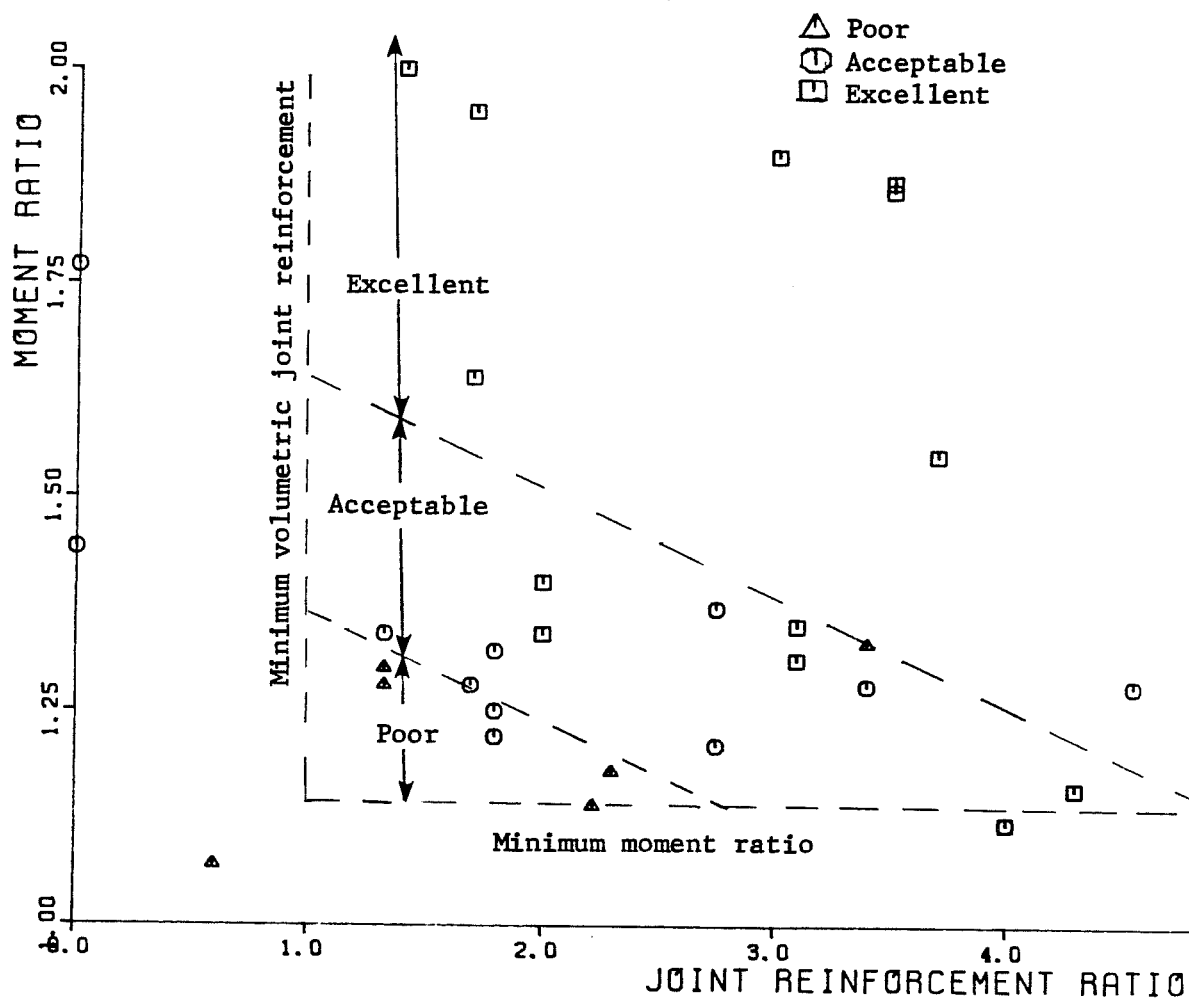


Figure 7-1 : Moment ratio vs. joint reinforcement (Interior)

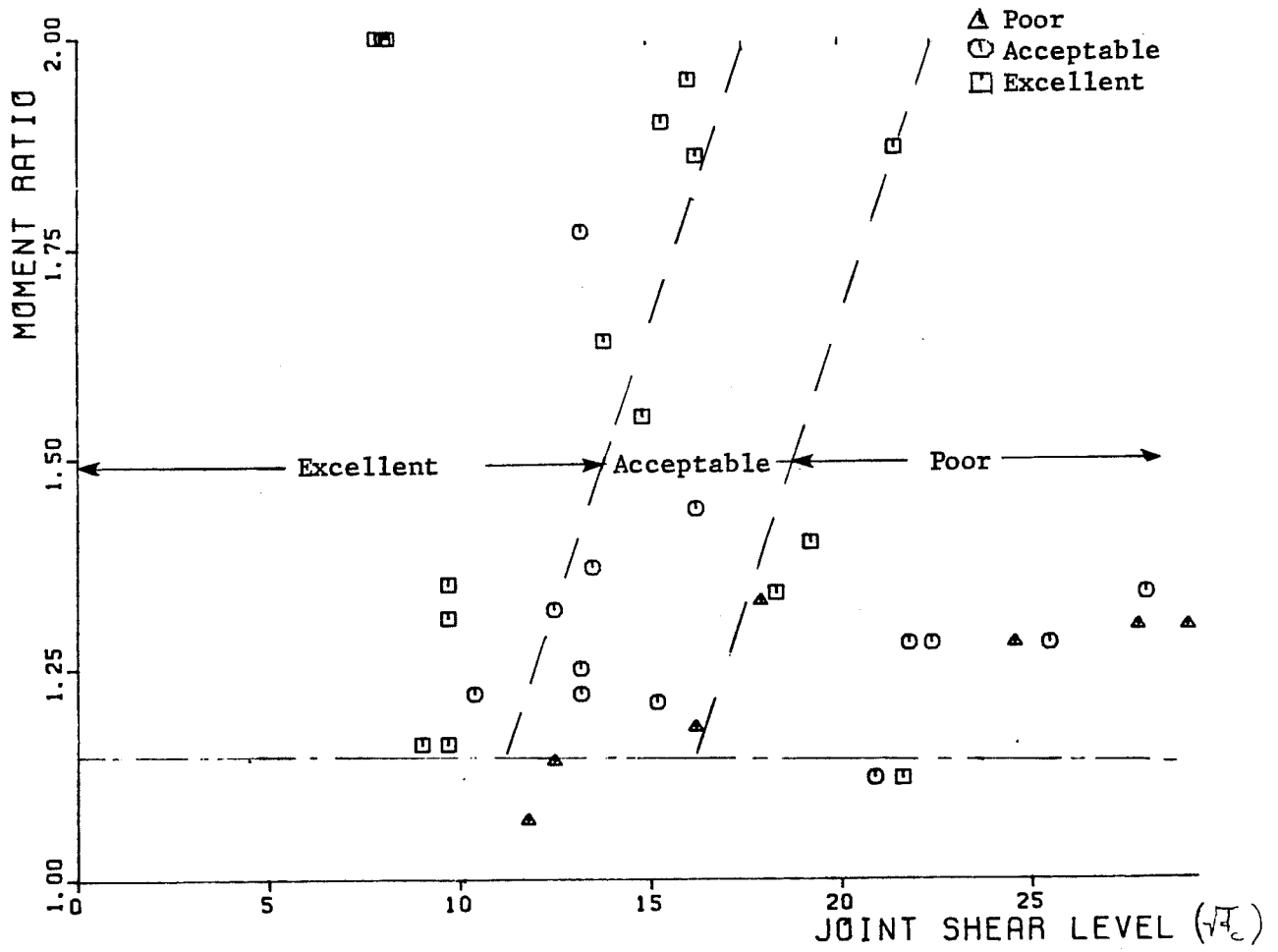


Figure 7-2: Moment ratio vs joint shear stress level

no other satisfactory technique could be found to compare tests run under very different load histories. Obviously the correlation between test performance described in Table 7-1 and the limits drawn in Fig. 7-1 is adequate but not outstanding. The reason for this is that most of these tests had other variables (axial load, presence of stub beams, transverse joint reinforcement, etc.) which influenced their behavior. The trends, however, are clear and excellent correlation should not be expected.

The parameter chosen for the horizontal axis is the amount of joint shear reinforcement. This is defined as the volume of steel in a given distance through the joint divided by the volume of the confined concrete over the same distance. Past research has focused on this as the key parameter for joint design. Fig. 7-1 clearly shows that good performance can be obtained utilizing low volumetric reinforcement ratios if the moment ratio is large enough. By increasing the moment ratio, the problems of congestion in a beam-column joint could be minimized.

The data presented shows that in general as the moment ratio increases, the overall behavior improves. The tests by Bertero [107] clearly show that good behavior can be obtained if the moment ratio is very high. The specimen behaved as expected, and no column inelasticity or cracking was observed. Due to the low shear stresses present in the joint, no visible shear cracking occurred and thus

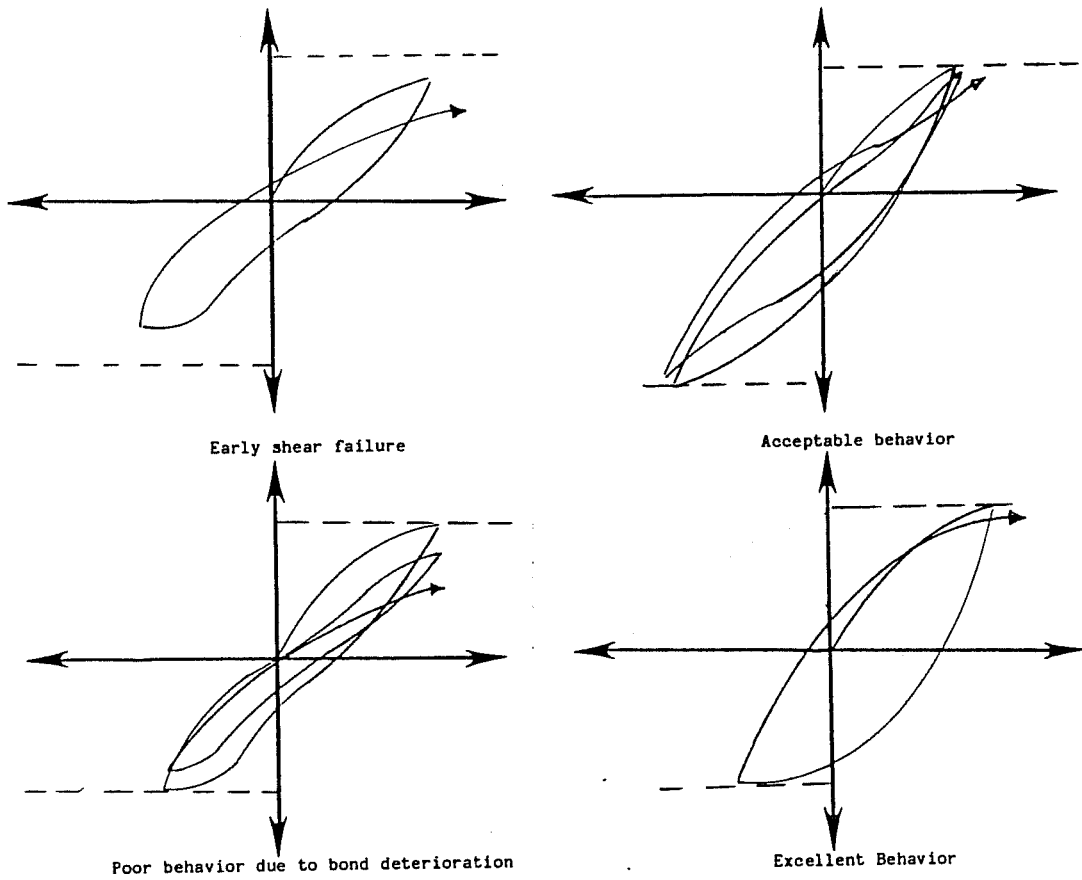


Figure 7-3: Performance classification for Table 7-1

deteriorating behavior was kept to a minimum. It was noted, however, that even with anchorage lengths of about 22.3 times the beam flexural bar diameters, bond deterioration and slip will occur with cycling at large deformations.

The data from Wight [29] shows that the combination of moderate moment ratios (1.2 to 1.3) and nominal shear stresses (10 to $15\sqrt{f'_c}$) begins to produce some undesirable joint behavior. Losses of strength and stiffness were evident at equivalent deformations for most tests. The losses, particularly stiffness losses, were not as high as for the BCJ series described here, where low moment ratios (1.1 to 1.3) and very high shear stresses (over $25\sqrt{f'_c}$) led to very poor behavior.

The tests from New Zealand [73, 74] show that for similar specimens (same level of nominal shear stress, but different moment ratios and axial load levels) very striking differences in behavior can be obtained. The test by Gaerty [73] points out that even at moderate nominal shear stress levels (10 to $15\sqrt{f'_c}$), a low moment ratio can lead to undesirable behavior.

The dotted lines in Fig. 7-1 show the authors interpretation of the limits to be used in design. The 1.0% volumetric ratio represents an absolute minimum to insure some confinement of the joint. This requirement must be tied to one specifying the maximum

bar spacing allowed without intermediate ties. Joints with intermediate ties have been hypothesized to provide better behavior than those without them, due to the better confinement provided by the latter. The 1.15 minimum moment ratio again represents a lower limit, and is intended to insure against wide variations in assumed and actual material properties. The tests discussed above clearly show that poor behavior is to be expected with low moment ratios unless very large joint reinforcement ratios are present. The inclined lines separating excellent, acceptable, and poor behavior are drawn somewhat above what the actual data shows, and are intended to be used as design limits rather than as a best fit to the data.

Figure 7-2 shows a similar plot, but the horizontal axis has been changed to the nominal shear stress on the joint area. It is clear that good performance can be achieved if the shear stress level is kept between $10 - 15\sqrt{f'_c}$, values commonly suggested as the limit in the more conservative codes [96, 7]. While these values are reasonable for low moment ratios, detailed examination of the experimental data shown in Table 7-1 will lead to the conclusion that these values could be increased to 15 to $20\sqrt{f'_c}$ as the moment ratio increases from 1.5 to 2.0.

Unfortunately not enough data is available to make the relationship between moment ratio, amount of volumetric joint reinforcement, and nominal shear stress levels clearer than described

above. The limits shown in Fig. 7-1 remain open to revision, but the author believes they are well within the bounds most researchers would consider acceptable.

From Figs. 7-1 and 7-2, it is clear that joints with moment ratios between 1.0 and 1.2 exhibited generally poor performance unless the shear stresses were low. Many researchers [50, 29] have reported that shear failures have occurred in tests with low moment ratios. However, most of this data needs to be reevaluated in light of the results reported herein and by Wight [29, 31]. It was shown in those studies that large bond stresses contributed significantly to the deteriorating behavior exhibited by specimens with low moment ratios. Due to the complex state of stress in a joint, it is impossible to separate the effect or relative contribution of each of these mechanisms (flexure, shear, and bond). The reader must bear in mind that since all the mechanism are related, the best solution to avoid deterioration may be to increase the moment ratio.

Reports from tests at the other end of the spectrum (moment ratios equal to or greater than 1.8) indicate very good behavior with little if any deterioration in strength and stiffness even under large deformations. Test with moment ratios between 1.40 and 1.8 indicate behavior somewhere between the two extremes. Thus the designer can obtain a wide spectrum of structural performance by adjusting the the moment ratio used and providing only minimum of joint reinforcement.

7.4.2 Conclusion form BCJ Test Series

The moment ratios used in the test series reported herein ranged from 1.13 to 1.28. As noted before, most of them displayed poor hysteretic performance and serious strength deterioration. Since the specimens were loaded biaxially, it is clear that the ratio decreased faster than under uniaxial loads, due to the crushing and spalling that occurred at the opposite corner of the joints along the diagonal loaded. The strains in both the concrete and steel are probably higher for the biaxial case than in the uniaxial case, and resulted in a faster loss of column flexural capacity with increasing deformation.

It is quite likely that at the latter stages of several tests the moment ratio dropped below one, since considerable column inelasticity and loss of stiffness occurred. This is particularly evident in specimens BCJ11, BCJ8, and BCJ9 after the first excursion at the second deflection level (drifts of about 4%). If the very large ductility demands imposed on these specimens is taken into account, it can be said that most exhibited poor to acceptable behavior for drifts below 2%. The exceptions were test BCJ11 and BCJ14. In BCJ11 the small framing beams did not provide adequate confinement to the joint, and the resultant spalling of the column corner sections led to a moment ratio lower than one. The anchorage failure in BCJ # 14 occurred before significant inelasticity could be

observed in the column. The behavior of BCJ11 clearly shows that unless the joint face is masked by the framing beam over more than 75% of its area, the effect of confinement from framing members is lost and should not be counted in design.

7.4.3 Structural Considerations

In selecting the desired level of performance for the joints in a ductile moment resisting frame, both the importance of the structure and the type of structural system to be used must be considered. Obviously, when designing a hospital or other lifeline facility, a large moment ratio is needed. On the other hand, for a warehouse or small office building the moment ratio would be smaller, according to the level of acceptable damage at different limit states.

The same reasoning must apply to the redundancy of the structural system. If the frame is to carry all the loads and no secondary system is available once the primary system is lost, then the the moment ratio ought to be very large. If the frame is to act as a secondary system to a set of shear walls, then the moment ratio could be substantially lowered.

7.4.4 Current Design Values

The use of a moment ratio greater than 1.0 had not been incorporated into design codes until very recently. Most past codes [3, 6, 2] only specified that the moment ratio had to be greater than one. The new ACI Code [5], in Appendix A, Section 4.2.2, requires that the ratio of the column-to-beam nominal flexural capacities be greater than 1.20 . In the new ACI-ASCE Joint Committee 352 Recommendations, still under balloting, consideration is being given to a moment ratio of about 1.40 . Both of these are based on engineering judgement , experimental data and field observations after past earthquakes. Although the ATC3-06 lacks specific recommendations for the the moment ratio factors to be used in joints, it is applied implicitly through the use of overstrength, importance, and structural system factors.

7.4.5 Suggested Values for the Moment Ratio

Careful study of the data in Table 7-1 indicates that reasonable values of the moment ratio should fall between 1.2 and 1.8 depending on the importance of the structure and the structural system. Since the design approach is based on selecting a value of the moment ratio, suggested ranges are shown in Table 7-4. The values suggested are in increments of 0.20, but any value in the range suggested may be used if it can be shown to be reasonable for that structure.

Importance(1)	Zone(2)	β (3)
1.5	3	1.8
1.5	2	1.6
1.0	3	1.6
1.0	2	1.4
1.5	1	1.4
1.0	1	1.2

- (1) Importance factor according to SEAOC Code
- (2) Zone factor according to SEAOC Code
- (3) Suggested value of moment ratio for structures with $K = 0.67$ according to SEAOC Code Structures with $K = 0.80$ should be designed for a moment ratio of 0.20 less than those of $K = 0.67$.

Table 7- : Suggested values for β

7.5 Proposed design approach

7.5.1 Background

In the previous section it was shown that the moment ratio can be selected as the key parameter in the design of beam-column joints. It is clear, moreover, that the size of the column determines the size of the joint and, indirectly, the width of the framing beams. Thus in any rational design approach for the design of beam-column joints a criteria involving moment ratios must be included in the preliminary design stage. The procedure proposed here is intended to give the engineer an idea of the preliminary sizes and reinforcement ratios to be used. A final check of the actual section capacities and the behavior of the complete structure under dynamic loads is obviously required.

7.6 Basis for Design Approach

The design approach to be proposed here is based on the acceptance of two concepts. The first is that the moment ratio can be utilized as the key design parameter to obtain any desired level of performance. Previous sections in this chapter have already proven this point. The second concept is that we must insure that the joint and columns remain in the elastic range as long as possible, even in the event of a major earthquake [75]. This second concept is an essential feature of the moment resisting frame design

philosophy as discussed in Chapter 1, and thus needs no further discussion.

The development of the design approach, however, requires that some choices be made with regard to the overstrength of the columns with respect to the beam. Since the intent is that the columns should remain elastic as long as possible, all the assumptions made in the development of the design approach will tend to underestimate the column capacity and overestimate that of the beams. Two approaches are possible, in principle, to the problem of insuring column overstrength even under very large earthquakes. The first is to design the columns according to working stress principles and the beams according to ultimate strength ones. This approach is impractical and inconsistent. The second approach is to design both the beams and columns according to ultimate strength considerations but to use a very low "phi factor" for the columns with respect to the beams. Ideally this will lead to the columns working in the elastic range under service loads and moderate earthquakes, and undergoing only some limited inelasticity under large earthquakes. This second approach is the one to be followed here.

Once the need for a substantial column overstrength is understood, the rest of the development of the design approach simplifies to finding expressions for the flexural and shear capacity of the sections involved. Once the flexural capacity of the members

is known, a relationship between the reinforcement ratios for the beam and the column can be found by using Eq. (7-3). Then the limiting values for the beam reinforcement ratio have to be checked against those provided by the shear and bond provisions. The intent of the procedure is to find the limiting values of beam and column reinforcement ratios associated with the limits for moment ratios, shear, and bond conditions found to have given the best performance in past tests.

The development of this design approach thus requires two steps. First, equations for the moment capacity of the members are developed. Second, limits on the moment capacity equations are established by shear and bond conditions. A number of approximations will be made in order to simplify the procedure. In most cases these approximations are conservative and of the nature commonly made in design. The intent of the procedure is guide the design towards section sizes and reinforcement ratios that have been found to perform well as evidenced by experimental, analytical, and field observations.

7.7 Derivation of Equations

The complete derivation of the following equations is given in Appendix E. Only the most important equations will be repeated here. The following symbols will be used :

- b_b = width of the beam , in.
 h_b = depth of the beam, in.
 ρ_t^+ = positive steel reinforcement ratio, %
 ρ_t^- = negative steel reinforcement ratio, %
 ρ_{tb} = summation of $\langle \rho_t^+ \rangle + \langle \rho_t^- \rangle$
 f_y = yield strength of beam steel, ksi
 $M_{u,b}$ = summation of beam capacities, kip-in
 b_c = width of the column, in.
 h_c = depth of the column, in.
 ρ_{tc} = column reinforcement ratio, %
 (P/P_u) = ratio of axial load present to
maximum allowable axial load
 (M_y/M_x) = ratio of moment in x-direction
to moment in y-direction
 $M_{u,c}$ = summation of column moment capacities, kip-in
 f_y = yield strength of column steel, ksi
 f'_c = compressive strength of concrete, ksi
 d_b = reinforcing bar diameter, in.
 $\psi = [h_c^2 b_c / h_b^2 b_b]$
 $r = [h_c b_c / h_b b_b]$

The definitions are illustrated in Fig. 7-4.

The equations will be developed separately for the case of uniaxial and biaxial loading. The procedure requires the use of the equations for biaxial loading when the ratio of the smaller to larger

$$M_y = M_y^- + M_y^+$$

$$M_x = M_x^- + M_x^+$$

Biaxial if $\left(\frac{M_y^-}{M_x}\right) > 0.25$

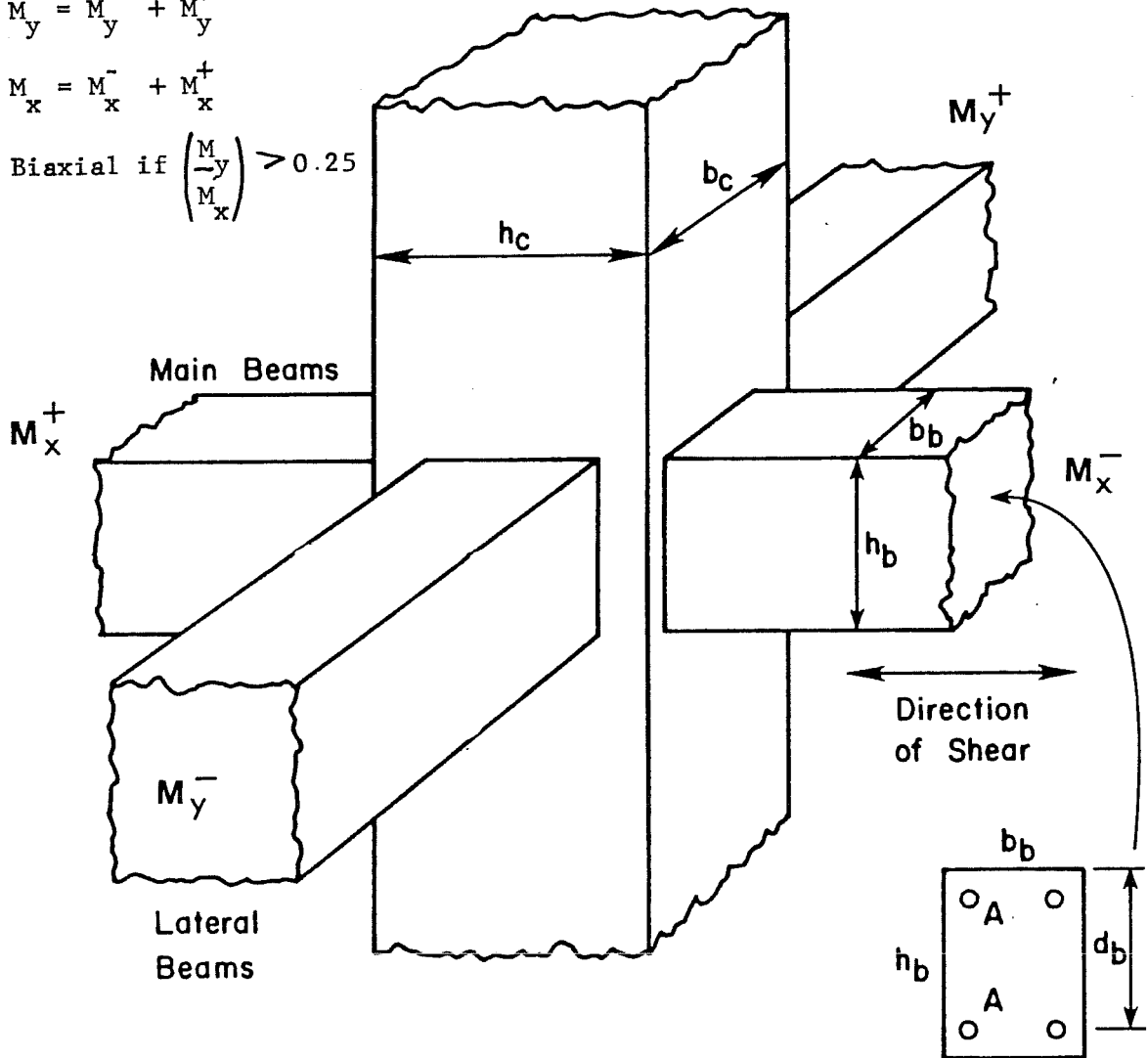


Figure 7-4: Definition of variables used.

moments required in two perpendicular directions exceeds 0.25 (See Fig. 7-4).

7.7.1 Uniaxial Loading

7.7.1.1. Beam Flexural Strength

The summation of the positive and negative beam moment capacities at the two faces of an interior beam-column joint can be approximated by:

$$\Sigma M_{b,u} = 0.87 \rho_{tb} h_b^2 b_b f_y \quad (7.4)$$

The effect of the presence of a slab or other floor members that may contribute to the beam flexural strength will be ignored in this development.

7.7.1.2. Column Flexural Strength

For the region between the balance and zero axial load points, the uniaxial moment capacity of a column section at a joint can be approximated by:

$$\Sigma M_{u,c} = 1.74 h_c^2 b_c K \quad (7.5)$$

where,

$$K = [0.45 + 15\rho_{tc}] [0.40 + 0.15f'_c] \quad (7.6)$$

7.7.1.3. Flexural Reinforcement Limits

Substituting the two equations derived for the beam and column moment capacities, into Eq. (7.3), and rearranging terms, we have :

$$\rho_{tb} < [1.40 K h_c \quad \Gamma \quad / B h_b f_y] \quad (7.7)$$

where the geometric parameter Γ has been defined as :

$$\Gamma = [h_c b_c / h_b b_b] \quad (7.8)$$

" Γ " is the ratio of the gross area of the column to the gross area of the beam.

Thus for a given set of material properties (f'_c and f_y) and a relationship between h_c and h_b , this equation fixes the limit for ρ_{tb} given any ρ_{tc} . This latter term is included in the expression for K .

7.7.1.4. Joint Shear Capacity

The joint shear strength for uniaxial loading will be assumed to be $20\sqrt{f'_c}$. Reducing this value by 0.70 to account for cyclic loading, and rearranging terms we obtain :

$$\rho_{tb} < 11.2 \quad f'_c \quad \Gamma \quad / f_y \quad (7.9)$$

7.7.1.5. Bond Stresses

To insure that bond deterioration and bar slippage do not govern the behavior of the beam-column joint, the following limits will be imposed on the joint size :

$$h_c > 24 d_{\text{largest beam bar}} \quad (7.10)$$

and,

$$h_b > 24 d_{\text{largest column bar}} \quad (7.11)$$

7.7.1.6. Geometric Considerations

As explained in Appendix E, the minimum beam width shall be taken as 0.60 times the column width, and the beam depth shall be taken as 1.15 times the column depth. Substituting these values into Eqs. (7.7) and (7.9), we obtain the following limits for p_{tb}

$$p_{tb} < 0.0292 K / \beta \quad (7.12)$$

and,

$$p_{tb} < 0.00027 \sqrt{f'_c} \quad (7.13)$$

The fact that Eq. (7.13) gives a maximum allowable p_{tb} for a given concrete strength, also put a limit on the amount of p_{tc} allowable. By equating Eqs. (7.12) and (7.13), and solving for K, we have :

$$K < 0.0092 \beta \sqrt{f'_c} \quad (7.14)$$

or substituting for K from eq. (7.6), we have:

$$[0.40 + 15\rho_{tc}] < 0.0092 \beta \sqrt{f'_c} h_b / [0.40 + 0.15 f'_c] h_c \quad (7.15)$$

Thus we have found limits for both the beam and column reinforcement ratios as the procedure requires. The equations contain only the limits given by flexure and shear, since bond conditions only put a limitation on the size of the bars that are allowed in either structural member.

7.7.2 Biaxial Loading

The procedure to be followed for biaxial loading is the same as that outlined above for the uniaxial case.

7.7.2.1. Beam Moment Capacity

The moment capacity of the beams is the same as given by Eq. (7.4), but the designer must be careful to always use the larger of the two perpendicular required moment capacities in his design.

7.7.2.2. Column Moment Capacity

The column moment capacity is the same as that given by Eq. (7.5), except for the fact that the the moment capacity of the column needs to be decreased to account for biaxial effects. It was found that a good approximation to the biaxial moment capacity of a column could be given by dividing the uniaxial moment capacity by:

$$\phi = (1.25 + 1.2 [P/P_u])(0.55 + 0.45[M_y/M_x])(1.00 + 10\rho_{tc}) \quad (7.16)$$

Since both this expression and K contain the term p_{tc} , a new quantity was defined to collect all the other terms, as :

$$\Omega = \beta [1.25 + 1.2(P/P_u)] [0.55 + 0.45(M_y/M_x)] / [0.40 + 0.15f'_c] \quad (7.17)$$

7.7.2.3. Joint Shear Strength

Since the joint will be confined by framing beams on all sides, the allowable joint shear strength has been increased to $24\sqrt{f'_c}$. Taking the usual 0.70 reduction for cyclic loading, a 0.7 reduction for biaxial effects, the limit for the beam reinforcement ratio is given as:

$$p_{tb} < 9.5 f'_c \Gamma / f_y \quad (7.18)$$

7.7.2.4. Geometric Parameters

For the case of biaxial loading, the minimum beam width was fixed as 0.75 times the column width, while the ratio between the beam and column depths was maintained at 1.15 as for the uniaxial case.

7.7.2.5. Synthesis

Substituting the values of the geometric parameters discussed into the limiting equations as done for the uniaxial case results in the following limits for the reinforcement ratios:

$$p_{tc} < 0.0233 K / \beta \Omega \quad (7.19)$$

$$p_{tc} < 0.00018\sqrt{f'_c} \quad (7.20)$$

$$K < 0.00771\sqrt{f'_c} \beta \rho \quad (7.21)$$

These three equations represent the limits for reinforcement in the beams and columns for the biaxial loading case.

7.7.3 Discussion

The significance of the equations derived above is shown in Figs. 7-5 and 7-6. For the case of uniaxial loading, it is clear that the shear requirements impose a limit not only on the beam directly, but also for the column indirectly. Thus, if the moment ratio of 1.6 and $f'_c = 4000$ psi are chosen, the column reinforcement ratio must be less than 3.0%. Thus, for a given the moment ratio the designer is already constrained in selecting the amount of steel in the column. For economic reasons the use of as large a column reinforcement ratio as possible is desirable. Fig. 7-5 gives us a starting point for the design approach. Note that most columns will need to be designed in the 2% to 3% range; if the designer feels that it is economical, he can obviously choose a lower column reinforcement ratio.

For the case of biaxial bending, flexure tends to control. Shear will be the limiting factor only if ξ becomes less than 2.0. This is the case only for unimportant structures in low to moderate seismic areas or for dual system structures of some importance in areas of high seismic risk. For most cases flexure will control

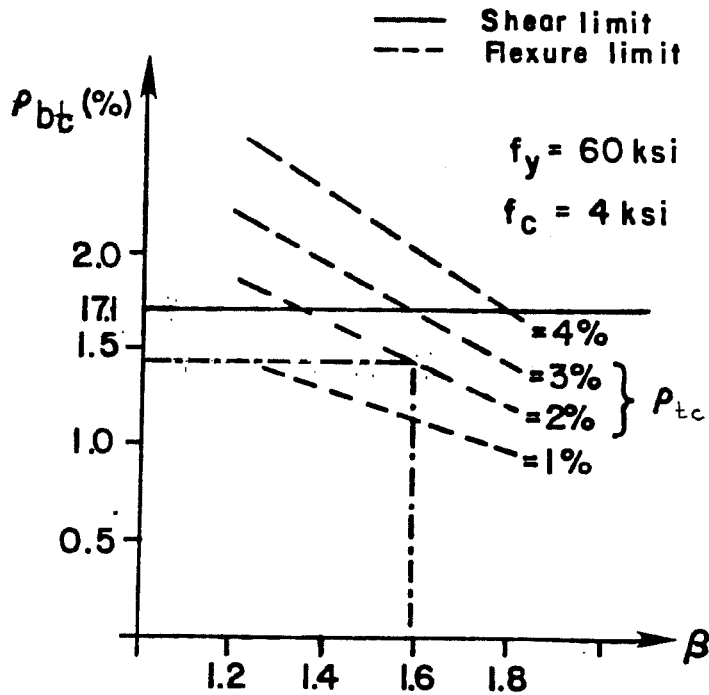


Figure 7-5 : Beam reinforcement vs. moment ratio - Uniaxial

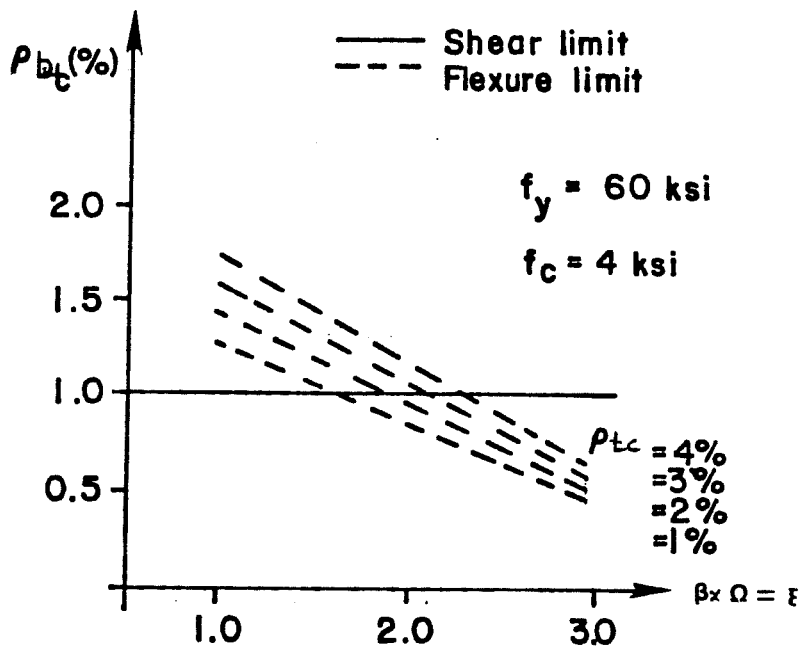


Figure 7-6 : Beam reinforcement vs. moment ratio - Biaxial

because the reduction in moment capacity can be substantial for the biaxial case (almost 50% for heavily reinforced square sections loaded along the diagonal). For the case of biaxial loading, then, the starting point will be given by Fig. 7-6.

The most important conclusion to be drawn from these two figures refers to the very low reinforcement ratios allowed in the beams, particularly in the biaxial case. The vertical axis refers to the sum of both positive and negative steel, and thus it is clear that for the uniaxial case that corresponds to about 60% of "rho balance", while for the biaxial case it is only about 35% of "rho balance" ($f_y = 60$ ksi and $f'_c = 4$ ksi). From the structural point of view, this has two effects. The first, and very beneficial effect, is that the ductility of these members will be very large if the proper detailing is carried out. The second, and potentially a damaging one, is that the dead load of the structure will increase. This second effect is particularly important because the mass of the structure will influence significantly its dynamic characteristics. However, the additional mass will come from the larger beam widths required by this procedure. This increase will probably be reflected in only a 5% to 10% increase in overall dead load, since most of the latter comes from the floor system and other non-structural elements rather than from the main frame. Thus the increase in mass cannot be considered a serious drawback of this procedure.

Another important feature of the procedure, and particularly of the biaxial case, is that it forces the designer to use large column reinforcement ratios in order to keep the beam reinforcement at a practical level. The ductility of columns depends both on its detailing and reinforcement ratio; it is quite possible that for the lower story columns, where hinging under extreme loading may be expected, special detailing would be required to insure the necessary column ductility.

7.7.4 Minimum Transverse Steel Requirements

The satisfactory performance of beam-column joints requires a minimum amount of steel in the joint to provide adequate confinement to the core concrete and to improve the bond characteristics of the column bars. It is felt that the new provisions for confined joints given by Appendix A of the ACI Code [5] are adequate to guarantee good performance. The amount of transverse steel required will be for both uniaxially and biaxially loaded joints:

$$A_{sh} = 0.15[s_h f'_c h'' / f_y] [(A_g / A_c) - 1.0] \quad (7.22)$$

or,

$$A_{sh} = 0.045 [s_{sh} f'_c h'' / f_y] \quad (7.23)$$

where,

- A_{sh} = area of steel required in the joint, in.²
- f'_c = concrete compressive strength, ksi.

- f_y = steel yield strength, ksi.
- s_{sh} = spacing of joint ties, in.
- A_g = gross concrete area of column, in.²
- A_c = confined area of the column, in.²

7.8 Design Approach

The intent of this procedure is to limit the shear and bond stresses in the joint to within values found by experiment to give good performance under severe cyclic loads. To accomplish this a moment ratio parameter is specified in design, and the size of the beams and columns fixed accordingly. Most design procedures do not take the joint into account until the sections have been designed. The joint is then reinforced with transverse steel to help it carry the computed shear forces. The proposed design approach does not consider the joint steel to be carrying any shear and should produce joints which are less congested and perform better.

The equations developed above can be transformed into a design approach by utilizing the following steps:

1. Select value of β from Table 7-2 . This is a straight forward choice involving only the importance and location of the structure.
2. Compute the required moment capacity for the column. For the uniaxial case this requires the multiplication of the required beam moment capacity by β . For the biaxial case, it requires the multiplication of the required beam capacity by β , by Θ to account for biaxial effects, and

to divide it by $[1.00 + 10 \rho_{tc}]$; the latter is required because at this stage we have not yet selected a ρ_{tc} , so we need to leave this term out of the equations.

3. Find the maximum reinforcement ratios allowed for the columns and beams.. These quantities are given by Eqs. (7-12), (7-13), and (7-14) for the uniaxial case and Eqs. (7-19), (7-20), and (7-21) for the biaxial case.
4. Assume a column reinforcement ratio. This should be as low as practically possible, but always at least 0.5% less than the one given by the limiting equations (Eq. (7-14) for the uniaxial and Eq. (7-21) for the biaxial case). This not be true if we are dealing with a large moment magnification factor (MFR), and the limiting value is given by 4%.
5. Find the required column size, as given by Eq. (7-5). Remember that the equations were developed for the case of square columns, so that h_c is equal to h_p . Recall also that Eq. (7-5) will underestimate the moment capacity at the balance point by about 10% and overestimate the one at the zero axial load by the same amount. The designer is encouraged to use this information to save himself some iterations and thus converge to a satisfactory solution faster.
6. From a handbook or set of tables, select a column with dimensions and reinforcement ratio similar to the ones computed in steps 4 and 5 above. Compute the moment capacity of the section selected, and check that the actual for the selected column is close to the originally assumed in the design If this check fails, go to step 4 and select a higher column reinforcement ratio.
7. For the actual ρ_{tc} used, calculate the limits of ρ_{tb} as given by Eqs. (7-12) and (7-19). Calculate the dimensions of the beam by using the assumed ratios of beam-to-column width and depth.
8. Select a beam size and reinforcement close to the values computed in step 7, and check that the beam moment capacity is close to that assumed initially in the design.
9. Check the bond conditions. If the column bars are too big go back to step 5 and select a section with smaller bars. If the beam bars do not meet the requirements go back to step 7 and select a different beam bar size.

10. Calculate the required transverse reinforcement as given by Eqs. (7-22) and (7-23), and check shear stress level.

The design approach is outlined in Fig. 7-7, and two design examples are summarized in Table 7-3. The complete solutions are shown in Appendix A comparison of the results given by this procedure and those obtained by Bertero et al [Zagajeski77] for a complete frame are shown in Fig. 7-7. It should be noted that the two procedures give very similar size columns, but that the beam widths are much larger for this procedure. This is due to the limitations in geometry assumed in the proposed design approach.

7.9 Evaluation and Comparison of Design Approach

The design approach proposed above differs from those discussed in Chapter 2 in two significant aspects. First, it assumes that in general flexural rather than shear strength should govern design. Second, it emphasizes the fact that the joint will control the size of the beams and columns in moment resisting frames.

The idea that flexural rather than shear strength should control design is based on both experimental evidence and analytical techniques. Few researchers have been able to obtain a true shear failure of a joint. In general, bond conditions and flexural cracking at the beam-column interface decreased the strength and stiffness of the subassemblages drastically before the shear deterioration of the joint became significant. More importantly,

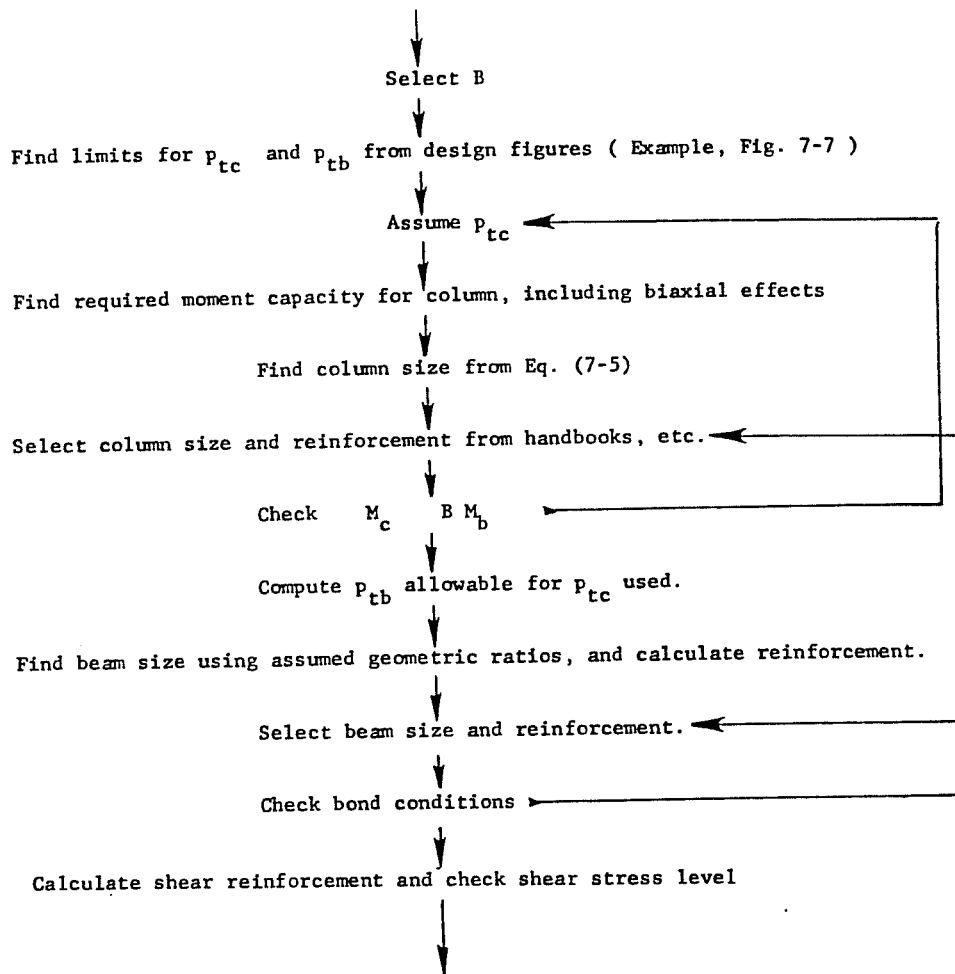


Figure 7-7: Outline of design approach

	Example # 1	Example # 2
Given	$Z = 3$ $I = 1.5$ $K = 0.67$ $M_b = 15,000$ kip-in. $f_y = 60$ ksi $f'_c = 4$ ksi $P = 0.2 P_u$ Uniaxial loading	$Z = 3$ $I = 1.5$ $K = 0.67$ $M_b = 15,000$ kip-in. $f_y = 60$ ksi $f'_c = 4$ ksi $P = 0.2 P_u$ Biaxial loading
Select B	$B = 1.8$ (Table 7.2)	$B = 1.8$ (Table 7.2)
Find limits	$P_{tb} = 0.0171$ (Fig. 7-6) $P_{tc} = 0.0400$ (Fig. 7-6)	$P_{tb} = 0.0099$ (Fig. 7-7) $P_{tc} = 0.0400$ (Fig. 7-7)
Select p_{tc}	$p_{tc} = 0.0250$	$p_{tc} = 0.0300$
Find column size and reinforcement	$h_c = 29.95$ " 28 " x 28 " 16 # 10 bars (2.59%)	$h_c = 36.26$ " 36 " x 36 " 16 # 14 bars (2.80%)
Check	$M_c = 13090$ kip-in. $B = 1.74$, O.K.	$M_c = 36,500$ kip-in. $B = 1.76$, O.K.
Find beam size and reinforcement	18 " x 32 " 6 # 8 top 7 # 6 bottom (1.51%)	28 " x 42 " 8 # 6 top 8 # 6 bottom (0.0065)
Find transverse reinforcement	3 # 4 at 4 "	3 # 4 at 4 "

Table 7-5: Design Examples

Beam Size	Col. Size	Col. Reinf.		Col. Reinf.	Col. Size	Beam Size
14" x 28"	26" x 26"	8 # 10	Roof	22" x 22"	4 # 10	18" x 24"
15" x 30"	26" x 26"	(8-12) #10	(10)	28" x 28"	(4-12) # 10	21" x 32"
15" x 30"	28" x 28"	12 #10	(9)	28" x 28"	12 # 10	21" x 32"
16" x 32"	28" x 28"	(12-16) #10	(8)	28" x 28"	12 # (10-11)	21" x 32"
16" x 32"	30" x 30"	16 #10	(7)	32" x 32"	12 # 11	24" x 38"
17" x 34"	30" x 30"	16 # 10	(6)	32" x 32"	(12-20) # 11	24" x 38"
17" x 34"	32" x 32"	16 # 10	(5)	34" x 34"	20 # 11	28" x 38"
17" x 34"	32" x 32"	(16-20) # 10	(4)	34" x 34"	20 # 11	28" x 38"
17" x 34"	34" x 34"	(20-32) # 10	(3)	34" x 34"	(28-20) # 11	28" x 38"
17" x 34"	34" x 34"	32 # 10	(2)	34" x 34"	28 # 11	28" x 38"

(a) Bartero & Zagajewski

(b) This procedure

Note : Assumed $\beta = 1.6$, $I = 1.0$, $K = 0.67$, $M_x/M_y = 0.5$, $P/P_u = 0.2$,
 $b_b = 0.75 b_c$, $f_y = 60 \text{ ksi}$, $f'_c = 4 \text{ ksi}$, $B = 1.8$ (first story)

Number in parenthesis refer to a change in reinforcement at midheight. Thus (20-32) # 10 indicates a transition from 32 to 20 # 10 bars.

Figure 7-8 : Comparison of member sizes and reinforcements given by this procedure and those given by an optimization solution by Bartero and Zagajewski (Ref. 112)

there is considerable evidence that the subassemblages that performed better under cyclic load were those having moment ratios greater than 1.50 . While increasing the amount of steel in the joint delayed deterioration, it clearly could not prevent it if a large number of cycles or large deformations were imposed. Evidence from field observations after past earthquakes shows that there are few documented cases of true joint shear failures. The most common source of joint failures are inadequate materials or poor detailing practices. If the latter two can be avoided, and the shear stress levels are maintained within the limits specified in Section 7.7.1, then it is likely that shear will not control design.

Several limitations to the procedure proposed above must be noted. The most important is the dependence of the equations on the geometric ratio of Eq. (7-8) . While the value of 1.00 for biaxially loaded joints is probably quite accurate, the 1.20 used for uniaxially loaded joints is open to debate. More research in this area is needed, since a small variation in the geometric ratio can cause large changes in beam reinforcement percentages. This is a particular problem for uniaxially loaded joints because the research summarized in Table 7-1 shows that the geometric ratio becomes less and less important as the joint increases in size. Tests with geometric ratios as large as 2.0 and as small as 0.80 have shown satisfactory performance if the moment ratio was high (>1.5).

Another limitation is that the procedure was derived for interior beam-column joints only. While similar equations can be written for external joints, the anchorage requirements for the beam bars must also be taken into account. There is insufficient data for behavior of exterior joints with different size framing beams, so a corresponding geometric ratio will have to be found empirically.

A third limitation is that the procedure as outlined above may be overconservative. The "phi factor" of 0.7 used for the column moment capacity combined with the 1.25 overstrength factor used for the beam steel will result in an initial margin against failure of about 1.50 even before the the moment ratio is applied. While this may seem excessive, there are two important mitigating factors. The first is that the assumed level of axial load can change drastically during an earthquake . In one side of the building the columns can be subjected to tension, while at the other side the compression load may exceed its balance point. In both cases the moment capacity, depending on the cross-section, can decrease rapidly and thus lead to an unsafe condition. The other factor to be taken into account is that beams and columns are generally cast monolithically with floor slabs. The contribution of the slab and other non-structural elements to the flexural strength of the beams cannot be safely ignored. Depending on the reinforcement ratio, the contribution of the slab may be as large as that of the beam. Ongoing research at the U. of Texas [55] will provide some insight into the beam-slab

interaction and help define more accurately parameter such as equivalent width necessary to take this effect into account. In the meantime it is probably safer to utilize the customary "phi factors" and maintain a conservative approach.

On the other hand, the procedure outlined above has several advantages. The main one is that it allows the designer to choose the level of performance desired with a high degree of confidence. Through the use of the the moment ratio, the engineer can achieve any desired type of behavior, a critical concern when dealing with moment resisting frames with little or no secondary lateral load-resisting system. The procedure outlined simultaneously satisfies flexural, shear, and bond requirements using values associated with satisfactory performance in past research.

Another advantage is that the procedure can be quickly automated. Thus, it could be added as a subroutine at the end of an computer analysis program to give immediately preliminary size and reinforcement ranges. To actually give sizes and reinforcement patterns the program would need access to a library of column interaction values. While this may seem cumbersome, only three values for each column (balance, no axial load, and $0.1f'_c A_g$) need to be stored. This procedure will work well if the program is designed to be interactive and the engineer can try several solutions before reaching a final decision.

A final advantage of the procedure developed above is that it will help the designer visualize better the interaction of the different structural requirements (bond, shear, and flexure) . The procedure clearly shows the significance of the different design parameters used in the design of beam-column joints and the results : beams with low reinforcement ratios and flexurally strong columns

Chapter 8

Conclusions

8.1 Summary of Test Program

Eight reinforced concrete beam-column joint subassemblages were tested to investigate the influence of floor members on their response under large cyclic load reversals. The tests were divided into three series. The first dealt with specimens with different framing beam sizes; the second with specimens with floor slabs; and the third with a comparison between interior and exterior joints. The intent was to clarify the effect of different floor member sizes and shapes on the behavior of these subassemblages.

Typically the subassemblages were 13 ft. high and consisted of four 13 in. by 18 in. beams framing into a 15 in. by 15 in. column. They were intended to represent a beam-column joint in the bottom stories of a moment resisting frame. The structural components between the midheight of adjacent floors and the points of inflection along the beams were modelled. The subassemblages were subjected to a severe load history consisting of 3 cycles at drifts of 2%, 4%, and 6%. The loads were applied biaxially simultaneously,

and were intended to model the worst loading condition to be expected from a major earthquake.

8.2 Summary of Results

The test series showed that beam geometry and floor slabs can have a significantly influence the behavior of beam-column joints. Severe degradation of stiffness and strength occurred in specimen with certain geometric characteristics.

8.2.1 Experimental Results

The main conclusion derived from the experimental phase of the program are:

1. Framing Beam Size - Under biaxial loading, the size of the members confining the joint was very important, particularly when the beam widths were smaller than 0.60 times that of the column. Except for the case of very narrow beams, it was shown that the beams can be counted to confine effectively the corners of the joint, and therefore prevent substantial changes in the moment ratio due to cover spalling.
2. Monolithic Slabs - the presence of monolithic slabs was important because :
 - (a) the additional flexural strength provided by the slab is generally not considered in design. The tests showed that for drifts of 2% or less the slab and beams acted as a T-section, thus greatly increasing the negative moment capacity of the beams. To prevent an early failure or lower moment ratios than those anticipated, the effect of the slab must be taken into account in design.
 - (b) the slab provided confinement to the upper

corners of the joint, which increased its shear strength and prevented spalling at drifts below 2%.

3. Biaxial Loading - For flexural strength design, the test series showed that biaxial loading of the column and the accompanying loss of section (spalling) under severe cyclic loading must be taken into account in design. For shear strength design, the tests showed that biaxial loads can be safely treated as two independent perpendicular forces, provided the vectorial sum of the two directions does not exceed $24\sqrt{f'_c}$.
4. Shear Strength - the shear strength of the beam-column joints tested was very high. The specimens withstood several cycles at nominal shear stresses higher than those allowed in practice ($24\sqrt{f'_c}$). The amount of shear introduced into the joint decreased with cycling, but this was due principally to bond deterioration rather than to actual shear strength degradation.
5. Axial Loads - the tests showed that for the practical range of axial loads in moment resisting frames (below the balance point), the effect of axial loads was small, and therefore would not help the joint appreciably in carrying the imposed loads.
6. Bond Conditions - the test showed that bond deterioration and yield penetration are very important mechanisms in beam-column joint behavior. This mechanisms can lead to an early failure not anticipated in current design codes or recommend, and the design engineer should be made aware of this shortcoming.

8.2.2 Design Recommendations

The results of the experimental work led to the following design recommendations for interior beam-column joints :

1. the use of small ratios of beam-to-column widths should be discouraged. For the case of uniaxially loaded frames the minimum allowed should not be less than 0.60, while for biaxially loaded frames the minimum should be increased to 0.80.

2. the use of large ratios of beam-to-column widths should be allowed only when a detailed analysis, including the effect of floor members, shows that the column overstrength is not endangered. If this detailed analysis is not carried out, the maximum allowable value for beam-to-column width should be set at 1.20.
3. the effect of the floor slab should be taken into account when the slab is very thick or heavily reinforced. The author suggest that until more research clarifies the issue of equivalent widths, current ACI provisions defining T-sections be used to calculate the total beam moment capacity.
4. for design purposes biaxial effects can be treated as independent, perpendicular forces, except for the flexural design of columns. For this latter case, a substantial "phi factor" should be used.
5. the maximum allowable shear stress in monotonically loaded joints should be fixed at $24\sqrt{f'_c}$. If biaxial loading is likely, this value should be reduced to $17\sqrt{f'_c}$ in each direction of loading.
6. the maximum allowable shear stress for cyclically loaded joints should not exceed 0.70 times that assumed for monotonically loaded ones.
7. the minimum anchorage length for bar across a joint should be 24 times the maximum bar diameter. This applies to both the beam and column, although the designer is strongly encouraged to use larger values for the column bars.

8.3 Proposed Design Approach

From the experimental work reported herein, and study of available data on other beam-column joint tests, a design approach was developed. It was shown that adequate joint performance required low shear stresses through the joint, favorable bond conditions, and a column flexural strength considerably greater than the flexural

strength of the floor members. Frames designed using this design approach will typically have large beams with low reinforcement ratios, and square columns with depths similar to those of the beams.

In general shear did not control the design of beam-column joints. Joints should be designed with flexure considerations in mind. In the proposed design procedures the contributions of the concrete strut and the truss mechanism were not separated. In fact, flexure dominated the design to the extent that only a minimum amount of transverse steel was required to confine the joint for axial effects and shear.

8.4 Additional Research Needs

Although this experimental work helped clarify some aspects of beam-column joint design, additional research is needed to improve design codes and verify the results of the research presented herein.

This is particularly true in three areas:

1. Bond stress-bar slip relationships : much work remains to be done in this area, both analytically and experimentally. Current models do not seem to match the data very well, and little is known of what kinds of limits on bond stresses should be allowable in design. This is particularly important in light of the observed behavior of column bars that tended to slip at levels below yield.
2. Influence of floor system geometry : although this work reports on a large test series, the number of available data for joints with large beams and stiff floor slabs is scant. More research is needed to fully verify some of

the conclusions presented here, and to extend the proposed design approach to a larger range of geometries.

3. Proposed design approach: the proposed design approach needs to be tried in practice to find out its strengths and shortcomings. As is always the case in earthquake engineering some structures will need to be built and undergo severe seismic loading before deciding whether it provides a satisfactory design solution.

REFERENCES

- [1] Abad de Aleman, M., Meinheit, D.F., and Jirsa, J.O.,
Influence of Lateral Beams on the Behavior of Beam-Column
Joints.
In Proceedings of the Sixth World Conference on Earthquake
Engineering - New Delhi. 1977.
- [2] ACI-ASCE Committee 352.
Recomendations for the Design of Beam-Column Joints in
Monolithic Reinforced Concrete Structures.
Journal of the American Concrete Institute 73(7):10-25, July,
1976.
- [3] American Concrete Institute.
Building Code Requirements for Reinforced Concrete (ACI - 318
77).
American Concrete Institute, Detroit, 1977.
103 pp.
- [4] American Concrete Institute.
Commentary on Building Requirements for Reinforced Concrete
(ACI - 318).
American Concrete Institute, Detroit, 1977.
132 pp.
- [5] American Concrete Institute.
Building Code Requirements for Reinforced Concrete (ACI
318-82).
ACI, Detroit, 1983.
- [6] Applied Technology Council.
Tentative Provisions for the Development of Seismic Regulations
for Buildings
Special Publication 510 (ATC3-6), National Bureau of Standards,
1978.

- [7] ASCE-ACI Committee 352.
Design Recommendations for Beam-Column Joints.
1982.
Updating of 1976 provisions currently under balloting (private communication).
- [8] Balint, P.S., and Taylor, H.P.J.,
Reinforcement Detailing of Frame Corner Joints with Particular Reference to Opening Corners.
Technical Report 42.462, Cement and Concrete Association,
February, 1972.
16 pp.
- [9] Beckingsale, C.W.,
Post-Elastic Behavior of Reinforced Concrete Beam-Column Joints.
PhD thesis, University of Canterbury, Christchurch New Zealand,
1980.
- [10] Bertero, V.V., Popov, E.P., and Viwathanatepa, S.,
Analytical and Experimental Hysteretic Loops for R/C
Subassemblages.
In Proceedings of the Fifth European Conference on Earthquake Engineering -Ankara. September, 1975.
- [11] Bertero, V.V., and Popov, E.P.,
Seismic Behavior of Ductile Moment-Resisting Reinforced
Concrete Frames.
In Reinforced Concrete Structures in Seismic Zones - SP 53,
pages 247-291. American Concrete Institute, 1977.
- [12] Bertero, V.V.
Seismic Behavior of Structural Concrete Linear Elements
(Beams, Columns) and their Connections.
In Symposium on Structural Concrete under Seismic Actions.
C.E.B. Rome, May, 1979.
- [13] Bertero, V.V., Popov, E.P., and Forzani, B.,
Seismic Behavior of Lightweight Concrete Beam-Column
Subassemblages.
Journal of the American Concrete Institute 77(1):44-52,
Jan.-Feb., 1980.
- [14] Bessho, S., et alia.
Tests of Beam-Column Joints of Reinforced Concrete Multistory
Buildings.
Transactions of the Architect's Institute of Japan
Extra(2448):000-000, Sept., 1979.
(In Japanese).

- [15] Birss, G.R.,
The Elastic Behavior of Earthquake-Resistant Interior Beam-Column Joints.
Master's thesis, University of Canterbury, Christchurch New Zealand, 1978.
- [16] Blakeley, R.W.G.,
Seismic Resistance of Prestressed Concrete Beam-Column Assemblies.
Journal of the American Concrete Institute 68(9):677-692, Sept., 1971.
- [17] Blakeley, R.W.G., and Park, R.,
Seismic Resistance of Prestressed Beam-Column Subassemblies.
Journal of the American Concrete Institute 68(9):677-692, September, 1971.
- [18] Blakeley, R.W.G., Megget, L.M., and Priestley, M.J.N.,
Seismic Performance of Two Full Size R.C. Beam-Column Units.
Bulletin of the New Zealand National Society for Earthquake Engineering 8(1):38-69, March, 1975.
- [19] Blakeley, R.W.G., Edmonds, F.D., Megget, L.M. and Priestley, M.J.N.,
Performance of Large R.C. Beam-Column Joint Units under Cyclic Loading.
In Proceedings of the Sixth World Conference on Earthquake Engineering - New Delhi. I.A.E.E., 1977.
- [20] Blakeley, R.W.G.,
Design of Beam-Column Joints.
Bulletin of the New Zealand National Society of Earthquake Engineering 10(4):000-000, Dec., 1977.
- [21] Bull, I.N.,
The Shear Strength of Relocated Plastic Hinges.
Technical Report 78/11, Department of Civil Engineering,
University of Canterbury, Christchurch, New Zealand, Feb., 1978.
- [22] Burns, N.H., and Siess, C.P.,
Load-Deflection Characteristics of Beam-Column Connections in Reinforced Concrete.
Civil Engineering Studies - Structural Research Series 234,
University of Illinois, January, 1962.
237 pp.

- [23] Bychenkov, Y.D.,
Strength and Crack-Resistance of Reinforced Concrete Frame
Joints in Multistory Earthquake-Resistant Buildings.
Concrete and Reinforced Concrete (2):10-13, 1971.
(In Russian).
- [24] Calcerano, G. and Moschella, A.
Comparison between the Behavior of Beam-Column External Joints
in both Fibre Bar Reinforced Concrete and Bar Reinforced
Concrete.
In Proceedings of the Seventh World Conference on Earthquake
Engineering - Ankara, pages 561-564 Vol. 6. I.A.E.E.,
1980.
- [25] Carvalho, E.C.,
Beam-Column Subassemblages Tested under Alternated Loads for
Seismic Design.
In Symposium on Structural Concrete under Seismic Actions,
pages 213-220. C.E.B., May, 1979.
Vol. 2 Rome.
- [26] Ciampi, V., Eligehausen, R., Bertero, V.V., and Popov, E.P.,
Hysteretic Behavior of Deformed Reinforcing Bars under Seismic
Excitations.
In Proceedings of the Seventh European Conference on Earthquake
Engineering, pages 179-187. September, 1982.
Athens, Greece.
- [27] Comité Euro-International du Béton.
Structural Concrete under Seismic Actions.
In Volumes 131, 132, 132bis. CEB, April, 1979.
- [28] Corley, W.G., and Hanson, N.W.,
Design of Beam-Column Joints for Seismic-Resistant Reinforced
Concrete Frames.
In Proceedings of the Fourth World Conference on Earthquake
Engineering. I.A.E.E., Santiago, January, 1969.
- [29] Durrani, A.J., and Wight, J.K.,
Experimental and Analytical Study of Internal Beam to Column
Connections Subjected to Reversed Cyclic Loading.
Technical Report UMEE 82R3, Department of Civil Engineering,
The University of Michigan, July, 1982.
- [30] Edgar, L. and Bertero, V.V.,
Evaluation of the Contribution of Floor System to the Dynamic
Characteristics of Moment-Resisting Space Frames.
In Proceedings of the Sixth World Conference on Earthquake
Engineering - New Delhi. I.A.E.E., 1977.

- [31] Ehsani, M. R., and Wight, J. K.,
Behavior of External Reinforced Concrete Beam to Column
Connections Subjected to Earthquake Type Loading.
Technical Report UMEE 82R5, Department of Civil Engineering,
The University of Michigan, July, 1982.
- [32] Eligehausen, R., Bertero, V.V., and Popov, E.P.,
Hysteretic Behavior of Reinforced Hooked Bars in R/C Joints.
In Proceedings of the Seventh European Conference on Earthquake
Engineering, pages 171-178. September, 1982.
Athens, Greece.
- [33] Fenwick, R.C., and Irvine, H.M.,
Reinforced Concrete Beam-Column Joints for Seismic Loading.
Technical Report 142, School of Engineering, University of
Auckland New Zealand, 1977.
- [34] Fenwick, R.C., and Nguyen, H.T.,
Reinforced Concrete Beam-Column Joints for Seismic Loading.
Technical Report 220, University of Auckland New Zealand, Jan.,
1981.
- [35] Fillippou, F.C., Popov, E. P., and Bertero, V.V.,
Analytical Model for Cyclic Deterioration of R/C Beam-Column
Joints.
In Proceedings of the Seventh European Conference on Earthquake
Engineering, pages 251-258. September, 1982.
Athens, Greece.
- [36] Galunic, B., Bertero, V.V., and Popov, E.P.,
An Approach for Improving the Seismic Behavior of R.C. Interior
Beam-Column Joints.
Technical Report UCB/EERC 77/30, Earthquake Engineering
Research Center - University of California at Berkeley,
Dec., 1977.
- [37] Gates, N.C.,
The Earthquake Response of Deteriorating Systems.
Technical Report EERL 77-03, California Institute of
Technology, March, 1977.
- [38] Gavrilovic, P., Velkov, M., Jurukovski, D., and Mamucervski, D.
Behavior of Beam-Column Joints Under Cyclic Loading.
In Proceedings of the Seventh World Conference on Earthquake
Engineering - Ankara, pages 289-296 Vol. 7. I.A.E.E.,
1980.

- [39] Hamada, K., and Kamimura, T.,
Tests of Reinforced Concrete Beam-Column Connections.
Transactions of the Architect's Institute of Japan Extra
2585:000-000, Sept., 1978.
(In Japanese).
- [40] Hamada, K., and Kamimura, T.,
Tests of Reinforced Concrete Beam-Column Connections (Part 2.
Character of Failure in Connections).
Transactions of the Architect's Institute of Japan Extra
2444:000-000, Sept., 1979.
(In Japanese).
- [41] Hanson, N.W., and Conner, H.W.
Seismic Resistance of Reinforced Concrete Beam-Column Joints.
Journal of the Structural Division A.S.C.E. 93(ST5):533-560,
October, 1967.
- [42] Hanson, N.W.,
Seismic Resistance of Concrete Frames with Grade 60
Reinforcement.
Journal of the Structural Division - ASCE 97(ST6):1683-1700,
June, 1971.
- [43] Hanson, N.W., and Conner, H.W.,
Tests of Reinforced Concrete Beam-Column Joints under Simulated
Seismic Loading.
Research and Development Bulletin RD012.01D, Portland Cement
Association, 1972.
- [44] Higashi, Y., and Ohwada, Y.,
Failing Behavior of Reinforced Concrete Beam-Column Joints
under Cyclic Loading.
Memoirs of the Faculty of Technology - Tokyo Metropolitan
University (19):91-101, 1969.
- [45] Ishibashi, K., Kamimura, T., and Sonobe, Y.
Behavior of R.C. Beam-Column Connections with Large Size
Deformed Bars under Cyclic Loads.
In Proceedings of the Sixth World Conference on Earthquake
Engineering - New Delhi. I.A.E.E., 1977.
- [46] Ishibashi, K., et alia.
Tests of Reinforced Concrete Beam-Column Connections with Large
Size Deformed Bars under Cyclic Loading (Part 1).
In Experimental Studies on Reinforced Concrete Members and
Composite Steel and Reinforced Concrete Members, pages
170-185. University of Tokyo, Dec., 1977.
(in Japanese).

- [47] Ishibashi, K., et alia.
Tests of Reinforced Concrete Beam-Column Connections with Large Size Deformed Bars under Cyclic Loads (Part 2).
In Experimental Studies on Reinforced Concrete Members and Composite Steel and Reinforced Concrete Members, pages 196-221. University of Tokyo, Dec., 1977.
(In Japanese).
- [48] Jirsa, J.O.,
Factors Influencing the Hinging Behavior of R.C. Members under Cyclic Overloads.
In Proceedings of the Fifth World Conference on Earthquake Engineering - Rome. I.A.E.E., 1973.
- [49] Jirsa, J.O., Meinheit, D.F., and Wooten, J.W.,
Factors Influencing the Shear Strength of Beam-Column Joints.
In Proceedings of the First U.S. National Conference on Earthquake Engineering - Ann Arbor, pages 297-305.
E.E.R.I., June, 1975.
- [50] Jirsa, J.O., and Meinheit, D.F.,
The Shear Strength of Beam-Column Joints.
Technical Report CESRL 77-1, University of Texas at Austin, January, 1977.
- [51] Jirsa, J.O., Burguières, S.T., and Longwell, J.E.,
The Behavior of Beam-Column Joints under Bidirectional Load Reversals.
In Symposium on Structural Concrete under Seismic Actions.
C.E.B. - Rome, May, 1979.
- [52] Jirsa, J.O., Burguières, S.T., and Longwell, J.E.
Shear and Bond Deterioration in Beam-Column Joints under Bidirectional Load Reversals.
In Proceedings of the Seventh World Conference on Earthquake Engineering - Ankara, pages 363-370 Vol. 6. I.A.E.E., 1980.
- [53] Jirsa, J.O.,
Seismic Behavior of R.C. Connections (Beam-Column Joints) State-of-the-Art.
In Proceedings of the Seventh World Conference on Earthquake Engineering - Ankara. I.A.E.E., Sept., 1980.
- [54] Jirsa, J.O.,
Beam-Column Joints : Irrational Solutions to a Rational Problem.
In Significant Developments in Engineering Practice and Research - SP 72. A.C.I., 1981.

- [55] Jirsa, J.O., and Joglekar, M.,
Results of Joint Tests from US-Japan Joint Project.
1983.
- [56] Keyong, Y.S.,
Prestressed Beam-Column Joints.
Technical Report 78/2, Department of Civil Engineering,
University of Canterbury, Christchurch New Zealand, Feb.,
1978.
- [57] Kokusho, S., et alia.
Tests of Reinforced Concrete Beam-Column Connections (Part 1
).
Transactions of the Architect's Institute of Japan
Extra(2531):000-000, Oct., 1974.
(In Japanese).
- [58] Lee, D.L.N.
Original and Repaired Behavior of R.C. Beam-Column
Subassemblages Subjected to Earthquake -Type Loadings.
Technical Report 76R4, Department of Civil Engineering,
University of Michigan, Ann Arbor, 1976.
- [59] Lee, D.L.N., Wight, J.K., and Hanson, R.D.,
Reinforced Concrete Beam-Column Joints under Large Load
Reversals.
Journal of the Structural Division - A.S.C.E.
103(ST12):2337-2350, December, 1977.
- [60] Longwell, J.E.
A Comparative Study of Biaxially Loaded Reinforced Concrete
Beam-Column Joints.
Master's thesis, University of Texas at Austin, December, 1980.
- [61] McCollister, H.M., Siess, C.P., and Newmark, N.M.,
Load-Deflection Characteristics of Simulated Beam-Column
Connections in Reinforced Concrete.
Civil Engineering Studies - Structural Research Series 76,
University of Illinois, June, 1954.
76 pp.
- [62] Megget, L.M.,
Anchorage of Beam Reinforcement in Seismic Resistant Reinforced
Concrete Frames.
Master's thesis, University of Canterbury, Christchurch New
Zealand, Feb., 1971.

- [63] Minami, K., and Nishimura, Y.,
Hysteretic Characteristics of Beam-to-Column Connections in
Steel R/C Structures.
In Proceedings of the Seventh World Conference on Earthquake
Engineering - Ankara , pages 305-309 Vol. 7. I.A.E.E.,
1980.
- [64] Minami, K., and Wakabayashi, M.,
Seismic Resistance of R.C. Beam and Column Assemblages with
Emphasis on Shear Failure of Column.
In Proceedings of the Sixth World Conference on Earthquake
Engineering - New Delhi. I.A.E.E., 1977.
- [65] Moss, P. J., and Carr, A. J.,
The Effects of Large Displacements on the Earthquake Response
of Tall Concrete Frame Structures.
Bulletin of the New Zealand National Society for Earthquake
Engineering 13(4):317-328, December, 1980.
- [66] Nakada, S., et alia.
Tests of R.P.C. Beam-Column Connections (Part 1).
In Experimental Studies on Reinforced Concrete Members and
Composite Steel and Reinforced Concrete Members - Vol. 2,
pages 155-165. University of Tokyo, Dec., 1977.
(In Japanese).
- [67] Nilsson, I.H.E., and Losberg, A.,
Reinforced Concrete Corners and Joints Subjected to Bending
Moment.
Journal of the Structural Division ASCE 102(ST6):1229-1254,
June, 1976.
- [68] Noguchi, H.,
Nonlinear Finite Element Analysis of Reinforced Concrete Beam-
Column Joints.
In Colloquium on Advanced Mechanics of Reinforced Concrete.
IABSE, June, 1981.
Delft, The Netherlands.
- [69] Ogura, K., et alia.
A Study on Flexural Capacity Deterioration of Members Passing
Through the Beam-Column Joints.
Transactions of the Architect's Institute of Japan
Extra(2585):000-000., Sept., 1978.
(In Japanese).

- [70] Ohwada, Y.,
A Study of the Effect of Lateral Beams on Reinforced Concrete
Beam-Column Joints (1).
Transactions of the Architect's Institute of Japan
Extra(2510):000-000, Oct., 1976.
(In Japanese).
- [71] Ohwada, Y.,
A Study of the Effect of Lateral Beams on Reinforced Concrete
Beam-Column Joints (2).
Conference of the Architect's Institute of Japan (61):000-000,
1977.
(In Japanese).
- [72] Park, R., and Thompson, K.J.,
Behavior of Prestressed, Partially Prestressed, and Reinforced
Concrete Beam-Column Assemblies under Cyclic Loading : Tests
Results of Units 1 to 7.
Technical Report 74-9, University of Canterbury, Christchurch
New Zealand, 1974.
- [73] Park, R., and Paulay, T.
Reinforced Concrete Structures.
John Wiley and Sons, New York, 1975.
- [74] Park, R., Gaerty, L., and Stevenson, E.C.,
Tests on an Interior Reinforced Concrete Beam-Column Joint.
Bulletin of the New Zealand National Society for Earthquake
Engineering 14(2):81-92, June, 1981.
- [75] Park, R., and Milburn, J.R.,
Comparison of Recent New Zealand and United States Seismic
Design Provisions for Reinforced Concrete Beam-Column
Joints.
1982.
Personal communication with J.O. Jirsa.
- [76] Paulay, T.
Capacity Design of Reinforced Concrete Ductile Frames.
In Bertero, V.V. (editor), Proceedings of a Workshop on
Earthquake-Resistant Reinforced Concrete Building
Construction - Vol. 3, pages 1043-1075. University of
California at Berkeley, 1977.
- [77] Paulay, T., Park, R., Priestley, M.J.N.,
Reinforced Concrete Beam-Column Joints Under Seismic Actions.
Journal of the American Concrete Institute 75(11):585-593,
November, 1978.

- [78] Poole, R.
R/C Ductile Frames - The Use of Diagonal Reinforcing to Solve the Joint Problem.
In Bertero, V.V. (editor), Proceedings of a Workshop on Earthquake-Resistant Reinforced Concrete Building Construction - Vol. 3, pages 1076-1097. University of California at Berkeley, 1977.
- [79] Popov, E.P., and Bertero, V.V.,
Hysteretic Behavior of Ductile Moment-Resisting Reinforced Concrete Frame Components.
Technical Report UCB/EERC 75/16, Earthquake Engineering Research Center - University of California at Berkeley, April, 1975.
- [80] Popov, E.P., Bertero, V.V., Galunic, B., and Lantaff, G.
On Seismic Design of R/C Interior Beam-Column Joints of Frames.
In Proceedings of the Sixth World Conference on Earthquake Engineering - New Delhi. I.A.E.E., 1977.
- [81] Popov, E.P.,
Seismic Behavior of Structural Subassemblages.
Journal of the Structural Division - A.S.C.E.
106(ST7):1451-1474, July, 1980.
- [82] Renton, G.,
The Behavior of R.C. Beam-Column Joints under Seismic Loading.
Master's thesis, University of Canterbury, Christchurch New Zealand, 1972.
- [83] Research Group on Anti-Seismic Joints.
Tests on Exterior Joints of Frame with Cast-in-Place Columns and Precast Beams.
Journal of Construction Technology, Structural Division
China:00-00, 1979.
(in Chinese).
- [84] Riddell, R. and Newmark, N. W.,
Statistical Analysis of the Response of Nonlinear Systems Subjected to Earthquakes.
Structural Research Series 468, Department of Civil Engineering, University of Illinois, August, 1979.
- [85] Rosenblueth, E., editor,
DEsign of Earthquake Resistant Structures.
John Wiley & Sons, New York, N.Y.,, 1980.

- [86] Saiidi, M., and Sozen, M.A.,
Simple and Complex Models for Nonlinear Seismic Response of Reinforced Concrete Structures.
Structural Research Series 465, University of Illinois at Urbana-Champaign, August, 1979.
- [87] Scarpas, A.,
The Inelastic Behavior of Earthquake Resistant Exterior Beam-Column Joints.
Technical Report 81-2, Department of Civil Engineering, University of Canterbury, Christchurch New Zealand, 1981.
- [88] Scribner, C.F., and Wight, J.K.,
Delaying Shear Strength Decay in R.C. Flexural Members under Large Load Reversals.
Technical Report UMEE 78R2, Department of Civil Engineering University of Michigan, May, 1978.
- [89] Seekin, M., and Uzumeri, S.M.,
Examination of Design Criteria for Beam-Column Joints.
In Proceedings of the Sixth European Conference on Earthquake Engineering, pages Vol. 3 , pp. 183-190. Dubrovnik, September, 1978.
- [90] Seekin, M., and Uzumeri, S.M.,
Examination of Design Criteria for Beam-Column Joints.
In Proceedings of the Sixth European Conference on Earthquake Engineering - Dubvronic, pages 183-190 Vol. 3. Sept., 1978.
- [91] Seekin, M. and Uzumeri, S.M.
Exterior Beam-Column Joints in Reinforced Concrete Frames.
In Proceedings of the Seventh World Conference on Earthquake Engineering - Ankara, pages 183-190. I.A.E.E., 1980.
- [92] Seismology Committee.
Recommened Lateral Force Requirements and Commentary
Structural Engineers Association of California edition, 1975.
- [93] Sekine, M., and Ogura, K.,
Experimental Studies on Reinforced Concrete Beam-Column Joints (Exterior).
Transactions of the Architect's Institute of Japan
Extra(2443):000-000, Sept., 1979.
(In Japanese).

- [94] Smith, B.J.,
Exterior Reinforced Concrete Joints with Low Axial Load under
Seismic Loading.
Master's thesis, University of Canterbury, Christchurch New
Zealand, 1972.
- [95] Soleimani, D.,
Reinforced Concrete Ductile Frames with Stiffness Degradation.
PhD thesis, University of California at Berkeley, December,
1978.
- [96] Soleimani, D., Popov, E.P., and Bertero, V.V.,
Hysteretic Behavior of Reinforced Concrete Beam-Column
Subassemblages.
Journal of the American Concrete Institute 76(11):1179-1196,
November, 1979.
- [97] Standards Association of New Zealand.
Code of Practice for the Design of Concrete Structures
DZ 3101 edition, 1980.
- [98] Sugano, S., and Koreishi, I.
An Empirical Evaluation of the Inelastic Behavior of Structural
Elements in Reinforced Concrete Frames Subjected to Lateral
Forces.
In Proceedings of the Fifth World Conference on Earthquake
Engineering - Rome. I.A.E.E., 1973.
- [99] Swan, R.A.,
Flexural Strength in Corners of Reinforced Concrete Portal
Frames.
Technical Report TRA 434, Cement and Concrete Association,
November, 1969.
14 pp.
- [100] Tada, T., Takeda, T., and Takemoto, Y.,
Tests of Reinforced Methods of Reinforced Concrete Beam-Column
Joints (Part 1).
In Proceedings of the Kanto District Conference. A.I.J., 1976.
(In Japanese).
- [101] Takizawa, H.
Biaxial and Gravity Effects in Modelling Strong Motion Response
of R.C. Structures.
In Proceedings of the Sixth World Conference on Earthquake
Engineering - New Delhi. I.A.E.E., 1977.

- [102] Tassios, T., Plainis, P., and Vassiliou, G.,
Column-Beam Joints Failed under Seismic Loading, Repaired and
Retested under Seismic Loading.
In Proceedings of the Sixth World Conference on Earthquake
Engineering - New Delhi . I.A.E.E., 1977.
- [103] Taylor, H.P.J.,
The Behavior of In-Situ Concrete Beam-Column Joints.
Technical Report Report 42.492, Cement and Concrete
Association, May, 1974.
London.
- [104] Thompson, K.J., and Park, R.,
Ductility of Concrete Frames under Seismic Loading.
Technical Report 75-14, Department of Civil Engineering,
University of Canterbury, Christchurch New Zealand, Oct.,
1975.
- [105] Uzumeri, S.M., and Seckin, M.,
Behavior of Reinforced Concrete Beam-Column Joints Subjected to
Slow Load Reversals.
Technical Report Report 74-05, Department of Civil Engineering,
University of Toronto, March, 1974.
85 pp.
- [106] Uzumeri, S.M.,
Strength and Ductility of Cast-in-Place Beam-Column Joints.
In SP 53. American Concrete Institute, 1977.
- [107] Viathanatepa, S., Popov, E.P., and Bertero, V.V.,
Seismic Behavior of Reinforced Concrete Beam-Column
Subassemblages.
Technical Report UCB/EERC - 79/14, University of California at
Berkeley, June, 1979.
- [108] Viathanatepa, S., Bertero, V.V., and Popov, E.P.,
Effects of Generalized Loadings on Bond of Reinforced Bars
Embedded in Confined Concrete Blocks.
Technical Report UCB/EERC 79/22, Earthquake Engineering
Research Center - University of California at Berkeley,
Aug., 1979.
- [109] Wakabayashi, M., Minami, K.,
Recent Studies on the Hysteretic Characteristics of Beam-to-
Column Connections in Composite structures.
Private communication with J.O. Jirsa.

- [110] Yamaguchi, I., et alia.
A Study on Reinforced Concrete Beam-Column Joints with U-Shaped Beam Reinforcement.
Takenaka Technical Research Report 16, T.I., Oct., 1976.
(in Japanese).
- [111] Yamaguchi, I., et alia.
A Study on Anchorages of Beam Reinforcement in Beam-Column Joints.
Takenaka Technical Research Report 20, T.I., Oct., 1978.
(In Japanese).
- [112] Zagajeski, S., and Bertero, V.V.,
Computer-Aided Optimum Design of Ductile R/C Moment-Resisting Frames.
In Bertero, V.V., (editor), Proceedings of a Workshop on Earthquake-Resistant Reinforced Concrete Construction, pages 1140-1174. University of California, Berkeley, July, 1977.
- [113] Zhang, L. and Jirsa, J.O.
Shear Strength of Beam-Column Joints.
1981.
Paper presented to Joint A.C.I.-A.S.C.E. Committee 352- A.C.I. Convention- Dallas.
- [114] Zhang, L., and Jirsa, J.O.,
Shear Strength of Reinforced Concrete Planar Frame Joints.
1981.
Paper presented at the US/PRC Workshop on Seismic Analysis and Design of Reinforced Concrete Structures, University of Michigan, Ann Arbor, May 1981.
- [115] Zhang, L. and Jirsa, J.O.,
A Study of Shear Behavior of Reinforced Concrete Beam-Column Joints.
PMFSEL Report 82-1, Department of Civil Engineering - The University of Texas at Austin, February, 1982.

VITA

Tomas Roberto Leon S. was born in San Jose, Costa Rica on November 3, 1955, the son of Maria Eugenia Saenz and Jorge Leon Arguedas. Upon graduation from Notre Dame International School, Rome, Italy, he entered the University of Massachusetts at Amherst in 1974. In May 1978 he received the degree of Bachelor of Science in Civil Engineering (cum laude) and then entered the Graduate School at Stanford University, receiving the degree of Master of Science in Structural Engineering in June 1979. In September 1979 he entered the Graduate School at the University of Texas at Austin to study for the Doctor of Philosophy degree. In September 1983 he was appointed to a faculty position in the Department of Civil and Mineral Engineering at the University of Minnesota.

Permanent Address: Dept. of Civil and Mineral Engineering
500 Pillsbury Drive, S.E.
University of Minnesota,
Minneapolis, MN 55455

This dissertation was typed by the author using the Scribe document formatting system created by Brian K. Reid. The current version has been maintained and enhanced by Unilogic, Ltd. The Scribe format definitions for thesis format for The University of Texas at Austin were developed by Richard M. Cohen.

